



GOLD-CATALYZED CYCLIZATIONS FOR THE SYNTHESIS OF SMALL AND MEDIUM-SIZED ARENES

Claudia Alejandra de León Solís

Dipòsit Legal: T. 196-2013

ADVERTIMENT. L'accés als continguts d'aquesta tesi doctoral i la seva utilització ha de respectar els drets de la persona autora. Pot ser utilitzada per a consulta o estudi personal, així com en activitats o materials d'investigació i docència en els termes establerts a l'art. 32 del Text Refós de la Llei de Propietat Intel·lectual (RDL 1/1996). Per altres utilitzacions es requereix l'autorització prèvia i expressa de la persona autora. En qualsevol cas, en la utilització dels seus continguts caldrà indicar de forma clara el nom i cognoms de la persona autora i el títol de la tesi doctoral. No s'autoritza la seva reproducció o altres formes d'explotació efectuades amb finalitats de lucre ni la seva comunicació pública des d'un lloc aliè al servei TDX. Tampoc s'autoritza la presentació del seu contingut en una finestra o marc aliè a TDX (framing). Aquesta reserva de drets afecta tant als continguts de la tesi com als seus resums i índexs.

ADVERTENCIA. El acceso a los contenidos de esta tesis doctoral y su utilización debe respetar los derechos de la persona autora. Puede ser utilizada para consulta o estudio personal, así como en actividades o materiales de investigación y docencia en los términos establecidos en el art. 32 del Texto Refundido de la Ley de Propiedad Intelectual (RDL 1/1996). Para otros usos se requiere la autorización previa y expresa de la persona autora. En cualquier caso, en la utilización de sus contenidos se deberá indicar de forma clara el nombre y apellidos de la persona autora y el título de la tesis doctoral. No se autoriza su reproducción u otras formas de explotación efectuadas con fines lucrativos ni su comunicación pública desde un sitio ajeno al servicio TDR. Tampoco se autoriza la presentación de su contenido en una ventana o marco ajeno a TDR (framing). Esta reserva de derechos afecta tanto al contenido de la tesis como a sus resúmenes e índices.

WARNING. Access to the contents of this doctoral thesis and its use must respect the rights of the author. It can be used for reference or private study, as well as research and learning activities or materials in the terms established by the 32nd article of the Spanish Consolidated Copyright Act (RDL 1/1996). Express and previous authorization of the author is required for any other uses. In any case, when using its content, full name of the author and title of the thesis must be clearly indicated. Reproduction or other forms of for profit use or public communication from outside TDX service is not allowed. Presentation of its content in a window or frame external to TDX (framing) is not authorized either. These rights affect both the content of the thesis and its abstracts and indexes.

Claudia A. De León Solís

**Gold-Catalyzed Cyclizations for the Synthesis of Small
and Medium-Sized Arenes**

DOCTORAL THESIS

Supervised by Prof. Antonio Echavarren

Institut Català d'Investigació Química (ICIQ)



UNIVERSITAT
ROVIRA I VIRGILI

Tarragona
2012

UNIVERSITAT ROVIRA I VIRGILI

GOLD-CATALYZED CYCLIZATIONS FOR THE SYNTHESIS OF SMALL AND MEDIUM-SIZED ARENES

Claudia Alejandra de León Solís

Dipòsit Legal: T. 196-2013



Av. Països Catalans, 16
43007 Tarragona
Tel. 977 920 218
Fax. 977 920 225

HAGO CONSTAR que este trabajo de investigación titulado “Gold-Catalyzed Cyclizations for the Synthesis of Small and Medium-Sized Arenes”, que presenta Claudia A. De León Solís para la obtención del título de doctor, ha sido realizado bajo mi dirección en el Institut Català d’Investigació Química vinculado a la Universidad Rovira I Virgili y que cumple los requisitos necesarios para poder optar a Mención Europea.

Tarragona, 15 de octubre de 2012

El director de la Tesis Doctoral

Prof. Antonio M. Echavarren

UNIVERSITAT ROVIRA I VIRGILI

GOLD-CATALYZED CYCLIZATIONS FOR THE SYNTHESIS OF SMALL AND MEDIUM-SIZED ARENES

Claudia Alejandra de León Solís

Dipòsit Legal: T. 196-2013

*To those who believed
and prayed for me.*

UNIVERSITAT ROVIRA I VIRGILI

GOLD-CATALYZED CYCLIZATIONS FOR THE SYNTHESIS OF SMALL AND MEDIUM-SIZED ARENES

Claudia Alejandra de León Solís

Dipòsit Legal: T. 196-2013

*First I shake the whole apple tree, that the ripest
might fall. Then I climb the tree and shake each
limb, and then each branch and then each twig,
and then I look under each leaf.*

Martin Luther

UNIVERSITAT ROVIRA I VIRGILI

GOLD-CATALYZED CYCLIZATIONS FOR THE SYNTHESIS OF SMALL AND MEDIUM-SIZED ARENES

Claudia Alejandra de León Solís

Dipòsit Legal: T. 196-2013

Este trabajo de tesis se realizó en el Institut Català d'Investigació Química bajo la dirección del Prof. Antonio M. Echavarren a quien quiero agradecer la confianza depositada en mí así como sus enseñanzas a lo largo de estos cuatro años.

Durante la realización de mi tesis doctoral he disfrutado de una beca del ICIQ de octubre de 2008 a marzo de 2009. A partir de abril del 2009 a diciembre de 2010, mi beca fue financiada por el Ministerio de Ciencia e Innovación, asociada al proyecto Explora y finalmente, a partir de enero del 2011, mi beca ha estado financiada por la Unión Europea, asociada al proyecto AtMol.

Asimismo, pude realizar una estancia de tres meses dentro del grupo del Prof. Matthew Gaunt a quien quiero agradecer el haberme abierto las puertas de su laboratorio y a su grupo en general, por el apoyo recibido durante el tiempo que estuve en Cambridge.

Quiero agradecer a todo el Echavarren Group el apoyo y la colaboración que he recibido durante estos cuatro años de tesis. En especial quiero agradecer a aquellos que han hecho de esta experiencia algo entrañable: Verónica López Carrillo y Patricia Pérez Galán quienes han sido mis mentores de las puertas del lab para adentro, siempre tendremos nuestros viajes express a la Habana con La Charanga; a Paula de Mendoza la herencia que me dejó, a Mibai Raducan de quien admiro su precisión de relojero suizo; a Rogelio Solorio de quien he aprendido que la perseverancia nos lleva lejos; a Núria Huguet, con quien inicié la aventura casi al mismo tiempo y casi al mismo tiempo retomaremos nuestra ruta; a Ana Escribano, Lorena Recio y Madeleine Livendahl, con quienes he podido compartir penas y alegrías a lo largo del camino; a María Moreno, quien me enseñó que el café de la máquina sabe mejor con buena compañía; y finalmente a Paul McGonigal y a Yabui Wang, sin quienes este trabajo no sería lo que es ni mi último año lo que fue (I owe you cherry cakes for life!), y a Antonio Echavarren, el nombre artístico que me acompañará de ahora en adelante: Claudia del Sol. Confío en que el lapsus haya sido el reflejo de la buena energía que siempre intenté transmitirle. Mención especial requieren Sónia Galaldà y Vanessa Martínez quienes han sido piedra angular del grupo. Nunca se han limitado a hacer su trabajo, sino que siempre han ido un paso más allá. Por todo ello, mil gracias. A todos por igual, les deseo éxitos en sus proyectos y ánimo, que soy prueba viviente de que la tesis, algún día se acaba.

A los que por los pasillos siempre han tenido palabras de ánimo para mí y me han ofrecido el hombro: Areli Flores, Isidoro López, Israel Macho, Judit Martínez, Kerman Gómez,

Mariona Urtasún, Noemí Cabello, Robert Haak y Sofía Arnal, muchísimas gracias. A veces, los pequeños gestos dejan una gran huella.

Me gustaría agradecer también el apoyo de mis profesores de Orléans. Gracias a ellos, me otorgaron la renovación de la beca para terminar el máster, y el resto fue posible.

No puedo dejar de agradecer el apoyo recibido de parte de mis padres, Pablo de León y Leslie Solís, quienes han sacrificado lo inimaginable para darnos a mi hermano y a mí lo mejor que nos podían dar: amor, unidad y una buena educación. A mi hermano José Ricardo de León, le agradezco el apoyo logístico que me brindó para mantenerme siempre cerca de mi gente.

A toda mi familia y amigos agradezco el apoyo, las oraciones y los consejos que nunca dejaron de fluir a pesar de la distancia.

A Juan, sin quien nunca me hubiera embarcado en esta aventura y quien cada mañana me exhortaba a “salvar el mundo de la química”, le agradezco el haber sido mi pilar, mi sostén y mi brújula a lo largo del camino.

Finalmente, doy gracias a Dios por ser el motor de mi vida y el artífice de una vivencia que ni en mis mejores sueños, pensé que tendría. Gracias por cerrar las puertas que se tenían que cerrar y por abrir aquellas que me han traído hasta aquí. Abba Padre.

Hasta el momento de redactar esta memoria, los resultados aquí descritos han dado lugar a la siguiente publicación:

“Gold for the Generation and Control of Fluxional Barbaralyl Cations”

Paul R. McGonigal, Claudia de León, Yahui Wang, Anna Homs, César R. Solorio-Alvarado, and Antonio M. Echavarren, *Angew. Chem. Int. Ed.* **2012**, DOI: 10.1002/anie.201207682.

UNIVERSITAT ROVIRA I VIRGILI

GOLD-CATALYZED CYCLIZATIONS FOR THE SYNTHESIS OF SMALL AND MEDIUM-SIZED ARENES

Claudia Alejandra de León Solís

Dipòsit Legal: T. 196-2013



UNIVERSITAT ROVIRA I VIRGILI

GOLD-CATALYZED CYCLIZATIONS FOR THE SYNTHESIS OF SMALL AND MEDIUM-SIZED ARENES

Claudia Alejandra de León Solís

Dipòsit Legal: T. 196-2013

Contents	Page
PRÓLOGO	17
RESUMEN	19
ABBREVIATIONS AND ACRONYMS	25
CHAPTER I: Generation and control of fluxional barbaralyl cations in gold-catalyzed cycloisomerization	27
1. Introduction	29
1.1 The relativistic affected gold-atom	29
1.2 Gold-promoted activation of alkynes	31
1.3 Frequently used Gold catalysts	33
<i>a) Gold Halides</i>	33
<i>b) Gold-phosphorous complexes</i>	33
<i>c) Gold (I)-NHC catalysts and related compounds</i>	35
<i>d) Gold (III) complexes</i>	36
1.4 Addition of carbon nucleophiles to alkynes	37
<i>a) Au (I)-catalyzed hydroarylation</i>	37
<i>b) Conia-ene type reactions</i>	39
1.5 Cycloisomerization of 1,6-enynes	40
<i>a) Single and double cleavage mechanisms</i>	41
<i>b) Trapping the carbene intermediate</i>	44
2. Objectives	47
3. Results and Discussion	49
3.1 Methodology	49
3.2 Intercepting barbaralyl intermediates with nucleophiles	55
3.3 The barbaralyl cation	58
3.4 Mass spectrometry experiments	60
3.5 Isotopic labeling studies	62
3.6 Mechanistic rationale	67
4. Conclusions	71

5. Experimental Section	73
6. Calculation Methods and Data	149
CHAPTER II: Towards well-defined nanographenes	161
1. Introduction	163
1.1 Fullerenes	165
1.2 Acenes	167
1.3 Crystallinity and transport of charge	171
1.4 Applications	173
1.5 Synthesis of polyaromatic hydrocarbons	177
2. Objectives	185
3. Results and Discussion	187
3.1 Synthesis of linear acenes	187
3.2 Synthesis of precursors of semi-buckminsterfullerenes (buckybowls)	195
4. Conclusions	209
5. Experimental Section	211

PRÓLOGO

Esta memoria de tesis Doctoral se ha dividido principalmente en un resumen en astellano y dos capítulos principales. Cada uno de estos últimos se compone por una introducción con sus correspondientes objetivos, resultados y discusión, conclusiones y parte experimental.

El trabajo aquí resumido incluye asimismo resultados obtenidos con la colaboración de César Rogelio Solorio Alvarado, Dr. Paul McGonigal y Yahui Wang, los cuales permiten una mejor comprensión de lo expuesto.

Todos los catalizadores utilizados han sido nombrados con letras, las cuales corresponden a las que aparecen en las figuras **3**, **4**, **5** y **7** del primer capítulo “Generation and control of fluxional barbaralyl cations in gold-catalyzed cycloisomerization”.

UNIVERSITAT ROVIRA I VIRGILI

GOLD-CATALYZED CYCLIZATIONS FOR THE SYNTHESIS OF SMALL AND MEDIUM-SIZED ARENES

Claudia Alejandra de León Solís

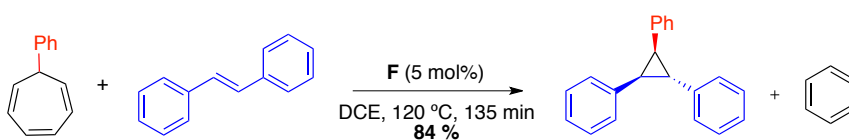
Dipòsit Legal: T. 196-2013

RESUMEN

La última década ha visto surgir al oro como uno de los catalizadores más interesantes. Su capacidad para coordinarse selectivamente a triples enlaces en presencia de otros sistemas insaturados ha provocado un auge importante en su utilización en diferentes transformaciones químicas. Esto, unido a las condiciones moderadas que se requieren con los catalizadores de oro y su bajo coste comparado a otros metales como el platino y el rodio, han colaborado para que las publicaciones relacionadas con este metal se dispararan exponencialmente.¹

A pesar de lo exhaustivo que parece ser la literatura relacionada con la química del oro, creemos que aun quedan muchos terrenos por explorar.

Estudios previos realizados en nuestro grupo con aril cicloheptatrienos mostraron que se podía generar un carbeno de oro libre, que podía ser atrapado posteriormente con un alqueno como el *trans*-estilbena. De esta forma se podía acceder a ciclopropanos triarilsustituídos con la pérdida de benceno.²

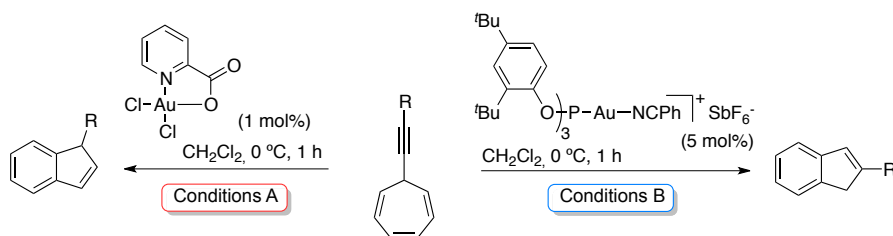


En este trabajo de tesis, nos hemos enfocado en la utilización de alquínil cicloheptatrienos como sustratos de la cicloisomerización catalizada por oro para extender los resultados obtenidos previamente.

¹ (a) A. S. K. Hashmi *Chem. Rev.* **2007**, *107*, 3180. (b) E. Jiménez-Núñez and A. M. Echavarren, *Chem. Rev.* **2008**, *108*, 3326. (c) A. Fürstner *Chem. Soc. Rev.* **2008**, *38*, 3208. (d) Gorin, D. J.; Sherry, B. D.; Toste, F. D. *Chem. Rev.* **2008**, *108*, 3351.

² Solorio-Alvarado, C. R.; Wang, Y.; Echavarren, A. M. J. *Am. Chem. Soc.* **2011**, *133*, 11952.

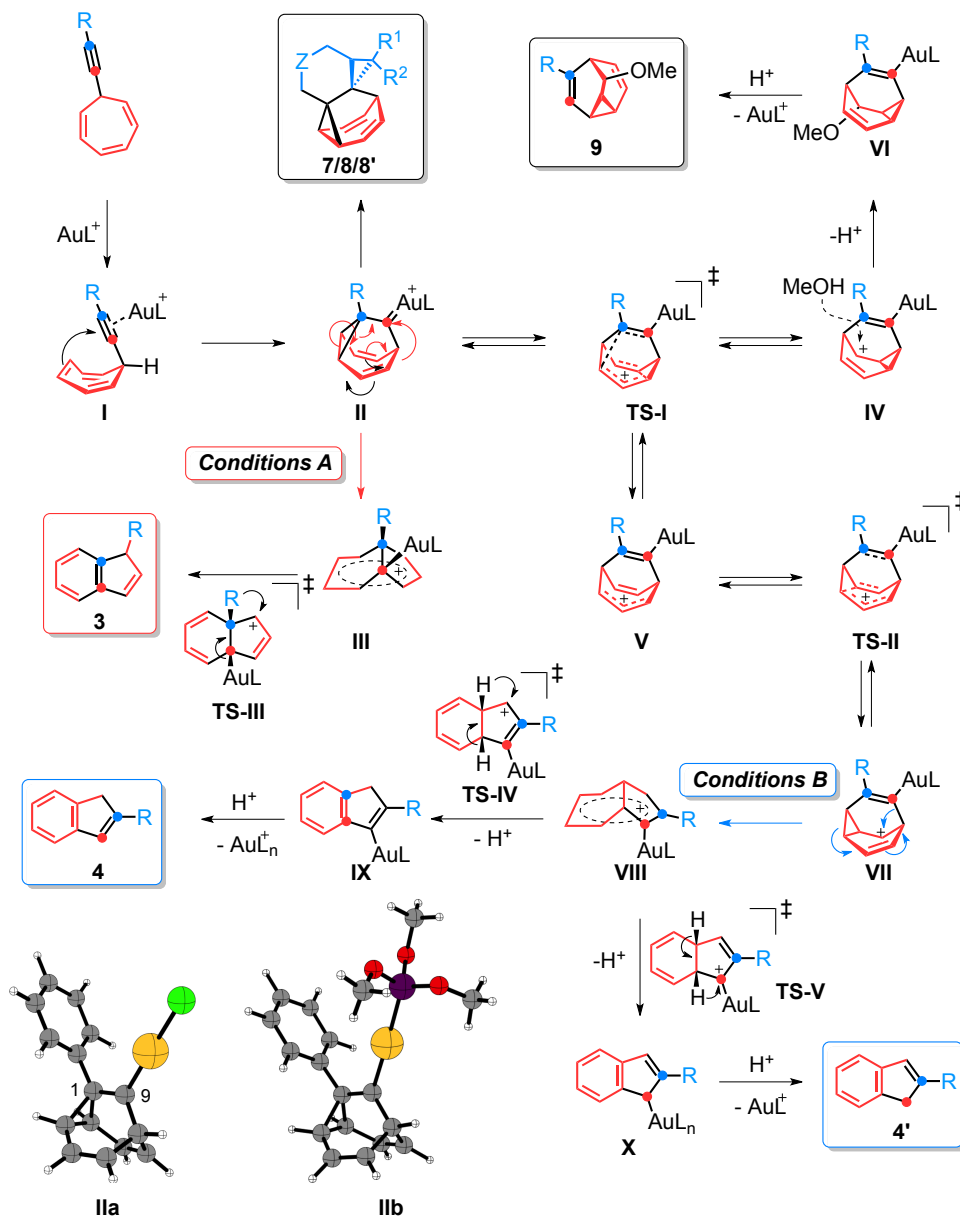
Tras la optimización de las condiciones, determinamos que se podían formar selectivamente indenos 1- y 2-arilsustituídos utilizando catalizadores de tipo picolinato y fosfito, respectivamente.



Esquema 2

A pesar de la sencillez de los productos, el mecanismo por el cual se accede a ellos no es simple. A través de marcajes isotópicos con ¹³C, experimentos de atrapamiento intra e intermolecular y cálculos teóricos, logramos determinar que la reacción se desarrolla a través de un intermedio catiónico de oro de tipo barbaralilo. El *Esquema 3* ilustra de forma condensada todos los pasos que nos llevan a obtener cada uno de los productos.

Esta metodología nos ha permitido determinar que la naturaleza del catalizador de oro puede afectar a la evolución de un intermediario catiónico, lo cual no tenía precedentes para los cationes barbaralilo. Además, hemos logrado sintetizar derivados del barbaralano en condiciones moderadas con la simple adición de nucleófilos externos o internos.



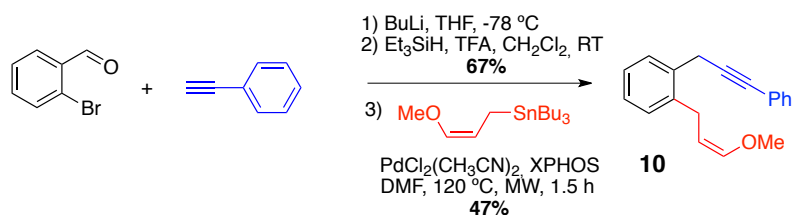
Esquema 3

Por otro lado, hemos intentado llevar a la química del oro a terrenos en los cuales su utilización aun no había sido explorada.

Desde el descubrimiento del fullereno C_{60} en 1985³ hasta la obtención de la primera molécula aislada de grafeno en 2004,⁴ el interés por la síntesis de hidrocarburos aromáticos policíclicos ha aumentado exponencialmente.

Muchos de los procesos que permiten obtener esta clase de moléculas requiere condiciones extremas de temperatura y/o presión.⁵ Basándonos en esto, nos propusimos emplear las ciclaciones catalizadas por oro para la síntesis de acenos lineares que permitirían posteriormente abrir la puerta la síntesis de nanografenos más complejos.

Partiendo de moléculas sencillas, ideamos una metodología que permitiera su ensamblaje para formar 1-6-eninos.



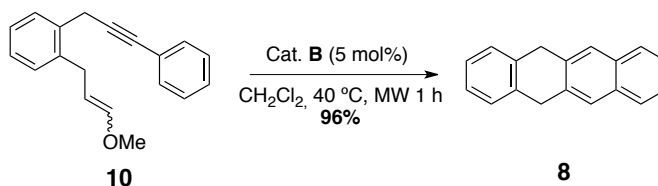
Esquema 4

El enino formado solamente pudo obtenerse con rendimientos moderados, debido a su poca estabilidad. Aun así, se llevó a cabo la reacción de ciclación catalizada por oro, la cual permitió la obtención de tetrahidrotetraceno con rendimientos excelentes.

³ Kroto, H. W.; Heath, J. R.; O'Brien, S. C.; Curl, R. F.; Smalley, R. E. *Nature* **1985**, *318*, 162.

⁴ Novoselov, K. S.; Geim, A. K.; Morozov, S. V.; Jiang, D.; Zhang, Y.; Dubonos, S. V.; Grigorieva, I. V.; Firsov, A. A. *Science* **2004**, *306*, 666.

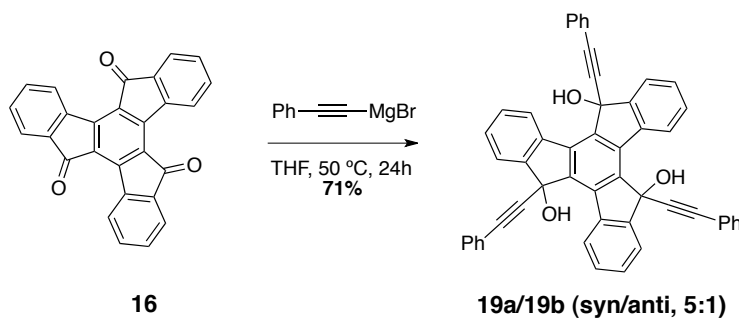
⁵ Feng, X.; Pisula, W.; Müllen, K. *Pure Appl. Chem.* **2009**, *81*, 2203.



Esquema 5

Desafortunadamente, el acoplamiento de Stille con alquinos más voluminosos no fue posible lo cual no permitió extender este procedimiento a la síntesis de acenos mayores.

Paralelamente, se intentó la síntesis de semifulerenos, partiendo de derivados de la truxentriona. La adición 1,2 de los reactivos de Grignard a la truxentriona, permitió obtener selectivamente el compuesto *syn*.



Esquema 6

La ciclación catalizada por oro y por otros ácidos de Lewis sólo permitió obtener un sólido negro, cuya masa correspondía la producto de partida y que resultó imposible identificar. Por otro lado, la ciclación promovida por ICl permitió la formación de una hélice cuya estructura pudo ser determinada por difracción de rayos X.

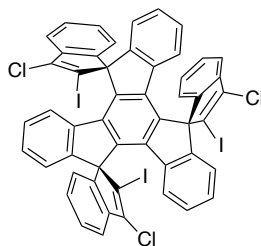


Figura 1

UNIVERSITAT ROVIRA I VIRGILI

GOLD-CATALYZED CYCLIZATIONS FOR THE SYNTHESIS OF SMALL AND MEDIUM-SIZED ARENES

Claudia Alejandra de León Solís

Dipòsit Legal: T. 196-2013

ABBREVIATIONS AND ACRONYMS

In this manuscript, abbreviations and acronyms have been used, according to the “Guidelines for authors” of the Journal of Organic Chemistry, which has been updated in January 2012.

Additional abbreviations and acronyms used in this manuscript are referenced in the list below.

HLG	HOMO-LUMO gap
PAH	Polyaromatic hydrocarbons
QTOF	Quadrupole Time of Flight
STM	Scanning Tunneling Microscope
TFP	Tri-(2-furyl)phosphine
TTFB	Tropyllium tetrafluoroborate

UNIVERSITAT ROVIRA I VIRGILI

GOLD-CATALYZED CYCLIZATIONS FOR THE SYNTHESIS OF SMALL AND MEDIUM-SIZED ARENES

Claudia Alejandra de León Solís

Dipòsit Legal: T. 196-2013

Chapter I

Generation and control of fluxional barbaralyl cations in gold-catalyzed cycloisomerization

UNIVERSITAT ROVIRA I VIRGILI

GOLD-CATALYZED CYCLIZATIONS FOR THE SYNTHESIS OF SMALL AND MEDIUM-SIZED ARENES

Claudia Alejandra de León Solís

Dipòsit Legal: T. 196-2013

Chapter I:

Generation and control of fluxional barbaralyl cations in gold-catalyzed cycloisomerization

1. Introduction

Gold emerged as a late bloomer in catalysis among other metals. For centuries, it was considered inert and only few derivatives were known, which made its applications in chemistry really scarce.¹ It was only in 1973 when Bond and co-workers² discovered that supported gold could catalyze the hydrogenation of mono-olefins. More than a decade later, the first examples using gold in homogeneous catalysis were published.³

1.1 The relativistic affected gold atom

The chemistry of gold can only be understood taking into consideration relativistic effects. Being a heavy metal, the electrons of gold are subjected to high electrostatic attraction. To keep them from crashing into the nucleus, their velocity is increased and approaches the speed of light. In consequence, the mass of the electrons increases and the Bohr radius is reduced proportionately, which translates into the contraction of the orbitals, especially those that are close to the nucleus like $1s$ electrons (*Figure 1*).

¹ Schmidbaur, H. *Gold Bull.* **1990**, *23*, 11.

² Bond, G. C.; Sermon, P. A.; Webb, G.; Buchanan, D. A.; Wells, P. B., *J. Chem. Soc., Chem. Commun.* **1973**, 444b.

³ a) Ito, Y.; Sawamura, M.; Hayashi, T. *J. Am. Chem. Soc.* **1986**, *108*, 6405. b) Fukuda, Y.; Utimoto, K.; Nozaki, H. *Heterocycles* **1987**, *25*, 297. c) Fukuda, Y.; Utimoto, K. *J. Org. Chem.* **1991**, *56*, 3729.

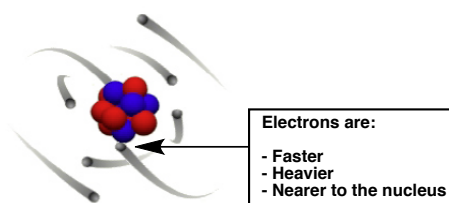


Figure 1: Relativistic effects on the electrons of the gold atom

However, s orbitals in the outer shells are also affected while p , d and f orbitals are affected in a lesser extent. On the other hand, the contraction of the s orbitals reduces the effective nuclear charge, and orbitals with higher angular momentum, like d and f orbitals, expand. Finally, there is a spin-orbit interaction, which accounts for the splitting of spectral lines.^{1,4,5,6,7,8} The contraction of the $6s$ orbital in the gold atom results in increased ionization potential, higher electron affinity, and strong gold-ligand (Au-L) bonds.^{1,7,8}

The most common oxidation states of gold are Au(I) and Au(III), the latter forming square planar complexes. The former tends to form linear two-coordinate complexes through particularly efficient s/p or s/d hybridization since due to the relativistic effects, s , p and d orbitals are brought much closer together in energy.¹

Relativistic effects also account for the high electronegativity of gold and superior Lewis acidity of Au(I) species since the contraction of the s and p orbitals corresponds to a low-lying LUMO.⁸

⁴ Pykko, P. *Chem. Rev.* **1988**, *88*, 563.

⁵ Schwerdtfeger, P.; Dolg, M.; Schwarz, W. H. E.; Bowmaker, G. A.; Boyd, P. D. W. *J. Chem. Phys.* **1989**, *91*, 1762.

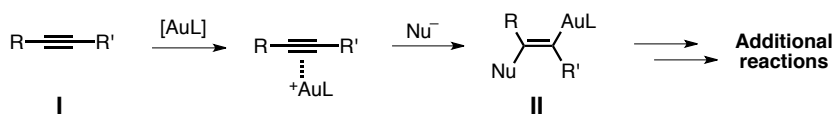
⁶ Bond, G. C.; Thompson, D. T. *Catal. Rev.* **1999**, *41*, 319.

⁷ Schwerdtfeger, P. *Heteroatom Chem.* **2002**, *13*, 578.

⁸ Gorin, D. J.; Toste, F. D. *Nature* **2007**, *446*, 395.

1.2 Gold-promoted activation of alkynes

The alkynophilicity of gold was the spark that started the gold rush in organic synthesis. Not only alkynes become highly reactive under the reaction conditions but also these transformations proceed with high selectivity.⁹ Indeed, alkynes are not prone to nucleophilic attack without some prior activation. Their lower HOMO and LUMO makes them more electrophilic and less nucleophilic than alkenes.^{8,10} The electrophilic gold complex usually coordinates to the triple bond withdrawing electron density from the alkyne: the metal fragment is considered a π -acid. As a consequence, the triple bond elongates and bends while the Au-C bond remains quite short (2.05-2.10 Å).^{10,11} Then the nucleophilic attack proceeds by forming a *trans*-alkenyl gold complex **I**, which in the presence of different electrophiles yields the corresponding products (*Scheme 1*).^{12,13}



Scheme 1

For terminal alkynes, another type of activation is possible: the substitution of the terminal hydrogen by gold to form a Au(I)-acetylide.^{10,14} These are stable species and until recently, were believed to be synthetically not useful. Li and Wei proposed the synthesis of propargylamines via a gold-acetylide

⁹ Cinellu, M. A. In *Modern Gold Catalyzed Synthesis*; Hashmi, S. K., Toste, F. D., Eds.; Wiley-VCH Verlag GmbH & Co. KGaA: 2012, p 153.

¹⁰ Hashmi, A. *Gold Bull.* **2003**, *36*, 3.

¹¹ Fürstner, A.; Davies, P. W. *Angew. Chem. Int. Ed.* **2007**, *46*, 3410.

¹² Hashmi, A. S. K. *Chem. Rev.* **2007**, *107*, 3180.

¹³ Jiménez-Núñez, E.; Echavarren, A. M. *Chem. Rev.* **2008**, *108*, 3326.

¹⁴ Li, Z.; Brouwer, C.; He, C. *Chem. Rev.* **2008**, *108*, 3239.

intermediate¹⁵ while Bertrand and co-workers reported an analogous intermediate in the cross-coupling reaction of enamines with terminal alkynes.¹⁶ Even though, a dual activation (*Figure 2*) had already been reported for some structures,¹⁷ it was not until recently that σ,π -activation was attributed to a gold catalyst.¹⁸

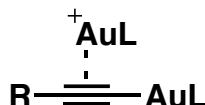


Figure 2: Dual σ,π -activation of terminal alkynes

The most common evolution of the *trans*-alkenyl gold intermediate **II** illustrated in *Scheme 1* is protodeauration promoted by the proton of the nucleophile to yield alkenes **III** (*Scheme 2*, path **a**). Aprotic nucleophiles such as alkenes could break down the vinyl-gold intermediate.⁸ For example, gold-catalyzed ring expansions¹⁹ and heterocyclizations^{3b} proceed through this path. Gold acts in this way as a Lewis acid. However, an alternative pathway is also possible: the trapping of the electrophile could be facilitated by backbonding from the relativistically expanded *5d* orbitals of the gold atom into the developing conjugated cation **IV** (*Scheme 2*, path **b**).⁸ Cycloisomerizations

¹⁵ Wei, C.; Li, C.-J. *J. Am. Chem. Soc.* **2003**, *125*, 9584.

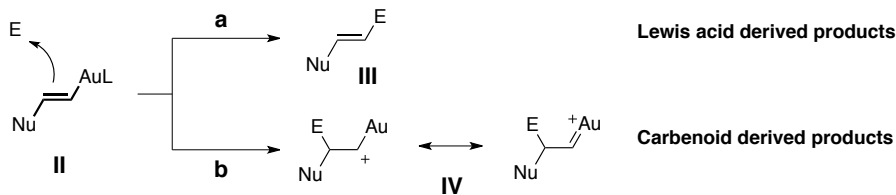
¹⁶ Lavallo, V.; Frey, G. D.; Kousar, S.; Donnadiou, B.; Bertrand, G. *Proc. Natl. Acad. Sci. U.S.A.* **2007**, *104*, 13569.

¹⁷ a) Coates, G. E.; Parkin, C. J. *Chem. Soc.* **1962**, 3220. b) Mingos, D. M. P.; Yau, J.; Menzer, S.; Williams, D. J. *Angew. Chem. Int. Ed.* **1995**, *34*, 1894.

¹⁸ a) Cheong, P. H.-Y.; Morganeli, P.; Luzung, M. R.; Houk, K. N.; Toste, F. D. *J. Am. Chem. Soc.* **2008**, *130*, 4517. b) Gaillard, S.; Bosson, J.; Ramón, R. S.; Nun, P.; Slawin, A. M. Z.; Nolan, S. P. *Chem. Eur. J.* **2010**, *16*, 13729. c) Brown, T. J.; Widenhoefer, R. A. *Organometallics* **2011**, *30*, 6003. d) Gorrane, A.; Garcia, H.; Corma, A.; Álvarez, E. *ACS Catal.* **2011**, *1*, 1647. e) Simonneau, A.; Jaroschik, F.; Lesage, D.; Karanik, M.; Guillot, R.; Malacria, M.; Tabet, J.-C.; Goddard, J.-P.; Fensterbank, L.; Gandon, V.; Gimbert, Y. *Chem. Sci.* **2011**, *2*, 2417.

¹⁹ Markham, J. P.; Staben, S. T.; Toste, F. D. *J. Am. Chem. Soc.* **2005**, *127*, 9708.

catalyzed by Au(I) were the first transformations that supported this mechanistic proposal.^{20,21,22}



Scheme 2

1.3 Frequently used Gold catalysts

a) Gold halides

The first contributions to homogeneous gold catalysis described the addition of many nucleophiles to alkynes catalyzed by gold halides⁸ and are still to date used in many synthetic transformations. In fact AuCl and NaAuCl₄ are the cheapest sources of Au(I) and Au(III) respectively. Unfortunately, they are also less stable: Au(III) might be reduced by easily oxidizable substrates and Au(I) disproportionates to Au(0) and Au(III).¹³

b) Gold(I)-phosphorous complexes

Phosphines are known to stabilize Au(I) cations due to their electrodonating character. Teles was the first to report the catalytic activity of cationic phosphine Au(I) for the hydration of alkynes using methyl(triphenylphosphane)gold(I) activated with a strong acid.²³ This opened the doors to further catalyst development and inspired by palladium-catalyzed

²⁰ (a) Nieto-Oberhuber, C.; Muñoz, M. P.; Buñuel, E.; Nevado, C.; Cárdenas, D. J.; Echavarren, A. M. *Angew. Chem. Int. Ed.* **2004**, *43*, 2402. (b) Nieto-Oberhuber, C.; Muñoz, M. P.; López, S.; Jiménez-Núñez, E.; Nevado, C.; Herrero-Gómez, E.; Raducan, M.; Echavarren, A. M. *Chem. Eur. J.* **2006**, *12*, 1677.

²¹ Mamane, V.; Gress, T.; Krause, H.; Fürstner, A. *J. Am. Chem. Soc.* **2004**, *126*, 8654.

²² Luzung, M. R.; Markham, J. P.; Toste, F. D. *J. Am. Chem. Soc.* **2004**, *126*, 10858.

²³ Teles, J. H.; Brode, S.; Chabanas, M. *Angew. Chem. Int. Ed.* **1998**, *37*, 1415.

reactions,²⁴ biphenyl phosphines proved to be suitable ligands (neutral catalysts **A-D**, *Figure 3*).

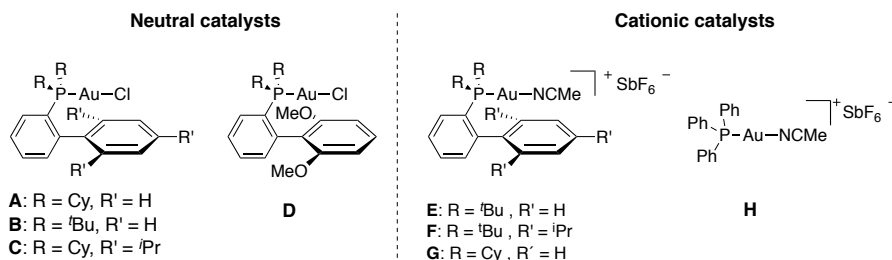


Figure 3: Phosphine-based gold catalysts

The abstraction of the chloride ligand can be performed in situ by addition of an equivalent of a silver salt with a non-coordinating anion or by addition of $\text{BF}_3 \cdot \text{Et}_2\text{O}$.^{20,25,26}

Phosphite gold complexes were early regarded as more active than phosphine gold complexes but they were also less stable.²³ *Figure 4* shows two of the most electrophilic gold(I) complexes bearing phosphite ligands.

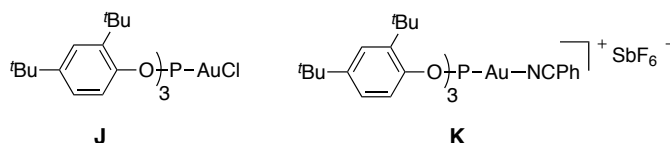


Figure 4: Phosphite gold-catalysts

²⁴ (a) Kaye, S.; Fox, J. M.; Hicks, F. A.; Buchwald, S. L. *Adv. Synth. Catal.* **2001**, *343*, 789. (b) Walker, S. D.; Barder, T. E.; Martinelli, J. R.; Buchwald, S. L. *Angew. Chem. Int. Ed.* **2004**, *43*, 1871. (c) Strieter, E. R.; Blackmond, D. G.; Buchwald, S. L. *J. Am. Chem. Soc.* **2003**, *125*, 13978. (d) Barder, T. E.; Walker, S. D.; Martinelli, J. R.; Buchwald, S. L. *J. Am. Chem. Soc.* **2005**, *127*, 4685. (e) Barder, T. E.; Buchwald, S. L. *J. Am. Chem. Soc.* **2007**, *129*, 5096.

²⁵ Marion, N.; Nolan, S. P. *Chem. Soc. Rev.* **2008**, *37*, 1776.

²⁶ Ferrer, C.; Raducan, M.; Nevado, C.; Claverie, C. K.; Echavarren, A. M. *Tetrahedron* **2007**, *63*, 6306.

c) Gold (I)-NHC catalysts and related compounds

Since the active species in gold catalysis is the monoligated cationic gold complex, it is important that the ancillary ligand manages to stabilize the charge both electronically and sterically. N-heterocyclic carbenes are excellent σ -donors and the corresponding catalysts have proven to be efficient in many chemical transformations.^{25,27}

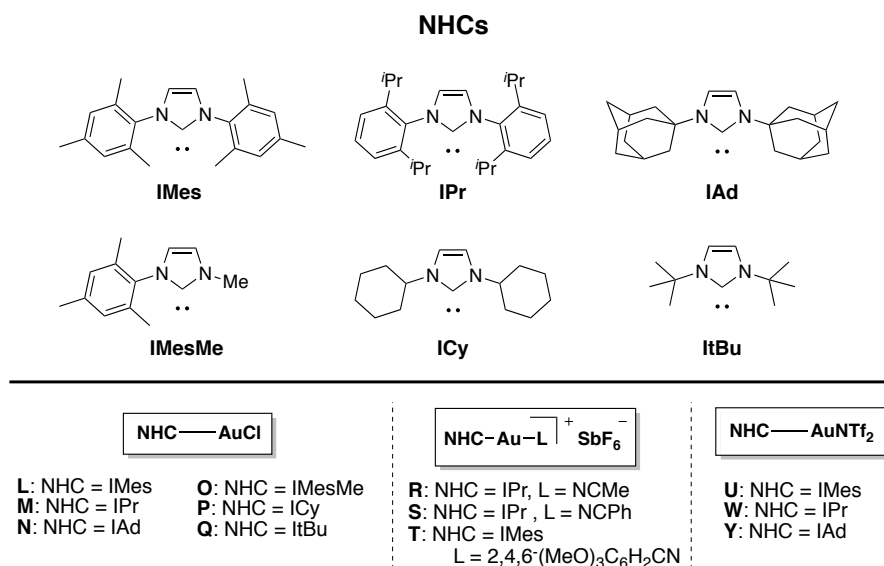


Figure 5: Some N-heterocyclic carbene-gold catalysts

Catalysts **R–Y** are catalytically active without the addition of silver salts.²⁷

²⁷ (a) de Frémont, P.; Scott, N. M.; Stevens, E. D.; Nolan, S. P. *Organometallics* **2005**, *24*, 2411. (b) de Fremont, P.; Stevens, E. D.; Fructos, M. R.; Mar Diaz-Requejo, M.; Perez, P. J.; Nolan, S. P. *Chem. Comm.* **2006**, 2045. (c) López, S.; Herrero-Gómez, E.; Pérez-Galán, P.; Nieto-Oberhuber, C.; Echavarren, A. M. *Angew. Chem. Int. Ed.* **2006**, *45*, 6029. (d) Kim, S. M.; Park, J. H.; Choi, S. Y.; Chung, Y. K. *Angew. Chem. Int. Ed.* **2007**, *46*, 6172. (e) Ricard, L.; Gagosz, F. *Organometallics* **2007**, *26*, 4704. (e) Witham, C. A.; Mauleón, P.; Shapiro, N. D.; Sherry, B. D.; Toste, F. D. *J. Am. Chem. Soc.* **2007**, *129*, 5838.

Other carbenes have also proved to be stabilizing ligands. Thus for example complex **Z** catalyzed the formation of allenes from enamines and terminal alkynes (*Figure 6*).²⁸

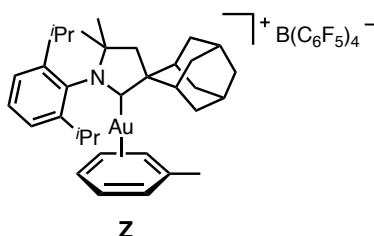


Figure 6 : Gold-carbene catalyst developed by Bertrand et al.

d) Gold (III) complexes

Contrary to Au(I)-complexes, Au(III)-organic compounds are more reactive and need to be stabilized by electronegative ligands such as halides.⁵

Hashmi reported the synthesis of stable complexes using pyridine derivatives as ligands (**AA-DD**, *Figure 7*), which were useful for the synthesis of tetrahydroisoquinolines.²⁹ The group of Nolan prepared Au(III)-NHC complexes and tested them in the addition of water to alkynes.

The group of Laguna found that complex **KK** and **LL** were good catalysts for some nucleophilic additions to triple bonds.³⁰

Finally a porphyrin-gold complex **MM** was reported to catalyze the reaction of allenones to give furan derivatives.³¹

²⁸ Lavallo, V.; Frey, G. D.; Kousar, S.; Donnadicu, B.; Bertrand, G. *Proc. Natl. Acad. Sci. U.S.A.* **2007**, *104*, 13569.

²⁹ Hashmi, A. S. K.; Weyrauch, J. P.; Rudolph, M.; Kurpejović, E. *Angew. Chem. Int. Ed.* **2004**, *43*, 6545.

³⁰ Casado, R.; Contel, M. A.; Laguna, M.; Romero, P.; Sanz, S. J. *Am. Chem. Soc.* **2003**, *125*, 11925.

³¹ Zhou, C.-Y.; Chan, P. W. H.; Che, C.-M. *Org. Lett.* **2005**, *8*, 325.

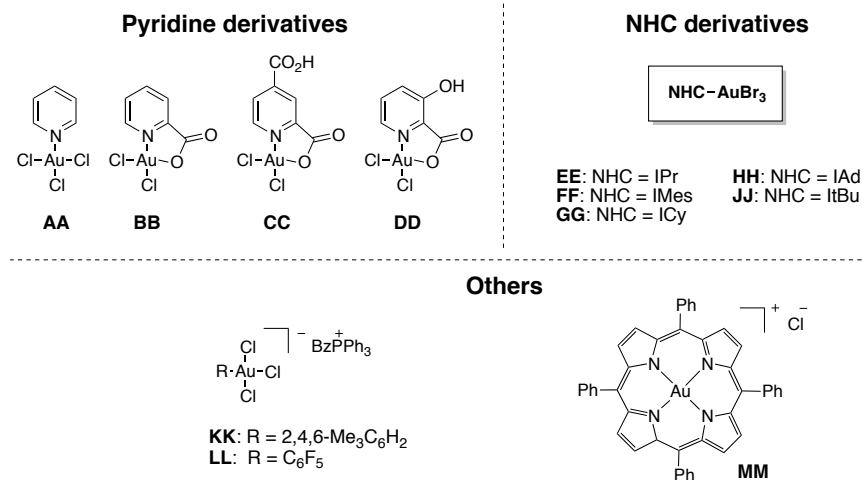


Figure 7: Au(III) catalysts

Due to its preference to form square planar complexes, Au(III) could be the template of choice for the design of chiral catalysts.³²

1.4 Addition of carbon nucleophiles to alkynes

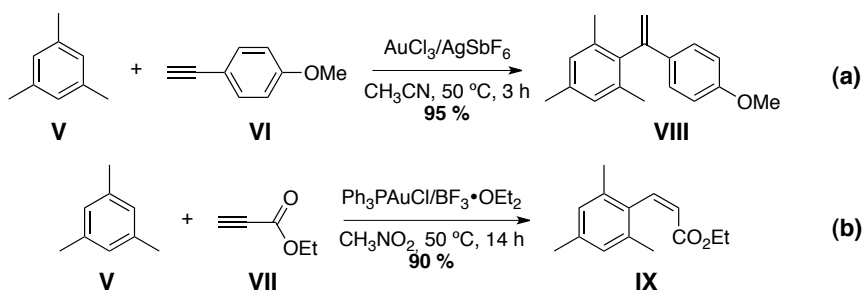
a) Au (I)-catalyzed hydroarylation

Electron-rich arenes and heteroarenes undergo an electrophilic aromatic substitution in a Friedel-Crafts process when submitted to a gold-catalyzed reaction with alkynes. Examples were reported by Reetz and Sommer in 2003 and 1,1-disubstituted olefins (*Scheme 3*, equation **a**) were obtained.³³ Complementary results were found using alkynes with electron-withdrawing groups (*Scheme 3*, equation **b**).³⁴

³² Sengupta, S.; Shi, X. *ChemCatChem* **2010**, *2*, 609.

³³ de Mendoza, P.; Echavarren, A. M. *Pure Appl. Chem.* **2010**, *82*, 801.

³⁴ Reetz, Manfred T.; Sommer, K. *Eur. J. Org. Chem.* **2003**, 3485.



Scheme 3

Hashmi reported the dual addition of unactivated alkynes to 2-methyl and 2-pentylfuran with the Schmidbaur-Bayler salt³⁵ something that He et al. had already detected while studying the reaction of heterocycles with electrodeficient alkynes.³⁶

Different heterocyclic moieties were accessed by gold-catalyzed intramolecular hydroarylation of alkynes. In 2000, Hashmi and co-workers described the cyclization of alkynylfurans to phenols catalyzed by AuCl_3 .³⁷ Our group developed the synthesis of *N*-tosyl-1,2-dihydroquinolines by cyclization of *N*-propargyl-*N*-tosylanilines.³⁸ More interesting was the intramolecular reaction of indoles with tethered alkynes, which afforded 7- or 8-membered rings depending on the oxidation state of the catalyst (+1 and +3, respectively, *Scheme 4*, equation a).³⁹ The 8-*endo-dig* process that yielded compounds **XII** had not been observed before in this context. Another example of the dichotomy of the catalytic behavior of Au(I) and Au(III) is illustrated in

³⁵ Hashmi, A. S. K.; Blanco, M. C. *Eur. J. Org. Chem.* **2006**, 4340.

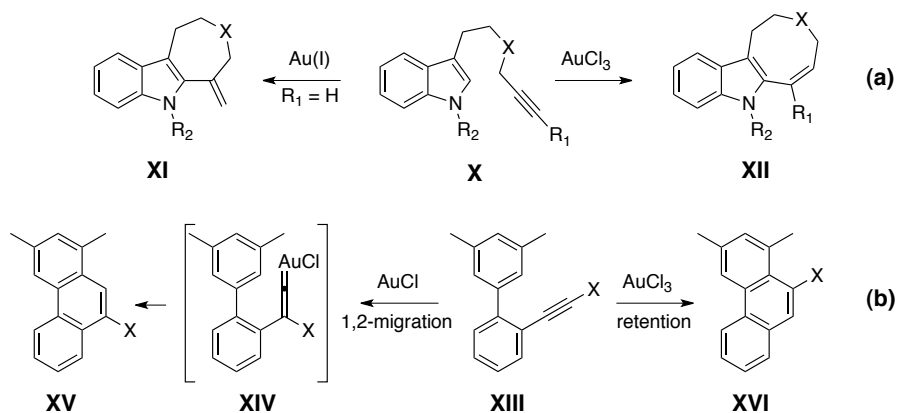
³⁶ Li, Z.; Shi, Z.; He, C. *J. Organomet. Chem.* **2005**, 690, 5049.

³⁷ Hashmi, A. S. K.; Frost, T. M.; Bats, J. W. *J. Am. Chem. Soc.* **2000**, 122, 11553.

³⁸ (a) Martín-Matute, B.; Nevado, C.; Cárdenas, D. J.; Echavarren, A. M. *J. Am. Chem. Soc.* **2003**, 125, 5757. (b) Nevado, C.; Echavarren, A. M. *Chem. Eur. J.* **2005**, 11, 3155.

³⁹ (a) Ferrer, C.; Echavarren, A. M. *Angew. Chem. Int. Ed.* **2006**, 45, 1105. (b) Ferrer, C.; Amijs, C. H. M.; Echavarren, A. M. *Chem. Eur. J.* **2007**, 13, 1358.

Scheme 4, equation **b**.⁴⁰ It has been reasoned that the Au(III) intermediate undergoes a Friedel-Crafts-type arylation due to the lesser ability of this metal cation to back-donate. On the other hand, the more electron-rich Au(I) was proposed to form a vinylidene intermediate, which via 1,2-migration affords the other regioisomer **XV**.



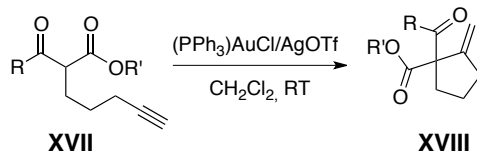
b) Conia-ene type reactions

Few examples of 1,3-dicarbonyl additions to triple bonds catalyzed by gold are found in the literature. Toste was the first one to describe the reaction of β -ketoesters with tethered alkynes.⁴¹ Vinylated ketones were produced in a 5-*exo-dig* pathway in excellent yields (*Scheme 5*). Labelling experiments supported their mechanistic proposal that involved the nucleophilic attack of the dicarbonyl to the Au(I)-alkyne complex. Further experiments showed that bringing the triple bond one carbon closer to the dicarbonyl yielded the 5-*endo-dig* product exclusively.⁴²

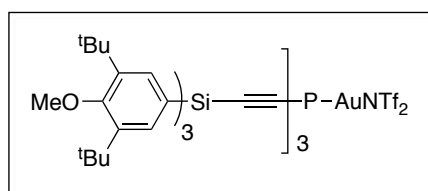
⁴⁰ (a) Mamane, V.; Hannen, P.; Fürstner, A. *Chem. Eur. J.* **2004**, *10*, 4556. (b) Theoretical support for the involvement of Au(I)-vinylidenes in this cyclization: Soriano, E.; Marco-Contelles, J. *Organometallics* **2006**, *25*, 4542.

⁴¹ Kennedy-Smith, J. J.; Staben, S. T.; Toste, F. D. *J. Am. Chem. Soc.* **2004**, *126*, 4526.

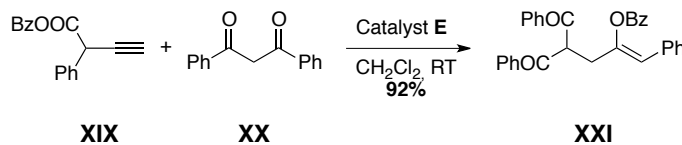
⁴² Staben, S. T.; Kennedy-Smith, J. J.; Toste, F. D. *Angew. Chem. Int. Ed.* **2004**, *43*, 5350.

*Scheme 5*

The design and synthesis of a new catalyst (*Figure 8*) allowed Sawamura and co-workers to access the 6-endo-dig product that was elusive using the conditions developed by Toste.⁴³

*Figure 8: The tris[(triarylsilyl)ethynyl]phosphinegold catalyst developed by Sawamura et al.*

Finally, our group also reported the formation of enol carboxylates by 1,2-acyl migration with high yields and chemoselectivity (*Scheme 6*).⁴⁴

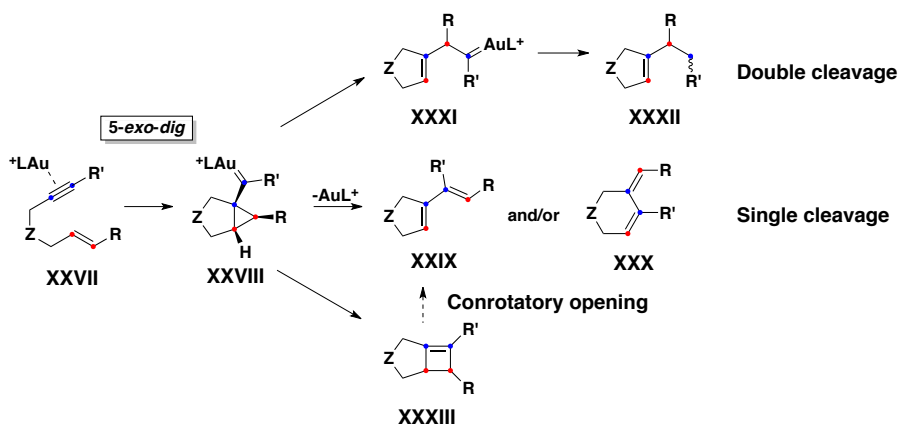
*Scheme 6*

1.5 Cycloisomerization of 1,6-enynes

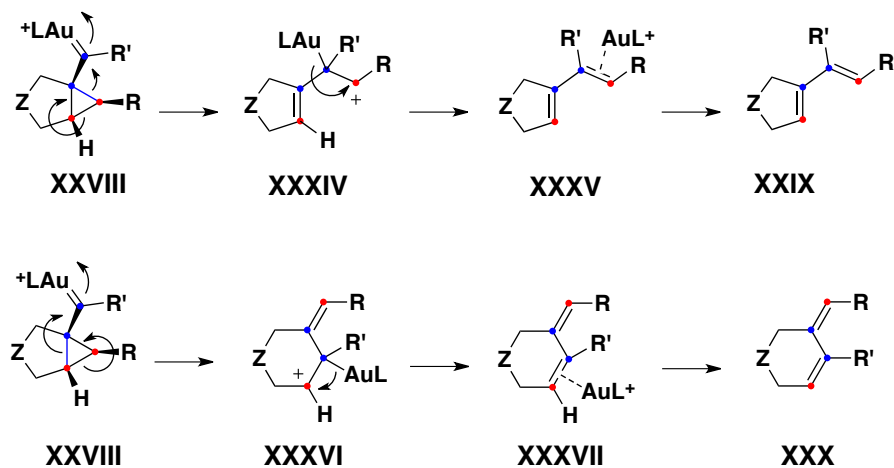
The cycloisomerization of 1,6-enynes is probably one of the most popular reactions in gold-catalysis, especially since many elegant transformations have

⁴³ Ochida, A.; Ito, H.; Sawamura, M. *J. Am. Chem. Soc.* **2006**, *128*, 16486.

⁴⁴ Amijs, C. H. M.; López-Carrillo, V.; Echavarren, A. M. *Org. Lett.* **2007**, *9*, 4021.

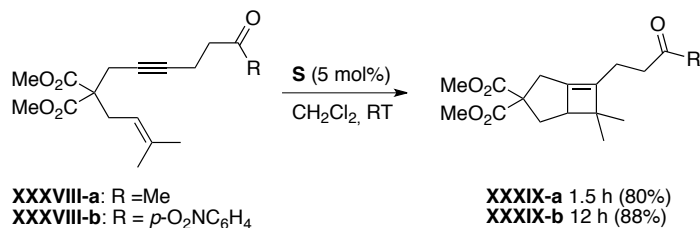


In the single cleavage mechanism, the initial *anti*-cyclopropyl gold carbene **XXVIII** gives carbocations **XXXIV** or **XXXVI**, which evolves by metal elimination to give dienes **XXIX** or **XXX** (*Scheme 8*).



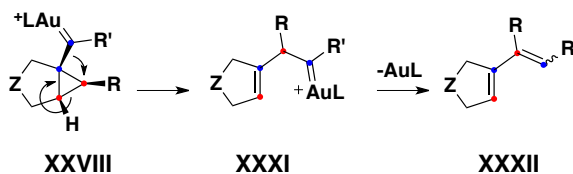
Even if earlier experimental and theoretical calculations considered unlikely the formation of the single cleavage product by conrotatory opening of

cyclobutenes **XXXIII** (*Scheme 7*),⁴⁶ newly evidence has arisen that supports this pathway. Indeed, cycloisomerization of 1,6-enynes **XXXVIII-a** and **XXXVIII-b** with gold catalyst **S** afforded the elusive bicyclo[3.2.0]hept-5enes **XXXIX-a** and **XXXIX-b** in good yields (*Scheme 9*). The structure of **XXXIX-b** was unequivocally assigned by X-ray diffraction of its crystalline 2,4-dinitrophenylhydrazone derivative.⁴⁷



Scheme 9

Intermediate **XXVIII** can also undergo a diotropic rearrangement to form carbene **XXXI**, followed by protodemetalation yielding dienes **XXXII** (*Scheme 10*). This corresponds to a double cleavage rearrangement. It is also possible to access **XXXI** through a 1,2-shift of the cyclic alkenyl group in **XXXV** (*Scheme 8*).¹³



Scheme 10

⁴⁶ Nieto-Oberhuber, C.; López, S.; Muñoz, M. P.; Cárdenas, D. J.; Buñuel, E.; Nevado, C.; Echavarren, A. M. *Angew. Chem. Int. Ed.* **2005**, *44*, 6146.

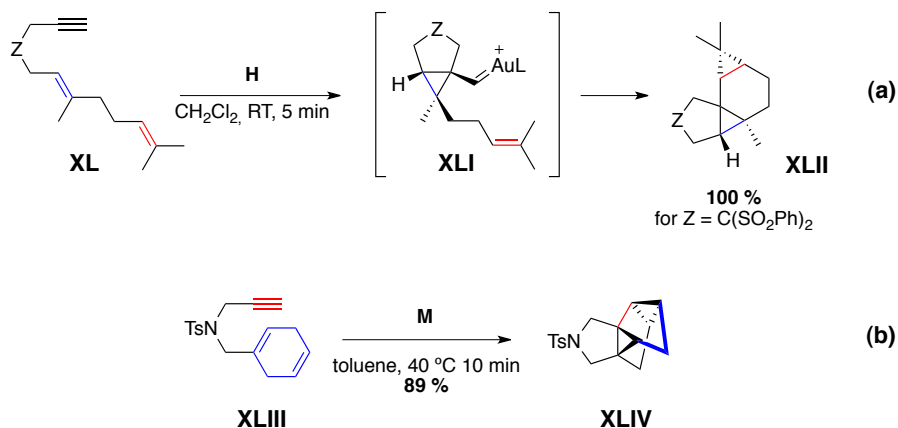
⁴⁷ Escribano-Cuesta, A.; Pérez-Galán, P.; Herrero-Gómez, E.; Sekine, M.; Braga, A. A. C.; Maseras, F.; Echavarren, A. M. *Org. Biomol. Chem.* **2012**, *10*, 6105.

1,6-Enynes with electron-donating substituents in the alkyne undergo single cleavage and those with electron-withdrawing substituents, yield selectively products of double cleavage.⁴⁷

b) Trapping the carbene intermediates

The structure of the cyclopropyl gold carbene intermediate **XXVIII** was the subject of certain debate. Theoretical studies showed that the C-C bond between the carbene and the cyclopropyl group had a substantial double bond character. It was concluded that the structure is highly distorted and is an intermediate between a gold-stabilized homoallylic carbocation and the cyclopropyl gold carbene. For comprehensive purposes, the latter is usually depicted in the mechanisms⁴⁸

1,6-Enynes with pendant alkenes allowed the trapping of the proposed cyclopropyl gold carbene. The cycloisomerization of dienynes provided tetracyclic compounds stereoselectively (*Scheme 11*).^{49,50}



Scheme 11

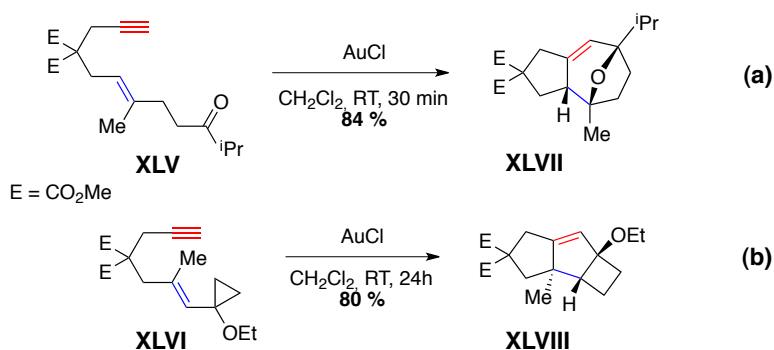
⁴⁸ Cabello, N.; Jiménez-Núñez, E.; Buñuel, E.; Cárdenas, D. J.; Echavarren, A. M. *Eur. J. Org. Chem.* **2007**, 4217.

⁴⁹ Nieto-Oberhuber, C.; López, S.; Muñoz, M. P.; Jiménez-Núñez, E.; Buñuel, E.; Cárdenas, D. J.; Echavarren, A. M. *Chem. Eur. J.* **2006**, *12*, 1694.

⁵⁰ Kim, S. M.; Park, J. H.; Choi, S. Y.; Chung, Y. K. *Angew. Chem. Int. Ed.* **2007**, *46*, 6172.

The intermolecular version of this reaction was also achieved with the IMes gold catalyst **L** or AuCl using.^{27c}

Substitution of the tethered alkene by a carbonyl group provided tricyclic products with a bridged oxygen in a Prins-type reaction (*Scheme 12*, equation **a**). Introducing a cyclopropan-2-ol instead, afforded an octahydrocyclobuta[α]pentalene framework (*Scheme 12*, equation **b**).⁵¹



Scheme 12

The intermolecular trapping of the gold carbene with ketones and aldehydes was carried out by Helmchen and co-workers⁵² and by our group,⁴⁷ leading to different products depending on the substitution at the alkene.

Other such as indoles^{53,54} and diphenylsulfoxide⁵⁵ have been used to trap the gold carbene.

Recently, our group reported the generation of a free gold carbene via a retro-

⁵¹ Jiménez-Núñez, E.; Claverie, C. K.; Nieto-Oberhuber, C.; Echavarren, A. M. *Angew. Chem. Int. Ed.* **2006**, *45*, 5452.

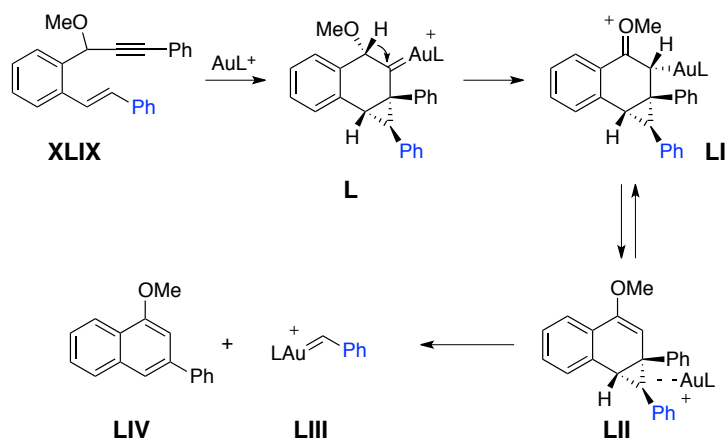
⁵² Schelwies, M.; Dempwolff, A. L.; Rominger, F.; Helmchen, G. *Angew. Chem. Int. Ed.* **2007**, *46*, 5598.

⁵³ Amijs, C. H. M.; Ferrer, C.; Echavarren, A. M. *Chem. Comm.* **2007**, 698

⁵⁴ Toullec, P. Y.; Genin, E.; Leseurre, L.; Genêt, J.-P.; Michelet, V. *Angew. Chem. Int. Ed.* **2006**, *45*, 7427.

⁵⁵ Witham, C. A.; Mauleon, P.; Shapiro, N. D.; Sherry, B. D.; Toste, F. D. *J. Am. Chem. Soc.* **2007**, *129*, 5838.

cyclopropanation reaction.⁵⁶ The cyclization of 1,6-enynes substituted with a methoxy group in the benzyl position afforded 1,3-substituted naphthalenes. The mechanistic proposal involved the formation of intermediate **L** by a 6-*endo-dig* cyclization, followed by a 1,2-shift to form **LI**. Then, retro-cyclopropanation via **LII** affords naphthalene **LIV** and free gold(I) carbene **LIII** (Scheme 13).

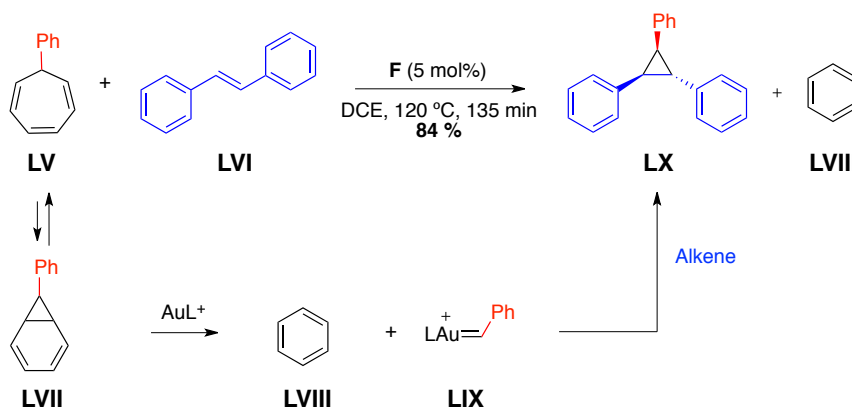


Scheme 13

⁵⁶ Solorio-Alvarado, C. R.; Echavarren, A. M. *J. Am. Chem. Soc.* **2010**, *132*, 11881.

2. Objectives

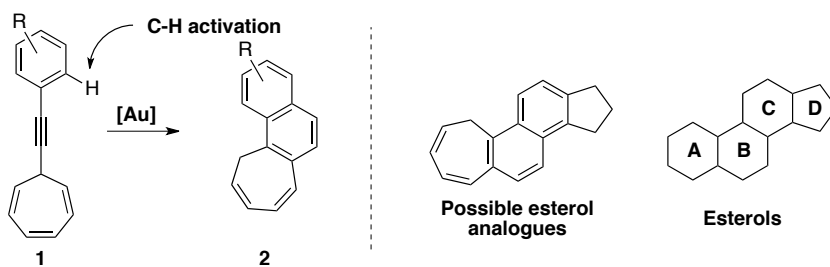
In 2011, our group established that a free gold-carbene could be generated from aryl-substituted cycloheptatrienes and subsequently trapped by an alkene such as *trans*-stilbene. Triaryl-substituted cyclopropanes were synthesized with loss of benzene (*Scheme 14*).⁵⁷



Scheme 14

We thought that we could extend these results to the gold-catalyzed cyclization of alkynyl cycloheptatrienes, expecting that tricyclic products could be obtained through a new type of annulation reaction. By tethering the aromatic ring, we could form tetracyclic compounds that could be considered analogues of esteroles.

⁵⁷ Solorio-Alvarado, C. R.; Wang, Y.; Echavarren, A. M. *J. Am. Chem. Soc.* **2011**, *133*, 11952.

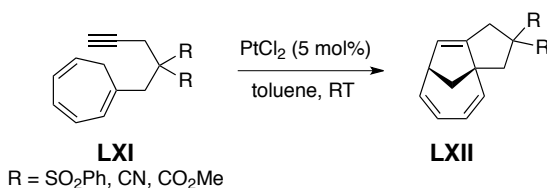
*Scheme 15*

Our goal was to prepare a set of aryl-substituted alkyne-cycloheptatrienes, which could undergo a gold-catalyzed cycloisomerization reaction.

3. Results and Discussion

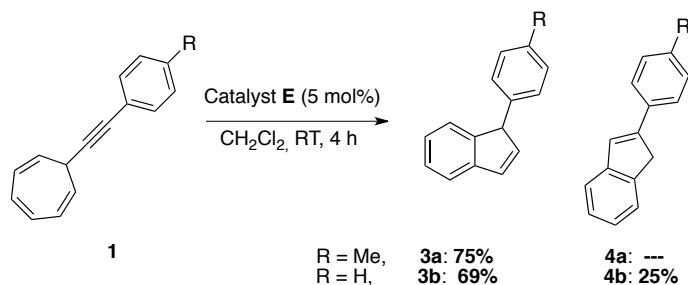
3.1 Methodology

When we first approached the gold-catalyzed cyclization of alkynyl cycloheptatrienes, we hypothesized that tricyclic products could be obtained through an annulation process. By tethering the aromatic ring, we could form tetracyclic compounds that could be considered analogues of esteroles. The only precedent for metal-catalyzed cyclization of alkynes tethered to cycloheptatriene was reported by Tenaglia and Gaillard,⁵⁸ in which tricyclic products were accessed by means of a PtCl₂-catalyzed [6+2] cycloaddition.



Scheme 16

The first tests that we carried out indicated that the product obtained was actually a mixture 1- and 2-substituted indenenes as illustrated in *Scheme 17*.⁵⁹



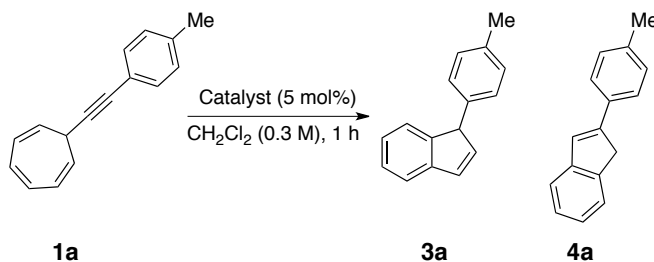
Scheme 17

⁵⁸ Tenaglia, A.; Gaillard, S. *Angew. Chem. Int. Ed.* **2008**, *47*, 2454.

⁵⁹ Work developed in collaboration with César Rogelio Solorio-Alvarado.

In order to improved the selectivity, we decided to screen different gold catalysts with alkynyl cycloheptatriene **1a** as substrate. We also investigated the rearrangement reaction in the presence of other known π -Lewis acids as catalysts.⁶⁰

Table 1



Entry	Catalyst	Temperature	Conversion [%] ^a	Ratio 3a: 4a ^a
1	E	23 °C	>99	75:25
2	E	0°C	>99	84:16
3	H^b	0°C	>99	48:52
4	F	0°C	>99	80:20
5	G	0°C	>99	62:38
6	S	0°C	>99	84:16
7	AuCl ₃	0°C	>99	87:13
8	AuCl	0°C	50	96:4
9	BB	0°C	>99	>99:1
10	K	0°C	>99	0:100
11	PtCl ₂	0°C	0	-
12	GaCl ₃	0°C	0	-
13	AgOTf	0°C	0	-
14	ICl	0°C	>99	- ^c
15	TfOH	0°C	>99	- ^c
16	BF ₃ ·OEt ₂	0°C	0	-
17	Hg(OAc) ₂	0°C	0	-
18	InCl ₃	0°C	0	-

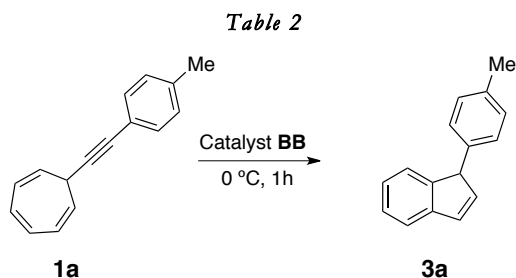
^aConversions and product ratios were determined by ¹H NMR analysis of the crude reaction mixtures. ^bGenerated in situ by mixing 5 mol% Ph₃PAuCl with 5 mol% AgSbF₆.

^cDecomposition of starting material observed without product formation.

⁶⁰ Work developed in collaboration with Dr. Paul McGonigal.

First, we realized that the reaction could be performed at 0 °C for 1 h, which increased the selectivity for **3a**. Treating **1a** with a variety of gold complexes led to rapid isomerization to indene products **3a** and **4a** (entries 1–10). Other common π -acids were found not to be catalytically active in this transformation (entries 11–18). The ratio of regioisomers **3a:4a** was sensitive to the gold source employed. Gold trichloride, cationic phosphine- and N-heterocyclic carbene gold(I) complexes generated mixtures (entries 1–7). However gold chloride and complexes **BB** and **K** exhibited excellent bias towards one regioisomer (entries 8–10), allowing either 1-(*p*-tolyl)-1*H*-indene **3a** or 2-(*p*-tolyl)-1*H*-indene **4a** to be formed selectively. The high selectivity and conversions obtained with **BB** and **K** prompted us to use these catalysts for further investigation.

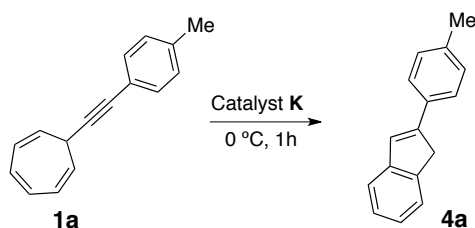
Then we focused on the optimization of the solvent and the catalyst loading for the rearrangement of substrate **1** catalyzed by complex **BB**. The best conditions are highlighted in *Table 2* (entry 6).



Entry	Catalyst loading (mol %)	Solvent	Yield ^a 3a (%)
1	5	CH ₂ Cl ₂	94
2	5	THF	93
3	5	Toluene	93
4	5	CH ₃ CN	80
5	2.5	CH ₂ Cl ₂	90
6	1	CH₂Cl₂	92 (88)^b
7	0.25	CH ₂ Cl ₂	92

^a Estimated by ¹H NMR analysis of crude reaction mixture. ^b Isolated yield.

The same was carried out with complex **K**, being the conditions depicted in entry 3 (*Table 3*) the best conditions for this transformation.

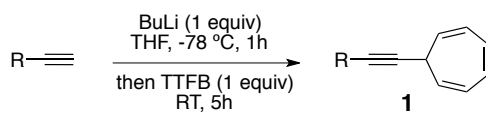
Table 3

Entry	Catalyst loading (mol %)	Solvent	Yield ^a 4a (%)
1	5	CH ₂ Cl ₂	45
2	5	THF	41
3	5	Toluene	74 (60^b)
4	2.5	Toluene	68
5	1	Toluene	64
6	0.25	Toluene	40
7	5	DCE	36
8	5	CH ₃ CN	22 (54 % conv.)
9	5	DMF	20 (85 % conv.)

^a Estimated by ¹H NMR analysis of crude reaction mixture. ^b Isolated yield.

In order to test the tolerance of this transformation towards changes in the alkyne substituent, a set of 7-alkynyl cyclohepta-1,3,5-triene substrates was synthesized by the reaction of commercially available tropylium tetrafluoroborate with lithium acetylides that were prepared in situ from the corresponding terminal alkynes.

Table 4



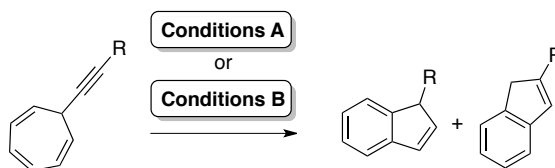
Entry	Alkyne	Product/Yield ^a
1	R = <i>p</i> -tolyl	1a 89%
2	R = phenyl	1b 74%
3	R = <i>m</i> -tolyl	1c 73%
4	R = <i>o</i> -tolyl	1d 71%
5	R = <i>p</i> -methoxyphenyl	1e 74%
6	R = <i>p</i> -fluorophenyl	1f 85%
7	R = <i>p</i> -chlorophenyl	1g 67%
8	R = <i>p</i> -bromophenyl	1h 47%
9	R = 2'-biphenyl	1i 88%
10	R = 2-naphtyl	1j 81%
11	R = 3-thienyl	1k 79%
12	R = ferrocenyl	1l 52%
13	R = Bn	1m 66%
14	R = CH ₂ Bn	1n 81%
15	R = H	1o ^b 70%
16	R = Bu	1p 86%
17	R = TMS	1q 40%
18		1r 67%
19		1s 23%

^aIsolated yields. ^bPrepared from 7-methoxycyclohepta-1,3,5-triene and ethylmagnesium bromide.⁶¹

These substrates were subjected to the optimized reaction conditions. The catalyst-controlled regioselectivity we observed in the cycloisomerization of **1a** was retained for the majority of substrates, although in two instances mixtures were obtained (*Table 5*, entries 4B and 13A). In general reactions were

⁶¹ Hoskinson, R. M. *Aust. J. Chem.* **1970**, *23*, 399.

complete within 1 hour at 0 °C, picolinate catalyst **BB** afforded 1-substituted indenyl products in good isolated yields (55–88%) whereas phosphite gold(I) catalyst **K** produced the 2-substituted indenyl isomers in slightly lower yields (30–76%), probably due to partial decomposition in the presence of the more reactive phosphite complex. Substrates bearing aryl groups with substituents in the 2-, 3-, or 4-positions performed similarly (*Table 5*, entries 1–9) and electron donating or withdrawing substituents were tolerated (e.g. *Table 5*, entries 5 and 6). Fused aromatic and heteroaromatic alkynyl cycloheptatrienes were also suitable substrates (*Table 5*, entries 10 and 11) although slightly more forcing conditions were necessary in order to achieve complete conversion of thiophenyl enyne **1n** with catalyst **BB**. Aside from aryl alkynes, benzyl substrate **1m** isomerized to indene products successfully (*Table 5*, entry 13). Terminal alkyne **1o** was also unreactive under set of conditions A, but could be converted to indene in moderate yield using phosphite catalyst **K** (entry 15).

Table 5

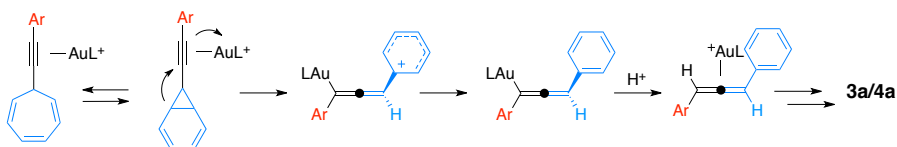
Entry	Substrate	Product/Yield ^a	
		Conditions A ^b	Conditions B ^c
1	1a	3a 86%	4a 60%
2	1b	3b 64%	4b 51%
3	1c	3c 55%	4c 50%
4	1d	3d 76%	3b/4d (1:1.8) ^d 48%
5	1e	3e 69%	4e 30%
6	1f	3f 63% ^e	4f 60%
7	1g	3g 80%	4g 59%
8	1h	3h 82%	4h 57%
9	1i	3i 77%	4i 76% ^f

10	1j	3j 75%	4m 51%
11	1k	3k ^e 66%	4n 41%
12	1l	-	4o 23%
13	1m	3m/4m (1:2) ^d 76%	4m 57%
14	1n	-	4n 31%
15	1o	-	3o = 4o 54% ^f
16	1p	-	-
17	1q	-	-
18	1r	- ^g	4r , 45%
19	1s	- ^g	4s , 36%

^aIsolated yields. ^bConditions A: **12** (1 mol%), CH₂Cl₂ (0.29 M), 0 °C, 1 h. ^cConditions B: **13** (5 mol%), PhMe (0.29 M), 0 °C, 1 h. ^dIsolated as a mixture. ^e**12** (5 mol%), rt, 2 h. ^fYield calculated by ¹H NMR. ^gReaction not performed as a mixture of diastereoisomers would be produced.

3.2 Intercepting barbaralyl intermediates with nucleophiles

The mechanism through which indenes were obtained was still a puzzle. We first hypothesized that it might proceed through an allene intermediate (*Scheme 18*) but that did not explain why substituents on the aryl group were never found in the indene moiety.

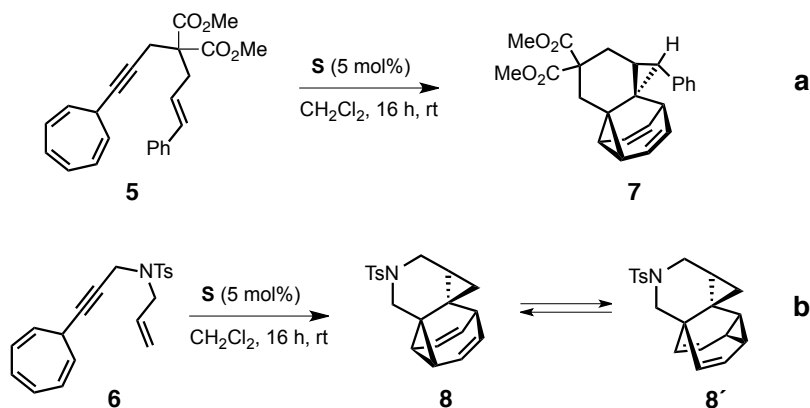


Scheme 18: First mechanistic proposal

We attempted the trapping of an intermediate that could shed some light into the mechanistic pathway followed by the gold-catalyzed cyclization of alkynyl cycloheptatrienes.

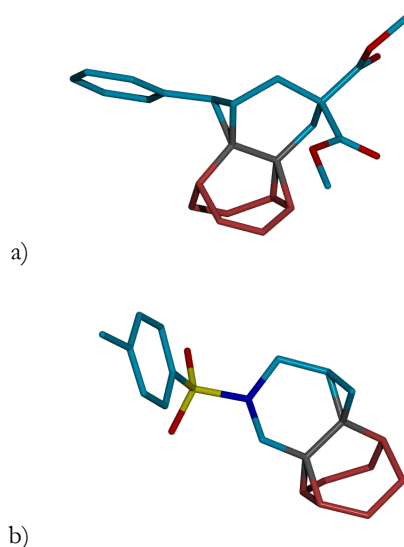
Substrates **5** and **6**, which feature pendant olefins attached to the cycloheptatriene ring via the alkyne, underwent cycloisomerization in the

presence of cationic gold catalyst **S** to form polycyclic products **7** and **8/8'** respectively (*Scheme 19*).⁶²

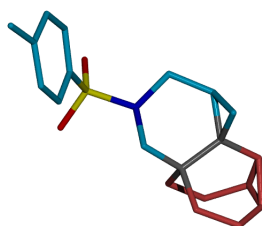


Scheme 19

Unambiguous structural assignment by X-ray diffraction of single crystals revealed the products to be barbaralanes (*Figure 10*).



⁶² Work developed in collaboration with Yahui Wang.



c)

Figure 10: X-Ray Crystal Structures of a) 7, b) 8 and c) 8'.

Tautomeric barbaralanes **8** and **8'** equilibrated rapidly on the NMR timescale at room temperature in deuteriochloroform via strain-assisted Cope rearrangement and were detected as a 1:1 mixture in the solid state whereas **7** was observed as a single tautomer. *Figure 11* illustrates the $^1\text{H-NMR}$ spectra recorded under ambient conditions of **8** and **8'**, which show sharp signals due to rapid exchange on the NMR timescale, averaging the resonances due to protons 2 and 4, or 6 and 8. As the temperature was lowered, the peaks broadened and merged with the baseline before reappearing at 148 K at which point exchange is slow on the NMR timescale and one isomer exists in solution as the major species. At room temperature, protons 3 and 7 resonate at 5.6 ppm but protons 2, 4, 5 and 8 do not appear in the C_{sp^2} region. At 148 K, four protons appear in the olefinic region (5.9–5.3 ppm), protons 3 and 7, as well as two more protons—either 2 and 8 or 4 and 6.

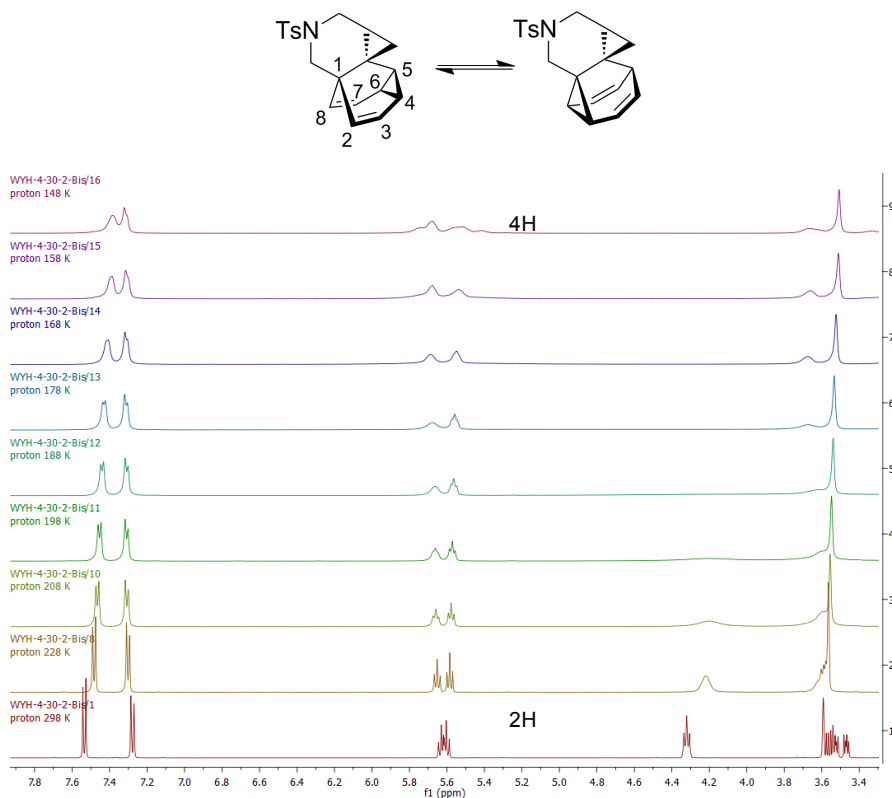
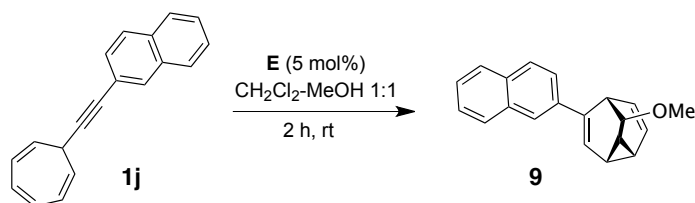


Figure 11: Variable temperature ^1H NMR (500 MHz, $\text{THF-d}_8/\text{CS}_2=1:5$) spectra of $8/8'$, region from 7.9 to 3.3 ppm.

These results strongly suggested that a barbaralyl cationic intermediate was indeed the key species in the mechanism we had at hand.

To gain more direct evidence for the intermediacy of a cationic barbaralyl species in the transformation of 7-alkynyl cyclohepta-1,3,5-trienes **5** to indenenes **6** and **7**, we sought to intercept an intermediate by employing methanol as co-solvent (*Scheme 20*). Thus, cyclization of substrate **1j** in 1:1 methanol-dichloromethane afforded barbaralane methyl ether **9** in 40% yield, along with minor amounts of indenenes **3j** and **4j**.



Scheme 20

The structure of **9** was confirmed by crystallographic analysis (*Figure 12*). The rigid tricyclo[3.3.1.0^{2,8}]nona-3,6-dien-9-yl carbon skeleton is clearly evident in all the solid state structures shown in *Figure 10* and *Figure 12*, suggesting that such a cage-like motif is prominent in the reactive intermediates formed during the course of the reaction.

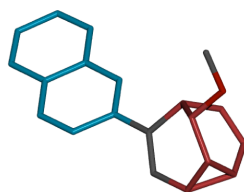


Figure 12: X-Ray crystal structure of 9.

3.3 The barbaralyl cation.

The 9-barbaralyl cation⁶³ (*Figure 13a*), is a hugely fluxional C₉H₉⁺ hydrocarbon that exists as a mixture of 181 400 degenerate forms⁶⁴ that interconvert rapidly at temperatures as low as -135 °C,⁶⁵ each carbon atom may exchange with every other carbon atom in the structure via a series of pericyclic reactions.

⁶³ Lambert, J. B. *Tetrahedron Lett.* **1963**, *4*, 1901.

⁶⁴ Cremer, D.; Svensson, P.; Kraka, E.; Ahlberg, P. *J. Am. Chem. Soc.* **1993**, *115*, 7445.

⁶⁵ Ahlberg, P.; Harris, D. L.; Winstein S. *J. Am. Chem. Soc.* **1970**, *92*, 4454.

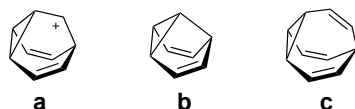
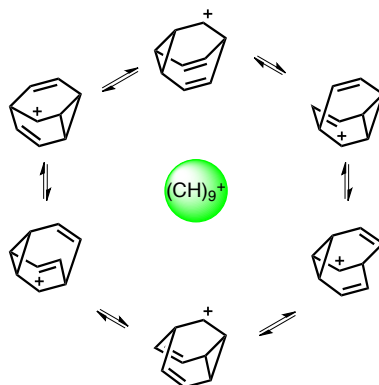


Figure 13: a) 9-barbaralyl cation, b) semibullvalene and c) bullvalene.

Barbaralanes⁶⁶ are known to ‘shape-shift’⁶⁷ via strain-assisted Cope rearrangements, analogous to the behavior of semibullvalene and bullvalene (Figure 13b and c, respectively).⁶⁸ However this mechanistic pathway is only followed in neutral systems and results in just two degenerate tautomers for barbaralane (C₉H₁₀). Seminal experimental and computational studies by Ahlberg^{64,6569} and others⁷⁰ have revealed that a dramatically different course is followed by cationic barbaralyl species, which can bring about complete scrambling of the core C₉ framework (Scheme 21).



Scheme 21

⁶⁶ Quast, H.; Geissler, E.; Mayer, A.; Jackman, L. M.; Colson, K. L. *Tetrahedron* **1986**, *42*, 1805.

⁶⁷ (a) Lippert, A. R.; Keleshian, V. L.; Bode, J. W. *Org. Biomol. Chem.* **2009**, *7*, 1529. (b) He, M.; Bode, J. W. *Proc. Natl. Acad. Sci. U.S.A.* **2011**, *108*, 14752. (c) Larson, K. K.; He, M.; Teichert, J. F.; Naganawa, A.; Bode, J. W. *Chem. Sci.* **2012**, *3*, 1825.

⁶⁸ Schröder, G. *Angew. Chem. Int. Ed.* **1963**, *2*, 481.

⁶⁹ (a) Ahlberg, P.; Grutzner, J. B.; Harris, D. L.; Winstein, S. *J. Am. Chem. Soc.* **1970**, *92*, 3478. (b) Engdahl, C.; Jonsäll, G.; Ahlberg, P. *J. Am. Chem. Soc.* **1983**, *105*, 891. (c) Engdahl, C.; Ahlberg, P. *J. Phys. Org. Chem.* **1990**, *3*, 349.

⁷⁰ (a) Barborak, J. C.; Daub, J.; Follweiler, D. M.; Schleyer, P. v. R. *J. Am. Chem. Soc.* **1969**, *91*, 7760. (b) Barborak, J. C.; Schleyer, P. V. R. *J. Am. Chem. Soc.* **1970**, *92*, 3184. (c) Grutzner, J. B.; Winstein, S. *J. Am. Chem. Soc.* **1972**, *94*, 2200. (d) Werstiuk, N. H. *Can. J. Chem.* **2010**, *88*, 1195.

3.4 Mass spectrometry experiments.

Since most of the barbaralyl intermediates seemed to be short-lived, we subjected the reaction to a mass spectrometry analysis in order to detect them. Since this technique detects only charged entities, we first tried the reaction using substrate **1a** with catalyst **E**, a cationic complex (Figure 14).

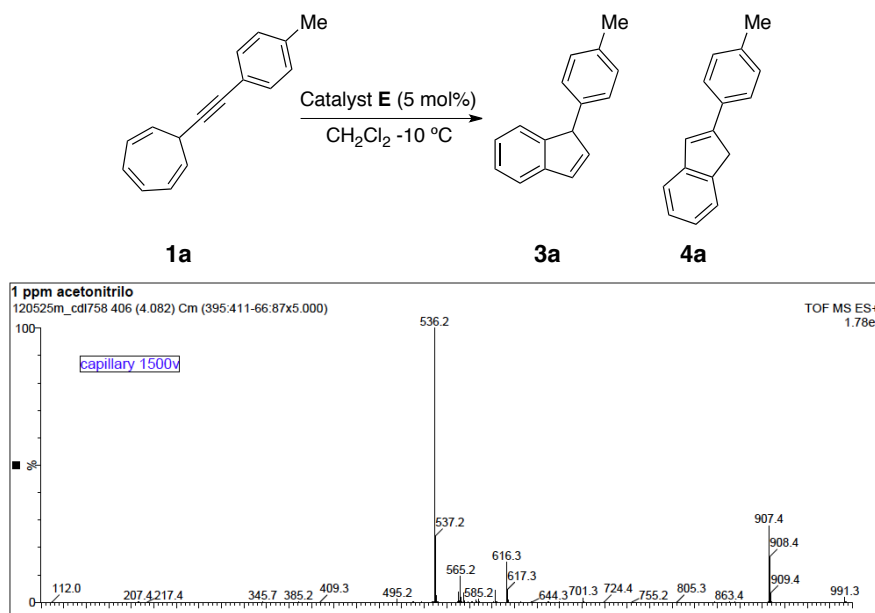


Figure 14: Mass spectrometry analysis of the cyclization of substrate **1a** with catalyst **E**.

We expected a signal with $m/z = 701$ which would correspond to coordination of the gold complex to the substrate. Indeed this peak was observable even if it was not intense. The peak with $m/z = 536$ correspond to the cationic part of the catalyst (Figure 15). The signal with $m/z = 907$ (Figure 14) was totally unexpected.

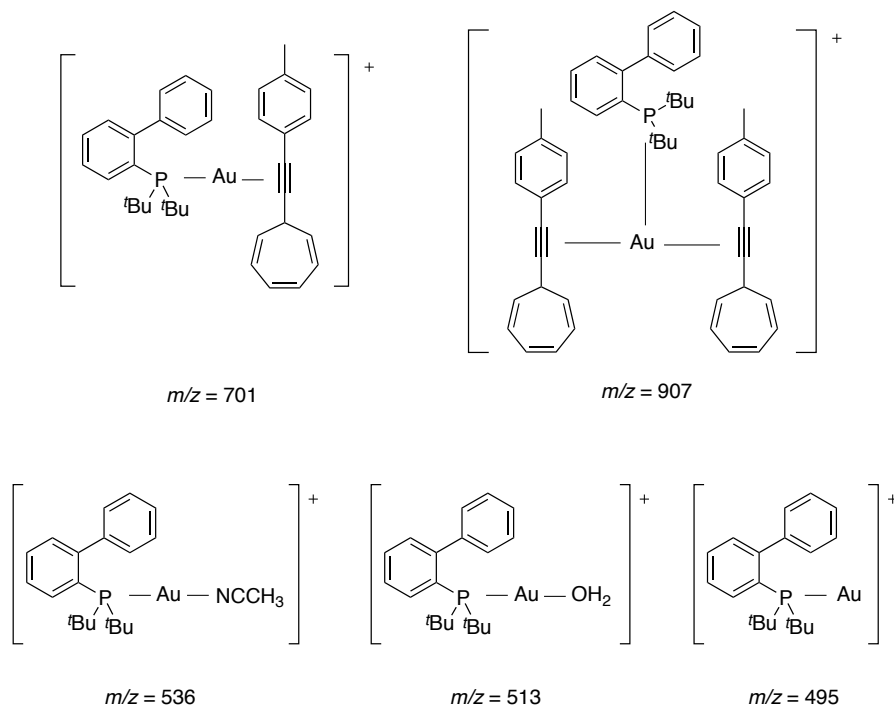


Figure 15: Fragments identified by Mass spectrometry analysis of the cyclization of substrate 1a with catalyst E.

This signal corresponds to the coordination of the gold complex with two molecules of substrate (Figure 15). Similar type of complexes has been reported by Das and co-workers⁷¹ who were able to isolate Au(I) bis(alkyne) complexes. Quadrupole time of flight (QTOF) experiments confirmed that a signal with $m/z = 701$ could be obtained from fragment with $m/z = 907$, along with fragments that corresponded to the gold catalyst ($m/z = 513$ and 495). (Figure 16).

⁷¹ Das, A.; Dash, C.; Yousufuddin, M.; Celik, M. A.; Frenking, G.; Dias, H. V. R. *Angew. Chem. Int. Ed.* **2012**, *51*, 3940.

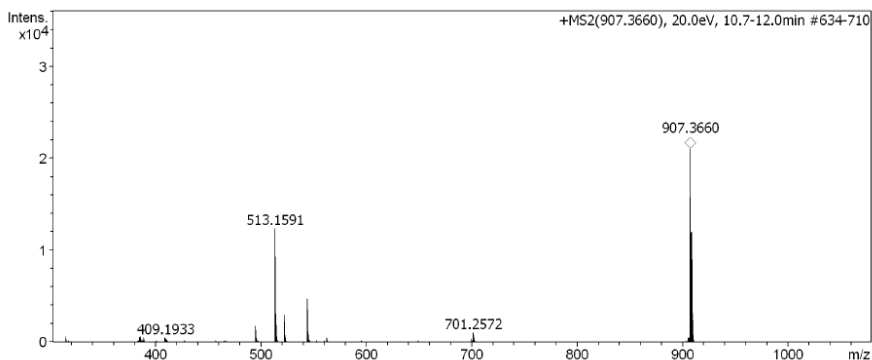


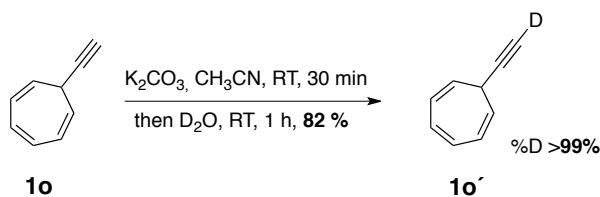
Figure 16: *Q*-TOF experiment performed on fragment with $m/z = 907$.

Repeating these experiments with AuCl and complex **BB** as catalysts did not provide any recognizable fragment. Ionization of the formed species seemed to be difficult in dichloromethane or acetonitrile as solvents. Unfortunately, carrying out the reaction in methanol was not viable since the reaction does not proceed cleanly in that solvent.

3.5 Isotopic labeling studies.

Having established the likely intermediacy of barbaralyl structures, we were still intrigued to understand how they developed into the final indene products and, importantly, we were unsure if the short-lived cationic barbaralyl species evolve via a short series of steps or whether they undergo numerous rearrangements. Accordingly, we undertook isotopic labeling studies using the deuterated ethynylcycloheptatriene **1o'**. The straightforward procedure described by Poullain and co-workers⁷² allowed us to prepare it with 82 % yield (*Scheme 22*).

⁷² Bew, S. P.; Hiatt-Gipson, G. D.; Lovell, J. A.; Poullain, C. *Org. Lett.* **2012**, *14*, 456.

*Scheme 22*

Gold-catalyzed cyclization of substrate **10'** with catalyst **E** did not provide a single isotopologue. Actually, analysis of the 1H NMR spectrum suggested that the deuterium label was lost since all the protons integrated for 1. On the other hand, we could identify satellite signals for each carbon signal (*Figure 17*) which was consistent with deuteration in different positions of the molecules but we could not assign the deuterated positions.

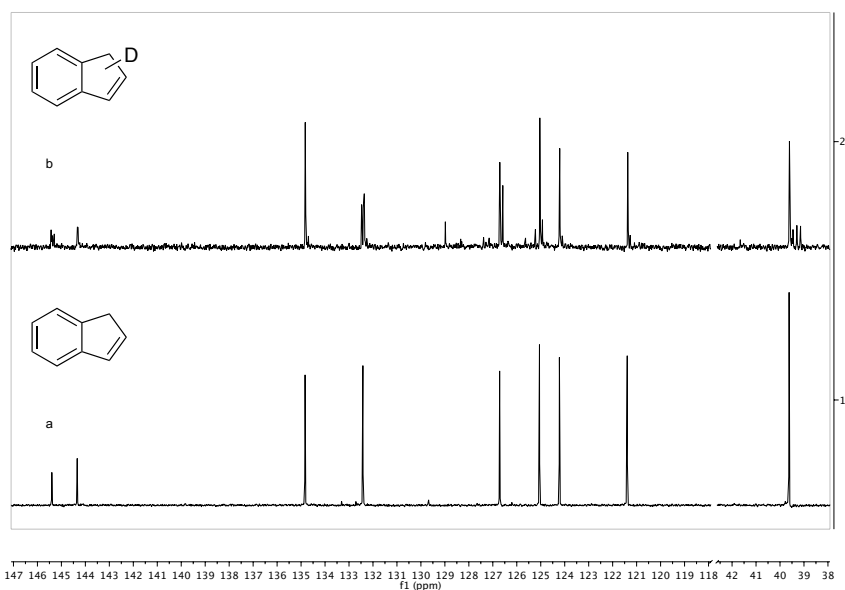
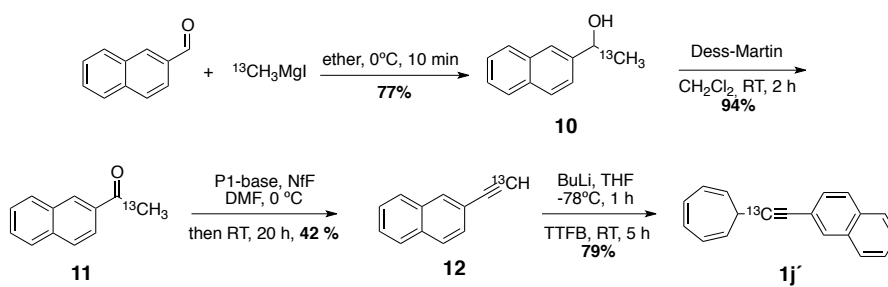


*Figure 17: Comparison of the ^{13}C NMR spectra of a) indene and b) product of gold-catalyzed cyclization of **5o'**.*

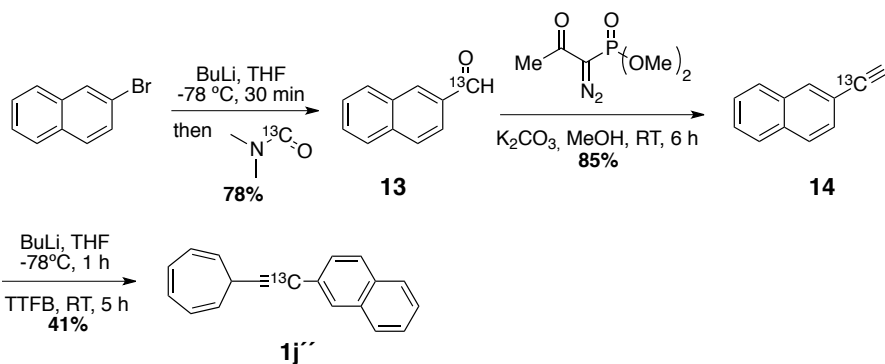
Since deuterium labeling did not provide any insight in the mechanism, we decided to prepare two alkynyl cycloheptatrienes bearing a ^{13}C label as part of

the alkyne at either the position adjacent to the cycloheptatriene moiety (**1j'**) or attached to the naphthyl ring system (**1j''**). The synthesis of the former labeled substrate is depicted in *Scheme 23*. We prepared the Grignard reagent from iodomethane- ^{13}C which was added to naphthaldehyde at $0\text{ }^{\circ}\text{C}$. The desired benzylic alcohol **10** was then oxidized with Dess-Martin periodinane to afford ketone **11**. Dehydration was achieved by means of a phosphazene base and nonafluorobutanesulfonyl fluoride to yield alkyne **12**. Finally substrate **1j'** was obtained in good yield by lithiation of the terminal alkyne and subsequent quenching with TTFB.



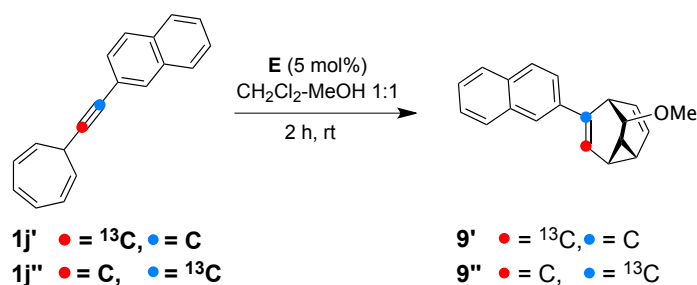
Scheme 23

The synthesis of substrate **1j''** was more straightforward as illustrated in *Scheme 24*. Lithium-halogen exchange followed by dimethyl formamide- ^{13}C quenching afforded the desired labeled naphthaldehyde **13**, which then underwent a Bestmann-Ohira reaction to afford the desired alkyne **14**. The desired substrate was obtained in moderate yield under the already described conditions.



Scheme 24

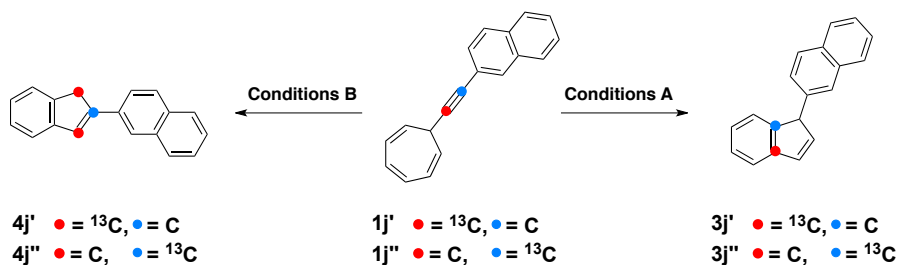
The two labeled substrates (red dot, **1j'**; blue dot, **1j''**) were subjected to methoxycyclization (Scheme 25) to capture isotopologues of barbaralane **9**.



Scheme 25

Methoxycyclization of either **1j'** or **1j''** generates **9'** or **9''** in which the ^{13}C label has been transferred with complete fidelity to a single position in the barbaralane products (Scheme 25), indicative of a mechanism proceeding via a small number of steps. If the barbaralyl intermediate could undergo manifold pericyclic rearrangements prior to interception with methanol, the ^{13}C label of **9'** (red dot) would be expected to disperse throughout the barbaralane skeleton.

These substrates were also subjected to the standard cyclization conditions A and B (Scheme 26) to yield 1-naphthyl and 3-naphthyl indenenes respectively.



Scheme 26

Generally, cycloisomerization under conditions A or B affords single isotopomers as products, however the transformation of $1j'$ catalyzed by phosphite complex **K** (conditions B, product $4j'$) yielded a mixture of two isotopomers in which the ^{13}C label was located in either the 1- or 3-position of the indene. Examination of the ^{13}C NMR spectra of 2-naphthyl indenenes $3j$, $3j'$, and $3j''$ (Figure 18) revealed unexpectedly that the ^{13}C labeled atoms are found at the quaternary positions of the indene core—separated from the naphthalene by an extra bond in comparison with the starting compounds $1j'$ and $1j''$.

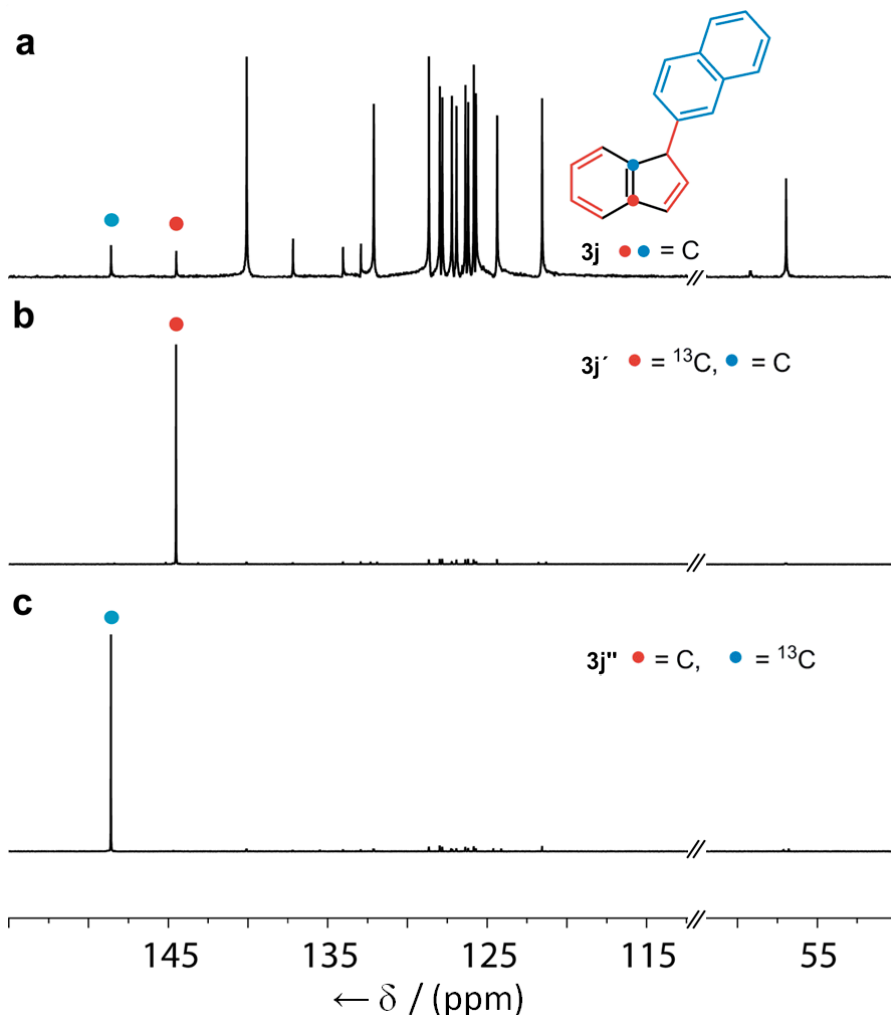
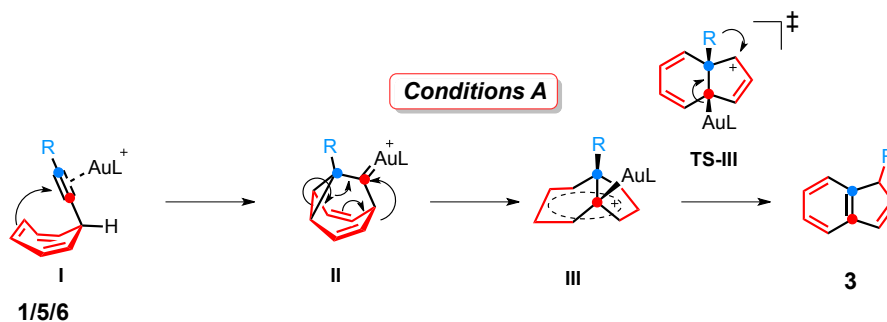


Figure 18: Determination of ^{13}C label position by NMR. ^{13}C NMR spectra (500 MHz, CDCl_3 , 298 K) of a, unlabeled product $3j$; b, product $3j'$ resulting from cycloisomerization of $1j'$; and c, product $3j''$ resulting from cycloisomerization of $1j''$.

3.6 Mechanistic rationale

Experimental and theoretical studies have established that the C_9H_9^+ barbaralyl cation fluctuates between degenerate isomers via a unique network of reaction paths involving 30240 degenerate divinylcyclopropylcarbanyl cation–divinylcyclopropylcarbanyl cation rearrangements (dvcpc–dvcpc, one

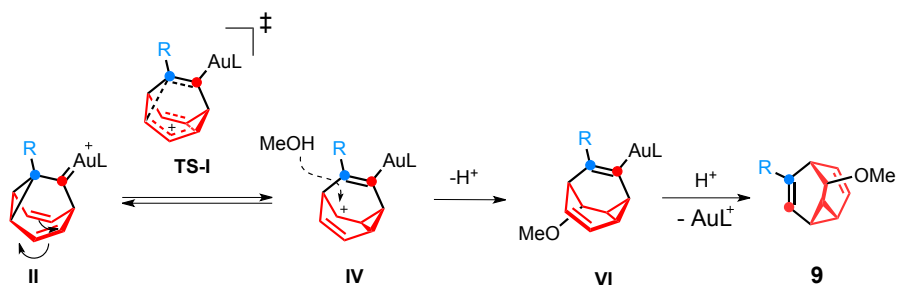
cyclopropyl bond is broken as another forms) and 90 720 rearrangements which pass through a bicyclo[3.2.2]nona-3,6,8-trien-2-yl transition state.⁶⁴ Although the number of energetically accessible non-degenerate isomers and, hence the number of possible rearrangements, is markedly reduced in substituted systems^{69c} such as ours, the key mechanistic features remain the same. The mechanistic rationale that accounts for our experimental observations was formulated based on these known steps and is presented in *Scheme 27*, *Scheme 28* and *Scheme 29*. We propose that coordination of the catalyst to the alkyne initiates a 6-endo-*dig* 1,6-enyne cyclization affording barbaralyl-gold complex **II**, pictured by invoking a gold carbene resonance form.⁷³ Intermediate **II** can irreversibly transform into homoaromatic bicyclo[6.3]nonatrienyl cation **III**,^{70d} which can suffer deauration with a concomitant 1,2-shift through **TS-III**, to establish aromaticity, liberate 1-substituted indene product **6**, and regenerate the catalytically active metal species (*Scheme 27*). As a consequence of the 1,2-shift, the R group separates from the carbon atoms that originated from the alkyne of **1** (red and blue dots) as detected in products **3j'** and **3j''** (*Scheme 26* and *Figure 18*).



Scheme 27

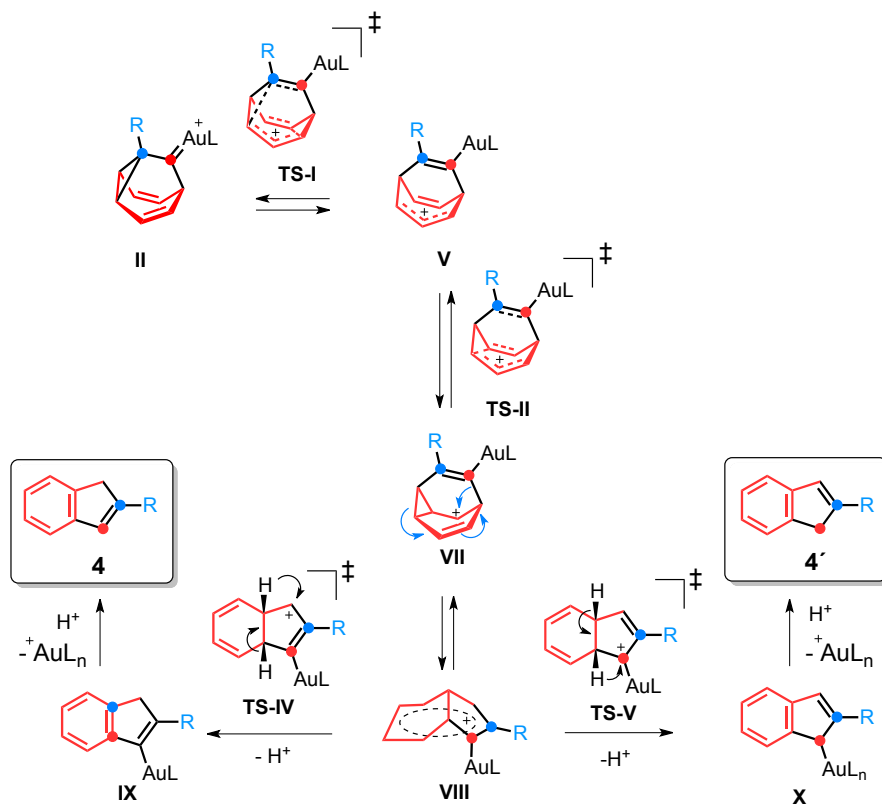
⁷³ (a) Benitez, D.; Shapiro, N. D.; Tkatchouk, E.; Wang, Y.; Goddard, W. A.; Toste, F. D. *Nature Chem.* **2009**, *1*, 482. (b) Pérez-Galán, P.; Herrero-Gómez, E.; Hog, D. T.; Martín, N. J. A.; Maseras, F.; Echavarren, A. M. *Chem. Sci.* **2011**, *2*, 141. (c) Pérez-Galán, P.; Martín, N. J. A.; Campaña, A. G.; Cárdenas, D. J.; Echavarren, A. M. *Chem. Asian J.* **2011**, *6*, 482.

Alternatively, reversible dvcpc-dvcpc rearrangement of **II** (*Scheme 28*) via transition state **TS-I** generates isomeric barbaralyl-gold complex **IV**, the precursor to methoxycyclization product **9**.



Scheme 28

By analogy to the reversible isomerization process in C_9H_9^+ ,⁶⁴ barbaralyl-gold complex **VII** can be accessed by evolution of **TS-I** via **V** and **TS-II** (*Scheme 29*). Homoaromatic bicyclo[6.3]nonatrienyl cation **VIII** is then formed irreversibly and can aromatize with concomitant proton loss and 1,2-hydride shift via two pathways to generate either **IX** or **X**. Protodeauration of either intermediate liberates the same 2-substituted indene products **4**, the preceding steps are only distinguishable in the case of ^{13}C labeled indene **4j'** which was isolated in a near 1:1 mixture of isotopomers.



Scheme 29

Gold-stabilized cations generated in this reaction fluctuate between a minimum of three barbaralyl structures **II**, **IV**, and **VII**. In the case of reactions performed using catalyst **E**, experimental evidence illustrates that all three of these intermediates are accessed as indenes **3** and **4**, and barbaralane **9** have all been isolated. Given this fact, it is remarkable that certain catalysts such as picolinate complex **BB** and phosphite complex **K** are able to exercise such a high level of control over the pathway that is followed. It is possible that other low energy, transient barbaralyl intermediates are also present during the course of these reactions but have escaped detection as they are not direct precursors to any of the compounds isolated in this study, however, ^{13}C labeling experiments have shown that the barbaralyl species are not sufficiently long-lived to allow carbon atoms of the cage-like skeleton to exchange positions.

The sheer number of conceivable permutations makes it impractical to perform calculations to calculate the relative energies of all possible isomers, however DFT modeling of our proposed intermediates with the M06 functional showed in all cases that the minimum structures correspond to 1-aryl-9-barbaralyl-gold species such as **IIa** and **IIb** with bond lengths between C1 and C-9 of 1.38-1.41 Å, intermediate between single and double carbon-carbons bonds (*Figure 19*). The C-Au bond distance in neutral **IIa**, with a more donating chloride ligand, is shorter than in cationic **IIb** (2.00 Å vs. 2.07 Å), corresponding to a more metal carbene-like structure for the former, neutral intermediate.

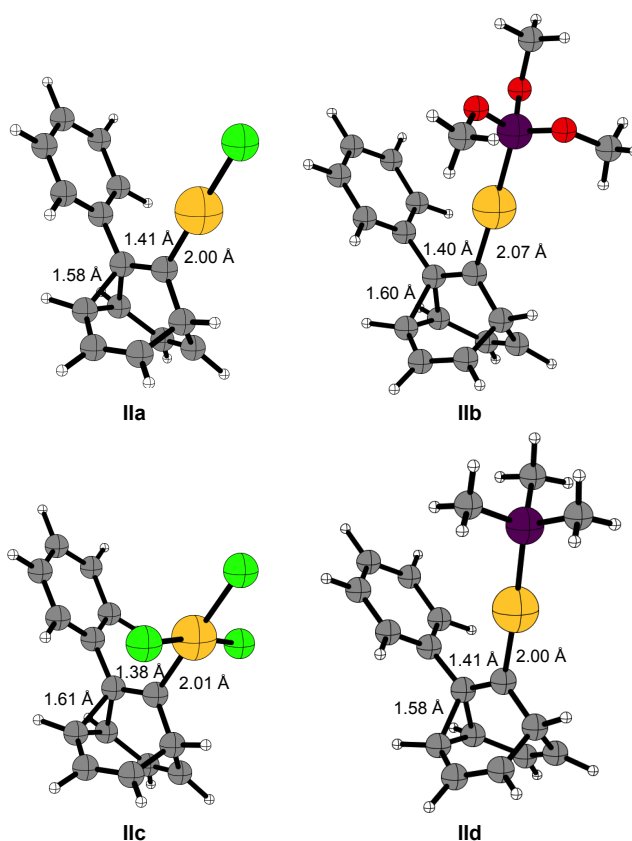


*Figure 19: DFT modeling of neutral intermediates **IIa** and **IIc** and cationic intermediates **IIb** and **IIId***

4. Conclusions

We have reported a new method that allows catalytic generation of fluxional barbaralyl cations directly either from easily-prepared 7-alkynyl cyclohepta-1,3,5-trienes **1**.

The reactions are catalyzed by gold complexes, under mild conditions and do not require inert atmosphere or exclusion of water. In the absence of nucleophiles, substituted indenenes are produced in good to high yields with catalyst-controlled regiochemistry.

The nature of the gold catalyst affects the evolution of the cationic intermediate. Such influence over the speciation of barbaralyl cations is unprecedented.

We have also demonstrated that this methodology can be exploited to synthesize barbaralanes in moderate yields simply by the addition of an internal or external nucleophile.

On the basis of ^{13}C labeling studies, nucleophilic trapping of intermediates, computational modeling and literature precedent we have presented a mechanistic rationale which accounts for our findings.

UNIVERSITAT ROVIRA I VIRGILI

GOLD-CATALYZED CYCLIZATIONS FOR THE SYNTHESIS OF SMALL AND MEDIUM-SIZED ARENES

Claudia Alejandra de León Solís

Dipòsit Legal: T. 196-2013

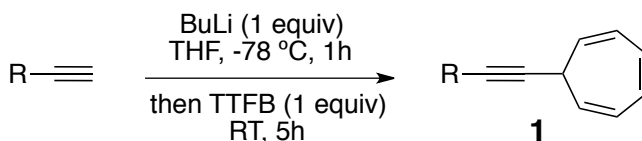
5. Experimental section

5.1 General

Unless otherwise stated, reactions were carried out under argon atmosphere in solvents dried by passing through an activated alumina column on a PureSolv™ solvent purification system (Innovative Technologies, Inc., MA). Analytical TLC was performed on precoated silica gel plates (0.2 mm thick, Gf234, Merck, Germany) and observed under UV light. Flash column chromatography purifications were carried out using flash grade silica gel (SDS Chromatogel 60 ACC, 40-60 μm) as the stationary phase. Preparative TLC was performed on 20 cm × 20 cm silica gel plates (2.0 mm thick, catalogue number 02015, Analtech). NMR spectra were recorded at 298 K on a Bruker Avance 400 Ultrashield and Bruker Avance 500 Ultrashield apparatus. Chemical shifts are reported in parts per million and referenced to residual solvent. Coupling constants (*J*) are reported in hertz (Hz). Mass spectra were recorded on a Waters LCT Premier Spectrometer (ESI and APCI) or on an Autoflex Bruker Daltonics (MALDI and LDI) or on a Maxis Impact Bruker (QTOF) or on an AgilentMSD-5975B (GC-MS). Melting points (M.p.) were determined using a Büchi melting point apparatus.

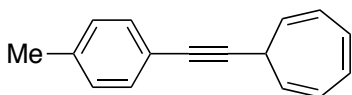
Unless otherwise stated, all reagents were purchased from commercial sources and used without further purification. Gold complexes were synthesized according to literature procedures (C. H. M. Amijs, V. López-Carrillo, M. Raducan, P. Pérez-Galán, C. Ferrer, A. M. Echavarren, *J. Org. Chem.* **2008**, *73*, 7721–7730). (Acetonitrile)[(2-biphenyl)di-*tert*-butylphosphine]gold(I) hexafluoroantimonate **8** which was also purchased from Aldrich.

5.2 General Procedure for the Synthesis of 7-Alkynylcyclohepta-1,3,5-trienes (**1**)



The terminal alkyne substrate (2.5 mmol) was placed in an oven-dried 25 mL screw-cap tube fitted with a septum under a nitrogen atmosphere. Dry THF (15 mL, 0.17 M) was added and the resulting solution was cooled to -78 °C before adding *n*-BuLi (1.6 M in hexanes, 1.6 mL, 2.56 mmol, 1.1 equiv) and stirring for 40 minutes at this temperature. Solid tropylium tetrafluoroborate (445 mg, 2.5 mmol, 1 equiv) was added, the cooling bath removed, and the mixture stirred at room temperature for 5 h. The reaction was quenched with an aqueous solution of NH₄Cl (30 mL, saturated) then extracted with EtOAc (3×20 mL). The combined organic extracts were dried over MgSO₄ and solvent was removed under reduced pressure. The crude residue was purified by column chromatography on silica gel with cyclohexane as eluent unless otherwise stated.

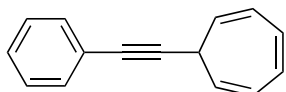
7-(*p*-Tolyloethynyl)cyclohepta-1,3,5-triene (**1a**)



The title compound **1a** was obtained from 1-ethynyl-4-methylbenzene (10 mmol scale) as a yellow, waxy solid (1.8389 g, 8.92 mmol, 89%). ¹H NMR (500 MHz, CDCl₃) δ 7.36 (d, *J* = 8.1 Hz, 2H), 7.12 (d, *J* = 8.0 Hz, 2H), 6.72 – 6.66 (m, 2H), 6.25 – 6.18 (m, 2H), 5.43 (dd, *J* = 9.0, 5.5 Hz, 2H), 2.70 (tt, *J* = 5.5, 1.6 Hz, 1H), 2.35 (s, 3H). ¹³C NMR (126 MHz, CDCl₃) δ 138.08, 131.73, 131.15, 129.14, 124.83, 123.53, 120.52, 90.42,

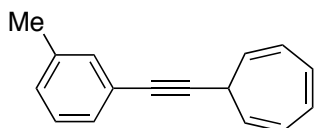
80.81, 32.44, 21.59. HRMS-APCI $m/z = 207.1162$ $[M+H]^+$, calculated for $C_{16}H_{15}$:
207.1174

7-(Phenylethynyl)cyclohepta-1,3,5-triene (1b)



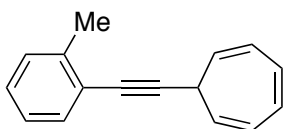
The title compound **1b** was obtained from phenylacetylene as a yellow oil (356 mg, 1.85 mmol, 74%). 1H NMR (500 MHz, $CDCl_3$) δ 7.49 – 7.44 (m, 2H), 7.33 – 7.29 (m, 3H), 6.69 (dd, $J = 3.6, 2.6$ Hz, 2H), 6.25 – 6.18 (m, 2H), 5.43 (dd, $J = 8.8, 5.4$ Hz, 2H), 2.71 (tt, $J = 5.5, 1.5$ Hz, 1H). ^{13}C NMR (126 MHz, $CDCl_3$) δ 131.86, 131.17, 128.39, 128.06, 124.91, 123.61, 123.35, 91.19, 80.76, 32.40. HRMS-APCI $m/z = 193.1018$ $[M+H]^+$, calculated for $C_{15}H_{13}$: 193.1017

*7-(*m*-Tolylethynyl)cyclohepta-1,3,5-triene (1c)*



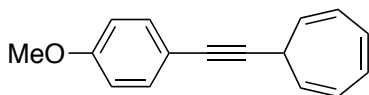
The title compound **1c** was obtained from 1-ethynyl-3-methylbenzene as a yellow oil (291 mg, 1.41 mmol, 73%). 1H NMR (500 MHz, $CDCl_3$) δ 7.32 – 7.24 (m, 2H), 7.19 (t, $J = 7.6$ Hz, 1H), 7.11 (d, $J = 7.5$ Hz, 1H), 6.69 (t, $J = 3.2$ Hz, 2H), 6.25 – 6.18 (m, 2H), 5.43 (dd, $J = 9.0, 5.4$ Hz, 2H), 2.70 (tt, $J = 5.5, 1.5$ Hz, 1H), 2.33 (s, 3H). ^{13}C NMR (126 MHz, $CDCl_3$) δ 138.05, 132.48, 131.16, 128.95, 128.91, 128.29, 124.87, 123.44, 123.39, 90.82, 80.89, 32.41, 21.37. HRMS-APCI $m/z = 207.1165$ $[M+H]^+$, calculated for $C_{16}H_{15}$: 207.1174

7-(o-Tolyethynyl)cyclohepta-1,3,5-triene (1d)



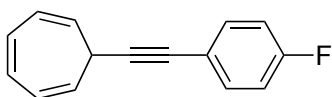
The title compound **1d** was obtained from 1-ethynyl-2-methylbenzene as a yellow oil (363 mg, 1.76 mmol, 71%). ¹H NMR (500 MHz, CDCl₃) δ 7.43 (d, *J* = 7.3 Hz, 1H), 7.22 – 7.17 (m, 2H), 7.13 (dt, *J* = 8.6, 4.3 Hz, 1H), 6.69 (dd, *J* = 3.7, 2.7 Hz, 2H), 6.26 – 6.19 (m, 2H), 5.45 (dd, *J* = 9.1, 5.5 Hz, 2H), 2.77 (tt, *J* = 5.5, 1.4 Hz, 1H), 2.46 (s, 3H). ¹³C NMR (126 MHz, CDCl₃) δ 140.31, 132.07, 131.18, 129.49, 128.04, 125.62, 124.91, 123.60, 123.33, 95.19, 79.61, 32.55, 20.89. HRMS-APCI *m/z* = 207.1164 [M+H]⁺, calculated for C₁₆H₁₅: 207.1174

7-((4-Methoxyphenyl)ethynyl)cyclohepta-1,3,5-triene (1e)



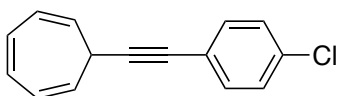
The title compound **1e** was obtained from 1-ethynyl-4-methoxybenzene as a yellow solid (356 mg, 1.85 mmol, 74%). The isolation of the product was achieved with CH₂Cl₂/cyclohexane (1:99). M.p. = 69 – 71 °C. ¹H NMR (500 MHz, CDCl₃) δ 7.44 – 7.36 (m, 2H), 6.86 – 6.82 (m, 2H), 6.68 (dd, *J* = 3.6, 2.7 Hz, 2H), 6.24 – 6.17 (m, 2H), 5.43 (dd, *J* = 8.6, 5.5 Hz, 2H), 3.81 (s, 3H), 2.68 (tt, *J* = 5.5, 1.5 Hz, 1H). ¹³C NMR (126 MHz, CDCl₃) δ 159.46, 133.22, 131.15, 124.80, 123.63, 115.74, 114.02, 89.66, 80.52, 55.43, 32.44. HRMS-APCI *m/z* = 223.1124 [M+H]⁺, calculated for C₁₆H₁₅O: 223.1123

7-((4-Fluorophenyl)ethynyl)cyclohepta-1,3,5-triene (1f)



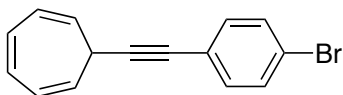
The title compound **1f** was obtained from 1-ethynyl-4-fluorobenzene as a yellow oil (446 mg, 2.12 mmol, 85%). ¹H NMR (500 MHz, CDCl₃) δ 7.47 – 7.41 (m, 2H), 7.04 – 6.97 (m, 2H), 6.72 – 6.67 (m, 2H), 6.25 – 6.19 (m, 2H), 5.42 (dd, *J* = 8.9, 5.5, 2H), 2.70 (t, *J* = 5.5, 1H). ¹³C NMR (126 MHz, CDCl₃) δ 133.40, 131.71, 131.27, 125.12, 122.96, 122.65, 122.29, 92.49, 79.85, 32.43. ¹⁹F NMR (376 MHz, CDCl₃) δ 111.69. HRAPCI-MS *m/z* = 211.0919, calc. for C₁₅H₁₂F = 211.0923. HRMS-APCI *m/z* = 211.0919 [M+H]⁺, calc. for C₁₅H₁₂F = 211.0923.

7-((4-Chlorophenyl)ethynyl)cyclohepta-1,3,5-triene (1g)



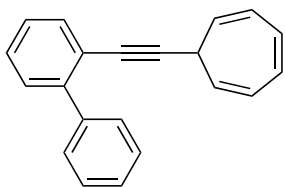
The title compound **1g** was obtained from 1-chloro-4-ethynylbenzene as a yellow oil (356 mg, 1.68 mmol, 67%). ¹H NMR (500 MHz, CDCl₃) δ 7.41 – 7.37 (m, 2H), 7.30 – 7.27 (m, 2H), 6.69 (dd, *J* = 3.5, 2.8, 2H), 6.22 (dddd, *J* = 8.7, 3.8, 2.5, 1.4, 2H), 5.41 (dd, *J* = 8.7, 5.6, 2H), 2.71 (tt, *J* = 5.5, 1.3, 1H). ¹³C NMR (126 MHz, CDCl₃) δ 134.11, 133.16, 131.27, 128.78, 125.10, 123.02, 122.18, 92.29, 79.79, 32.41. HRMS-APCI *m/z* = 227.0616 [M+H]⁺, calc. for C₁₅H₁₂Cl = 227.0628.

7-((4-Bromophenyl)ethynyl)cyclohepta-1,3,5-triene (1b)



The title compound **1b** was obtained from 1-bromo-4-ethynylbenzene as a colorless oil that solidified upon standing (319 mg, 1.18 mmol, 47%). M.p. = 60 – 61 °C. ¹H NMR (500 MHz, CDCl₃) δ 7.48 – 7.41 (m, 2H), 7.35 – 7.29 (m, 2H), 6.72 – 6.66 (m, 2H), 6.22 (dddd, *J* = 8.7, 3.8, 2.6, 1.4, 2H), 5.41 (dd, *J* = 8.7, 5.5, 2H), 2.70 (ddd, *J* = 5.5, 4.2, 1.3, 1H). ¹³C NMR (126 MHz, CDCl₃) δ 133.40, 131.71, 131.27, 125.12, 122.96, 122.65, 122.29, 92.49, 79.85, 32.43. HRMS-APCI *m/z* = 271.0118 [M+H]⁺, calc. for C₁₅H₁₂⁷⁹Br = 271.0122.

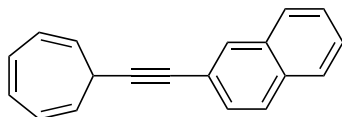
2-(Cyclohepta-2,4,6-trien-1-ylethynyl)-1,1'-biphenyl (1i)



2-ethynyl-1,1'-biphenyl (177 mg, 993 μmol, prepared according to a literature procedure: John, J. A.; Tour, J. M. *Tetrahedron* **1997**, *53*, 15515–15534) was placed in an oven-dried 25 mL screw-cap tube fitted with a septum under a nitrogen atmosphere. Dry THF (8 mL, 0.125 M) was added and resulting solution was cooled to -78 °C before adding *n*-BuLi (1.6 M in hexanes, 0.68 mL, 1.09 mmol, 1.1 equiv) and stirring for 40 minutes at this temperature. Solid tropyllium tetrafluoroborate (194 mg, 1.09 mmol, 1.1 equiv) was added, the cooling bath removed, and the mixture stirred at room temperature for 5 h. The reaction was quenched with an aqueous solution of NH₄Cl (30 mL, saturated) then extracted with EtOAc (3×20 mL). The combined

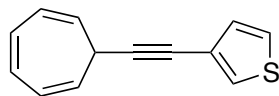
organic extracts were dried over MgSO_4 and solvent was removed under reduced pressure. The crude residue was purified by column chromatography on silica gel with 9:1 cyclohexane- CH_2Cl_2 as eluent. The title compound **1i** was obtained as a yellow oil (234 mg, 0.87 mmol, 88%). ^1H NMR (500 MHz, CDCl_3) δ 7.67 – 7.62 (m, 2H), 7.59 (d, $J = 7.3$ Hz, 1H), 7.45 – 7.35 (m, 5H), 7.30 (td, $J = 7.5, 1.9$ Hz, 1H), 6.68 – 6.60 (m, 2H), 6.20 – 6.12 (m, 2H), 5.27 (dd, $J = 8.9, 5.5$ Hz, 2H), 2.62 (t, $J = 5.5$ Hz, 1H). ^{13}C NMR (126 MHz, CDCl_3) δ 144.09, 140.79, 133.24, 131.08, 129.56, 129.45, 128.30, 127.98, 127.50, 127.10, 124.80, 123.15, 121.89, 93.97, 80.38, 32.49. HRMS-APCI m/z = 269.1317 $[\text{M}+\text{H}]^+$, calc. for $\text{C}_{21}\text{H}_{17}$ = 269.1330.

2-(Cyclohepta-2,4,6-trien-1-ylethynyl)naphthalene (1j)



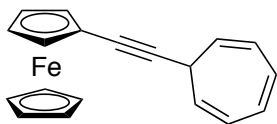
The title compound **1j** was obtained from 2-ethynynaphthalene as a pale yellow oil that solidified upon standing (489 mg, 2.02 mmol, 81%). M.p. = 62 – 64 °C. ^1H NMR (500 MHz, CDCl_3) δ 7.99 (d, $J = 1.6$ Hz, 1H), 7.85 – 7.76 (m, 3H), 7.55 – 7.45 (m, 3H), 6.71 (t, $J = 3.1$ Hz, 2H), 6.25 (ddd, $J = 10.7, 3.8, 1.6$ Hz, 2H), 5.48 (dd, $J = 8.9, 5.4$ Hz, 2H), 2.77 (tt, $J = 5.5, 1.5$ Hz, 1H). ^{13}C NMR (126 MHz, CDCl_3) δ 133.16, 132.80, 131.55, 131.20, 128.83, 128.03, 127.87, 127.80, 126.59, 124.96 (2 \times C), 123.29, 120.92, 91.56, 81.12, 32.49. HRMS-APCI m/z = 243.1181 $[\text{M}+\text{H}]^+$, calc. for $\text{C}_{19}\text{H}_{15}$ = 243.1174.

3-(Cyclohepta-2,4,6-trien-1-ylethynyl)thiophene (1k)



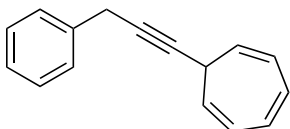
The title compound **1k** was obtained from 3-ethynylthiophene as a pale yellow oil (392 mg, 1.97 mmol, 79%). ^1H NMR (500 MHz, CDCl_3) δ 7.43 (dd, $J = 3.0, 1.2$ Hz, 1H), 7.26 (dd, $J = 5.2, 3.0$ Hz, 1H), 7.13 (dd, $J = 5.1, 1.2$ Hz, 1H), 6.69 (t, $J = 3.2$ Hz, 2H), 6.25 – 6.17 (m, 2H), 5.42 (dd, $J = 9.0, 5.5$ Hz, 2H), 2.69 (tt, $J = 5.5, 1.5$ Hz, 1H). ^{13}C NMR (126 MHz, CDCl_3) δ 131.17, 130.18, 128.39, 125.28, 124.92, 123.25, 122.57, 90.72, 75.84, 32.39. HRMS-APCI $m/z = 199.0582$ $[\text{M}+\text{H}]^+$, calc. for $\text{C}_{13}\text{H}_{11}\text{S} = 199.0581$.

(Cyclohepta-2,4,6-trien-1-ylethynyl)ferrocene (1l)



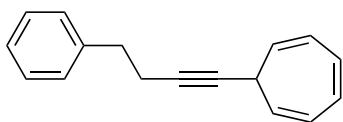
The title compound **1l** was obtained from ethynylferrocene (1.0 mmol scale) as an orange solid (155 mg, 0.52 mmol, 52%). M.p.: 98 – 100 °C. ^1H NMR (400 MHz, CDCl_3) δ 6.72 – 6.63 (m, 2H), 6.28 – 6.12 (m, 2H), 5.47 – 5.32 (m, 2H), 4.44 – 4.39 (m, 2H), 4.21 (s, 5H), 4.19 – 4.15 (m, 2H), 2.59 (tt, $J = 5.4, 1.4$ Hz, 1H). ^{13}C NMR (101 MHz, CDCl_3) δ 131.13, 124.70, 123.82, 87.38, 78.68, 71.49, 70.04, 68.50, 65.86, 32.57. HRMS-ESI $m/z = 300.0607$ $[\text{M}]^+$, calc. for $\text{C}_{19}\text{H}_{16}\text{Fe} = 300.0601$.

7-(3-Phenylprop-1-yn-1-yl)cyclohepta-1,3,5-triene (1m)



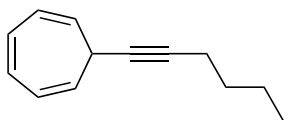
The title compound **1m** was obtained from prop-2-yn-1-ylbenzene as a yellow oil (341 mg, 1.65 mmol, 66%). ¹H NMR (500 MHz, CDCl₃) δ 7.41 – 7.35 (m, 2H), 7.35 – 7.30 (m, 2H), 7.26 – 7.21 (m, 1H), 6.65 (dd, *J* = 3.6, 2.6 Hz, 2H), 6.23 – 6.10 (m, 2H), 5.37 (dd, *J* = 8.9, 5.5 Hz, 2H), 3.66 (d, *J* = 2.3 Hz, 2H), 2.58 – 2.49 (m, 1H). ¹³C NMR (126 MHz, CDCl₃) δ 137.29, 131.11, 128.60, 128.01, 126.65, 124.70, 124.10, 83.96, 78.09, 32.00, 25.24. HRMS-APCI *m/z* = 207.1164 [M+H]⁺, calculated for C₁₆H₁₅: 207.1174.

7-(4-Phenylbut-1-yn-1-yl)cyclohepta-1,3,5-triene (1n)



The title compound **1n** was obtained from but-3-yn-1-ylbenzene (1.0 mmol scale) as a yellow oil (177.4 mg, 0.805 mmol, 81%). ¹H NMR (500 MHz, CDCl₃) δ 7.34 – 7.27 (m, 2H), 7.26 – 7.19 (m, 3H), 6.64 (dd, *J* = 3.7, 2.5 Hz, 2H), 6.18 – 6.10 (m, 2H), 5.29 (dd, *J* = 8.8, 5.5 Hz, 2H), 2.85 (t, *J* = 7.6 Hz, 2H), 2.52 (td, *J* = 7.6, 2.3 Hz, 2H), 2.47 – 2.40 (m, 1H). ¹³C NMR (126 MHz, CDCl₃) δ 141.00, 131.07, 128.66, 128.46, 126.36, 124.59, 124.25, 82.46, 79.95, 35.57, 31.92, 21.16. HRMS-APCI *m/z* = 221.1325 [M+H]⁺, calculated for C₁₇H₁₇: 221.1330.

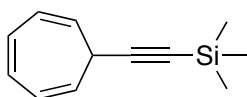
7-(Hex-1-yn-1-yl)cyclohepta-1,3,5-triene (1p)



The title compound **1p** was obtained from hex-1-yne as a colorless oil (369 mg, 2.14 mmol, 86%). ¹H NMR (500 MHz, CDCl₃) δ 6.64 (dd, *J* = 3.6, 2.7 Hz, 2H), 6.15 (dddd, *J* = 8.9, 3.9, 2.5, 1.5 Hz, 2H), 5.35 – 5.29 (m, 2H), 2.47 – 2.41 (m, 1H), 2.23 (td, *J* = 7.0,

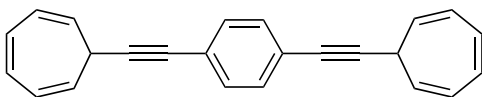
2.2 Hz, 2H), 1.56 – 1.39 (m, 4H), 0.93 (t, $J = 7.2$ Hz, 3H). ^{13}C NMR (126 MHz, CDCl_3) δ 131.07, 124.52 (2 \times C), 81.59, 80.72, 31.96, 31.22, 22.09, 18.56, 13.80. HRMS-APCI $m/z = 173.1331$ $[\text{M}+\text{H}]^+$, calculated for $\text{C}_{13}\text{H}_{17}$: 173.1330.

(Cyclohepta-2,4,6-trien-1-ylethynyl)trimethylsilane (1q)



The title compound **1q** was obtained from ethynyltrimethylsilane as a red oil (139 mg, 0.74 mmol, 30%) following the general procedure but performing the lithiation step at 0 °C. ^1H NMR (500 MHz, CDCl_3) δ 6.66 – 6.63 (m, 2H), 6.19 – 6.14 (m, 2H), 5.32 (dd, $J = 8.7, 5.5$ Hz, 2H), 2.50 (tt, $J = 5.4, 1.4$ Hz, 1H), 0.19 (s, 9H). ^{13}C NMR (126 MHz, CDCl_3) δ 131.07, 124.81, 123.18, 108.18, 84.73, 32.74, 0.26. HRMS-APCI $m/z = 187.0948$ $[\text{M}-\text{H}]^+$, calc. for $\text{C}_{12}\text{H}_{15}\text{Si}$ = 187.0943.

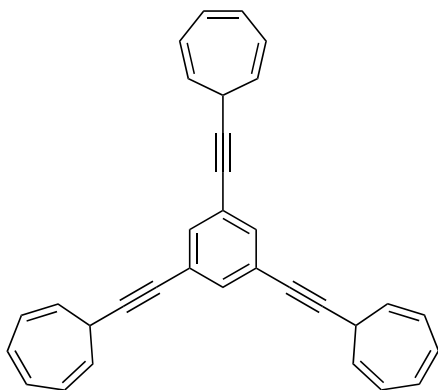
1,4-Bis(cyclohepta-2,4,6-trien-1-ylethynyl)benzene (1r)



1,4-diethynylbenzene (315 mg, 2.5 mmol, 1 equiv) was placed in an oven-dried 25 mL screw-cap tube fitted with a septum under a nitrogen atmosphere and dry THF (20 mL, 0.125 M) was added. The resulting solution was cooled to -78 °C before adding *n*-BuLi (1.6 M in hexanes, 3.4 mL, 5.5 mmol, 2.2 equiv) and stirring for 40 minutes at this temperature. Solid tropyllium tetrafluoroborate (934 mg, 5.25 mmol, 2.1 equiv) was added, the cooling bath removed, and the mixture stirred at room temperature for 5 h. The reaction was quenched with an aqueous solution of NH_4Cl (30 mL, saturated)

then extracted with EtOAc (3×20 mL). The combined organic extracts were dried over MgSO₄ and solvent was removed under reduced pressure. The crude residue was purified by column chromatography (SiO₂, cyclohexane) to give the title compound **1r** as a colorless solid (512 mg, 1.67 mmol, 67%). M.p. = 93 – 96 °C. ¹H NMR (400 MHz, CDCl₃) δ 7.40 (s, 4H), 6.73 – 6.66 (m, 4H), 6.22 (dddd, *J* = 8.8, 3.8, 2.5, 1.4 Hz, 4H), 5.46 – 5.38 (m, 4H), 2.72 (tt, *J* = 5.5, 1.4 Hz, 2H). ¹³C NMR (101 MHz, CDCl₃) δ 131.72, 131.19, 125.00, 123.15, 123.06, 92.84, 80.51, 32.43. HRMS-APCI *m/z* = 307.1491 [M+H]⁺, calc. for C₂₄H₁₉ = 307.1487.

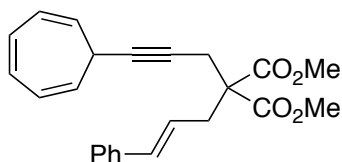
1,3,5-Tris(cyclohepta-2,4,6-trien-1-ylethynyl)benzene (1s)



1,3,5-triethynylbenzene (375 mg, 2.5 mmol, 1 equiv) was placed in an oven-dried 25 mL screw-cap tube fitted with a septum under a nitrogen atmosphere and dry THF (20 mL, 0.125 M) was added. The resulting solution was cooled to -78 °C before adding *n*-BuLi (1.6 M in hexanes, 5.0 mL, 8.0 mmol, 3.2 equiv) and stirring for 40 minutes at this temperature. Solid tropyllium tetrafluoroborate (1.38 g, 7.75 mmol, 3.1 equiv) was added, the cooling bath removed, and the mixture stirred at room temperature for 5 h. The reaction was quenched with an aqueous solution of NH₄Cl (30 mL, saturated) then extracted with EtOAc (3×20 mL). The combined organic extracts were dried over MgSO₄ and solvent was removed under reduced pressure. The crude residue was purified by column chromatography (SiO₂, eluent 1. cyclohexane then 2. 9:1

cyclohexane-CH₂Cl₂) followed by recrystallization from cyclohexane (7 mL) to give the title compound **1s** as a colorless solid (240 mg, 0.57 mmol, 23%). M.p. = 158 – 161 °C. ¹H NMR (500 MHz, CDCl₃) δ 7.49 (s, 3H), 6.72 – 6.67 (m, 6H), 6.26 – 6.19 (m, 6H), 5.40 (dd, *J* = 9.1, 5.5 Hz, 6H), 2.72 (t, *J* = 5.4 Hz, 3H). ¹³C NMR (126 MHz, CDCl₃) δ 134.34, 131.20, 125.07, 124.07, 122.90, 92.22, 79.42, 32.29. HRMS-APCI *m/z* = 421.1954 [M+H]⁺, calc. for C₃₃H₂₅ = 421.1956.

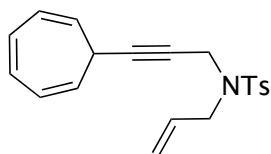
Dimethyl 2-cinnamyl-2-(3-(cyclohepta-2,4,6-trien-1-yl)prop-2-yn-1-yl)malonate
(**5**)



LiHMDS (1.0 M, 5.0 mL, 5.0 mmol) was added dropwise to the solution of dimethyl 2-cinnamyl-2-(prop-2-yn-1-yl)malonate (1.2 g, 4.2 mmol, synthesized according to the procedure reported in: Jiménez-Núñez, E.; Claverie, C. K.; Bour, C.; Cárdenas, D. J.; Echavarren, A. M. *Angew. Chem. Int. Ed.* **2008**, *47*, 7892–7895) in 10 mL dry THF at -78 °C. The mixture was stirred for 30 min at -78 °C then tropylium tetrafluoroborate (822 mg, 4.62 mmol) was added in one portion. The cooling bath was removed and the reaction was stirred at rt overnight. The reaction was quenched by addition of a saturated aqueous solution of NH₄Cl. The aqueous phase was extracted with diethyl ether, the combined organic extracts were dried over MgSO₄, and the solvent was evaporated under reduced pressure. The crude reaction mixture was purified by chromatography using cyclohexane/EtOAc as eluent (30:1) to give the title compound **5** (555 mg, 1.47 mmol, 35%) as a yellow oil. ¹H NMR (400 MHz, CDCl₃) δ 7.38 – 7.25 (m, 5H), 6.67 (dd, *J* = 3.7, 2.7 Hz, 2H), 6.54 (d, *J* = 15.7 Hz, 1H), 6.21 – 6.16 (m, 2H), 6.06 (dt, *J* = 15.5, 7.6 Hz, 1H), 5.31 (dd, *J* = 9.0, 5.4 Hz, 2H), 3.78 (s, 6H), 3.01 (dd, *J* = 7.6, 1.3 Hz, 2H), 2.91 (d, *J* = 2.3 Hz, 2H), 2.52 - 2.49 (m, 1H). ¹³C NMR (126 MHz,

CDCl_3) δ 170.4, 137.0, 134.4, 130.9, 128.4, 127.4, 126.2, 124.6, 123.6, 123.4, 85.1, 74.8, 57.6, 52.7, 36.0, 31.6, 23.2. HRMS-APCI m/z = 399.1567 $[\text{M}+\text{Na}]^+$, calc. for $\text{C}_{24}\text{H}_{24}\text{O}_4\text{Na}$ = 399.1572.

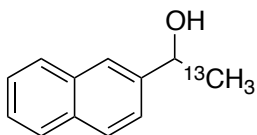
N-Allyl-N-(3-(cyclohepta-2,4,6-trien-1-yl)prop-2-yn-1-yl)-4-methylbenzenesulfonamide (6)



BuLi (1.6 M, 1.5 mL, 2.4 mmol) was added dropwise to the solution of *N*-allyl-4-methyl-*N*-(prop-2-yn-1-yl)benzenesulfonamide (500 mg, 2 mmol, synthesized according to the procedure reported in: Jiménez-Núñez, E.; Claverie, C. K.; Bour, C.; Cárdenas, D. J.; Echavarren, A. M. *Angew. Chem. Int. Ed.* **2008**, *47*, 7892–7895) in dry THF (20mL, 0.1 M) at -78 °C. The mixture was stirred for 30 min at -78 °C, and then tropylium tetrafluoroborate (356 mg, 2 mmol) was added in one portion. The cooling bath was removed and the reaction was stirred at rt overnight. The reaction was quenched by addition of a saturated aqueous solution of NH_4Cl . The aqueous phase was extracted with diethyl ether, the combined organic extracts were dried over MgSO_4 , and the solvent was evaporated under reduced pressure. The crude reaction mixture was purified by chromatography using cyclohexane/EtOAc as eluent (20:1) to give the title compound **6** (378 mg, 1.11 mmol, 56%) as yellow solid. M.p. = $72.4 - 73.6$ °C. ^1H NMR (500 MHz, CDCl_3) δ 7.77 (d, J = 8.3 Hz, 2H), 7.29 (d, J = 8.2 Hz, 2H), 6.64 (t, J = 3.1 Hz, 2H), 6.18 – 6.06 (m, 2H), 5.80 (ddt, J = 16.7, 10.1, 6.5 Hz, 1H), 5.33 (dd, J = 17.1, 1.5 Hz, 1H), 5.27 (dd, J = 10.0, 1.4 Hz, 1H), 4.97 (dd, J = 9.0, 5.4 Hz, 2H), 4.15 (d, J = 2.1 Hz, 2H), 3.88 (d, J = 6.4 Hz, 2H), 2.39 (s, 3H), 2.20 – 2.17 (m, 1H). ^{13}C NMR (126 MHz, CDCl_3) δ 143.4, 136.0, 132.1, 130.9, 129.5, 127.8, 124.6,

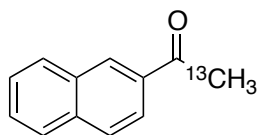
122.9, 119.8, 87.3, 72.5, 49.1, 36.2, 31.3, 21.5. HRMS-APCI $m/z = 362.1191$ $[M+Na]^+$,
calc. for $C_{20}H_{21}NO_2SNa = 362.1198$.

1-(Naphthalen-2-yl)-(2-¹³C)ethanol (10)



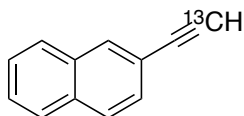
A solution of iodomethane-¹³C (1.0 g, 7.0 mmol) in dry diethyl ether (1.2 mL) was added at a rate of 0.2 mL/min to a suspension of magnesium turnings (170 mg, 7.0 mmol) in dry diethyl ether (5 mL) under an argon atmosphere. The resulting mixture was refluxed for 1.5 h and then cooled to 0 °C. A solution of naphthaldehyde (1.203 g) in dry diethyl ether (15.5 mL) was added at the same rate as previously and the mixture was stirred at 0 °C for 10 minutes after the addition was completed. The reaction was quenched with aqueous NH₄Cl (saturated), the phases were separated and the aqueous phase was extracted with diethyl ether. The solvent was removed under reduced pressure and the crude was purified by column chromatography using ethyl acetate/cyclohexane (5:95) as eluent. The title compound **10** was obtained as a white solid (939 mg, 5.42 mmol, 77 %). ¹H NMR (400 MHz, CDCl₃) δ 7.98 – 7.73 (m, 4H), 7.60 – 7.42 (m, 3H), 5.11 (d, *J* = 6.5 Hz, 1H), 1.61 (dd, *J*_{CH} = 126.8 Hz, *J* = 6.5 Hz, 3H). ¹³C NMR (126 MHz, CDCl₃) δ 143.32, 133.48, 133.08, 128.48, 128.08, 127.82, 126.31, 125.96, 125.46 (d, *J*_{CC} = 37.0 Hz), 123.95, 70.71 (d, *J*_{CC} = 38.4 Hz), 25.31 (¹³C label). LRMS-EI $m/z = 173.1$ $[M]^+$, calc. for $C_{11}^{13}CH_{12}O = 173.09$.

¹³C-Methyl naphthyl ketone (11)



A solution of 1-(naphthalen-2-yl)-(2-¹³C)ethanol (767 mg, 4.43 mmol) in dry CH₂Cl₂ (6.3 mL) was added to a stirred solution of the Dess-Martin periodinane reagent (2.25 g, 5.31 mmol) in dry CH₂Cl₂ (19 mL) under a nitrogen atmosphere at room temperature. The reaction was stirred for 2 h and then poured into a separatory funnel containing aqueous NaOH (10 %, 6 mL) and diethyl ether (12 mL). The layers were separated and the organic layer was washed with water (2 × 6 mL), dried over MgSO₄ and the solvent removed under reduced pressure. The crude was purified by flash chromatography using cyclohexane as eluent. The desired product **11** was obtained as a yellow solid (709 mg, 4.14 mmol, 94%). ¹H NMR (400 MHz, CDCl₃) δ 8.47 (s, 1H), 8.04 (dd, *J* = 8.7, 1.8 Hz, 1H), 8.00 – 7.95 (m, 1H), 7.94 – 7.85 (m, 2H), 7.66 – 7.51 (m, 2H), 2.73 (d, *J*_{CH} = 127.5 Hz, 3H). ¹³C NMR (101 MHz, CDCl₃) δ 198.21 (d, *J*_{CC} = 42.9 Hz), 135.73, 134.65 (d, *J*_{CC} = 13.5 Hz), 130.32, 129.68, 128.60, 128.56, 127.92, 126.91 (2×C), 124.04, 26.83 (¹³C label). LRMS-EI *m/z* = 171.1 [M]⁺, calc. for C₁₁¹³CH₁₀O = 171.08.

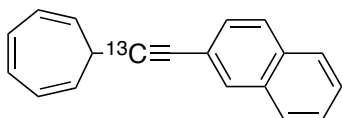
2-[(2-¹³C)Ethyne]naphthalene (12)



Phosphazene base P1-t-Bu-tris(tetramethylene) (242 μL, 0.79 mmol, 2.2 equiv) was added in one lot to a vigorously stirred mixture of ¹³C-methyl naphthyl ketone (62 mg, 0.36 mmol) and nonafluorobutanesulfonyl fluoride (78 μL, 0.43 mmol, 1.2 equiv) in

dry DMF (0.4 mL) at -10 °C. The reaction mixture was allowed to warm to 20 °C for the following 2 hours. Then it was stirred for 20 hours at room temperature. The resulting solution was adsorbed on fluorisil and it was purified by flash chromatography. Elution with cyclohexane afforded the title compound **12** as a yellow oil that solidified upon standing (23.3 mg, 0.15 mmol, 42%). ¹H NMR (500 MHz, CDCl₃) δ 8.03 (s, 1H), 7.84 – 7.76 (m, 3H), 7.54 – 7.48 (m, 3H), 3.15 (d, ¹J_{CH} = 251.0 Hz, 1H). ¹³C NMR (126 MHz, CDCl₃) δ 133.19, 132.97, 132.45 (d, J_{CC} = 3.2 Hz), 128.69 (d, J_{CC} = 2.3 Hz), 128.17, 127.93, 127.91, 127.05, 126.76, 119.52 (d, J_{CC} = 12.7 Hz), 84.20 (d, ¹J_{CC} = 176.1 Hz), 77.54 (¹³C label). LRMS-EI *m/z* = 153.1 [M]⁺, calc. for C₁₁¹³CH₈ = 153.07.

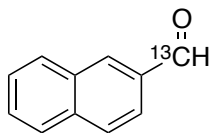
2-(Cyclohepta-2,4,6-trien-1-yl(2-¹³C)ethynyl)naphthalene (**1j'**)



2-[(2-¹³C)Ethynyl]naphthalene (14.6 mg, 95 μmol) was placed in an oven-dried 2 mL microwave vial under a nitrogen atmosphere. Dry THF (0.76 mL, 0.125 M) was added and the resulting solution was cooled to -78 °C before adding n-BuLi (1.6 M in hexanes, 71.5 μL, 114 μmol, 1.2 equiv) and stirring for 40 minutes at this temperature. Solid tropylium tetrafluoroborate (33.9 mg, 191 μmol, 2 equiv) was added, the cooling bath removed, and the mixture stirred at room temperature for 5 h. The reaction was quenched with an aqueous solution of NH₄Cl (5 mL, saturated) then extracted with EtOAc (3×5 mL). The combined organic extracts were dried over MgSO₄ and solvent was removed under reduced pressure. The crude residue was purified by preparative TLC with cyclohexane as eluent to give the title compound **1j'** (18.3 mg, 75 μmol, 79%) as a yellow oil that solidified upon standing. ¹H NMR (500 MHz, CDCl₃) δ 7.99 (s, 1H), 7.84 – 7.76 (m, 3H), 7.54 – 7.46 (m, 3H), 6.74 – 6.68 (m, 2H), 6.28 – 6.22 (m,

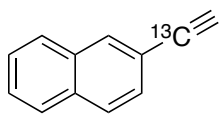
2H), 5.48 (dt, $J = 9.0, 5.3$ Hz, 2H), 2.77 (t, $^2J_{CH} = 10.0$ Hz, $J = 6.5$ Hz, 1H). ^{13}C NMR (126 MHz, CDCl_3) δ 133.16, 132.80, 131.53, 131.20, 128.82 (d, $J = 2.6$ Hz), 128.03, 127.87, 127.80, 126.59, 124.96 (d, $J_{CC} = 6.3$ Hz), 123.28 (d, $J_{CC} = 3.6$ Hz), 120.92 (d, $J_{CC} = 12.9$ Hz), 91.56 (^{13}C label), 81.04 (d, $^1J_{CC} = 179.4$ Hz), 32.48 (d, $^1J_{CC} = 73.6$ Hz). HRMS-APCI $m/z = 244.1196$ $[\text{M}+\text{H}]^+$, calc. for $\text{C}_{18}\text{H}_{15}^{13}\text{C} = 244.1207$.

2- Naphthaldehyde-(carbonyl- ^{13}C) (**13**)



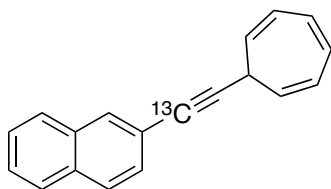
n-Butyl lithium (5.1 mL, 8.17 mmol, 1.1 equiv) was added to a stirred solution of 2-bromonaphthalene (1.538 g, 7.43 mmol, 1 equiv) in THF (25 mL, 0.3 M) at -78 °C under an argon atmosphere. The resulting mixture was stirred for 30 minutes at the same temperature and then *N,N*-dimethyl formamide-(carbonyl- ^{13}C) (0.52 mL, 6.75 mmol, 0.9 equiv) was added. The mixture was warmed to room temperature and finally quenched with aqueous NH_4Cl (saturated). The phases were separated and the organic phase was dried over MgSO_4 . The solvent was removed under reduced pressure and the crude material was purified by flash chromatography (ethyl acetate/cyclohexane, 1:9) to afford the desired product **13** as a white solid (823.8 mg, 5.24 mmol, 78%). ^1H NMR (400 MHz, CDCl_3) δ 10.17 (d, $^2J_{CH} = 174.3$ Hz, 1H), 8.35 (dd, $J = 6.5, 1.1$ Hz, 1H), 8.02 (ddd, $J = 8.1, 1.5, 0.7$ Hz, 1H), 7.99 – 7.94 (m, 2H), 7.94 – 7.89 (m, 1H), 7.62 (dddd, $J = 22.8, 8.2, 6.9, 1.3$ Hz, 2H). ^{13}C NMR (101 MHz, CDCl_3) δ 192.41 (^{13}C label), 136.62, 134.70 (d, $J_{CC} = 5.4$ Hz), 134.26 (d, $J_{CC} = 53.8$ Hz), 132.80 (d, $J_{CC} = 5.4$ Hz), 129.68, 129.25 (d, $J_{CC} = 3.4$ Hz), 128.23, 127.24, 122.93 (d, $J_{CC} = 2.8$ Hz). LRMS-EI $m/z = 157.1$ $[\text{M}]^+$, calc. for $\text{C}_{10}^{13}\text{CH}_8\text{O} = 157.06$.

2-[(1-¹³C)Ethyanyl]naphthalene (14)



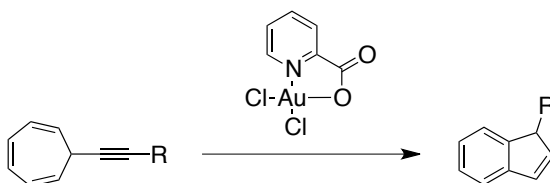
To a solution of 2-naphthaldehyde-(carbonyl-¹³C) (157.2 mg, 1.0 mmol) and K₂CO₃ (276 mg, 2.0 mmol, 2 equiv) in dry methanol (15 mL, 0.067 M) was added dimethyl-1-diazo-oxopropylphosphonate (230 mg, 1.2 mmol, 1.2 equiv) at room temperature (following the procedure of Müller, S.; Liepold, B.; Roth, G. J.; Bestman, H. J. *Synlett* **1996**, 521-522). The resulting mixture was stirred for 6 hours until the starting material was consumed (verification by TLC). The reaction was diluted with diethyl ether and washed with aqueous NaHCO₃ (saturated). The solvents were removed under reduced pressure and the crude was purified by flash chromatography (ethyl acetate/cyclohexane, 1:9) to afford the desired product **14** as a yellow solid (128.7 mg, 0.85 mmol, 85%). ¹H NMR (300 MHz, CDCl₃) δ 8.02 (d, *J* = 5.8 Hz, 1H), 7.90 – 7.70 (m, 3H), 7.65 – 7.37 (m, 3H), 3.14 (d, ²*J*_{CH} = 49.5 Hz, 1H). ¹³C NMR (101 MHz, CDCl₃) δ 133.18 (d, *J*_{CC} = 1.4 Hz), 132.96 (d, *J*_{CC} = 6.1 Hz), 132.44 (d, *J*_{CC} = 1.5 Hz), 128.68 (d, *J*_{CC} = 2.2 Hz), 128.16 (d, *J*_{CC} = 5.3 Hz), 127.92, 127.90, 127.04, 126.75, 119.51 (d, *J*_{CC} = 89.6 Hz), 84.15 (¹³C label), 77.41 (d, *J*_{CC} = 176.0 Hz). LRMS-EI *m/z* = 153.1 [M]⁺, calc. for C₁₁¹³CH₈ = 153.07.

2-(Cyclohepta-2,4,6-trien-1-yl(1-¹³C)ethynyl)naphthalene (1j'')



2-[(1-¹³C)ethynyl]naphthalene (300 mg, 1.96 mmol) was placed in dry schlenk flask under a argon atmosphere. Dry THF (12 mL, 0.16 M) was added and the resulting solution was cooled to -78 °C before adding n-BuLi (1.6 M in hexanes, 1.2 mL, 1.96 mmol, 1.0 equiv) and stirring for 40 minutes at this temperature. Solid tropylium tetrafluoroborate (697 mg, 3.92 mmol, 2 equiv) was added, the cooling bath removed, and the mixture stirred at room temperature for 5 h. The reaction was quenched with an aqueous solution of NH₄Cl (25 mL, saturated) then extracted with EtOAc (3×25 mL). The combined organic extracts were dried over MgSO₄ and solvent was removed under reduced pressure. The crude mixture was purified by flash chromatography (cyclohexane) to afford the desired product **1j**¹³ as a white solid (199.5 mg, 0.08 mmol, 41%). ¹H NMR (400 MHz, CDCl₃) δ 7.98 (d, *J* = 5.9 Hz, 1H), 7.88 – 7.72 (m, 3H), 7.60 – 7.41 (m, 3H), 6.71 (dd, *J* = 3.7, 2.7 Hz, 2H), 6.33 – 6.17 (m, 2H), 5.48 (ddd, *J* = 9.4, 5.6, 0.8 Hz, 2H), 2.84 – 2.69 (m, 1H). ¹³C NMR (101 MHz, CDCl₃) δ 133.16 (d, *J*_{CC} = 6.0 Hz), 132.80 (d, *J*_{CC} = 1.4 Hz), 131.55 (d, *J*_{CC} = 1.6 Hz), 131.20, 128.83 (d, *J*_{CC} = 2.1 Hz), 128.03 (d, *J*_{CC} = 5.3 Hz), 127.87, 127.80, 126.59, 124.97, 123.30, 123.27, 120.92 (d, *J*_{CC} = 91.2 Hz), 91.61 (d, *J*_{CC} = 179.3 Hz), 81.12 (¹³C label), 32.49 (d, *J*_{CC} = 11.7 Hz). HRMS-APCI *m/z* = 244.1218 [M+H]⁺, calc. for C₁₈H₁₅¹³C = 244.1207.

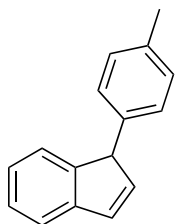
5.3 General Procedure for the Synthesis of 1-Substituted-1*H*-indenes (Conditions A)



A solution of the cycloheptatriene substrate (0.145 mmol) in CH₂Cl₂ (0.5 mL, 0.29 M) was sealed in a 3 mL screw cap vial and cooled to 0 °C, with no special precautions taken to exclude air or moisture. (Pyridine-2-carboxylato)gold(III) dichloride **12** (1

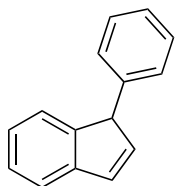
mol% unless otherwise stated) was then added and the mixture stirred at 0 °C for 1 h. The solvent was removed under reduced pressure and the crude yield assessed by ¹H NMR analysis (CDCl₃, 1,4-diacetylbenzene as internal standard). Purification by preparative TLC (eluent: 9:1 pentane-CH₂Cl₂) afforded the *1H*-indene product.

1-(p-Tolyl)-1H-indene (3a)



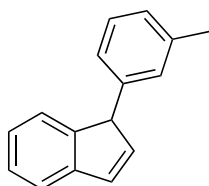
The title compound **3a** was obtained from 7-(*p*-tolylethynyl)cyclohepta-1,3,5-triene as a pale yellow oil (25.8 mg, 0.125 mmol, 86%). ¹H NMR (400 MHz, CDCl₃) δ 7.43 – 7.39 (m, 1H), 7.31 – 7.25 (m, 2H), 7.19 – 7.13 (m, 1H), 7.10 (d, *J* = 7.8, 2H), 7.05 – 7.00 (m, 2H), 6.91 (ddd, *J* = 5.5, 2.1, 0.5, 1H), 6.60 (dd, *J* = 5.5, 2.0, 1H), 4.60 (s, 1H), 2.33 (s, 3H). ¹³C NMR (101 MHz, CDCl₃) δ 148.56, 144.27, 140.14, 136.55, 136.34, 131.53, 129.56, 127.88, 126.89, 125.45, 124.04, 121.29, 56.34, 21.27. HRMS-APCI *m/z* = 207.1165 [M+H]⁺, calc. for C₁₆H₁₅ = 207.1174.

1-Phenyl-1H-indene (3b)



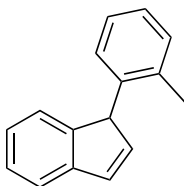
The title compound **3b** was obtained from 7-(phenylethynyl)cyclohepta-1,3,5-triene as a pale yellow oil (17.9 mg, 0.093 mmol, 64%). ^1H NMR (400 MHz, CDCl_3) δ 7.46 (dd, $J = 7.4, 1.3$ Hz, 1H), 7.36 – 7.27 (m, 5H), 7.24 – 7.15 (m, 3H), 6.97 (dd, $J = 5.5, 2.1$ Hz, 1H), 6.66 (dd, $J = 5.5, 2.0$ Hz, 1H), 4.67 (s, 1H). ^{13}C NMR (101 MHz, CDCl_3) δ 148.32, 144.20, 139.86, 139.43, 131.65, 128.79, 127.95, 126.92, 126.90, 125.42, 124.02, 121.28, 56.63. The spectroscopic data were consistent with those previously reported: Odedra, A.; Datta, S.; Liu, R.-S. *J. Org. Chem.* **2007**, *72*, 3289–3292.

1-(*m*-Tolyl)-1H-indene (**3c**)



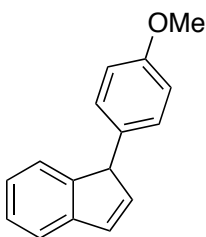
The title compound **3c** was obtained from 7-(*m*-tolylethynyl)cyclohepta-1,3,5-triene as a pale yellow oil (16.4 mg, 0.080 mmol, 55%). ^1H NMR (500 MHz, CDCl_3) δ 7.44 – 7.41 (m, 1H), 7.31 – 7.27 (m, 2H), 7.21 – 7.16 (m, 2H), 7.06 (d, $J = 7.4$ Hz, 1H), 6.96 (d, $J = 7.7$ Hz, 1H), 6.95 – 6.92 (m, 2H), 6.62 (dd, $J = 5.4, 1.9$ Hz, 1H), 4.60 (s, 1H), 2.32 (s, 3H). ^{13}C NMR (126 MHz, CDCl_3) δ 148.36, 144.21, 139.96, 139.27, 138.42, 131.55, 128.67, 128.51, 127.72, 126.85, 125.39, 125.08, 124.02, 121.24, 56.60, 21.52. HRMS-APCI $m/z = 207.1183$ $[\text{M}+\text{H}]^+$, calc. for $\text{C}_{16}\text{H}_{15} = 207.1174$.

1-(*o*-Tolyl)-1H-indene (3d)



The title compound **3d** was obtained from 7-(*o*-tolylethynyl)cyclohepta-1,3,5-triene as a pale yellow oil (22.7 mg, 0.110 mmol, 76%). ¹H NMR (500 MHz, CDCl₃) δ 7.45 (d, *J* = 7.5 Hz, 1H), 7.31 (t, *J* = 7.5 Hz, 1H), 7.27 – 7.21 (m, 2H), 7.21 – 7.13 (m, 2H), 7.05 (t, *J* = 7.2 Hz, 1H), 6.95 (dd, *J* = 5.5, 2.2 Hz, 1H), 6.81 (d, *J* = 7.7 Hz, 1H), 6.61 (dd, *J* = 5.5, 2.0 Hz, 1H), 4.87 (s, 1H), 2.42 (s, 3H). ¹³C NMR (126 MHz, CDCl₃) δ 148.13, 144.51, 139.35, 137.47, 136.64, 131.45, 130.75, 127.74, 126.91, 126.81, 126.35, 125.34, 123.87, 121.40, 56.63, 19.76. HRMS-APCI *m/z* = 207.1172 [M+H]⁺, calc. for C₁₆H₁₅ = 207.1174.

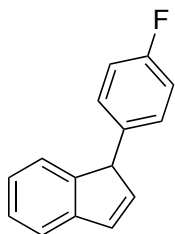
1-(4-Methoxyphenyl)-1H-indene (3e)



The title compound was obtained from 7-((4-methoxyphenyl)ethynyl)cyclohepta-1,3,5-triene as a colorless solid (22.2 mg, 0.100 mmol, 69%). M.p. = 58 – 60 °C. ¹H NMR (400 MHz, CDCl₃) δ 7.41 (dt, *J* = 7.4, 1.0 Hz, 1H), 7.31 – 7.24 (m, 2H), 7.17 (td, *J* = 7.4, 1.1 Hz, 1H), 7.07 – 7.02 (m, 2H), 6.90 (ddd, *J* = 5.5, 2.1, 0.7 Hz, 1H), 6.86 – 6.80 (m, 2H), 6.59 (dd, *J* = 5.5, 2.0 Hz, 1H), 4.58 (s, 1H), 3.79 (s, 1H). ¹³C NMR (101 MHz, CDCl₃) δ 158.63, 148.62, 144.12, 140.16, 131.35, 131.23, 128.89, 126.82, 125.38,

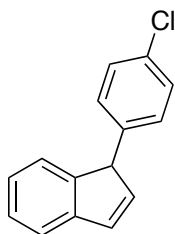
123.94, 121.23, 114.23, 55.86, 55.39. The spectroscopic data were consistent with those previously reported: Odedra, A.; Datta, S.; Liu, R.-S. *J. Org. Chem.* **2007**, *72*, 3289–3292.

1-(4-Fluorophenyl)-1H-indene (3f)



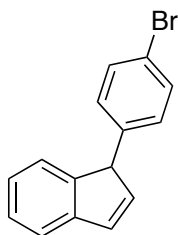
The title compound **3f** was obtained from 7-((4-fluorophenyl)ethynyl)cyclohepta-1,3,5-triene as a yellow oil (19.2 mg, 0.091 mmol, 63%) using 5 mol% (pyridine-2-carboxylato)gold(III) dichloride. ^1H NMR (400 MHz, CDCl_3) δ 7.42 – 7.38 (m, 1H), 7.31 – 7.25 (m, 1H), 7.25 – 7.20 (m, 1H), 7.16 (td, $J = 7.4, 1.2$ Hz, 1H), 7.09 – 7.04 (m, 2H), 6.99 – 6.92 (m, 2H), 6.91 (dd, $J = 5.5, 2.1$ Hz, 1H), 6.56 (dd, $J = 5.5, 2.0$ Hz, 1H), 4.58 (s, 1H). ^{13}C NMR (101 MHz, CDCl_3) δ 161.82 (d, $J_{\text{CF}} = 244.8$ Hz), 148.08, 143.92, 139.54, 134.91, 131.64, 129.22 (d, $J = 7.9$ Hz), 126.89, 125.38, 123.78, 121.23, 115.45 (d, $J = 21.3$ Hz), 55.62. ^{19}F NMR (376 MHz, CDCl_3) δ -116.37. HRMS-MALDI $m/z = 210.0809$ $[\text{M}]^+$, calc. for $\text{C}_{15}\text{H}_{11}\text{F} = 210.0839$.

1-(4-chlorophenyl)-1H-indene (3g)



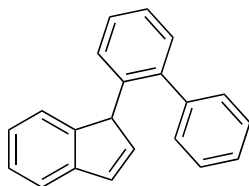
The title compound **3g** was obtained from 7-((4-chlorophenyl)ethynyl)cyclohepta-1,3,5-triene as a colorless oil (26.3 mg, 0.116 mmol, 80%). ¹H NMR (400 MHz, Chloroform-d) δ 7.40 (dt, $J = 7.6, 0.9$ Hz, 1H), 7.31 – 7.25 (m, 1H), 7.25 – 7.20 (m, 3H), 7.16 (td, $J = 7.5, 1.2$ Hz, 1H), 7.07 – 7.01 (m, 2H), 6.92 (dd, $J = 5.6, 2.1$ Hz, 1H), 6.55 (dd, $J = 5.4, 2.0$ Hz, 1H), 4.57 (s, 1H). ¹³C NMR (101 MHz, Chloroform-d) δ 147.93, 144.10, 139.37, 137.99, 132.62, 132.04, 129.29, 128.93, 127.12, 125.59, 123.93, 121.42, 55.86. HRMS-EI $m/z = 226.0558$ [M]⁺, calc. for C₁₅H₁₁³⁵Cl = 226.0549.

1-(4-Bromophenyl)-1H-indene (3b)



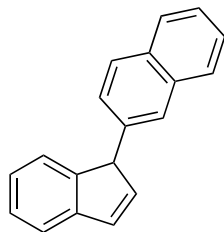
The title compound **3h** was obtained from 7-((4-bromophenyl)ethynyl)cyclohepta-1,3,5-triene as a colorless oil (32.0 mg, 0.119 mmol, 82%). ¹H NMR (400 MHz, CDCl₃) δ 7.43 – 7.35 (m, 3H), 7.31 – 7.25 (m, 1H), 7.24 – 7.19 (m, 1H), 7.16 (td, $J = 7.4, 1.2$ Hz, 1H), 7.01 – 6.95 (m, 2H), 6.91 (dd, $J = 5.5, 2.1$ Hz, 1H), 6.55 (dd, $J = 5.5, 2.0$ Hz, 1H), 4.55 (s, 1H). ¹³C NMR (101 MHz, CDCl₃) δ 147.85, 144.11, 139.29, 138.54, 132.09, 131.88, 129.69, 127.14, 125.60, 123.94, 121.43, 120.65, 55.92. HRMS-EI $m/z = 270.0040$ [M]⁺, calc. for C₁₅H₁₁⁷⁹Br = 270.0044.

1-([1,1'-Biphenyl]-2-yl)-1H-indene (3i)



The title compound **3i** was obtained from 2-(cyclohepta-2,4,6-trien-1-ylethynyl)-1,1'-biphenyl as a pale yellow oil (30.0 mg, 0.112 mmol, 77%). ¹H NMR (400 MHz, CDCl₃) δ 7.56 – 7.51 (m, 2H), 7.48 (t, *J* = 7.5 Hz, 2H), 7.41 – 7.35 (m, 3H), 7.27 (t, *J* = 7.6 Hz, 2H), 7.20 (d, *J* = 7.1 Hz, 1H), 7.18 – 7.12 (m, 2H), 6.86 (dd, *J* = 5.2, 2.0 Hz, 1H), 6.67 (dd, *J* = 7.8, 1.1 Hz, 1H), 6.56 (dd, *J* = 5.5, 2.0 Hz, 1H), 4.89 (s, 1H). ¹³C NMR (101 MHz, CDCl₃) δ 149.58, 144.46, 142.80, 141.74, 140.81, 136.76, 131.17, 130.30, 129.74, 128.44, 127.83, 127.47, 127.23, 126.74, 126.62, 125.32, 123.96, 121.23, 52.94. HRMS-APCI *m/z* = 269.1331 [M+H]⁺, calc. for C₂₁H₁₇ = 269.1330.

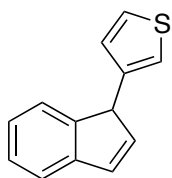
2-(1H-inden-1-yl)naphthalene 3j



The title compound **3j** was obtained from 2-(cyclohepta-2,4,6-trien-1-ylethynyl)naphthalene as a yellow oil (26.4 mg, 0.109 mmol, 75%). ¹H NMR (400 MHz, CDCl₃) δ 7.85 – 7.78 (m, 2H), 7.78 – 7.70 (m, 2H), 7.52 – 7.43 (m, 3H), 7.36 – 7.28 (m, 2H), 7.19 (td, *J* = 7.4, 1.1 Hz, 1H), 7.05 (dd, *J* = 8.5, 1.8 Hz, 1H), 7.00 (dd, *J* = 5.5, 2.1 Hz, 1H), 6.69 (dd, *J* = 5.4, 2.0 Hz, 1H), 4.80 (s, 1H). ¹³C NMR (101 MHz, CDCl₃) δ

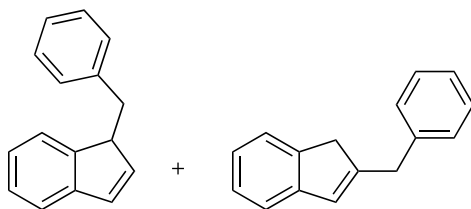
148.39, 144.30, 139.88, 136.98, 133.84, 132.72, 131.91, 128.45, 127.77, 127.61, 127.01, 126.72, 126.16, 125.99, 125.64, 125.50, 124.17, 121.35, 56.76. HRMS-APCI $m/z = 243.1172$ $[M+H]^+$, calc. for $C_{19}H_{15} = 243.1174$.

3-(1H-inden-1-yl)thiophene (3k)



The title compound **3k** was obtained from 3-(cyclohepta-2,4,6-trien-1-ylethynyl)thiophene as a colorless oil (19.0 mg, 0.096 mmol, 66%) using 5 mol% (pyridine-2-carboxylato)gold(III) dichloride and stirring for 2 h at rt. 1H NMR (500 MHz, $CDCl_3$) δ 7.43 (d, $J = 7.5$ Hz, 1H), 7.39 – 7.36 (m, 1H), 7.34 – 7.29 (m, 1H), 7.26 (dd, $J = 5.0, 2.9$ Hz, 1H), 7.21 (td, $J = 7.4, 1.0$ Hz, 1H), 7.12 (d, $J = 2.4$ Hz, 1H), 6.92 (dd, $J = 5.5, 2.2$ Hz, 1H), 6.81 (dd, $J = 5.0, 1.2$ Hz, 1H), 6.62 (dd, $J = 5.5, 2.0$ Hz, 1H), 4.77 (s, 1H). HRMS-APCI $m/z = 199.0589$ $[M+H]^+$, calc. for $C_{13}H_{11}S = 199.0581$.

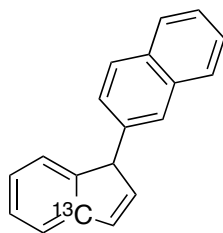
2:1 Mixture of 1-benzyl-1H-indene and 2-benzyl-1H-indene (3m + 4m)



An inseparable 2:1 mixture (determined by 1H NMR) of the title compounds **3m** and **4m** was obtained from 7-(3-phenylprop-1-yn-1-yl)cyclohepta-1,3,5-triene as a colorless

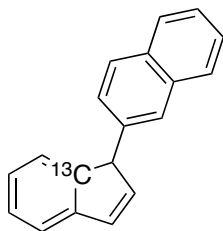
oil (22.6 mg, 0.110 mmol, 76% combined). The components of the mixture could be assigned by ^1H NMR with reference to previously reported spectra: a) Alt, G. H.; Jung, M.; Milius, W. *J. Organomet. Chem.* **1998**, *558*, 111–121. b) Martinez, A.; Fernandez, M.; Estevez, J. C.; Estevez, R. J.; Castedo, L. *Tetrahedron* **2005**, *61*, 485–492.

2-(1H-[4'- ^{13}C]inden-1-yl)naphthalene (3j')



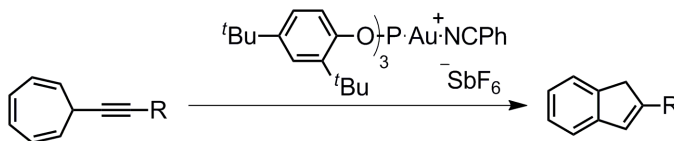
The title compound **3j'** was obtained from 2-(cyclohepta-2,4,6-trien-1-yl(2- ^{13}C)ethynyl)naphthalene (9.9 mg, 41 μmol) as a yellow film (5.4 mg, 22 μmol , 55%) according to the general procedure. ^1H NMR (500 MHz, CDCl_3) δ 7.79 (d, $J = 9.2$ Hz, 2H), 7.73 (s, 1H), 7.70 (d, $J = 8.4$ Hz, 1H), 7.49 – 7.41 (m, 3H), 7.32 – 7.25 (m, 2H), 7.15 (t, $J = 7.4$ Hz, 1H), 7.02 (dd, $J = 8.5, 1.7$ Hz, 1H), 6.97 (ddd, $J_{\text{CH}} = 7.0$ Hz, $J = 5.9, 2.0$ Hz, 1H), 6.66 (ddd, $J_{\text{CH}} = 10.4$ Hz, $J = 5.5, 2.0$ Hz, 1H), 4.77 (s, 1H). ^{13}C NMR (126 MHz, CDCl_3) δ 148.39 (d, $J_{\text{CC}} = 51.8$ Hz), 144.32 (^{13}C label), 139.90, 136.99, 133.85, 132.74, 131.91 (d, $J_{\text{CC}} = 52.0$ Hz), 128.46, 127.78, 127.62, 127.02 (d, $J_{\text{CC}} = 1.8$ Hz), 126.73, 126.17, 126.00, 125.65, 125.51 (d, $J_{\text{CC}} = 9.0$ Hz), 124.18, 121.34 (d, $J_{\text{CC}} = 60.1$ Hz), 56.77 (d, $J = 6.7$ Hz). HRMS-APCI $m/z = 244.1204$ [$\text{M}+\text{H}$] $^+$, calc. for $\text{C}_{18}\text{H}_{15}^{13}\text{C} = 244.1207$.

2-(1H-[7'-¹³C]inden-1-yl)naphthalene (3j'')



The title compound **3j''** was obtained from 2-(cyclohepta-2,4,6-trien-1-yl(1-¹³C)ethynyl)naphthalene (20 mg, 82 μ mol) as a yellow film (9.7 mg, 40 μ mol, 49 %) according to the general procedure. ¹H NMR (500 MHz, CDCl₃) δ 7.79 (dd, J = 7.8, 1.6 Hz, 2H), 7.74 (d, J = 1.6 Hz, 1H), 7.71 (d, J = 8.5 Hz, 1H), 7.45 (pd, J = 6.9, 1.4 Hz, 3H), 7.33 – 7.26 (m, 2H), 7.16 (q, J = 7.3 Hz, 1H), 7.03 (dd, J = 8.4, 1.8 Hz, 1H), 6.98 (td, J = 6.0, 2.0 Hz, 1H), 6.67 (td, J = 5.6, 2.0 Hz, 1H), 4.79 – 4.75 (m, 1H). ¹³C NMR (126 MHz, CDCl₃) δ 148.39, 144.28 (d, J_{CC} = 51.8 Hz), 139.89 (d, J = 3.6 Hz), 136.99 (d, J_{CC} = 1.7 Hz), 133.84, 132.73, 131.92 (d, J_{CC} = 6.4 Hz), 128.46, 127.78, 127.62, 127.02 (d, J = 9.0 Hz), 126.73 (d, J = 1.8 Hz), 126.17, 126.00 (d, J_{CC} = 1.3 Hz), 125.64, 125.51 (d, J_{CC} = 1.6 Hz), 124.16 (d, J_{CC} = 62.0 Hz), 121.36, 56.76 (d, J_{CC} = 42.5 Hz). HRMS-APCI m/z = 244.1206 [M+H]⁺, calc. for C₁₈H₁₅¹³C = 244.1207.

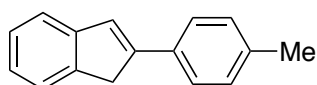
5.4 General Procedure for the Synthesis of 2-Substituted-1H-indenes (Conditions B)



A solution of the cycloheptatriene substrate (0.145 mmol) in toluene (0.5 mL, 0.29 M) was sealed in a 3 mL screw cap vial and cooled to 0 °C, with no special precautions

taken to exclude air or moisture. Au(I)-phosphite catalyst **13** (5 mol%) was then added and the mixture stirred at 0 °C for 1 h. The solvent was removed under reduced pressure and the crude yield assessed by ¹H NMR analysis (CDCl₃, 1,4-diacetylbenzene as internal standard). Purification by preparative TLC (eluent: 9:1 pentane-CH₂Cl₂) afforded the *1H*-indene product.

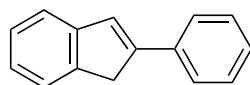
2-(p-Tolyl)-1H-indene (4a)



The title compound **4a** was obtained from 7-(*p*-tolylethynyl)cyclohepta-1,3,5-triene (30 mg, 0.145 mmol) as a waxy solid (17.9 mg, 87 μmol, 60%).

¹H NMR (400 MHz, CDCl₃) δ 7.53 (d, *J* = 8.0 Hz, 2H), 7.45 (d, *J* = 7.2 Hz, 1H), 7.38 (d, *J* = 7.6 Hz, 1H), 7.29 – 7.24 (m, 1H), 7.21 – 7.14 (m, 4H), 3.76 (s, 2H), 2.36 (s, 3H).
¹³C NMR (100 MHz, CDCl₃) δ 146.5, 145.5, 143.0, 137.4, 133.2, 129.4, 126.6, 125.6, 125.5, 124.5, 123.6, 120.8, 39.0, 21.2. The spectroscopic data were consistent with those previously reported: Fuchibe, K.; Mitomi, K.; Akiyama, T. *Chem. Lett.* **2007**, *36*, 24-25.

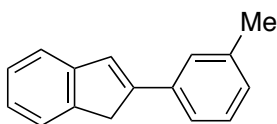
2-Phenyl-1H-indene (4b)



The title compound **4b** was obtained from 7-(phenylethynyl)cyclohepta-1,3,5-triene (27.4 mg, 0.143 mmol) as a yellow oil (14 mg, 0.073 mmol, 51%). ¹H NMR (500 MHz, CDCl₃) δ 7.63 – 7.61 (m, 2H), 7.46 (dd, *J* = 7.5, 1.0 Hz, 1H), 7.40 – 7.35 (m, 3H), 7.28

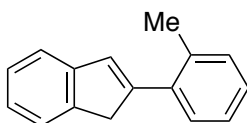
– 7.24 (m, 2H), 7.21 (t, $J = 0.5$ Hz, 1H), 7.17 (dt, $J = 7.5, 1.0$ Hz, 1H), 3.77 (s, 2H). ^{13}C NMR (125 MHz, CDCl_3) δ 146.7, 145.6, 143.4, 136.3, 129.0, 127.8, 126.9, 126.8, 125.9, 125.0, 123.9, 121.3, 39.3. The spectroscopic data were consistent with those previously reported: a) Bors, D. A.; Kaufman, M. J.; Streitwieser, A. Jr. *J. Am. Chem. Soc.* **1985**, *107*, 6975. b) Greifenstein, L. G.; Lambert, J. B.; Nienhuis, R. J.; Fried, H. E.; Pagani, G. A. *J. Org. Chem.* **1981**, *46*, 5125.

2-(*m*-Tolyl)-1H-indene (**4c**)



The title compound **4c** was obtained from 7-(*m*-tolylethynyl)cyclohepta-1,3,5-triene (28.9 mg, 0.140 mmol) as a yellow oil (14.3 mg, 0.069 mmol, 50%). ^1H NMR (400 MHz, CDCl_3) δ 7.53 – 7.46 (m, 2H), 7.43 (dt, $J = 7.6, 0.9$ Hz, 1H), 7.36 – 7.27 (m, 3H), 7.29 – 7.23 (m, 1H), 7.22 (td, $J = 7.4, 1.2$ Hz, 1H), 7.13 (dt, $J = 7.4, 1.0$ Hz, 1H), 3.82 (s, 2H), 2.43 (s, 3H). The spectroscopic data were consistent with those previously reported: Greifenstein, L. G.; Lambert, J. B.; Nienhuis, R. J.; Fried, H. E.; Pagani, G. A. *J. Org. Chem.* **1981**, *46*, 5125–5132.

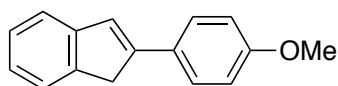
2-(*o*-Tolyl)-1H-indene (**4d**)



The title compound **4d** was obtained from 7-(*o*-tolylethynyl)cyclohepta-1,3,5-triene (29.2 mg, 0.142 mmol) as a yellow oil (14.1 mg, 0.068 mmol, 48%). ^1H NMR (400

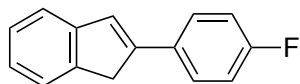
MHz, CDCl₃) δ 7.49 (d, J = 7.4 Hz, 1H), 7.41 (t, J = 8.9 Hz, 2H), 7.32 – 7.18 (m, 5H), 6.95 (s, 1H), 3.80 (s, 2H), 2.50 (s, 3H). ¹³C NMR (100 MHz, CDCl₃) δ 147.26, 145.68, 143.32, 137.02, 135.99, 131.20, 130.59, 128.96, 127.35, 126.74, 126.05, 124.82, 123.66, 121.12, 42.43, 21.98. The spectroscopic data were consistent with those previously reported: Pantelev, J.; Huang, R. Y.; Lui, E. K. J.; Lautens, M. *Org. Lett.* **2011**, *13*, 5314–5317.

2-(4-Methoxyphenyl)-1H-indene (4e)



The title compound **4e** was obtained from 7-((4-methoxyphenyl)ethynyl)cyclohepta-1,3,5-triene as a colorless solid (8.4 mg, 0.043 mmol, 30%). ¹H NMR (500 MHz, CDCl₃) δ 7.58 – 7.55 (m, 2H), 7.44 (d, J = 7.5 Hz, 1H), 7.36 (d, J = 7.5 Hz, 1H), 7.25 (t, J = 7.5 Hz, 1H), 7.15 (dt, J = 7.5, 1.0 Hz, 1H), 7.09 (s, 1H), 6.93-6.90 (m, 2H), 3.84 (s, 3H), 3.75 (s, 2H). ¹³C NMR (125 MHz, CDCl₃) δ 159.5, 146.4, 146.0, 143.1, 129.1, 127.1, 126.8, 124.9, 124.6, 123.8, 120.8, 114.3, 55.6, 39.3. The spectroscopic data were consistent with those previously reported: a) Wolff, T.; Schmidt, F.; Volz, P. *J. Org. Chem.* **1992**, *57*, 4255–4262. b) Deng, R.; Sun, L.; Li, Z. *Org. Lett.*, **2007**, *9*, 5207–5210

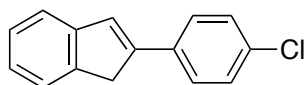
2-(4-Fluorophenyl)-1H-indene (4f)



The title compound **4f** was obtained from 7-((4-fluorophenyl)ethynyl)cyclohepta-1,3,5-triene (31.4 mg, 0.149 mmol) as a colorless solid (18.8 mg, 0.089 mmol, 60%). ¹H

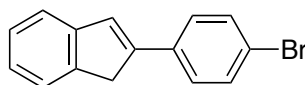
NMR (500 MHz, CDCl_3) δ 7.63 – 7.59 (m, 2H), 7.50 – 7.48 (m, 1H), 7.42 (dd, $J = 1.0$ Hz, 1H), 7.32 – 7.29 (m, 1H), 7.21 (dt, $J = 1.0, 7.5$ Hz, 1H), 7.17 (s, 1H), 7.11 – 7.07 (m, 2H), 3.77 (s, 2H). ^{13}C NMR (125 MHz, CDCl_3) δ 162.6 (d, $J_{\text{CF}} = 237.5$ Hz), 145.5, 143.2, 132.5, 127.5 (d, $J_{\text{CF}} = 12.5$ Hz), 126.9, 126.5, 125.0, 123.9, 121.2, 115.9, 115.8, 39.4. The spectroscopic data were consistent with those previously reported: a) Bors, D. A.; Kaufman, M. J.; Streitwieser, A. Jr. *J. Am. Chem. Soc.* **1985**, *107*, 6975–6982. b) Greifenstein, L. G.; Lambert, J. B.; Nienhuis, R. J.; Fried, H. E.; Pagani, G. A. *J. Org. Chem.* **1981**, *46*, 5125–5132. c) Deng, R.; Sun, L.; Li, Z. *Org. Lett.*, **2007**, *9*, 5207–5210.

2-(4-Chlorophenyl)-1H-indene (4g)



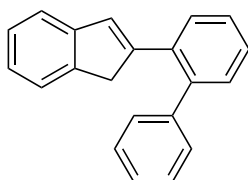
The title compound **4g** was obtained from 7-((4-chlorophenyl)ethynyl)cyclohepta-1,3,5-triene (32.4 mg, 0.143 mmol) as a colorless solid (19.1 mg, 0.084 mmol, 59%). ^1H NMR (400 MHz, CDCl_3) δ 7.56 – 7.51 (m, 2H), 7.46 (dq, $J = 7.3, 0.9$ Hz, 1H), 7.39 (dt, $J = 7.6, 1.0$ Hz, 1H), 7.35 – 7.30 (m, 2H), 7.27 (td, $J = 7.5, 1.1$ Hz, 1H), 7.21 – 7.16 (m, 2H), 3.74 (s, 2H). The spectroscopic data were consistent with those previously reported: Greifenstein, L. G.; Lambert, J. B.; Nienhuis, R. J.; Fried, H. E.; Pagani, G. A. *J. Org. Chem.* **1981**, *46*, 5125–5132.

2-(4-Bromophenyl)-1H-indene (4b)



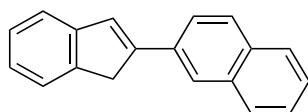
The title compound **4h** was obtained from 7-((4-bromophenyl)ethynyl)cyclohepta-1,3,5-triene (26.6 mg, 0.098 mmol) as a colorless solid (15.1 mg, 0.056 mmol, 57%). ¹H NMR (400 MHz, CDCl₃) δ 7.48 (s, 4H), 7.46 (dd, *J* = 7.6, 1.1 Hz, 1H), 7.41 – 7.38 (m, 1H), 7.32 – 7.23 (m, 1H), 7.23 – 7.15 (m, 2H), 3.74 (s, 2H). The spectroscopic data were consistent with those previously reported: Greifenstein, L. G.; Lambert, J. B.; Nienhuis, R. J.; Fried, H. E.; Pagani, G. A. *J. Org. Chem.* **1981**, *46*, 5125–5132.

2-([1,1'-Biphenyl]-2-yl)-1H-indene (4i)



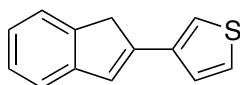
The title compound **4i** was obtained from 2-(cyclohepta-2,4,6-trien-1-ylethynyl)-1,1'-biphenyl (44 mg, 0.164 mmol) as a yellow oil (25.4 mg, 0.095 mmol, 76%) ¹H NMR (500 MHz, CDCl₃) δ 7.54 – 7.50 (m, 1H), 7.40 – 7.26 (m, 10H), 7.25 – 7.17 (m, 1H), 7.10 (td, *J* = 7.4, 1.2 Hz, 1H), 6.68 – 6.64 (m, 1H), 3.26 (s, 2H). ¹³C NMR (126 MHz, CDCl₃) δ 147.98 , 145.21 , 143.94 , 142.47 , 140.82 , 136.21 , 130.95 , 130.85 , 129.62 , 129.41 , 128.44 , 127.58 , 127.55 , 127.12 , 126.43 , 124.55 , 123.58 , 120.98 , 41.21 . The spectroscopic data were consistent with those previously reported: Ijpeij, E. G.; Beijer, F. H.; Arts, H. J.; Newton, C.; Vries, J. G. de; Gruter, G.-J. M. *J. Org. Chem.* **2002**, *67*, 169-176.

2-(1H-inden-2-yl)naphthalene (4j)



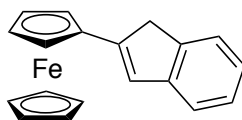
The title compound **4j** was obtained from 2-(cyclohepta-2,4,6-trien-1-ylethynyl)naphthalene (30 mg, 0.124 mmol) as a colorless solid (15.3 mg, 0.063 mmol, 51%). ^1H NMR (500 MHz, CDCl_3) δ 8.00 (s, 1H), 7.88 – 7.81 (m, 4H), 7.54 – 7.43 (m, 4H), 7.37 (s, 1H), 7.32 (t, $J = 7.2$ Hz, 1H), 7.23 (td, $J = 7.4, 1.1$ Hz, 1H), 3.94 (s, 2H). ^{13}C NMR (126 MHz, CDCl_3) δ 146.54, 145.54, 143.34, 133.81, 133.53, 133.02, 128.33, 128.25, 127.82, 127.34, 126.83, 126.52, 126.06, 125.04, 124.43, 124.08, 123.84, 121.20, 39.21. The spectroscopic data were consistent with those previously reported: Kohei, F.; Ken, M.; Takahiko, A. *Chem. Lett.* **2007**, *36*, 24–25.

3-(1*H*-inden-2-yl)thiophene (**4k**)



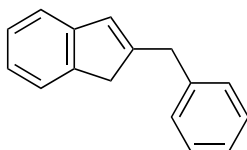
The title compound **4k** was obtained from 3-(cyclohepta-2,4,6-trien-1-ylethynyl)thiophene (32.3 mg, 0.163 mmol) as a colorless solid (13.2 mg, 0.067 mmol, 41%). M.p. = 181 – 184 °C. ^1H NMR (500 MHz, CDCl_3) δ 7.43 (d, $J = 7.4$ Hz, 1H), 7.39 – 7.34 (m, 2H), 7.32 (d, $J = 3.2$ Hz, 2H), 7.25 (t, $J = 8.2$ Hz, 1H), 7.16 (t, $J = 7.4$ Hz, 1H), 7.01 (s, 1H), 3.74 (s, 2H). ^{13}C NMR (126 MHz, CDCl_3) δ 145.51, 142.71, 142.00, 138.58, 126.77, 126.25, 126.20, 125.85, 124.76, 123.74, 121.03, 120.53, 39.73. HRAPCI-MS $m/z = 199.0585$ $[\text{M}+\text{H}]^+$, calc. for $\text{C}_{13}\text{H}_{11}\text{S} = 199.0581$.

2-Ferrocenylindene (**4l**)



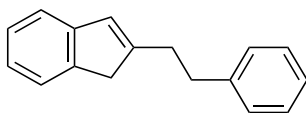
The title compound **4l** was obtained from (cyclohepta-2,4,6-trien-1-ylethynyl)ferrocene (40.7 mg, 0.136 mmol) as an orange solid (9.3 mg, 0.031 mmol, 23%). ^1H NMR (500 MHz, CDCl_3) δ 7.41 (dd, $J = 7.3, 1.0$ Hz, 1H), 7.29 (d, $J = 7.4$ Hz, 1H), 7.23 (d, $J = 6.5$ Hz, 1H), 7.13 (td, $J = 7.4, 1.2$ Hz, 2H), 6.81 (q, $J = 1.3$ Hz, 1H), 4.55 (t, $J = 1.9$ Hz, 2H), 4.31 (t, $J = 1.8$ Hz, 2H), 4.08 (s, 4H), 3.65 (s, 2H). ^{13}C NMR (126 MHz, CDCl_3) δ 146.63, 146.16, 142.74, 126.73, 124.04, 123.88, 123.64, 120.07, 81.10, 69.59, 69.20, 66.60, 40.01. The spectroscopic data were consistent with those previously reported: Plenio, H. *Organometallics* **1992**, *11*, 1856-1859.

2-Benzyl-1H-indene (**4m**)



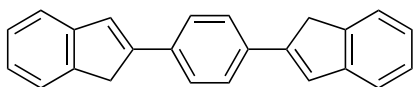
The title compound **4m** was obtained from 7-(3-phenylprop-1-yn-1-yl)cyclohepta-1,3,5-triene (29.8 mg, 0.144 mmol) as a yellow oil (16.8 mg, 0.081 mmol, 57%). ^1H NMR (500 MHz, CDCl_3) δ 7.37 – 7.18 (m, 8H), 7.09 (td, $J = 7.3, 1.2$ Hz, 1H), 6.50 (t, $J = 1.7$ Hz, 1H), 3.81 (s, 2H), 3.27 (s, 3H). ^{13}C NMR (101 MHz, CDCl_3) δ 149.40, 145.46, 143.57, 140.16, 129.02, 128.61, 127.95, 126.42, 126.35, 124.01, 123.61, 120.34, 40.98, 38.12. The spectroscopic data were consistent with those previously reported: Licht, E. H.; Alt, H. G.; Karim, M. M. *J. Organomet. Chem.* **2000**, *599*, 275–287.

2-Phenethyl-1H-indene (**4n**)



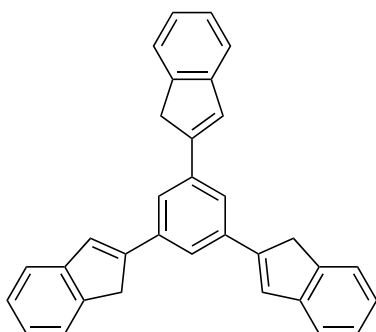
The title compound **4n** was obtained from 7-(4-phenylbut-1-yn-1-yl)cyclohepta-1,3,5-triene (29.7 mg, 0.135 mmol) as a yellow oil (9.1 mg, 0.0413 mmol, 31%). ¹H NMR (500 MHz, CDCl₃) δ 7.37 (dd, *J* = 7.4, 0.9 Hz, 1H), 7.32 – 7.24 (m, 3H), 7.24 – 7.17 (m, 4H), 7.10 (td, *J* = 7.3, 1.3 Hz, 1H), 6.54 (d, *J* = 1.0 Hz, 1H), 3.32 (s, 2H), 2.96 – 2.92 (m, 2H), 2.85 – 2.78 (m, 2H). ¹³C NMR (126 MHz, CDCl₃) δ 149.96, 145.66, 143.20, 141.98, 128.54, 128.46, 126.78, 126.40, 126.10, 123.85, 123.55, 120.17, 41.39, 35.55, 33.17. The spectroscopic data were consistent with those previously reported: Licht, E. H.; Alt, H. G.; Karim, M. M. *J. Organomet. Chem.* **2000**, *599*, 275–287.

1,4-Di(1H-inden-2-yl)benzene (**4r**)



The title compound **4r** was obtained from 1,4-bis(cyclohepta-2,4,6-trien-1-ylethynyl)benzene (100 mg, 0.326 mmol) as a highly insoluble yellow solid (44.7 mg, 0.146 mmol, 45%). Decomposes over 320 °C. ¹H NMR (500 MHz, C₂Cl₄D₂; 398 K) δ 7.69 (s, 4H), 7.53 (d, *J* = 7.3 Hz, 2H), 7.46 (d, *J* = 7.5 Hz, 2H), 7.33 (t, *J* = 7.4 Hz, 2H), 7.28 (s, 2H), 7.24 (t, *J* = 7.3 Hz, 2H), 3.88 (s, 4H). ¹³C NMR (126 MHz, C₂Cl₄D₂; 398 K) δ 146.08, 145.25, 143.05, 135.30, 126.63, 126.50, 125.84, 124.69, 123.40, 120.82, 39.02. HRMS-MALDI *m/z* = 306.1402 [M]⁺, calculated for C₂₄H₁₈ = 306.1403.

1,3,5-Tri(1H-inden-2-yl)benzene (4s)



A solution of the 1,3,5-tris(cyclohepta-2,4,6-trien-1-ylethynyl)benzene (50 mg, 0.119 mmol) in toluene (0.5 mL, 0.29 M) was sealed in a 3 mL screw cap vial and cooled to 0 °C, with no special precautions taken to exclude air or moisture. Au(I)-phosphite catalyst **12** (6.7 mg, 5 mol%) was then added and the mixture stirred at 0 °C for 1 h. The reaction mixture was then evaporated to dryness, 1,1'-(1,4-phenylene)diethanone added as an internal standard, and the crude yield assessed by ¹H NMR. The product was purified by column chromatography (SiO₂, eluent 1. 9:1 cyclohexane-DCM 2. 4:1) followed by recrystallization from refluxing cyclohexane (25 mL) to give compound **4s** (18 mg, 0.043 mmol, 36%) as a colorless solid. M.p. = 300 – 320 °C. ¹H NMR (500 MHz, CDCl₃) δ 7.79 (s, 3H), 7.52 (d, *J* = 7.3 Hz, 3H), 7.45 (d, *J* = 7.3 Hz, 3H), 7.36 (s, 3H), 7.32 (t, *J* = 7.4 Hz, 3H), 7.23 (td, *J* = 7.4, 1.2 Hz, 3H), 3.90 (s, 6H). ¹³C NMR (126 MHz, CDCl₃) δ 146.28, 145.38, 143.32, 136.91, 127.42, 126.89, 125.14, 123.88, 122.22, 121.28, 39.39. HRMS-MALDI *m/z* = 420.1816 [M]⁺, calc. for C₃₃H₂₄ = 420.1873.

X-Ray Crystal Structure:

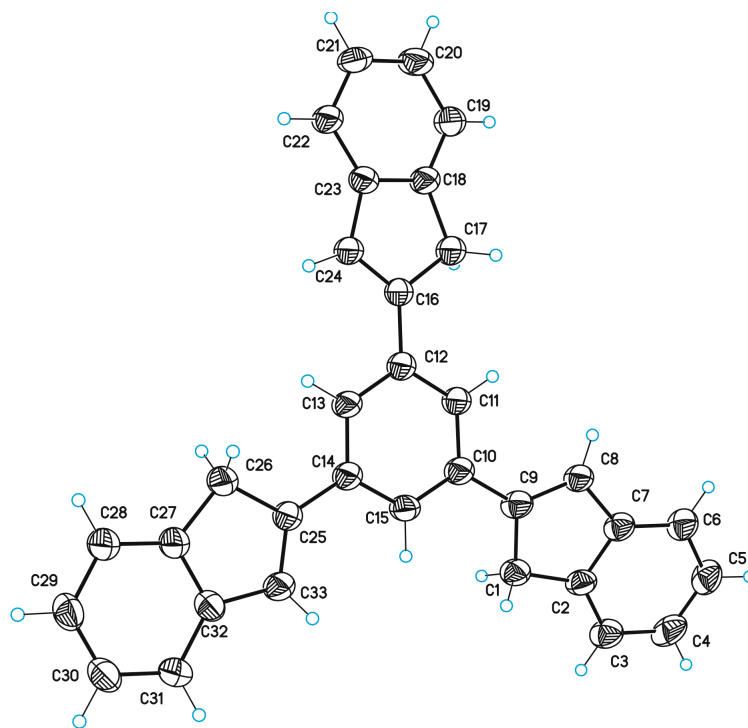


Table 1. Crystal data and structure refinement for PM2190.

Identification code	PM2190	
Empirical formula	C ₃₃ H ₂₄	
Formula weight	420.52	
Temperature	100(2)K	
Wavelength	0.71073 Å	
Crystal system	Orthorhombic	
Space group	Pbca	
Unit cell dimensions	a = 23.3720(16) Å	a =
90.00 °.	b = 6.9309(6) Å	b =
90.00 °.		

	$c = 27.463(2) \text{ \AA}$	$g =$
90.00 °.		
Volume	4448.8(6) \AA^3	
Z	8	
Density (calculated)	1.256 Mg/m^3	
Absorption coefficient	0.071 mm^{-1}	
F(000)	1776	
Crystal size	0.20 x 0.02 x 0.02 mm^3	
Theta range for data collection	1.48 to 24.76 °.	
Index ranges	-27 $\leq h \leq 27$, -8 $\leq k \leq 8$, -32 $\leq l \leq 32$	
Reflections collected	53514	
Independent reflections	3759 [R(int) = 0.0927]	
Completeness to theta =24.76 °	0.987 %	
Absorption correction	Empirical	
Max. and min. transmission	0.9986 and 0.9860	
Refinement method	Full-matrix least-squares on F^2	
Data / restraints / parameters	3759 / 0 / 298	
Goodness-of-fit on F^2	1.147	
Final R indices [$I > 2\sigma(I)$]	R1 = 0.0634 , wR2 = 0.1683	
R indices (all data)	R1 = 0.1146 , wR2 = 0.2082	
Largest diff. peak and hole	0.280 and -0.321 e.\AA^{-3}	

Table 2. Bond lengths [\AA] and angles [$^\circ$] for PM2190.

Bond lengths----

C1-C9	1.475(4)
C1-C2	1.494(4)
C2-C3	1.379(4)

Chapter I: Generation and control of fluxional barbaralyl cations in gold-catalyzed cycloisomerizations

C2-C7	1.409(4)
C3-C4	1.389(4)
C4-C5	1.394(5)
C5-C6	1.385(4)
C6-C7	1.380(4)
C7-C8	1.468(4)
C8-C9	1.378(4)
C9-C10	1.471(4)
C10-C15	1.398(4)
C10-C11	1.401(4)
C11-C12	1.397(4)
C12-C13	1.401(4)
C12-C16	1.468(4)
C13-C14	1.396(4)
C14-C15	1.403(4)
C14-C25	1.469(4)
C16-C24	1.359(4)
C16-C17	1.506(4)
C17-C18	1.503(4)
C18-C19	1.387(4)
C18-C23	1.404(4)
C19-C20	1.389(4)
C20-C21	1.387(4)
C21-C22	1.391(4)
C22-C23	1.388(4)
C23-C24	1.465(4)
C25-C33	1.356(4)
C25-C26	1.506(4)
C26-C27	1.501(4)
C27-C28	1.380(4)

C27-C32	1.397(4)
C28-C29	1.391(4)
C29-C30	1.374(4)
C30-C31	1.391(4)
C31-C32	1.392(4)
C32-C33	1.458(4)

Angles-----

C9-C1-C2	104.8(2)
C3-C2-C7	120.2(3)
C3-C2-C1	131.3(3)
C7-C2-C1	108.5(2)
C2-C3-C4	119.0(3)
C3-C4-C5	120.6(3)
C6-C5-C4	120.8(3)
C7-C6-C5	118.7(3)
C6-C7-C2	120.8(2)
C6-C7-C8	131.4(3)
C2-C7-C8	107.8(2)
C9-C8-C7	109.2(2)
C8-C9-C10	126.5(3)
C8-C9-C1	109.6(2)
C10-C9-C1	123.9(3)
C15-C10-C11	118.3(3)
C15-C10-C9	121.0(3)
C11-C10-C9	120.6(2)
C12-C11-C10	121.8(3)
C11-C12-C13	117.9(3)
C11-C12-C16	121.1(2)
C13-C12-C16	121.1(3)
C14-C13-C12	122.3(3)

Chapter I: Generation and control of fluxional barbaralyl cations in gold-catalyzed cycloisomerizations

C13-C14-C15	117.9(3)
C13-C14-C25	120.2(3)
C15-C14-C25	121.9(2)
C10-C15-C14	121.7(3)
C24-C16-C12	126.5(3)
C24-C16-C17	109.8(2)
C12-C16-C17	123.6(2)
C18-C17-C16	103.2(2)
C19-C18-C23	119.8(3)
C19-C18-C17	131.0(3)
C23-C18-C17	109.2(2)
C18-C19-C20	119.3(3)
C21-C20-C19	120.5(3)
C20-C21-C22	121.0(3)
C23-C22-C21	118.4(3)
C22-C23-C18	121.0(3)
C22-C23-C24	131.3(3)
C18-C23-C24	107.7(2)
C16-C24-C23	110.0(2)
C33-C25-C14	128.3(3)
C33-C25-C26	109.7(2)
C14-C25-C26	122.1(2)
C27-C26-C25	103.2(2)
C28-C27-C32	121.0(3)
C28-C27-C26	129.9(3)
C32-C27-C26	109.1(2)
C27-C28-C29	118.8(3)
C30-C29-C28	120.5(3)
C29-C30-C31	121.4(3)
C30-C31-C32	118.4(3)

C31-C32-C27	120.0(3)
C31-C32-C33	131.9(3)
C27-C32-C33	108.1(2)
C25-C33-C32	110.0(2)

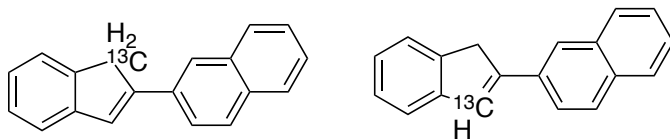
Table 3. Torsion angles [°] for PM2190.

C9-C1-C2-C3	-178.4(3)
C9-C1-C2-C7	2.9(3)
C7-C2-C3-C4	1.4(5)
C1-C2-C3-C4	-177.2(3)
C2-C3-C4-C5	0.1(5)
C3-C4-C5-C6	-1.4(5)
C4-C5-C6-C7	1.3(5)
C5-C6-C7-C2	0.2(5)
C5-C6-C7-C8	179.7(3)
C3-C2-C7-C6	-1.6(5)
C1-C2-C7-C6	177.3(3)
C3-C2-C7-C8	178.8(3)
C1-C2-C7-C8	-2.3(3)
C6-C7-C8-C9	-178.7(3)
C2-C7-C8-C9	0.7(4)
C7-C8-C9-C10	-179.4(3)
C7-C8-C9-C1	1.1(4)
C2-C1-C9-C8	-2.4(3)
C2-C1-C9-C10	178.1(3)
C8-C9-C10-C15	-159.0(3)
C1-C9-C10-C15	20.4(5)
C8-C9-C10-C11	20.8(5)
C1-C9-C10-C11	-159.8(3)

C15-C10-C11-C12	0.2(4)
C9-C10-C11-C12	-179.5(3)
C10-C11-C12-C13	0.6(5)
C10-C11-C12-C16	-178.9(3)
C11-C12-C13-C14	-0.7(5)
C16-C12-C13-C14	178.8(3)
C12-C13-C14-C15	0.0(5)
C12-C13-C14-C25	179.8(3)
C11-C10-C15-C14	-1.0(5)
C9-C10-C15-C14	178.8(3)
C13-C14-C15-C10	0.9(5)
C25-C14-C15-C10	-178.9(3)
C11-C12-C16-C24	-176.1(3)
C13-C12-C16-C24	4.3(5)
C11-C12-C16-C17	5.4(5)
C13-C12-C16-C17	-174.2(3)
C24-C16-C17-C18	-0.7(4)
C12-C16-C17-C18	178.0(3)
C16-C17-C18-C19	-179.2(3)
C16-C17-C18-C23	0.5(3)
C23-C18-C19-C20	0.3(5)
C17-C18-C19-C20	180.0(3)
C18-C19-C20-C21	-0.8(5)
C19-C20-C21-C22	0.6(6)
C20-C21-C22-C23	0.0(5)
C21-C22-C23-C18	-0.5(5)
C21-C22-C23-C24	-179.7(3)
C19-C18-C23-C22	0.4(5)
C17-C18-C23-C22	-179.4(3)
C19-C18-C23-C24	179.7(3)

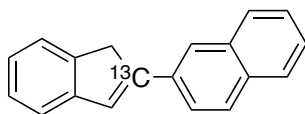
C17-C18-C23-C24	0.0(4)
C12-C16-C24-C23	-177.9(3)
C17-C16-C24-C23	0.7(4)
C22-C23-C24-C16	178.8(3)
C18-C23-C24-C16	-0.4(4)
C13-C14-C25-C33	-179.4(3)
C15-C14-C25-C33	0.4(5)
C13-C14-C25-C26	0.0(5)
C15-C14-C25-C26	179.7(3)
C33-C25-C26-C27	0.3(3)
C14-C25-C26-C27	-179.1(3)
C25-C26-C27-C28	-179.8(3)
C25-C26-C27-C32	-0.1(3)
C32-C27-C28-C29	0.9(5)
C26-C27-C28-C29	-179.5(3)
C27-C28-C29-C30	-0.9(5)
C28-C29-C30-C31	0.2(5)
C29-C30-C31-C32	0.5(5)
C30-C31-C32-C27	-0.5(5)
C30-C31-C32-C33	179.8(3)
C28-C27-C32-C31	-0.2(5)
C26-C27-C32-C31	-179.9(3)
C28-C27-C32-C33	179.6(3)
C26-C27-C32-C33	-0.1(3)
C14-C25-C33-C32	179.0(3)
C26-C25-C33-C32	-0.4(4)
C31-C32-C33-C25	-179.9(3)
C27-C32-C33-C25	0.3(4)

3:2 Mixture of 2-(1H-(1-¹³C)inden-2-yl)naphthalene and 2-(1H-(3-¹³C)inden-2-yl)naphthalene (4j')



The title compounds **4j'** were obtained as an inseparable mixture from 2-(cyclohepta-2,4,6-trien-1-yl(2-¹³C)ethynyl)naphthalene (8.1 mg, 33 μ mol) in the form of a colorless solid (3.4 mg, 42%). ¹H NMR (500 MHz, CDCl₃) δ 8.00 (s, 1H), 7.87 – 7.80 (m, 4H), 7.54 – 7.34 (m, 5H), 7.30 (dd, $J = 7.3, 7.3$ Hz, 1H), 7.21 (dd, $J = 7.3, 7.3$ Hz, 1H), 3.94 (d, $^3J_{CH} = 3.4$ Hz, 0.8H), 3.94 (d, $^1J_{CH} = 128.4$ Hz, 1.2H). ¹³C NMR (126 MHz, CDCl₃) δ 146.95 – 146.15 (m), 145.88 – 145.26 (m), 143.60 – 143.11 (m), 133.83, 133.55 (d, $J_{CC} = 2.5$ Hz), 133.04, 128.35, 128.26, 127.83, 127.36 (¹³C label), 126.84, 126.54, 126.08, 125.06 (d, $J_{CC} = 2.3$ Hz), 124.45 (d, $J_{CC} = 2.4$ Hz), 124.10 (d, $J_{CC} = 2.6$ Hz), 123.85 (d, $J_{CC} = 2.9$ Hz), 121.21 (d, $J_{CC} = 2.5$ Hz), 39.24 (¹³C label). HRMS-APCI $m/z = 244.1210$ [M+H]⁺, calc. for C₁₈H₁₅¹³C = 244.1207.

2-(1H-(2-¹³C)-inden-2-yl)naphthalene (4j'')

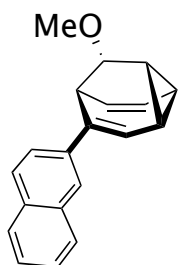


The title compound **4j''** was obtained from 2-(cyclohepta-2,4,6-trien-1-yl(1-¹³C)ethynyl)naphthalene (20 mg, 82 μ mol) in the form of a colorless solid (2.9 mg, 12 μ mol, 15 %). ¹H NMR (500 MHz, CDCl₃) δ 8.00 (d, $J = 4.9$ Hz, 1H), 7.87 – 7.80 (m, 4H), 7.54 – 7.41 (m, 4H), 7.36 (q, $J = 1.9$ Hz, 1H), 7.30 (t, $J = 7.3$ Hz, 1H), 7.21 (td, $J = 7.4, 1.1$ Hz, 1H), 3.94 (d, $J = 5.8$ Hz, 2H). ¹³C NMR (126 MHz, CDCl₃) δ 146.56 (¹³C

label), 133.84, 133.79 (d, $J_{CC} = 3.8$ Hz), 133.30, 133.03, 128.34 (d, $J_{CC} = 4.6$ Hz), 128.26, 127.83, 127.60, 127.05, 126.84, 126.54, 126.08, 125.06, 124.45, 124.09 (d, $J_{CC} = 1.8$ Hz), 123.85 (d, $J_{CC} = 2.9$ Hz), 121.21 (d, $J_{CC} = 6.4$ Hz), 39.22 (d, $J_{CC} = 40.5$ Hz). HRMS-APCI $m/z = 244.1208$ $[M+H]^+$, calc. for $C_{18}H_{15}^{13}C = 244.1207$.

5.5 Trapping of the intermediates

(±)(1R,5S,8R,9S)-9-methoxy-4-(naphthalen-2-yl)tricyclo[3.3.1.0^{2,8}]nona-3,6-diene (9)



A solution of 2-(cyclohepta-2,4,6-trien-1-ylethynyl)naphthalene (100 mg, 0.41 mmol) in 1:1 MeOH-CH₂Cl₂ (0.5 mL, 0.29 M) was sealed in a 3 mL screw cap vial and cooled to 0 °C, with no special precautions taken to exclude air or moisture. Catalyst **7** (5.6 mg, 5 mol%) was then added and the mixture stirred at 0 °C for 1 h. The solvent was removed under reduced pressure and the crude residue was purified by preparative TLC (eluent: 1:4 pentane-CH₂Cl₂) afforded the title compound **9** as a colorless solid (45.5 mg, 0.17 mmol, 40 %). ¹H NMR (500 MHz, CDCl₃) δ 7.86 (s, 1H), 7.85 – 7.77 (m, 3H), 7.59 (dd, $J = 8.6, 1.9$ Hz, 1H), 7.50 – 7.41 (m, 2H), 6.10 (dd, $J = 6.7, 1.1$ Hz, 1H), 6.00 (dd, $J = 9.1, 6.0$ Hz, 1H), 5.94 – 5.88 (m, 1H), 3.72 – 3.68 (m, 1H), 3.51 – 3.49 (m, 1H), 3.42 (s, 3H), 2.54 – 2.48 (m, 1H), 2.39 – 2.31 (m, 2H). ¹³C NMR (126 MHz, CDCl₃) δ 137.60, 137.15, 133.68, 132.52, 128.18, 128.09, 127.65, 126.36, 125.73, 124.01, 123.48, 123.46, 123.14, 118.82, 72.98, 56.74, 37.94, 25.57, 22.90, 21.54. HRMS-APCI $m/z = 275.1434$ $[M+H]^+$, calc. for $C_{17}H_{19}O = 275.1436$.

X-Ray Crystal Structure:

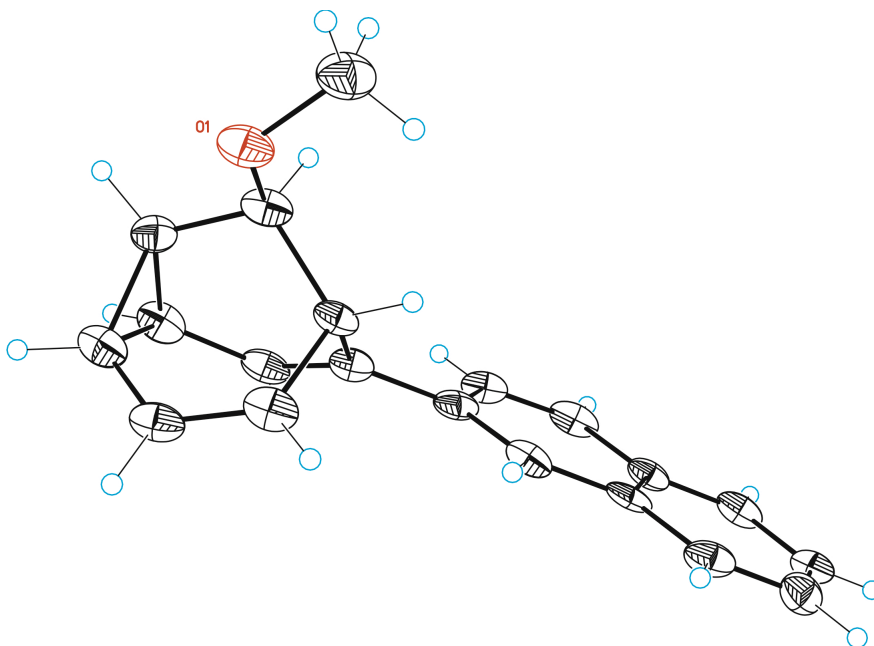


Table 1. Crystal data and structure refinement for PM3183.

Identification code	PM3183	
Empirical formula	C ₂₀ H ₁₈ O	
Formula weight	274.34	
Temperature	100(2) K	
Wavelength	0.71073 Å	
Crystal system	Orthorhombic	
Space group	Pca2(1)	
Unit cell dimensions	a = 15.006(4) Å	a =
90.00 °.	b = 15.379(5) Å	b =
90.00 °.	c = 6.095(3) Å	g =

90.00 °.	
Volume	1406.6(9) Å ³
Z	4
Density (calculated)	1.296 Mg/m ³
Absorption coefficient	0.078 mm ⁻¹
F(000)	584
Crystal size	0.01 x 0.01 x 0.001 mm ³
Theta range for data collection	1.32 to 25.35 °.
Index ranges	-17 <=h<=16 ,-18 <=k<=18 ,-7
<=l<=7	
Reflections collected	16373
Independent reflections	2540 [R(int) = 0.1386]
Completeness to theta =25.35 °	99.5%
Absorption correction	Empirical
Max. and min. transmission	0.9999 and 0.9992
Refinement method	Full-matrix least-squares on F ²
Data / restraints / parameters	2540 / 1 / 191
Goodness-of-fit on F ²	1.049
Final R indices [I>2sigma(I)]	R1 = 0.0605 , wR2 = 0.1079
R indices (all data)	R1 = 0.1336 , wR2 = 0.1382
Flack parameter	x =1(4)
Largest diff. peak and hole	0.240 and -0.211 e.Å ⁻³

Table 2. Bond lengths [Å] and angles [°] for PM3183.

Bond lengths----

C1-O1	1.421(5)
C2-O1	1.443(5)
C2-C7	1.513(6)
C2-C3	1.547(6)

Chapter I: Generation and control of fluxional barbaralyl cations in gold-catalyzed cycloisomerizations

C3-C4	1.509(6)
C3-C10	1.535(5)
C4-C5	1.336(6)
C5-C6	1.449(6)
C6-C7	1.512(6)
C6-C8	1.582(7)
C7-C8	1.514(6)
C8-C9	1.460(6)
C9-C10	1.340(6)
C10-C11	1.471(6)
C11-C20	1.374(6)
C11-C12	1.435(7)
C12-C13	1.363(6)
C13-C14	1.426(6)
C14-C15	1.420(6)
C14-C19	1.434(5)
C15-C16	1.361(6)
C16-C17	1.402(7)
C17-C18	1.361(6)
C18-C19	1.410(6)
C19-C20	1.431(6)
Angles-----	
O1-C2-C7	107.1(4)
O1-C2-C3	111.4(3)
C7-C2-C3	110.2(3)
C4-C3-C10	106.9(3)
C4-C3-C2	111.6(4)
C10-C3-C2	107.7(3)
C5-C4-C3	118.6(4)
C4-C5-C6	120.9(4)

C5-C6-C7	119.6(4)
C5-C6-C8	120.6(4)
C7-C6-C8	58.5(3)
C6-C7-C2	115.5(4)
C6-C7-C8	63.0(3)
C2-C7-C8	113.7(4)
C9-C8-C7	118.2(4)
C9-C8-C6	121.0(4)
C7-C8-C6	58.4(3)
C10-C9-C8	122.5(4)
C9-C10-C11	123.6(4)
C9-C10-C3	116.5(4)
C11-C10-C3	119.9(4)
C20-C11-C12	118.0(4)
C20-C11-C10	122.5(4)
C12-C11-C10	119.5(4)
C13-C12-C11	121.3(4)
C12-C13-C14	121.7(5)
C15-C14-C13	122.9(4)
C15-C14-C19	119.2(4)
C13-C14-C19	118.0(4)
C16-C15-C14	120.3(5)
C15-C16-C17	120.8(5)
C18-C17-C16	120.3(5)
C17-C18-C19	121.6(5)
C18-C19-C20	123.6(4)
C18-C19-C14	117.9(4)
C20-C19-C14	118.6(4)
C11-C20-C19	122.5(4)
C1-O1-C2	112.3(3)

Symmetry transformations used to generate equivalent atoms:

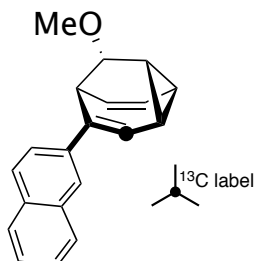
Table 3. Torsion angles [°] for PM3183.

O1-C2-C3-C4	64.3(4)
C7-C2-C3-C4	-54.4(4)
O1-C2-C3-C10	-178.7(3)
C7-C2-C3-C10	62.6(4)
C10-C3-C4-C5	-75.9(5)
C2-C3-C4-C5	41.6(5)
C3-C4-C5-C6	-3.1(6)
C4-C5-C6-C7	-21.4(6)
C4-C5-C6-C8	47.4(6)
C5-C6-C7-C2	4.8(6)
C8-C6-C7-C2	-104.9(4)
C5-C6-C7-C8	109.7(5)
O1-C2-C7-C6	-89.5(4)
C3-C2-C7-C6	31.8(5)
O1-C2-C7-C8	-159.7(4)
C3-C2-C7-C8	-38.4(5)
C6-C7-C8-C9	-110.9(5)
C2-C7-C8-C9	-3.2(6)
C2-C7-C8-C6	107.7(5)
C5-C6-C8-C9	-2.0(6)
C7-C6-C8-C9	106.2(4)
C5-C6-C8-C7	-108.2(4)
C7-C8-C9-C10	22.6(7)
C6-C8-C9-C10	-45.7(6)
C8-C9-C10-C11	-178.0(4)
C8-C9-C10-C3	4.1(6)
C4-C3-C10-C9	73.9(5)

C2-C3-C10-C9	-46.1(5)
C4-C3-C10-C11	-104.0(5)
C2-C3-C10-C11	135.9(4)
C9-C10-C11-C20	-143.6(4)
C3-C10-C11-C20	34.2(6)
C9-C10-C11-C12	38.1(7)
C3-C10-C11-C12	-144.1(4)
C20-C11-C12-C13	0.2(6)
C10-C11-C12-C13	178.5(4)
C11-C12-C13-C14	1.4(6)
C12-C13-C14-C15	178.2(4)
C12-C13-C14-C19	-1.4(6)
C13-C14-C15-C16	-178.9(4)
C19-C14-C15-C16	0.6(6)
C14-C15-C16-C17	-0.6(6)
C15-C16-C17-C18	0.0(6)
C16-C17-C18-C19	0.7(6)
C17-C18-C19-C20	179.0(4)
C17-C18-C19-C14	-0.7(6)
C15-C14-C19-C18	0.1(5)
C13-C14-C19-C18	179.6(4)
C15-C14-C19-C20	-179.7(4)
C13-C14-C19-C20	-0.1(5)
C12-C11-C20-C19	-1.7(6)
C10-C11-C20-C19	180.0(4)
C18-C19-C20-C11	-178.0(4)
C14-C19-C20-C11	1.7(6)
C7-C2-O1-C1	-158.3(4)
C3-C2-O1-C1	81.2(4)

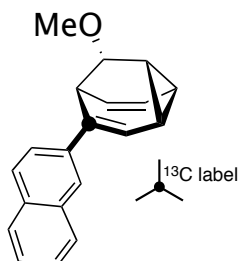
Symmetry transformations used to generate equivalent atoms:

(±)(1*R*,5*S*,8*R*,9*S*)-9-methoxy-4-(naphthalen-2-yl)-3(¹³C)tricyclo[3.3.1.0^{2,8}]nona-3,6-diene (9')



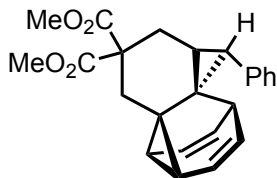
The title compound **9'** was obtained from 2-(cyclohepta-2,4,6-trien-1-yl(2-¹³C)ethynyl)naphthalene (20 mg, 82 μ mol) following the procedure for (±)(1*R*,5*S*,8*R*,9*S*)-9-methoxy-4-(naphthalen-2-yl)tricyclo[3.3.1.0^{2,8}]nona-3,6-diene as a white solid (8.6 mg, 31 μ mol, 38 %). ¹H NMR (500 MHz, CDCl₃) δ 7.85 (s, 1H), 7.83 – 7.77 (m, 3H), 7.58 (dd, J = 8.6, 1.9 Hz, 1H), 7.48 – 7.41 (m, 2H), 6.09 (ddd, J = 0.86, 6.63 Hz, J_{CH} = 158.65 Hz, 1H), 5.99 (dd, J = 9.2, 6.0 Hz, 1H), 5.90 (dd, J = 9.2, 6.6 Hz, 1H), 3.75 – 3.64 (m, 2H), 3.50 (s, 2H), 3.42 (s, 5H), 2.51 (q, J = 7.2 Hz, 2H), 2.39 – 2.30 (m, 4H). ¹³C NMR (126 MHz, CDCl₃) δ 137.88, 137.25 (d, J_{CC} = 18.9 Hz), 133.69, 132.54, 128.20, 128.10, 127.67, 126.38, 125.76, 124.01, 123.50 (d, J_{CC} = 4.0 Hz) (plus one masked carbon signal), 123.15, 118.84 (¹³C label), 73.03, 56.76, 37.95, 25.57 (d, J_{CC} = 53.4 Hz), 22.91, 21.56. HRMS-APCI m/z = 276.1465 [M+H]⁺, calc. for C₁₉¹³CH₁₉O = 276.1469.

(±)(1R,5S,8R,9S)-9-methoxy-4-(naphthalen-2-yl)-4(¹³C)tricyclo[3.3.1.0^{2,8}]nona-3,6-diene (9'')



The title compound **9''** was obtained from 2-(cyclohepta-2,4,6-trien-1-yl(1-¹³C)ethynyl)naphthalene (20 mg, 82 μmol) following the procedure for (±)(1R,5S,8R,9S)-9-methoxy-4-(naphthalen-2-yl)tricyclo[3.3.1.0^{2,8}]nona-3,6-diene as a white solid (9.4 mg, 34 μmol, 41%). ¹H NMR (500 MHz, CDCl₃) δ 7.90 – 7.86 (m, 2H), 7.86 – 7.80 (m, 5H), 7.61 (ddd, *J* = 8.6, 3.2, 1.9 Hz, 2H), 7.47 (dddd, *J* = 19.3, 8.0, 6.9, 1.4 Hz, 3H), 6.15 – 6.09 (m, 2H), 6.05 – 5.99 (m, 2H), 5.93 (ddd, *J* = 9.1, 6.6, 1.0 Hz, 2H), 3.75 – 3.67 (m, 1H), 3.52 (ddd, *J* = 3.6, 2.3, 1.2 Hz, 1H), 3.44 (s, 2H), 2.53 (qd, *J* = 7.4, 6.1 Hz, 1H), 2.43 – 2.31 (m, 2H). ¹³C NMR (126 MHz, CDCl₃) δ 137.64 (¹³C label) (plus one masked carbon signal), 133.68, 132.54, 128.20 (d, *J*_{CC} = 3.7 Hz), 128.11, 127.67, 126.39, 125.76, 124.02, 123.50, 123.48, 123.16 (d, *J* = 3.8 Hz), 118.82 (d, *J*_{CC} = 70.1 Hz), 73.01, 56.77, 37.95 (d, *J*_{CC} = 38.0 Hz), 25.59, 22.92, 21.55. HRMS-APCI *m/z* = 276.1465 [M+H]⁺, calc. for C₁₉¹³CH₁₉O = 276.1469.

8(±)(1*R*,1*aS*,4*aS*,5*S*,5*aR*,6*R*)-dimethyl 5-phenyl-1,4,4*a*,5,6,8*a*-hexahydro-1,6-ethenodicyclopropa[*d*,*i*]naphthalene-3,3(2*H*)-dicarboxylate (7)



A solution of gold complex **11** (5 mol%) and dimethyl 2-cinnamyl-2-(3-(cyclohepta-2,4,6-trien-1-yl)prop-2-yn-1-yl)malonate (0.1 mmol) in CH₂Cl₂ (1 mL, 0.1 M) was stirred for 16 h at rt. The crude reaction mixture was purified by preparative TLC using cyclohexane/EtOAc (10:1) to give the title compound **7** as a colorless solid (49%). M. p. 171.6 – 173.1 °C. ¹H NMR (400 MHz, CDCl₃) δ 7.26 – 7.12 (m, 5H), 5.77 (ddd, *J* = 9.1, 6.7, 1.3 Hz, 1H), 5.69 (ddd, *J* = 9.1, 6.4, 0.8 Hz, 1H), 5.62 (dd, *J* = 9.0, 6.4 Hz, 1H), 5.33 (ddd, *J* = 9.1, 6.6, 1.3 Hz, 1H), 3.80 (s, 3H), 3.72 (s, 3H), 2.99 (ddd, *J* = 14.5, 8.4, 1.9 Hz, 1H), 2.55 (d, *J* = 14.2 Hz, 1H), 2.35 (ddd, *J* = 7.9, 6.5, 1.4 Hz, 1H), 2.11 (ddd, *J* = 7.6, 6.4, 1.3 Hz, 1H), 2.00 (dd, *J* = 14.2, 1.8 Hz, 1H), 1.89 (d, *J* = 5.2 Hz, 1H), 1.80 – 1.67 (m, 3H). ¹³C NMR (101 MHz, CDCl₃) δ 172.4, 171.4, 139.2, 129.0, 127.6, 125.7, 124.8, 122.5, 122.2, 121.0, 52.7, 52.6, 52.3, 35.6, 35.1, 34.7, 32.4, 31.3, 30.4, 28.2, 25.8, 17.8. HRMS-APCI *m/z* = 399.1585 [M+Na]⁺, calc. for C₂₄H₂₄O₄Na = 399.1572.

X-Ray Crystal Structure:

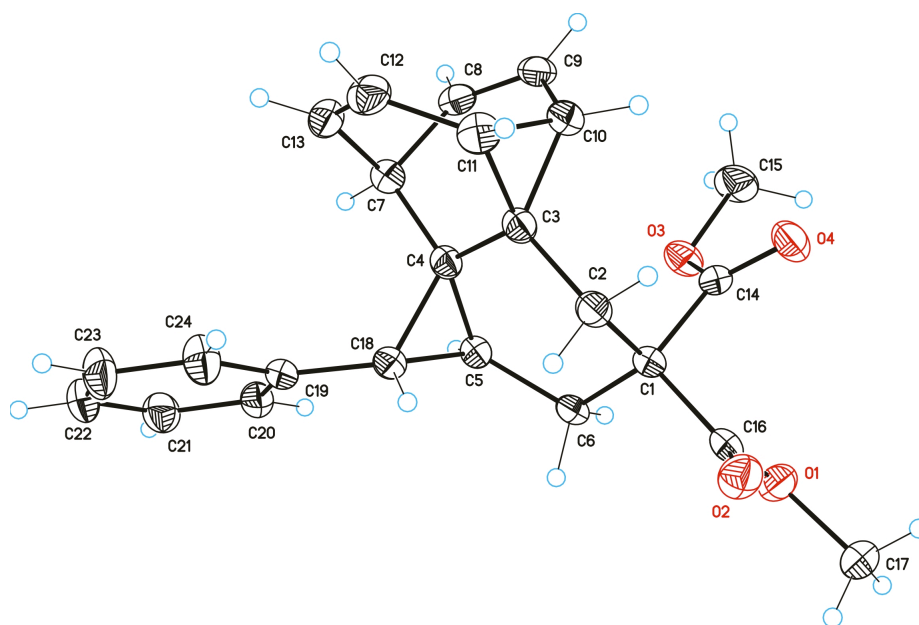


Table 1. Crystal data and structure refinement for mo_WYH4662_0m.

Identification code	mo_WYH4662_0m	
Empirical formula	C ₂₄ H ₂₄ O ₄	
Formula weight	376.43	
Temperature	100(2)K	
Wavelength	0.71073 Å	
Crystal system	Monoclinic	
Space group	C2/c	
Unit cell dimensions	a = 43.104(13) Å	∠ = 90.00 °.
	b = 6.2652(18) Å	∠ = 99.96 °.
	c = 13.842(4) Å	∠ = 90.00 °.
Volume	3681.6(18) Å ³	
Z	8	

Density (calculated)	1.358 Mg/m ³
Absorption coefficient	0.091 mm ⁻¹
F(000)	1600
Crystal size	0.15 x 0.15 x 0.1 mm ³
Theta range for data collection	1.92 to 27.56 °.
Index ranges	-55 <=h<=56 , -8 <=k<=8 , -12 <=l<=17
Reflections collected	12242
Independent reflections	4229 [R(int) = 0.0660]
Completeness to theta =27.56 °	0.995 %
Absorption correction	Empirical
Max. and min. transmission	0.9909 and 0.9864
Refinement method	Full-matrix least-squares on F ²
Data / restraints / parameters	4229 / 0 / 255
Goodness-of-fit on F ²	1.010
Final R indices [I>2sigma(I)]	R1 = 0.0516 , wR2 = 0.1083
R indices (all data)	R1 = 0.1086 , wR2 = 0.1273
Largest diff. peak and hole	0.253 and -0.244 e.Å ⁻³

Table 2. Bond lengths [Å] and angles [°] for mo_WYH4662_0m.

Bond lengths----

C1-C16	1.523(3)
C1-C14	1.535(3)
C1-C2	1.543(3)
C1-C6	1.548(3)
C2-C3	1.509(3)
C3-C4	1.492(3)
C3-C11	1.501(3)
C3-C10	1.521(3)

C4-C5	1.507(3)
C4-C18	1.523(3)
C4-C7	1.525(3)
C5-C18	1.519(3)
C5-C6	1.531(3)
C7-C8	1.510(3)
C7-C13	1.516(3)
C8-C9	1.322(3)
C9-C10	1.462(3)
C10-C11	1.583(3)
C11-C12	1.469(3)
C12-C13	1.334(3)
C14-O4	1.204(2)
C14-O3	1.331(3)
C15-O3	1.452(2)
C16-O2	1.201(3)
C16-O1	1.343(3)
C17-O1	1.458(3)
C18-C19	1.497(3)
C19-C24	1.387(3)
C19-C20	1.388(3)
C20-C21	1.389(3)
C21-C22	1.374(3)
C22-C23	1.374(3)
C23-C24	1.384(3)

Angles-----

C16-C1-C14	105.36(15)
C16-C1-C2	108.81(17)
C14-C1-C2	106.96(16)
C16-C1-C6	109.80(16)

C14-C1-C6	113.95(17)
C2-C1-C6	111.65(16)
C3-C2-C1	110.01(17)
C4-C3-C11	114.71(17)
C4-C3-C2	116.01(17)
C11-C3-C2	120.55(18)
C4-C3-C10	114.80(18)
C11-C3-C10	63.18(14)
C2-C3-C10	117.10(16)
C3-C4-C5	117.51(17)
C3-C4-C18	118.63(17)
C5-C4-C18	60.15(13)
C3-C4-C7	111.98(17)
C5-C4-C7	122.25(18)
C18-C4-C7	117.27(16)
C4-C5-C18	60.45(13)
C4-C5-C6	121.20(17)
C18-C5-C6	117.79(17)
C5-C6-C1	115.25(17)
C8-C7-C13	103.44(17)
C8-C7-C4	110.66(16)
C13-C7-C4	108.56(18)
C9-C8-C7	119.0(2)
C8-C9-C10	121.39(19)
C9-C10-C3	118.59(18)
C9-C10-C11	120.45(18)
C3-C10-C11	57.80(13)
C12-C11-C3	118.34(19)
C12-C11-C10	118.89(19)
C3-C11-C10	59.02(13)

C13-C12-C11	120.9(2)
C12-C13-C7	119.3(2)
O4-C14-O3	124.51(19)
O4-C14-C1	121.99(19)
O3-C14-C1	113.49(17)
O2-C16-O1	124.2(2)
O2-C16-C1	125.1(2)
O1-C16-C1	110.72(18)
C19-C18-C5	124.77(19)
C19-C18-C4	121.96(18)
C5-C18-C4	59.40(13)
C24-C19-C20	118.08(19)
C24-C19-C18	118.1(2)
C20-C19-C18	123.82(19)
C19-C20-C21	120.5(2)
C22-C21-C20	120.5(2)
C23-C22-C21	119.7(2)
C22-C23-C24	120.0(2)
C23-C24-C19	121.3(2)
C16-O1-C17	115.34(17)
C14-O3-C15	115.45(17)

Table 3. Torsion angles [°] for mo_WYH4662_0m.

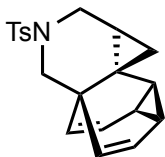
C16-C1-C2-C3	178.95(15)
C14-C1-C2-C3	65.6(2)
C6-C1-C2-C3	-59.7(2)
C1-C2-C3-C4	54.6(2)
C1-C2-C3-C11	-159.52(17)
C1-C2-C3-C10	-86.2(2)
C11-C3-C4-C5	-173.71(17)

C2-C3-C4-C5	-25.8(3)
C10-C3-C4-C5	115.8(2)
C11-C3-C4-C18	-104.5(2)
C2-C3-C4-C18	43.4(3)
C10-C3-C4-C18	-174.97(17)
C11-C3-C4-C7	37.1(2)
C2-C3-C4-C7	-175.02(17)
C10-C3-C4-C7	-33.4(2)
C3-C4-C5-C18	108.9(2)
C7-C4-C5-C18	-105.2(2)
C3-C4-C5-C6	2.5(3)
C18-C4-C5-C6	-106.4(2)
C7-C4-C5-C6	148.33(18)
C4-C5-C6-C1	-8.9(3)
C18-C5-C6-C1	-79.5(2)
C16-C1-C6-C5	158.00(17)
C14-C1-C6-C5	-84.1(2)
C2-C1-C6-C5	37.2(2)
C3-C4-C7-C8	55.0(2)
C5-C4-C7-C8	-92.5(2)
C18-C4-C7-C8	-162.85(18)
C3-C4-C7-C13	-57.9(2)
C5-C4-C7-C13	154.59(17)
C18-C4-C7-C13	84.3(2)
C13-C7-C8-C9	75.3(2)
C4-C7-C8-C9	-40.8(3)
C7-C8-C9-C10	3.1(3)
C8-C9-C10-C3	20.4(3)
C8-C9-C10-C11	-47.0(3)
C4-C3-C10-C9	-3.4(3)

C11-C3-C10-C9	-109.8(2)
C2-C3-C10-C9	137.8(2)
C4-C3-C10-C11	106.4(2)
C2-C3-C10-C11	-112.4(2)
C4-C3-C11-C12	1.9(3)
C2-C3-C11-C12	-144.43(19)
C10-C3-C11-C12	108.5(2)
C4-C3-C11-C10	-106.54(19)
C2-C3-C11-C10	107.1(2)
C9-C10-C11-C12	-0.9(3)
C3-C10-C11-C12	-107.5(2)
C9-C10-C11-C3	106.6(2)
C3-C11-C12-C13	-20.7(3)
C10-C11-C12-C13	47.6(3)
C11-C12-C13-C7	-2.9(3)
C8-C7-C13-C12	-75.9(2)
C4-C7-C13-C12	41.6(3)
C16-C1-C14-O4	-50.5(3)
C2-C1-C14-O4	65.2(2)
C6-C1-C14-O4	-170.89(19)
C16-C1-C14-O3	129.94(18)
C2-C1-C14-O3	-114.37(18)
C6-C1-C14-O3	9.5(2)
C14-C1-C16-O2	119.7(2)
C2-C1-C16-O2	5.2(3)
C6-C1-C16-O2	-117.2(2)
C14-C1-C16-O1	-60.7(2)
C2-C1-C16-O1	-175.09(15)
C6-C1-C16-O1	62.4(2)
C4-C5-C18-C19	109.8(2)
C6-C5-C18-C19	-138.3(2)

C6-C5-C18-C4	112.0(2)
C3-C4-C18-C19	138.6(2)
C5-C4-C18-C19	-114.3(2)
C7-C4-C18-C19	-1.0(3)
C3-C4-C18-C5	-107.1(2)
C7-C4-C18-C5	113.4(2)
C5-C18-C19-C24	-165.2(2)
C4-C18-C19-C24	-92.4(3)
C5-C18-C19-C20	17.0(3)
C4-C18-C19-C20	89.8(3)
C24-C19-C20-C21	-1.1(3)
C18-C19-C20-C21	176.7(2)
C19-C20-C21-C22	0.7(3)
C20-C21-C22-C23	0.1(4)
C21-C22-C23-C24	-0.5(4)
C22-C23-C24-C19	0.1(4)
C20-C19-C24-C23	0.7(3)
C18-C19-C24-C23	-177.2(2)
O2-C16-O1-C17	-4.0(3)
C1-C16-O1-C17	176.33(15)
O4-C14-O3-C15	-3.1(3)
C1-C14-O3-C15	176.44(18)

(±)(3*a*S,5*a*R,6*a*S,6*b*S)-2-tosyl-1,2,3,5*a*,6,6*a*,7,7*a*-octahydro-3*a*,6-ethenodicyclopropa[*d*,*f*]isoquinoline (8 and 8')



A solution of gold complex **11** (5 mol%) and *N*-allyl-*N*-(3-(cyclohepta-2,4,6-trien-1-yl)prop-2-yn-1-yl)-4-methylbenzenesulfonamide (0.1 mmol) in CH₂Cl₂ (1 mL, 0.1 M) was stirred for 16 h at rt. The crude reaction mixture was purified by preparative TLC using cyclohexane/EtOAc (10:1) to give the title compound as a colorless solid (51%). M.p. 101.7 – 103.2 °C. ¹H NMR (400 MHz, CDCl₃) δ 7.67 (d, *J* = 8.3 Hz, 2H), 7.33 (d, *J* = 8.2 Hz, 2H), 5.71 (td, *J* = 7.7, 3.4 Hz, 2H), 4.51 – 4.42 (m, 2H), 3.69 (dd, *J* = 12.0, 5.3 Hz, 1H), 3.59 (ddd, *J* = 7.7, 4.8, 1.2 Hz, 1H), 3.51 (ddd, *J* = 7.5, 4.9, 1.1 Hz, 1H), 3.29 (d, *J* = 12.0 Hz, 1H), 3.25 (dd, *J* = 12.0, 1.8 Hz, 1H), 2.83 (d, *J* = 11.8 Hz, 1H), 2.45 (s, 3H), 1.66 (t, *J* = 6.8 Hz, 1H), 1.08 – 1.03 (m, 1H), 0.36 (dd, *J* = 8.5, 5.5 Hz, 1H), 0.30 (t, *J* = 5.1 Hz, 1H). ¹³C NMR (101 MHz, CDCl₃) δ 143.2, 134.6, 129.6, 127.2, 122.0, 121.5, 85.8, 85.2, 71.4, 67.6, 49.0, 43.3, 35.6, 31.6, 21.5, 15.5, 13.9, 11.2 HRMS-APCI *m/z* = 362.1196 [M+Na]⁺, calc. for C₂₀H₂₁NO₂SNa = 362.1191.

X-Ray Crystal Structure:

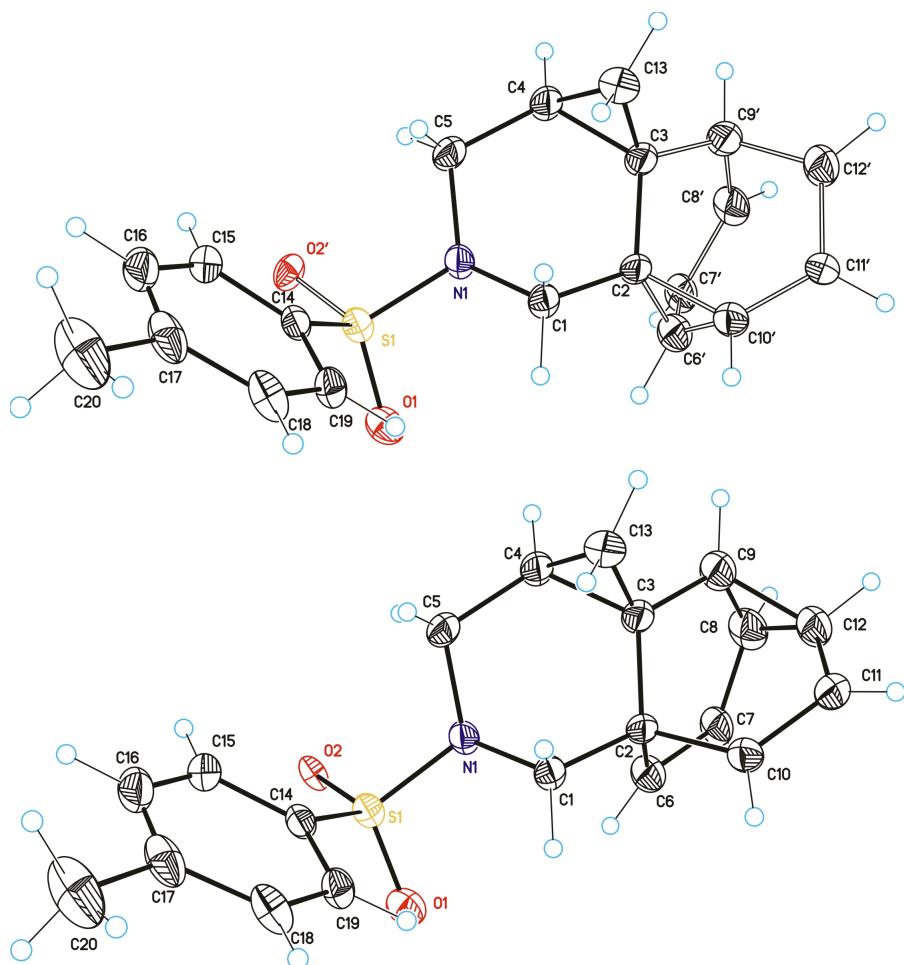


Table 1. Crystal data and structure refinement for mo_WYH4302_0m.

Identification code	mo_WYH4302_0m
Empirical formula	C ₂₀ H ₂₁ N O ₂ S
Formula weight	339.44
Temperature	100(2)K

Wavelength	0.71073 Å	
Crystal system	Monoclinic	
Space group	Cc	
Unit cell dimensions	a = 19.6378(14) Å	a =
90.00 °.	b = 6.2264(4) Å	b =
113.794(3) °.	c = 15.1429(11) Å	g =
90.00 °.		
Volume	1694.2(2) Å ³	
Z	4	
Density (calculated)	1.331 Mg/m ³	
Absorption coefficient	0.203 mm ⁻¹	
F(000)	720	
Crystal size	0.10 x 0.10 x 0.05 mm ³	
Theta range for data collection	2.27 to 32.40 °.	
Index ranges	-29 <=h<=29 , -8 <=k<=9 , -22	
<=l<=19		
Reflections collected	9225	
Independent reflections	4389 [R(int) = 0.0275]	
Completeness to theta =32.40 °	0.915 %	
Absorption correction	Empirical	
Max. and min. transmission	0.9899 and 0.9800	
Refinement method	Full-matrix least-squares on F ²	
Data / restraints / parameters	4389 / 262 / 266	
Goodness-of-fit on F ²	1.069	
Final R indices [I>2sigma(I)]	R1 = 0.0677 , wR2 = 0.1964	
R indices (all data)	R1 = 0.0722 , wR2 = 0.2017	
Flack parameter	x =0.05(12)	

Largest diff. peak and hole

1.135 and -0.718 e.Å⁻³

Table 2. Bond lengths [Å] and angles [°] for mo_WYH4302_0m.

Bond lengths----

S1-O2	1.411(9)
S1-O1	1.440(3)
S1-O2'	1.443(11)
S1-N1	1.629(3)
S1-C14	1.755(4)
N1-C5	1.475(5)
N1-C1	1.475(4)
C1-C2	1.509(5)
C2-C6'	1.438(7)
C2-C10'	1.482(8)
C2-C3	1.514(5)
C2-C10	1.514(8)
C2-C6	1.560(7)
C3-C13	1.496(6)
C3-C4	1.504(5)
C3-C9	1.507(8)
C3-C9'	1.512(8)
C4-C5	1.507(5)
C4-C13	1.524(6)
C6-C7	1.476(8)
C7-C8	1.465(8)
C8-C9	1.466(9)
C8-C12	1.503(9)
C9-C12	1.518(9)
C10-C11	1.435(8)

C11-C12	1.520(9)
C6'-C7'	1.518(8)
C6'-C10'	1.543(9)
C7'-C8'	1.463(8)
C8'-C9'	1.508(9)
C9'-C12'	1.549(9)
C10'-C11'	1.428(8)
C11'-C12'	1.482(8)
C14-C15	1.388(5)
C14-C19	1.396(5)
C15-C16	1.392(6)
C16-C17	1.378(7)
C17-C18	1.397(6)
C17-C20	1.507(6)
C18-C19	1.386(5)

Angles-----

O2-S1-O1	111.7(4)
O2-S1-O2'	15.6(5)
O1-S1-O2'	124.1(4)
O2-S1-N1	107.3(3)
O1-S1-N1	106.86(16)
O2'-S1-N1	108.7(4)
O2-S1-C14	114.6(3)
O1-S1-C14	106.62(16)
O2'-S1-C14	100.3(4)
N1-S1-C14	109.58(16)
C5-N1-C1	114.9(3)
C5-N1-S1	116.4(2)
C1-N1-S1	117.2(2)
N1-C1-C2	106.7(3)

C6'-C2-C10'	63.8(4)
C6'-C2-C1	119.2(4)
C10'-C2-C1	116.3(5)
C6'-C2-C3	120.0(4)
C10'-C2-C3	116.2(5)
C1-C2-C3	112.8(3)
C6'-C2-C10	74.9(6)
C10'-C2-C10	12.3(7)
C1-C2-C10	116.7(5)
C3-C2-C10	106.7(5)
C6'-C2-C6	27.6(4)
C10'-C2-C6	91.4(5)
C1-C2-C6	108.3(4)
C3-C2-C6	109.3(4)
C10-C2-C6	102.4(6)
C13-C3-C4	61.1(3)
C13-C3-C9	112.5(6)
C4-C3-C9	117.8(5)
C13-C3-C9'	118.5(6)
C4-C3-C9'	124.0(5)
C9-C3-C9'	7.4(9)
C13-C3-C2	119.7(3)
C4-C3-C2	117.4(3)
C9-C3-C2	116.7(5)
C9'-C3-C2	109.3(5)
C3-C4-C5	121.0(3)
C3-C4-C13	59.2(3)
C5-C4-C13	118.9(3)
N1-C5-C4	112.0(3)
C7-C6-C2	113.9(7)

C8-C7-C6	121.8(9)
C7-C8-C9	120.8(10)
C7-C8-C12	106.6(9)
C9-C8-C12	61.5(5)
C8-C9-C3	115.3(11)
C8-C9-C12	60.4(5)
C3-C9-C12	112.3(8)
C11-C10-C2	121.8(9)
C10-C11-C12	112.5(10)
C8-C12-C9	58.1(5)
C8-C12-C11	136.4(9)
C9-C12-C11	115.4(9)
C2-C6'-C7'	117.0(7)
C2-C6'-C10'	59.5(4)
C7'-C6'-C10'	136.6(8)
C8'-C7'-C6'	106.2(8)
C7'-C8'-C9'	121.9(9)
C8'-C9'-C3	114.8(10)
C8'-C9'-C12'	98.3(9)
C3-C9'-C12'	107.2(7)
C11'-C10'-C2	119.2(9)
C11'-C10'-C6'	109.5(9)
C2-C10'-C6'	56.7(4)
C10'-C11'-C12'	121.0(10)
C11'-C12'-C9'	113.3(9)
C3-C13-C4	59.7(3)
C15-C14-C19	120.7(4)
C15-C14-S1	119.0(3)
C19-C14-S1	120.0(3)
C14-C15-C16	119.3(4)
C17-C16-C15	120.9(4)

C16-C17-C18	119.2(4)
C16-C17-C20	119.4(4)
C18-C17-C20	121.3(5)
C19-C18-C17	120.9(4)
C18-C19-C14	118.9(4)

Table 3. Torsion angles [°] for mo_WYH4302_0m.

O2-S1-N1-C5	51.0(5)
O1-S1-N1-C5	170.9(3)
O2'-S1-N1-C5	34.8(5)
C14-S1-N1-C5	-73.9(3)
O2-S1-N1-C1	-167.4(5)
O1-S1-N1-C1	-47.5(3)
O2'-S1-N1-C1	176.3(5)
C14-S1-N1-C1	67.7(3)
C5-N1-C1-C2	-68.6(4)
S1-N1-C1-C2	149.3(3)
N1-C1-C2-C6'	-92.6(5)
N1-C1-C2-C10'	-165.9(5)
N1-C1-C2-C3	56.3(4)
N1-C1-C2-C10	-179.6(5)
N1-C1-C2-C6	-64.8(5)
C6'-C2-C3-C13	-167.0(5)
C10'-C2-C3-C13	-93.6(6)
C1-C2-C3-C13	44.4(5)
C10-C2-C3-C13	-85.1(6)
C6-C2-C3-C13	164.9(4)
C6'-C2-C3-C4	122.4(5)

C10'-C2-C3-C4	-164.2(6)
C1-C2-C3-C4	-26.3(5)
C10-C2-C3-C4	-155.7(6)
C6-C2-C3-C4	94.3(5)
C6'-C2-C3-C9	-25.8(9)
C10'-C2-C3-C9	47.6(9)
C1-C2-C3-C9	-174.4(7)
C10-C2-C3-C9	56.1(9)
C6-C2-C3-C9	-53.9(8)
C6'-C2-C3-C9'	-25.7(8)
C10'-C2-C3-C9'	47.8(8)
C1-C2-C3-C9'	-174.3(6)
C10-C2-C3-C9'	56.2(8)
C6-C2-C3-C9'	-53.8(7)
C13-C3-C4-C5	-107.3(4)
C9-C3-C4-C5	151.0(8)
C9'-C3-C4-C5	146.1(7)
C2-C3-C4-C5	3.2(6)
C9-C3-C4-C13	-101.7(8)
C9'-C3-C4-C13	-106.6(8)
C2-C3-C4-C13	110.5(4)
C1-N1-C5-C4	44.9(4)
S1-N1-C5-C4	-172.6(3)
C3-C4-C5-N1	-11.2(5)
C13-C4-C5-N1	-80.7(4)
C6'-C2-C6-C7	-72.5(10)
C10'-C2-C6-C7	-72.6(9)
C1-C2-C6-C7	169.0(7)
C3-C2-C6-C7	45.8(8)
C10-C2-C6-C7	-67.1(8)
C2-C6-C7-C8	-22.7(13)

Chapter I: Generation and control of fluxional barbaralyl cations in gold-catalyzed cycloisomerizations

C6-C7-C8-C9	3.6(17)
C6-C7-C8-C12	69.9(13)
C7-C8-C9-C3	-9.1(16)
C12-C8-C9-C3	-102.3(9)
C7-C8-C9-C12	93.2(12)
C13-C3-C9-C8	179.9(8)
C4-C3-C9-C8	-112.0(8)
C9'-C3-C9-C8	35(7)
C2-C3-C9-C8	36.0(12)
C13-C3-C9-C12	113.2(9)
C4-C3-C9-C12	-178.7(7)
C9'-C3-C9-C12	-32(7)
C2-C3-C9-C12	-30.7(13)
C6'-C2-C10-C11	88.4(10)
C10'-C2-C10-C11	113(4)
C1-C2-C10-C11	-156.1(9)
C3-C2-C10-C11	-28.9(11)
C6-C2-C10-C11	85.9(10)
C2-C10-C11-C12	-20.6(14)
C7-C8-C12-C9	-116.5(11)
C7-C8-C12-C11	-22.0(19)
C9-C8-C12-C11	94.4(14)
C3-C9-C12-C8	107.4(12)
C8-C9-C12-C11	-130.4(10)
C3-C9-C12-C11	-23.0(15)
C10-C11-C12-C8	-20.7(19)
C10-C11-C12-C9	48.7(14)
C10'-C2-C6'-C7'	-130.3(9)
C1-C2-C6'-C7'	122.8(6)
C3-C2-C6'-C7'	-23.8(8)

C10-C2-C6'-C7'	-124.7(7)
C6-C2-C6'-C7'	49.9(8)
C1-C2-C6'-C10'	-106.9(6)
C3-C2-C6'-C10'	106.5(6)
C10-C2-C6'-C10'	5.6(9)
C6-C2-C6'-C10'	-179.8(10)
C2-C6'-C7'-C8'	52.6(10)
C10'-C6'-C7'-C8'	-20.5(15)
C6'-C7'-C8'-C9'	-33.5(14)
C7'-C8'-C9'-C3	-13.6(15)
C7'-C8'-C9'-C12'	99.7(12)
C13-C3-C9'-C8'	-174.7(7)
C4-C3-C9'-C8'	-102.0(9)
C9-C3-C9'-C8'	-138(8)
C2-C3-C9'-C8'	43.4(10)
C13-C3-C9'-C12'	77.3(9)
C4-C3-C9'-C12'	150.0(6)
C9-C3-C9'-C12'	114(8)
C2-C3-C9'-C12'	-64.6(9)
C6'-C2-C10'-C11'	95.3(10)
C1-C2-C10'-C11'	-153.4(8)
C3-C2-C10'-C11'	-17.0(11)
C10-C2-C10'-C11'	-59(4)
C6-C2-C10'-C11'	95.3(9)
C1-C2-C10'-C6'	111.3(5)
C3-C2-C10'-C6'	-112.2(5)
C10-C2-C10'-C6'	-154(4)
C6-C2-C10'-C6'	0.1(5)
C2-C6'-C10'-C11'	-112.7(8)
C7'-C6'-C10'-C11'	-14.5(14)
C7'-C6'-C10'-C2	98.2(11)

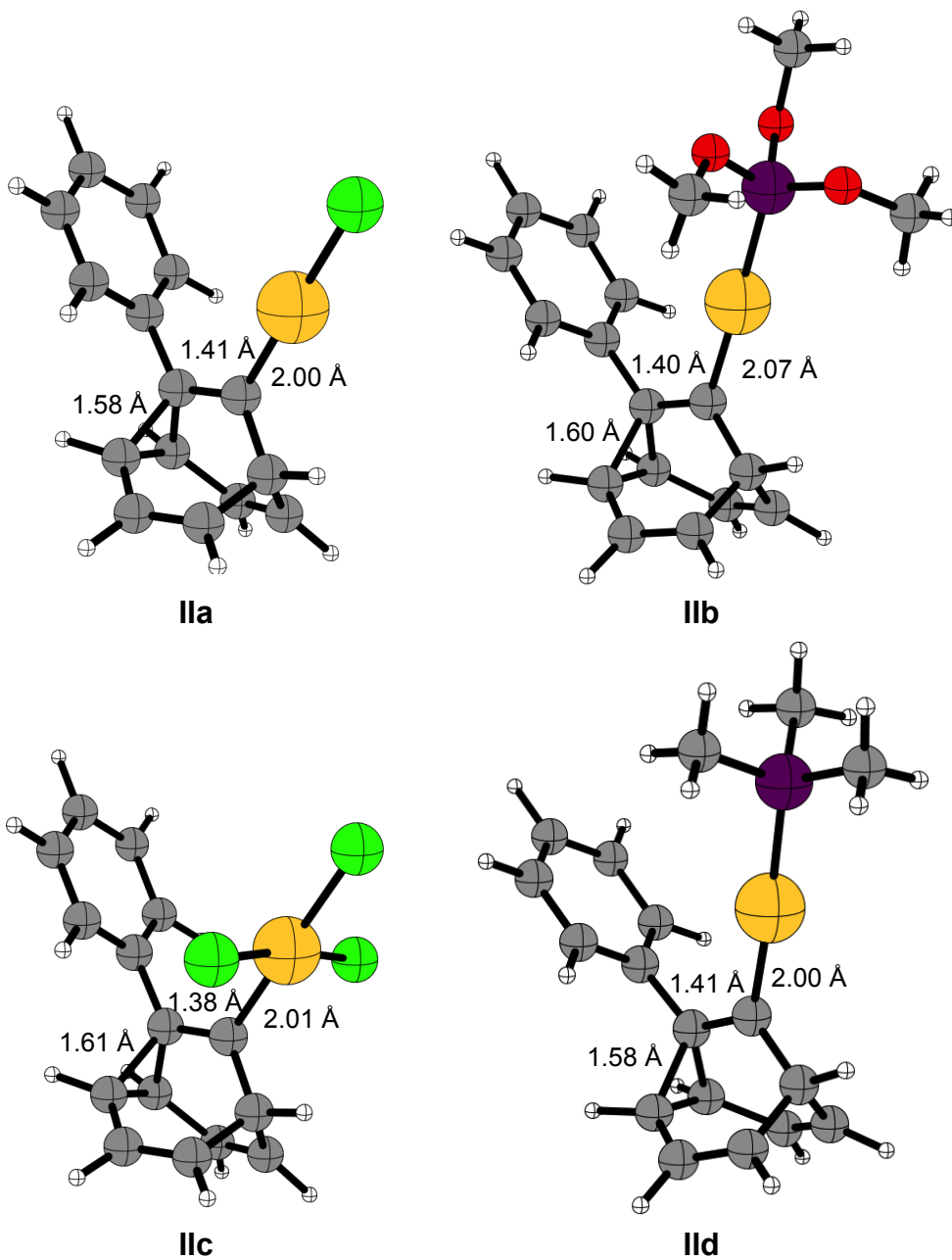
C2-C10'-C11'-C12'	5.0(15)
C6'-C10'-C11'-C12'	67.1(13)
C10'-C11'-C12'-C9'	-24.0(16)
C8'-C9'-C12'-C11'	-66.0(10)
C3-C9'-C12'-C11'	53.3(13)
C9-C3-C13-C4	110.4(6)
C9'-C3-C13-C4	115.3(6)
C2-C3-C13-C4	-106.9(4)
C5-C4-C13-C3	110.8(4)
O2-S1-C14-C15	-12.8(5)
O1-S1-C14-C15	-136.8(3)
O2'-S1-C14-C15	-6.4(5)
N1-S1-C14-C15	107.9(3)
O2-S1-C14-C19	162.0(4)
O1-S1-C14-C19	38.0(3)
O2'-S1-C14-C19	168.4(5)
N1-S1-C14-C19	-77.3(3)
C19-C14-C15-C16	-2.2(5)
S1-C14-C15-C16	172.5(3)
C14-C15-C16-C17	-0.4(6)
C15-C16-C17-C18	3.3(6)
C15-C16-C17-C20	-174.1(4)
C16-C17-C18-C19	-3.6(5)
C20-C17-C18-C19	173.8(4)
C17-C18-C19-C14	1.0(5)
C15-C14-C19-C18	1.9(5)
S1-C14-C19-C18	-172.8(3)

6. Calculation Methods and Data

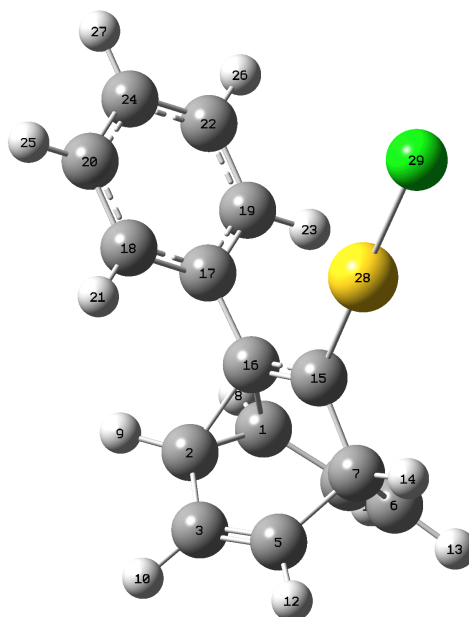
6.1 General Methods

DFT Calculations were carried out using Meta-Hybrid Generalized Gradient Approximation (MH-GGA) M06 functional (Zhao, Y.; Truhlar, D. G. *Theor. Chem. Acc.* **2008**, *120*, 215–241) as implemented in Gaussian 09 (Frisch, M. J.; Trucks, G. W.; Schlegel, H. B.; Scuseria, G. E.; Robb, M. A.; Cheeseman, J. R.; Scalmani, G.; Barone, V.; Mennucci, B.; Petersson, G. A.; Nakatsuji, H.; Caricato, M.; Li, X.; Hratchian, H. P.; Izmaylov, A. F.; Bloino, J.; Zheng, G.; Sonnenberg, J. L.; Hada, M.; Ehara, M.; Toyota, K.; Fukuda, R.; Hasegawa, J.; Ishida, M.; Nakajima, T.; Honda, Y.; Kitao, O.; Nakai, H.; Vreven, T.; Montgomery, J. A., Jr.; Peralta, J. E.; Ogliaro, F.; Bearpark, M.; Heyd, J. J.; Brothers, E.; Kudín, K. N.; Staroverov, V. N.; Kobayashi, R.; Normand, J.; Raghavachari, K.; Rendell, A.; Burant, J. C.; Iyengar, S. S.; Tomasi, J.; Cossi, M.; Rega, N.; Millam, J. M.; Klene, M.; Knox, J. E.; Cross, J. B.; Bakken, V.; Adamo, C.; Jaramillo, J.; Gomperts, R.; Stratmann, R. E.; Yazyev, O.; Austin, A. J.; Cammi, R.; Pomelli, C.; Ochterski, J. W.; Martin, R. L.; Morokuma, K.; Zakrzewski, V. G.; Voth, G. A.; Salvador, P.; Dannenberg, J. J.; Dapprich, S.; Daniels, A. D.; Farkas, O.; Foresman, J. B.; Ortiz, J. V.; Cioslowski, J.; Fox, D. J. *Gaussian 09, Revision A.02*, Gaussian, Inc., Wallingford CT, **2009**). The 6-31G(d) basis set (a. Hehre, W. J.; Ditchfield, R.; Pople, J. A. *J. Chem. Phys.* **1972**, *56*, 2257–2258. b. Francl, M. M.; Pietro, W. J.; Hehre, W. J.; Binkley, J. S.; Gordon, M. S.; Defrees D. J.; Pople, J. A. *J. Chem. Phys.*, **1982**, *77*, 3654–3665. c. Clark, T.; Chandrasekhar, J.; Spitznagel, G. W.; Schleyer, P. v. R.; *J. Comput. Chem.*, **1983**, *4*, 294–301) was used for all atoms except gold, which was treated with SDD and the associated effective core potential (Andrae, D.; Haussermann, U.; Dolg, M.; Stoll, H.; Preuss, H. *Theor. Chim. Acta* **1990**, *77*, 123–141). The solvent effect (CH₂Cl₂) was taken into account by single-point calculations using the polarizable continuum model (PCM) (Miertus S.; Tomasi, J. *J. Chem. Phys.* **1982**, *65*, 239–245).

6.2 Barbaralyl Au Intermediates



6.3 Intermediate IIa



(E = -1174.26945339; zpe corrected = -1174.047718; Enthalpy = -1174.031912; Free energy = -1174.092878 u.a.)

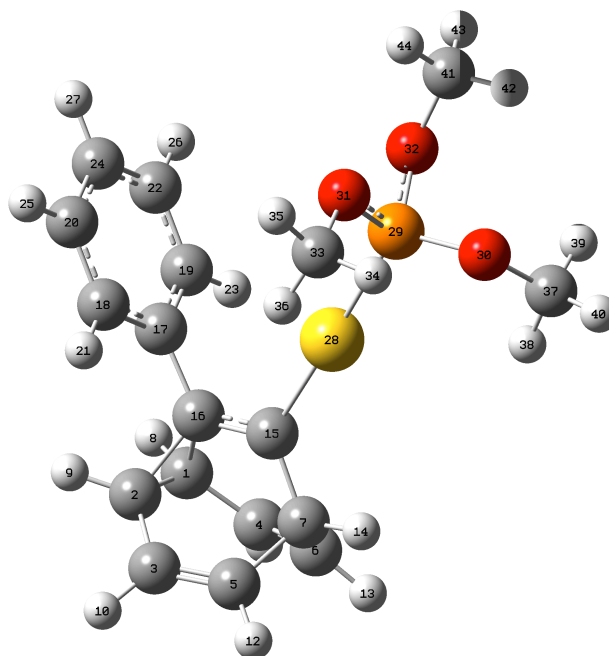
Cartesian coordinates for IIa

Coordinates (Å)

Atom	X	Y	Z
C	-2.947859	0.163196	-0.746305
C	-2.947570	0.162900	0.747236
C	-3.115383	-1.075244	1.513302
C	-3.116064	-1.074727	-1.512716
C	-2.425020	-2.169499	1.178298
C	-2.425566	-2.169123	-1.178479
C	-1.459952	-2.090335	-0.000283
H	-3.288939	1.091874	-1.204073

H	-3.288311	1.091572	1.205301
H	-3.849805	-1.080574	2.316536
H	-3.850875	-1.079729	-2.315609
H	-2.561489	-3.136389	1.657688
H	-2.562284	-3.135839	-1.658149
H	-0.764095	-2.932503	-0.000568
C	-0.743269	-0.778659	-0.000234
C	-1.570243	0.367301	0.000104
C	-0.990928	1.743788	0.000211
C	-0.694505	2.382751	1.206121
C	-0.695480	2.383001	-1.205835
C	-0.112767	3.648262	1.206679
H	-0.913005	1.878728	2.149162
C	-0.113821	3.648525	-1.206728
H	-0.914825	1.879039	-2.148721
C	0.175667	4.283757	-0.000066
H	0.117716	4.137999	2.151545
H	0.115906	4.138446	-2.151672
H	0.629161	5.273657	-0.000149
Au	1.251406	-0.686983	-0.000138
Cl	3.609786	-0.612352	0.000106

6.4 Intermediate IIb



(E = -1400.49502775; zpe corrected = -1400.143279; Enthalpy = -1400.118021; Free energy = -1400.201096 u.a.)

Cartesian coordinates for IIb

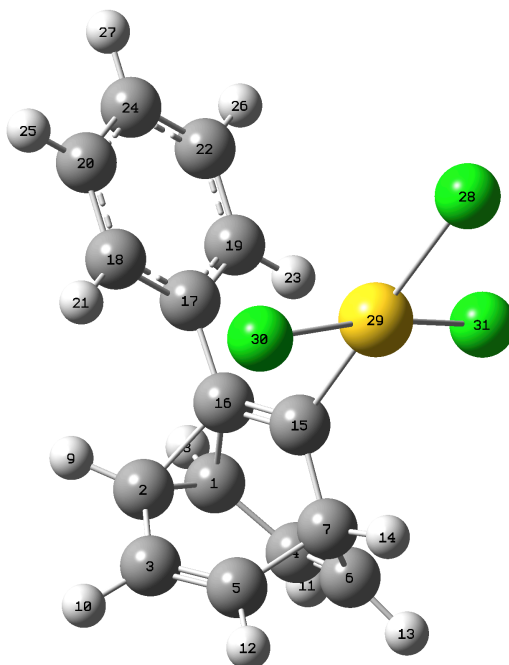
Coordinates (Å)

Atom	X	Y	Z
C	-3.900394	-0.019100	-0.761122
C	-3.893316	-0.000394	0.721320
C	-3.975575	-1.234898	1.503557
C	-3.988859	-1.272725	-1.511787
C	-3.224553	-2.290670	1.175632
C	-3.234611	-2.319902	-1.164368
C	-2.257577	-2.163086	-0.000538
H	-4.282734	0.886423	-1.232840

H	-4.269881	0.917577	1.173501
H	-4.701300	-1.273335	2.313607
H	-4.720973	-1.331309	-2.314845
H	-3.307271	-3.261970	1.657819
H	-3.320593	-3.302357	-1.622797
H	-1.514165	-2.963714	0.006739
C	-1.631493	-0.812540	-0.018519
C	-2.508646	0.276352	-0.030588
C	-2.004830	1.680828	-0.050325
C	-1.715924	2.339479	1.146871
C	-1.744504	2.315922	-1.266599
C	-1.170788	3.620857	1.127979
H	-1.908650	1.837736	2.096818
C	-1.198513	3.597047	-1.285983
H	-1.960279	1.796296	-2.201748
C	-0.912637	4.251235	-0.088651
H	-0.945894	4.127925	2.064921
H	-0.995692	4.084738	-2.238090
H	-0.488347	5.253755	-0.103610
Au	0.413093	-0.520160	-0.013663
P	2.736419	-0.135283	0.042837
O	3.684131	-1.437258	-0.054373
O	3.336739	0.554794	1.358185
O	3.190623	0.863485	-1.114059
C	3.131418	-0.070126	2.633104
H	3.697479	-1.005917	2.689611
H	3.497205	0.633178	3.383091
H	2.063324	-0.263114	2.800497
C	3.468898	-2.367474	-1.123765

H	2.407636	-2.641107	-1.196747
H	3.807896	-1.937560	-2.074181
H	4.058930	-3.254845	-0.887955
C	4.565114	1.273526	-1.254414
H	5.219365	0.398038	-1.332203
H	4.613186	1.858014	-2.174454
H	4.858902	1.889321	-0.399137

10.5 Intermediate IIc



(E = -2094.60942643; zpe corrected = -2094.385331; Enthalpy = -2094.365684; Free energy = -2094.436324 u.a.)

Cartesian coordinates for IIc

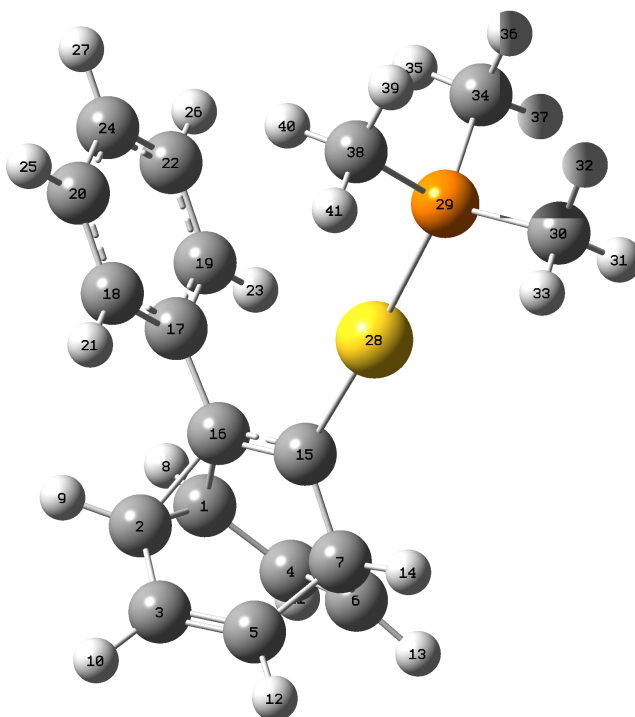
Coordinates (Å)

Atom	X	Y	Z
------	---	---	---

C	-3.103838	-0.229344	-0.773374
C	-3.134784	-0.192760	0.703783
C	-3.105599	-1.416314	1.506445
C	-3.043330	-1.490970	-1.513055
C	-2.248222	-2.397736	1.212972
C	-2.201665	-2.457424	-1.136763
C	-1.275544	-2.192313	0.051433
H	-3.548255	0.633623	-1.270087
H	-3.603253	0.691245	1.137331
H	-3.831848	-1.508278	2.311335
H	-3.737065	-1.621642	-2.340916
H	-2.235151	-3.363781	1.711186
H	-2.170688	-3.448059	-1.583242
H	-0.444945	-2.902432	0.085952
C	-0.819613	-0.786384	0.020501
C	-1.756589	0.231503	-0.012885
C	-1.397927	1.678182	-0.032570
C	-1.267195	2.377106	1.169886
C	-1.149689	2.327070	-1.244581
C	-0.887416	3.715989	1.160423
H	-1.454413	1.866243	2.115304
C	-0.771000	3.666667	-1.251334
H	-1.241289	1.777319	-2.182390
C	-0.639383	4.361381	-0.049948
H	-0.781814	4.254202	2.100706
H	-0.574906	4.167482	-2.197781
H	-0.340886	5.408314	-0.056975
Cl	3.510712	0.006719	-0.006075
Au	1.156371	-0.410689	0.011675

Cl 1.003401 -0.421170 2.366557
Cl 0.981298 -0.566590 -2.338033

6.6 Intermediate *IId*



(E = -1174.89548984; zpe corrected = -1174.559899; Enthalpy = -1174.538064; Free energy = -1174.610969 u.a.)

Cartesian coordinates for IId

Coordinates (Å)

Atom X Y Z

C	-3.527499	0.246598	-0.671196
C	-3.462115	0.220428	0.813461
C	-3.632176	-1.023005	1.567723

C	-3.764348	-0.973272	-1.446876
C	-2.995975	-2.134224	1.185264
C	-3.097210	-2.094386	-1.156538
C	-2.069191	-2.063597	-0.027447
H	-3.851872	1.194568	-1.101065
H	-3.732634	1.154968	1.305641
H	-4.329256	-1.016407	2.403466
H	-4.530646	-0.941769	-2.218937
H	-3.148605	-3.106366	1.648571
H	-3.288484	-3.050592	-1.638261
H	-1.404287	-2.929760	-0.069169
C	-1.318673	-0.777796	-0.031780
C	-2.097151	0.388662	0.005547
C	-1.452730	1.735310	0.015178
C	-0.977638	2.268886	1.216028
C	-1.237625	2.427544	-1.177772
C	-0.286117	3.477462	1.223298
C	-1.141178	1.722753	2.146858
C	-0.547438	3.638159	-1.171375
C	-1.599036	2.008456	-2.118200
C	-0.068458	4.162644	0.028056
H	0.085131	3.884271	2.162719
H	-0.379540	4.169975	-2.106601
H	0.472774	5.107435	0.032111
Au	0.743179	-0.653756	-0.043761
P	3.097782	-0.398432	0.000847
C	4.076029	-1.934748	-0.079325
H	3.849215	-2.475540	-1.005055
H	5.147929	-1.698191	-0.053154

H	3.828309	-2.578881	0.771876
C	3.750771	0.631930	-1.354224
H	3.277102	1.620258	-1.327921
H	4.837098	0.749025	-1.245394
H	3.533115	0.165023	-2.321216
C	3.677562	0.438368	1.513279
H	4.767433	0.566238	1.479970
H	3.199385	1.421927	1.594782
H	3.410065	-0.153968	2.395556

UNIVERSITAT ROVIRA I VIRGILI

GOLD-CATALYZED CYCLIZATIONS FOR THE SYNTHESIS OF SMALL AND MEDIUM-SIZED ARENES

Claudia Alejandra de León Solís

Dipòsit Legal: T. 196-2013

Chapter II

Towards well-defined nanographenes

UNIVERSITAT ROVIRA I VIRGILI

GOLD-CATALYZED CYCLIZATIONS FOR THE SYNTHESIS OF SMALL AND MEDIUM-SIZED ARENES

Claudia Alejandra de León Solís

Dipòsit Legal: T. 196-2013

Chapter II: Towards well-defined nanographenes

1. Introduction

The Nobel Prize awarded to Geim and Novoselov in 2009 for their studies on graphene discovered to the non-scientific world a wonderful material. Behind them, there was decades of theoretical studies but it was only in 2004 when the first free-standing graphene was found and its electronic properties were later established.¹ The philosopher's stone of all materials was discovered. Geim described it as "the thinnest material ever known and the strongest ever measured" (*Figure 1*).²

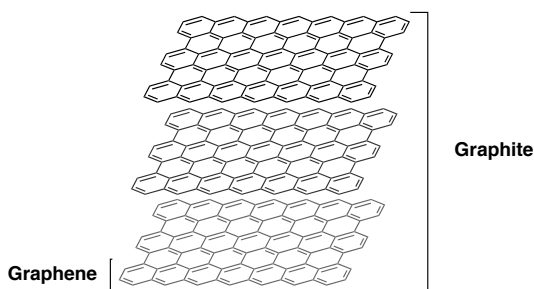


Figure 1: Graphene 2D- and Graphite 3D-crystals

There are two different pathways that allow the isolation of 2D crystals such as graphene: one is the mechanical splitting of a strongly layered material such as graphite, and second is the growth of the layers epitaxially on top of other crystals. Before all these techniques were developed, scientists focused on the synthesis of molecules that contained discrete parts of graphene as models for

¹ (a) Geim, A. K.; Novoselov, K. S. *Nat. Mater.* **2007**, *6*, 183. (b) Novoselov, K. S.; Geim, A. K.; Morozov, S. V.; Jiang, D.; Zhang, Y.; Dubonos, S. V.; Grigorieva, I. V.; Firsov, A. A. *Science* **2004**, *306*, 666. (c) Novoselov, K. S.; Geim, A. K.; Morozov, S. V.; Jiang, D.; Katsnelson, M. I.; Grigorieva, I. V.; Dubonos, S. V.; Firsov, A. A. *Nature* **2005**, *438*, 197.

² Geim, A. K. *Science* **2009**, *324*, 1530.

deeper understanding of such molecules. Indeed, graphene can be wrapped up to form buckminsterfullerenes or rolled to form 1D nanotubes. In addition, small polyaromatic hydrocarbons such as acenes were the subject of deep study and continue to be of interest for applications in electronic devices (*Figure 2*).^{1a}

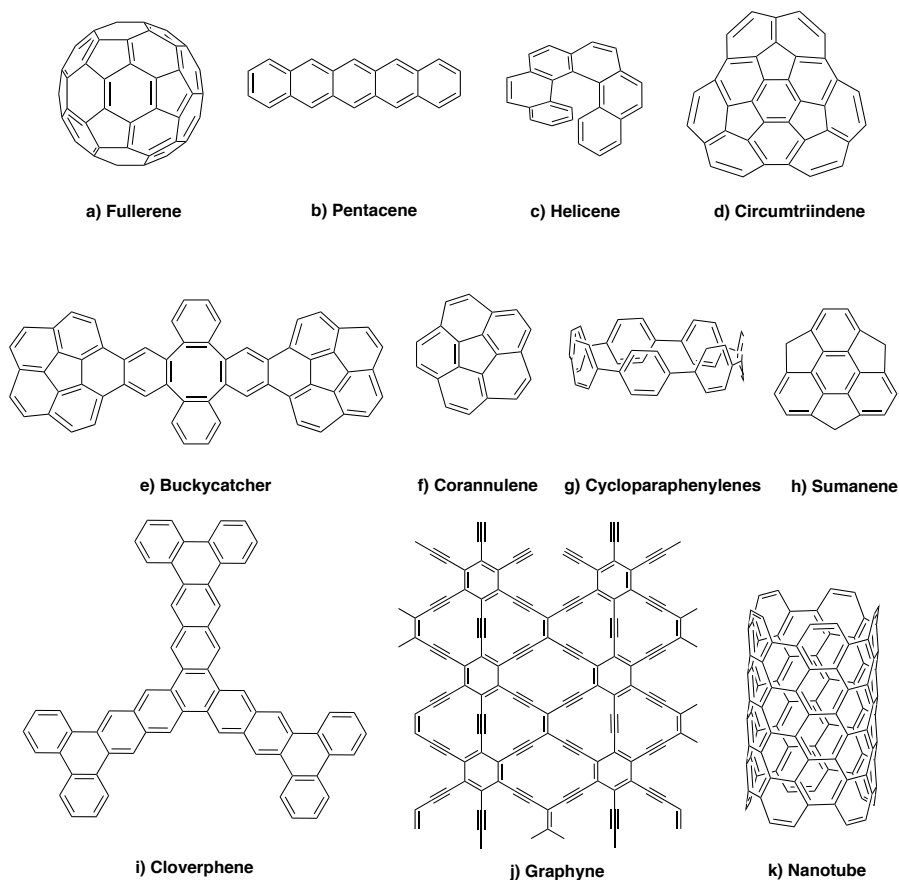


Figure 2: Graphene-related compounds and materials

1.1 Fullerenes

In 1985, Smalley and co-workers detected by mass spectrometry a stable cluster containing 60 atoms of carbon formed by laser irradiation-induced vaporization of graphite. The molecule appeared to be aromatic and they had to consult Buckminster Fuller's studies to find a plausible structure to their finding. They suggested that the more stable C_{60} species should be an icosahedral symmetry closed-cage structure, similar to a football. In homage to the American engineer, the molecule was baptized buckminsterfullerene and they were honored in 1996 with the Nobel Prize.³

It was in 1990 when Krätschmer and Huffman found that fullerenes could be synthesized in gram quantities by electric arc discharge between graphite electrodes immersed in a noble gas.⁴ This was a breakthrough since its solid state and molecular properties could finally be studied. On the other hand, other members of the fullerene family were described and some of them are depicted in *Figure 3*.

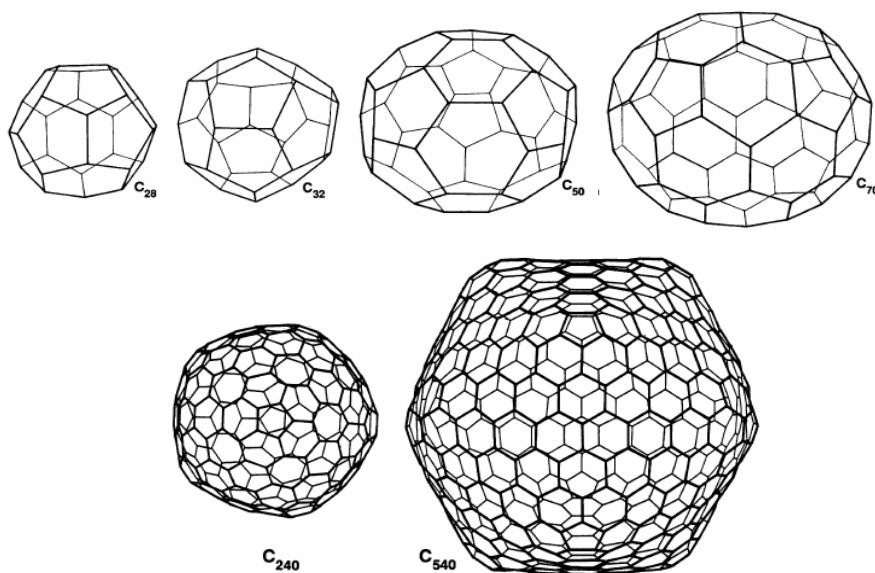


Figure 3: Members of the fullerene family

The more stable fullerene after C_{60} is C_{70} and then the subsequent higher fullerenes. The smallest possible fullerene is C_{20} which along with C_{28} is stable

³ Kroto, H. W.; Heath, J. R.; O'Brien, S. C.; Curl, R. F.; Smalley, R. E. *Nature* **1985**, *318*, 162.

⁴ Krätschmer, W.; Lamb, L. D.; Fostiropoulos, K.; Huffman, D. R. *Nature* **1990**, *347*, 354.

in gas phase cluster-beam experiments.⁵ Schiller and co-workers have analyzed the electronic structure of C₆₀ adsorbed on a vicinal Au (887) surface using photoemission, X-ray absorption, and scanning tunneling microscopy/spectroscopy (STM/STS).⁶ The HOMO-LUMO energy separation has served as a measure of kinetic stability and has acquired higher relevance since the discovery of a photoinduced electron transfer between conjugated polymers and fullerenes.⁷

It has been demonstrated that fullerenes can encapsulate metal ions,⁸ noble gases, nitrogen atoms,⁹ and even a single molecule of water.¹⁰ These doped fullerenes show different properties from their empty counterparts. In 1991, Hebard et al discovered superconductivity in potassium-doped C₆₀,^{8b} and the interest in these molecules exploded. The doping can occur not only in the inside of the cage, but also on the outside producing fulleride salts, and even on the side of the cage by replacing one carbon atom by another one such as boron.¹¹

Long before C₆₀ was introduced into the chemical arena, fullerenes fragments had already been the subject of several studies. Indeed, the first synthesis of corannulene (see structure **f**, *Figure 2*) was reported by Barth and Lawton in 1966.¹² This bowl-shaped molecule allowed chemists to “extend our basic

⁵ Kim, K. H.; Han, Y.-K.; Jung, J. *Theor. Chem. Acc.* **2005**, *113*, 233.

⁶ Schiller, F.; Ruiz-Osés, M.; Ortega, J. E.; Segovia, P.; Martínez-Blanco, J.; Doyle, B. P.; Pérez-Dieste, V.; Lobo, J.; Néel, N.; Berndt, R.; Kröger, J. J. *Chem. Phys* **2006**, *125*, 144719.

⁷ Sariciftci, N. S.; Smilowitz, L.; Heeger, A. J.; Wudl, F. *Science* **1992**, *258*, 1474.

⁸ (a) Chai, Y.; Guo, T.; Jin, C.; Haufler, R. E.; Chibante, L. P. F.; Fure, J.; Wang, L.; Alford, J. M.; Smalley, R. E. *J. Phys. Chem.* **1991**, *95*, 7564. (b) Hebard, A. F.; Rosseinsky, M. J.; Haddon, R. C.; Murphy, D. W.; Glarum, S. H.; Palstra, T. T. M.; Ramirez, A. P.; Kortan, A. R. *Nature* **1991**, *350*, 600.

⁹ Ge, Z.; Duchamp, J. C.; Cai, T.; Gibson, H. W.; Dorn, H. C. *J. Am. Chem. Soc.* **2005**, *127*, 16292.

¹⁰ Kurotobi, K.; Murata, Y. *Science* **2011**, *333*, 613.

¹¹ Smalley, R. E. In *Fullerenes*; American Chemical Society: 1992; Vol. 481, p 141.

¹² Barth, W. E.; Lawton, R. G. *J. Am. Chem. Soc.* **1966**, *88*, 380.

understanding of the nature of aromaticity in three dimensions".¹³ It also showed great potential for the synthesis of fullerenes and nanotubes when the fullerene fever spread.^{13,14} Other related structures derived from corannulene such as the buckycatcher (see structure **e**, *Figure 2*) which complexate C₆₀ and C₇₀.¹⁵

1.2 Acenes

Benzenoid hydrocarbons have been the subject of many studies for the better comprehension of aromaticity. The best-known series of these compounds are *n*-acenes, planar and linearly annelated benzene rings, which comprise naphthalene (2 rings), anthracene (3 rings), naphthacene (4 rings) and pentacene (5 rings). It has been established that the reactivity of the members of the series increases with the addition of each fused benzene ring (*Figure 4*).¹⁶

¹³ Sygula, A. *Eur. J. Org. Chem.* **2011**, 1611.

¹⁴ Tsefrikas, V. M.; Scott, L. T. *Chem. Rev.* **2006**, *106*, 4868.

¹⁵ Sygula, A.; Fronczek, F. R.; Sygula, R.; Rabideau, P. W.; Olmstead, M. M. *J. Am. Chem. Soc.* **2007**, *129*, 3842.

¹⁶ Portella, G. P., J.; Bofill, J. M.; Alemany, P.; Solà, M. *J. Org. Chem.* **2005**, *70*, 2509.

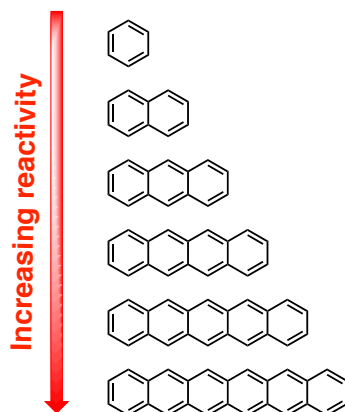


Figure 4: Increased reactivity in some family members of *n*-acenes

Contradictory, the aromatic character increases from the outer to the inner ring (Figure 5) according to different indicators of aromaticity (HOMA index, NCIS data and paradelocalization index).

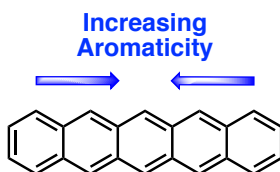


Figure 5: Variation of the aromatic character of each ring in pentacene

The acene that has acquired the higher relevance due to its electronic properties is pentacene. It has one of the highest charge-carrier mobilities and is the standard used for the newly developed devices that bear a small molecule inside.¹⁷ However, pentacene is prone to photodegradation and has poor solubility, which limits its applications. Molecular engineering of pentacene to overcome these drawbacks has been the subject of the study in many groups.^{17,18,19} Miller and co-workers have quantitated how different

¹⁷ Murphy, A. R.; Fréchet, J. M. J. *Chem. Rev.* **2007**, *107*, 1066.

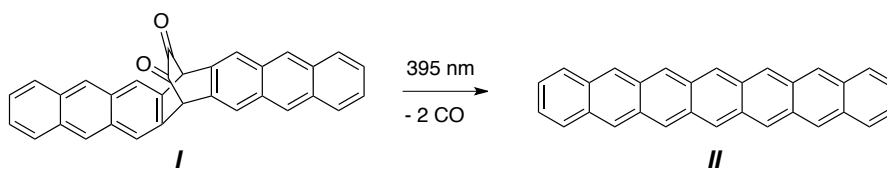
¹⁸ Meng, H.; Bendikov, M.; Mitchell, G.; Helgeson, R.; Wudl, F.; Bao, Z.; Siegrist, T.; Kloc, C.; Chen, C. H. *Adv. Mater.* **2003**, *15*, 1090.

¹⁹ Tang, Q.; Zhang, D.; Wang, S.; Ke, N.; Xu, J.; Yu, J. C.; Miao, Q. *Chem. Mater.* **2009**, *21*, 1400.

substituents affect the HOMO-LUMO gaps (HLG) and the photooxidative resistance for a large series of pentacene derivatives: in general, alkylthio and arylthio substituted pentacenes proved to be the more stable compounds with the smaller HLG.²⁰

It has also been important to understand how its outstanding electrical performance is related to the thin film morphology and to the molecular and crystal structure.¹⁹

Preparation of higher acenes has also been a hot topic since some organic electronics should benefit of higher conjugation length but larger *n*-acenes are light and air-sensitive, have low solubilities and tend to dimerize.²¹ Pure heptacene was first synthesized by Neckers and co-workers by photodecarbonylation of a dione precursor (*Scheme 1*) over a poly(methyl methacrylate) matrix.²²



Scheme 1

Anthony, Wudl and Miller have made great progress introducing bulky substituents in the heptacene core making them more stable (*Figure 6*).²³

²⁰ Kaur, I.; Jia, W.; Kopreski, R. P.; Selvarasah, S.; Dokmeci, M. R.; Pramanik, C.; McGruer, N. E.; Miller, G. P. *J. Am. Chem. Soc.* **2008**, *130*, 16274.

²¹ Zade, S. S.; Bendikov, M. *Angew. Chem. Int. Ed.* **2010**, *49*, 4012.

²² Mondal, R.; Shah, B. K.; Neckers, D. C. *J. Am. Chem. Soc.* **2006**, *128*, 9612.

²³ (a) Payne, M. M.; Parkin, S. R.; Anthony, J. E. *J. Am. Chem. Soc.* **2005**, *127*, 8028. (b) Chun, D.; Cheng, Y.; Wudl, F. *Angew. Chem.* **2008**, *120*, 8508. (c) Kaur, I.; Stein, N. N.; Kopreski, R. P.; Miller, G. P. *J. Am. Chem. Soc.* **2009**, *131*, 3424.

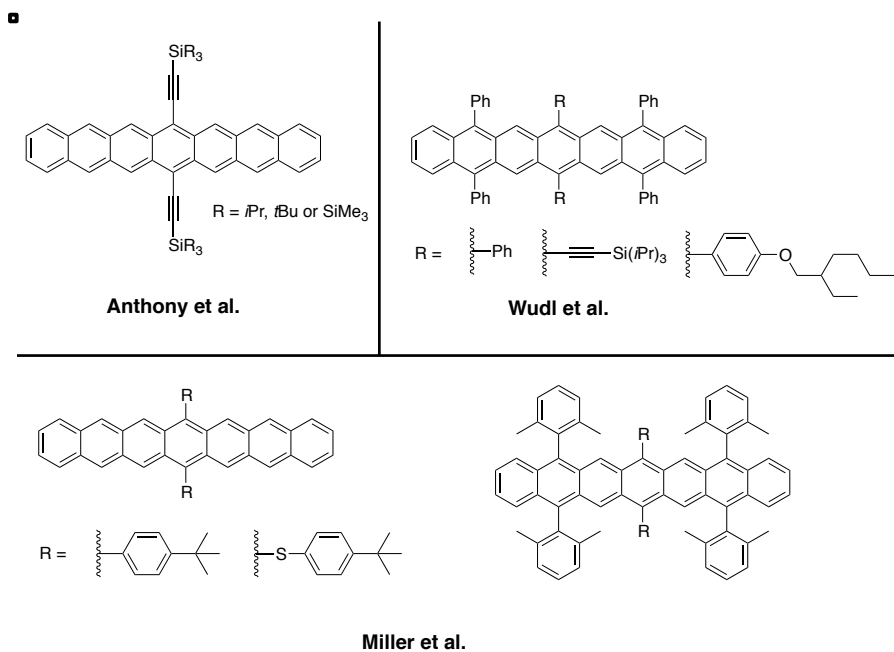


Figure 6: Molecular engineering of heptacene

Finally, Miller²⁴ has also reported the synthesis and characterization of two nonacene derivatives (*Figure 7*), which presented closed-shell ground states and small HLGs.

²⁴ Kaur, I.; Jazdyk, M.; Stein, N. N.; Prusevich, P.; Miller, G. P. *J. Am. Chem. Soc.* **2010**, *132*, 1261.

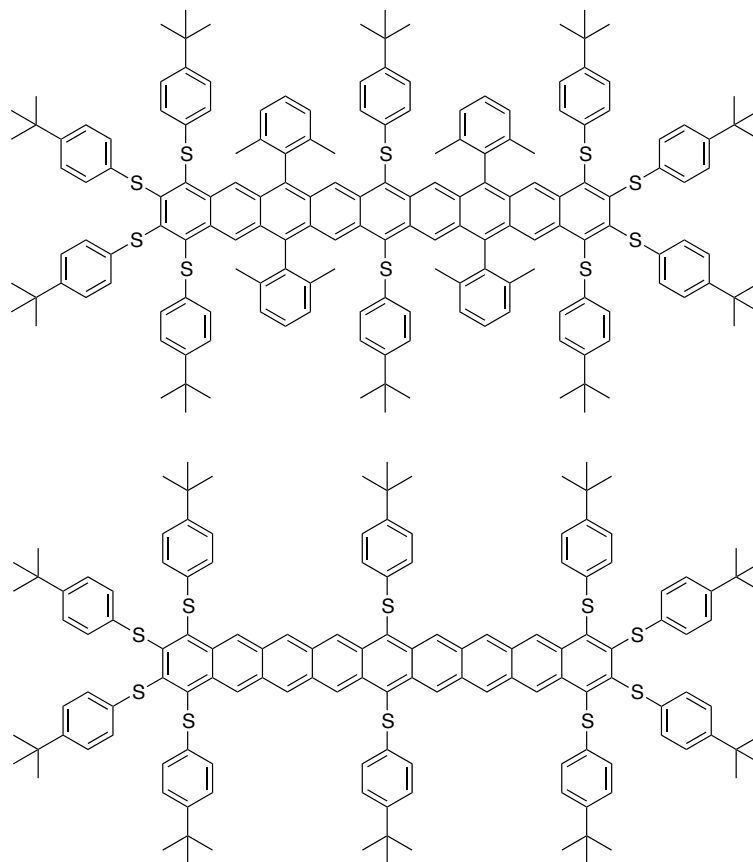


Figure 7: Nonacene derivatives reported by Miller et al.

1.3 Crystallinity and transport of charge

In the solid state, *n*-acenes, among other polyaromatic compounds, tend to adopt two different intermolecular orders: herringbone and coplanar arrangements (*Figure 8*).²⁵ Studies carried out by Gavezzotti and co-workers concluded that the carbon to hydrogen ratio (C:H) determines which disposition will adopt the material in the solid state: the larger C:H is, the more

²⁵ Anthony, J. E. *Chem. Rev.* **2006**, *106*, 5028.

favoured is the π stacking.²⁶ These dispositions in the space permit electronic coupling between the π -electron clouds of the aromatic molecules, especially when they face each other.²⁷ Strong electronic coupling enables efficient transport of charge along the molecules.

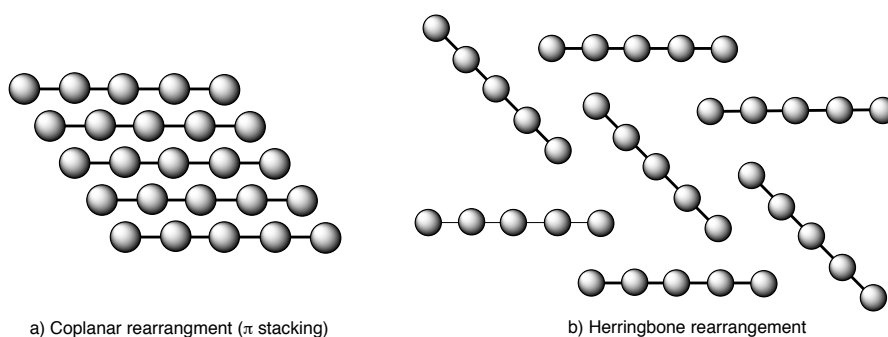


Figure 8: Arrangements of acenes in the solid state

The charge carrier mobility is intrinsically related to the film quality or the crystallinity of the molecule and small variations in their disposition in the space lead to important variations in their electronic properties. It becomes evident how the functionalization of such compounds is essential to obtain the strongest couplings.²⁵ Indeed, in the case of unsubstituted acenes, the packing is dominated by the herringbone rearrangement.²⁷ The addition of a strong electron withdrawing substituent interrupts the edge to face interaction, reduces the repulsion between the π faces and creates a significant dipole that has to be cancelled by a π stacked disposition. Small substituents in the central ring(s) of the acene lead to disruption of edge to edge interactions, favoring the π stacking (*Figure 9*). Larger substituents may revert this trend.

²⁶ (a) Gavezzotti, A.; Desiraju, G. R. *Acta. Cryst. B* **1988**, *44*, 427. (b) Desiraju, G. R.; Gavezzotti, A. *Acta. Cryst. B* **1989**, *45*, 473. (c) Dunitz, J. D.; Gavezzotti, A. *Acc. Chem. Res.* **1999**, *32*, 677.

²⁷ Anthony, J. E. In *Functional Organic Materials*; Wiley-VCH Verlag GmbH & Co. KGaA: 2007, p 511.

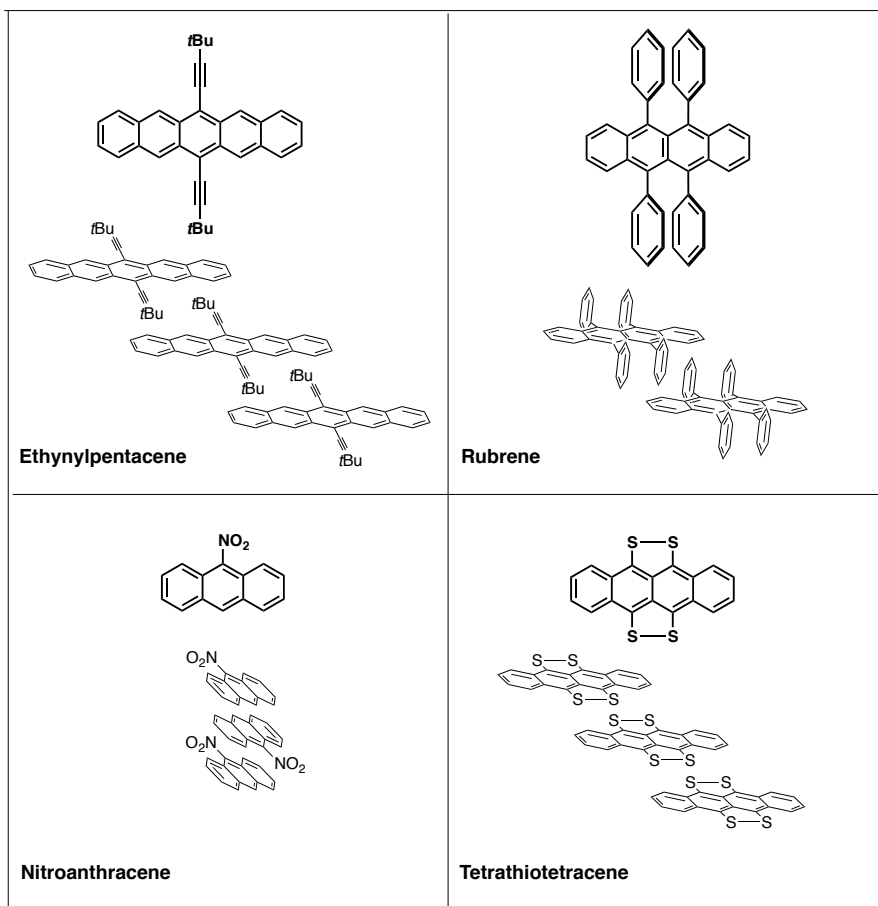


Figure 9: Examples of induced π -stacking in acenes

1.4 Applications

Due to their properties, fullerenes have found applications in different fields. In medicine, soluble functionalized fullerenes have presented interesting biological properties as inhibitors of the protease of HIV1 virus²⁸ and as

²⁸ Bosi, S.; Da Ros, T.; Spalluto, G.; Balzarini, J.; Prato, M. *Bioorg. Med. Chem. Lett.* **2003**, *13*, 4437.

antiretroviral drugs.²⁹ Some of them are inhibitors of bacterial respiration³⁰ and they've also been used in antimicrobial treatments.³¹

However, the area that has been mainly revolutionized by these compounds is nanotechnology. The electronic properties of PAHs were first exploited in the eighties when the first organic field transistors appeared:³² Koezuka and coworkers fabricated a polythiophene-based field effect transistor³³ in 1986. The same year, Tang introduced a two layer organic photovoltaic containing copper phthalocyanine and a perylene tetracarboxylic derivative³⁴ followed one year later by a light emitting diode coated with an aromatic diamine and a chelated complex.³⁵

The exact nature of the charge transport in organic semiconductors is still a subject of debate. Some theories include hopping of charge between localized states and transport of charge through polarons, which are deformations of the conjugated chain under the action of the charge.³⁶

The performance of organic transistors that have been fabricated after those first ones has been improved and nowadays we can find semiconductors with mobility values superior to $1 \text{ cm}^2 \text{ V}^{-1} \text{ s}^{-1}$. The appeal on these devices has not arisen from their performance though, most of them are still less competitive compared to silicon-based semiconductors, but rely on their application on large area electronics, their biodegradability and above all, their low-cost of production and processability.^{32,37,38} These organic materials can be easily

²⁹ Schinazi, R. F.; Sijbesma, R.; Srdanov, G.; Hill, C. L.; Wudl, F. *Antimicrob. Agents Chemother.* **1993**, *37*, 1707.

³⁰ Mashino, T.; Usui, N.; Okuda, K.; Hirota, T.; Mochizuki, M. *Bioorg. Med. Chem.* **2003**, *11*, 1433.

³¹ Tegos, G. P.; Demidova, T. N.; Arcila-Lopez, D.; Lee, H.; Wharton, T.; Gali, H.; Hamblin, M. R. *Chem. Biol.* **2005**, *12*, 1127.

³² Braga, D.; Horowitz, G. *Adv. Mater.* **2009**, *21*, 1473.

³³ Tsumura, A.; Koezuka, K.; Ando, T. *Appl. Phys. Lett.* **1986**, *49*, 1210.

³⁴ Tang, C. W. *Appl. Phys. Lett.* **1986**, *48*, 1983.

³⁵ Tang, C. W.; van Slyke, S. A. *Appl. Phys. Lett.* **1987**, *51*, 913.

³⁶ Horowitz, G. *Advanced Materials* **1998**, *10*, 365.

³⁷ Feng, X.; Pisula, W.; Müllen, K. *Pure Appl. Chem.* **2009**, *81*, 2203.

³⁸ Sheats, J. R. *J. Mater. Res.* **2004**, *19*, 1974.

modified to make them compatible with solution processing techniques contrary to the silicon-based ones which require expensive lithography and vacuum deposition.

Organic semi-conductors are found in organic field-effect transistors (OFET), organic light-emitting diodes (OLED), photovoltaic cells, sensors and radio frequency identification tags. In our everyday life, these are the components of a great variety of gadgets ranging from the electronic paper that can be flexed, bent, rolled-up, and folded³⁹ to the electronic ink popularized by Amazon's Kindle and Barnes and Noble's Nook Tablet⁴⁰ to the so called e-textiles that may play music or monitor vitals signs.⁴¹ But what lies ahead seems to follow a trend of miniaturization, which will need the development of new devices using few or a single molecule embedded between the electrodes.⁴² Such concept was already described by Aviram and Ratner in 1974: a hypothetical molecule (*Figure 10*) with an HLG of 0.3 eV was predicted to act as a unimolecular rectifier.⁴³

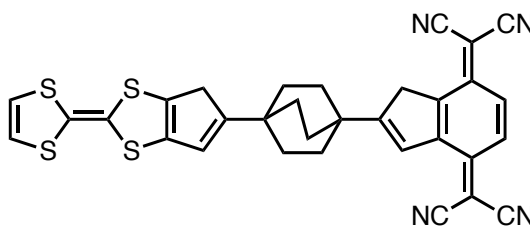


Figure 10: organic donor-acceptor (D-A) complex of tetrathiafulvalene and tetracyanoquinodimethane

³⁹ Rogers, J. A. *Science* **2001**, *291*, 1502.

⁴⁰ Rainie, L. Tablet and E-book reader Ownership Nearly Double Over the Holiday Gift-Giving Period. Pew Internet and American Life Project. January 23, 2012, <http://pewinternet.org/Reports/2012/E-readers-and-tablets.aspx>, accessed on October 3, 2012.

⁴¹ Service, R. F. *Science* **2003**, *301*, 909.

⁴² Joachim, C.; Gimzewski, J. K.; Aviram, A. *Nature* **2000**, *408*, 541.

⁴³ Aviram, A.; Ratner, M. A. *Chem. Phys. Lett.* **1974**, *29*, 277.

Nonetheless, it was only in the last decade that the technology has developed enough to have the first operative molecular logic gates constructed. Different polyaromatic compounds have been tested: starphenes have proved to be suitable molecules for such tasks. Recently, the group of Joachim deposited trinaphthylene (*Figure 11*) on a Au(111) surface. Single atoms of Au were attached to each branch by STM manipulation (two inputs and one reference) and several tests were performed. It was demonstrated that a single molecule of trinaphthylene was able to perform the logic function of a NOR gate.⁴⁴

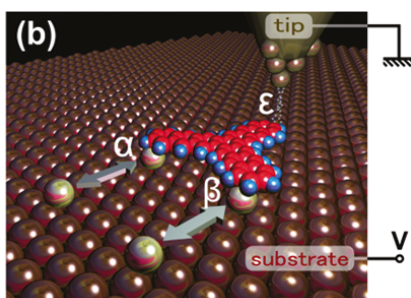


Figure 11: experimental implementation of a trinaphthylene molecule NOR gate where the “tip \leftrightarrow output branch end \leftrightarrow Au(111) surface” tunnel junction is used to measure the logic status of the NOR gate via the tunnel current intensity.

Further experiments have also been performed using larger starphenes such a decastarphene (*Figure 12*), which showed promising results.⁴⁵

⁴⁴ Soe, W.-H.; Manzano, C.; Renaud, N.; de Mendoza, P.; De Sarkar, A.; Ample, F.; Hliwa, M.; Echavarren, A. M.; Chandrasekhar, N.; Joachim, C. *ACS Nano* **2011**, *5*, 1436.

⁴⁵ Guillermet, O.; Gauthier, S.; Joachim, C.; Mendoza, P. d.; Lauterbach, T.; Echavarren, A. *Chem. Phys. Lett.* **2011**, *511*, 482.

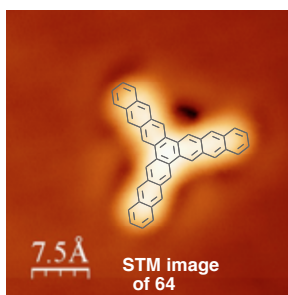


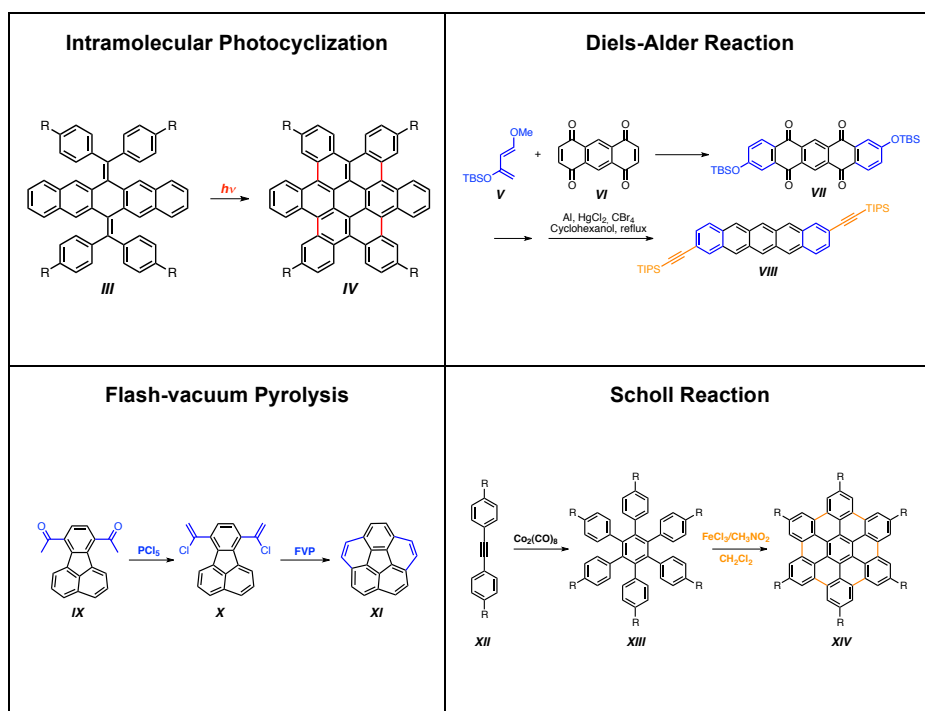
Figure 12: Molecular model of decastarphene superposed on a constant-current STM image of the molecule adsorbed on Cu(1 1 1). Size: 4.5 _ 4.5 nm. Imaging conditions: $V_t = -210$ mV, $I_t = 0.65$ nA.

1.5 Synthesis of polyaromatic hydrocarbons.

Since the architecture of the molecule at the heart of the device is a key feature, the synthesis of polyaromatics compounds has gained relevance in the last decade. Some examples of synthetic approaches to access these compounds are pictured in *Scheme 2*.³⁷ The Diels-Alder reaction has been one of the most favourite tools to create C-C bonds. The method is efficient although it usually deal with harsh conditions. The oxidative cyclodehydrogenation, also known as the Scholl reaction, is a more general procedure since it generates a C-C bond between two unfunctionalized aryl vertices and has the great advantage that the reagents are cheap, being FeCl_3 the most widely used. However, the products are not always predictable and small, unfunctionalized arenes may undergo oligomerization. The latter can be suppressed by placing blocking groups such as *t*-butyl.⁴⁶

Flash-vacuum pyrolysis (FVP) deals only with thermal-stable compounds bearing reactive sites and the intramolecular photocyclization is mostly used for the synthesis of condensed PAHs.³⁷

⁴⁶ King, B. T.; Kroulík, J.; Robertson, C. R.; Rempala, P.; Hilton, C. L.; Korinek, J. D.; Gortari, L. M. *J. Org. Chem.* **2007**, *72*, 2279.

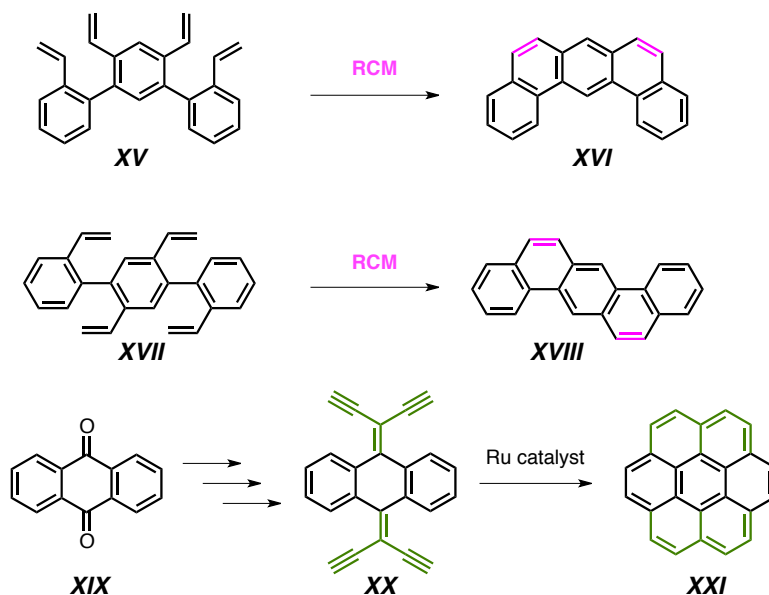


Scheme 2: Some methods for the synthesis of PAHs^{47,47}

Ring-closing metathesis (RCM) and benzannulation reactions (*Scheme 3*) have also been used for the synthesis of PAHs due to their milder conditions but the reagents are much more expensive since the ruthenium catalysts are added in ratios up to 15 mol% for each new C-C bond formed.⁴⁸

⁴⁷ (a) Scott, L. T.; Hashemi, M. M.; Meyer, D. T.; Warren, H. B. *J. Am. Chem. Soc.* **1991**, *113*, 7082. (b) Watson, M. D.; Fechtenkötter, A.; Müllen, K. *Chem. Rev.* **2001**, *101*, 1267. (c) Xiao, S.; Myers, M.; Miao, Q.; Sanaur, S.; Pang, K.; Steigerwald, M. L.; Nuckolls, C. *Angew. Chem. Int. Ed.* **2005**, *44*, 7390. (d) Bénard, C. P.; Geng, Z.; Heuft, M. A.; VanCrey, K.; Fallis, A. G. *J. Org. Chem.* **2007**, *72*, 7229.

⁴⁸ (a) Donovan, P. M.; Scott, L. T. *J. Am. Chem. Soc.* **2004**, *126*, 3108. (b) Bonifacio, M. C.; Robertson, C. R.; Jung, J.-Y.; King, B. T. *J. Org. Chem.* **2005**, *70*, 8522.



Scheme 3 Example of RCM and benzannulation reactions for the synthesis of PAHs

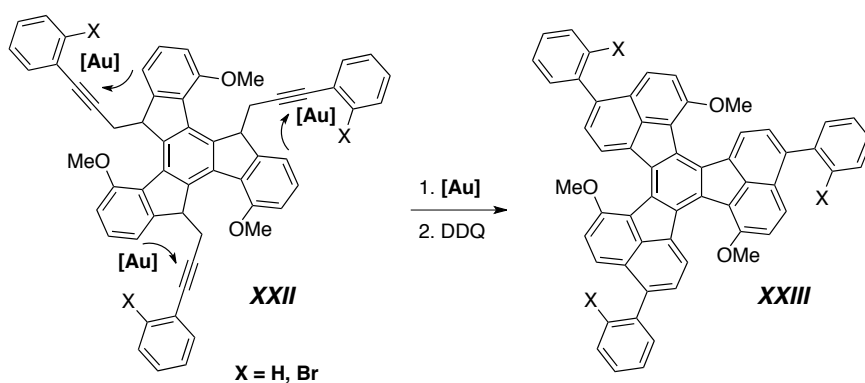
These drawbacks have encouraged the development of new strategies for the rational synthesis of well-defined molecular-sized sections of graphite single layers (nanographenes) and other acenes based on new reactions that might limit the problems of handling insoluble materials. It was also desirable that the transformations leading to planarization could be delayed until the last step(s) of the synthesis.

The last few years, our group has been developing methods based on palladium chemistry for the synthesis of polyarenes,⁴⁹ and the study of mechanistic aspects of the Pd-catalyzed arylation.⁵⁰ Thus, as part of a program

49. (a) Pascual, S.; de Mendoza, P.; Echavarren, A. M. *Org. Biol. Chem.* **2007**, *5*, 2727. (b) de Frutos, Ó.; Gómez-Lor, B.; Granier, T.; Monge, M. Á.; Gutiérrez-Puebla, E.; Echavarren, A. M. *Angew. Chem. Int. Ed.* **1999**, *38*, 204. (c) Gómez-Lor, B.; Echavarren, A. M. *Org. Lett.* **2004**, *6*, 3191.

50. (a) García-Cuadrado, D.; Braga, A. A. C.; Maseras, F.; Echavarren, A. M. *J. Am. Chem. Soc.* **2006**, *128*, 1066. (b) García-Cuadrado, D.; de Mendoza, P.; Braga, A. A. C.; Maseras, F.; Echavarren, A. M. *J. Am. Chem. Soc.* **2007**, *129*, 6880. (c) Pascual, S.; de Mendoza, P.; Braga, A. A. C.; Maseras, F.; Echavarren, A. M. *Tetrahedron* **2008**, *64*, 6021.

on the synthesis of bowl-shaped polyarenes,⁵¹ we have reported the synthesis of fullerene C₆₀ and triazafullerene by cyclodehydrogenation of the corresponding planar precursors.⁵² The Y shaped molecules portrayed in the work of Joachim have also been synthesized by our group by palladium-catalyzed cyclotrimerization of arynes^{44, 53} or by trimerization of 1,4-anthraquinone in the presence of freshly prepared 1,4-dihydroxyanthracene.⁴⁵ Another approach was introducing the Au(I)-catalyzed cycloisomerization reactions into the synthesis of PAHs. The synthesis of planar polyarenes with OMe and X substituents at strategic positions could be carried out by a triple Au(I)-catalyzed hydroarylation⁵⁴ of truxene derivatives to give 3,9,15-triaryldiacenaphtho[1,2-j:1',2'-l]fluoranthenes (*Scheme 4*).⁵⁵



Scheme 4: Au (I)-catalyzed synthesis of 3,9,15-triaryldiacenaphtho[1,2-j:1',2'-l]fluoranthenes

51. (a) Wu, Y.-T.; Siegel, J. S. *Chem. Rev.* **2006**, *106*, 4843. (b) Tsefrikas, V. M.; Scott, L. T. *Chem. Rev.* **2006**, *106*, 4868.

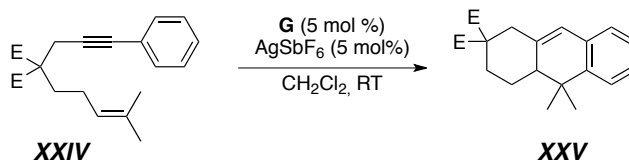
52. Otero, G.; Biddau, G.; Sánchez-Sánchez, C.; Caillard, R.; López, M. F.; Rogero, C.; Palomares, F. J.; Cabello, N.; Basanta, M. A.; Ortega, J.; Méndez, J.; Echavarren, A. M.; Pérez, R.; Gómez-Lor, B.; Martín-Gago, J. A. *Nature* **2008**, *454*, 865.

53 (a) Peña, D.; Escudero, S.; Pérez, D.; Guitián, E.; Castedo, L. *Angew. Chem. Int. Ed.* **1998**, *37*, 2659. (b) Romero, C.; Peña, D.; Pérez, D.; Guitián, E. *Chem. Eur. J.* **2006**, *12*, 5677.

54. (a) Nevado, C.; Echavarren, A. M. *Chem. Eur. J.* **2005**, *11*, 3155-3164. (b) Nevado, C.; Echavarren, A. M. *Synthesis* **2005**, 167.

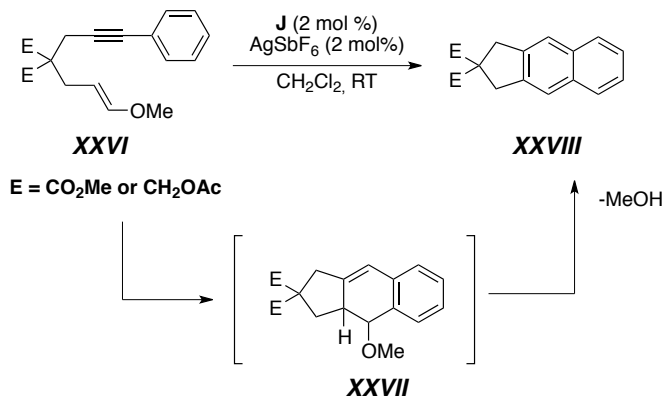
55. S. Pascual, C. Bour, P. de Mendoza, Unpublished results, ICIQ, ICIQ, **2009-2010**.

These results supported the idea that cyclization reactions of 1,6- and 1,7-enynes could be applicable to access more complex molecules. Indeed, the Au(I)-catalyzed cyclization of fully substituted 1,7-enynes yielded polyhydrogenated anthracene moieties (*Scheme 5*) that in principle, could be templated to obtain other polyhydrogenated acenes.



Scheme 5: Au(I)-catalyzed cyclization of 1,7-enynes

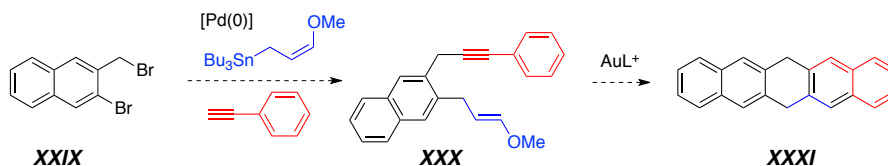
On the other hand, cyclization of 1,6-enynes bearing a methoxy group in the alkene produced tricyclic products with two aromatic rings. The aromatization proceeded by elimination of methanol (*Scheme 6*).⁵⁶



Scheme 6: Cyclization of arylalkynes with enol ethers

⁵⁶ (a) Nieto-Oberhuber, C.; López, S.; Echavarren, A. M. *J. Am. Chem. Soc.* **2005**, *127*, 6178. (b) Nieto-Oberhuber, C.; Pérez-Galán, P.; Herrero-Gómez, E.; Lauterbach, T.; Rodríguez, C.; López, S.; Bour, C.; Rosellón, A.; Cárdenas, D. J.; Echavarren, A. M. *J. Am. Chem. Soc.* **2007**, *130*, 269. (c) Cabello, N.; Rodríguez, C.; Echavarren, A. M. *Synlett* **2007**, 1753.

Thus, for example, the synthesis of 6,13-dihydropentacene **XXIX** could be carried out by two consecutive Pd-catalyzed cross-coupling reactions from known starting materials⁵⁷ to form enyne **XXX**, followed by a Au(I)-catalyzed [4+2] cycloaddition reaction (*Scheme 7*).



Scheme 7: Synthesis proposal for 6,3-dihydropentacene

In a similar Lego-type approach, the 1,7-enyne **XXXV** pictured in *Scheme 8* could be assembled starting from known compounds.^{58,59} A gold-catalyzed cyclization would form **XXXVI**, which would undergo an oxidative cyclodehydrogenation⁶⁰ to give the planar C₅₄ derivative **XXXVII**, which is still an unknown compound.⁶¹ The Diels-Alder reaction at the bay regions⁶² could lead to the C₆₆ nanographene **XXXVIII**.⁶³ Similarly, starting from known 1,6-

57. (a) Smith, J. G.; Dibble, P. W.; Sandborn, R. E. *J. Org. Chem.* **1986**, *51*, 3762. (b) Kadota, I.; Sakaiharu, T.; Yamamoto, Y. *Tetrahedron Lett.* **1996**, *37*, 3195.

58. (a) Washburn, L. C.; Pearson, D. E. *J. Med. Chem.* **1974**, *17*, 676. (b) Nishigaichi, Y.; Takuwa, A. *Chem. Lett.* **1994**, 1429.

59. Naphthalene and other electron-rich fragments could be added to the corresponding propargylic alcohol intermediates by a Au(III)-catalyzed reaction: Georgy, M.; Boucard, V.; Debleds, O.; Zotto, C. D.; Campagne, J.-M. *Tetrahedron* **2009**, *65*, 1758.

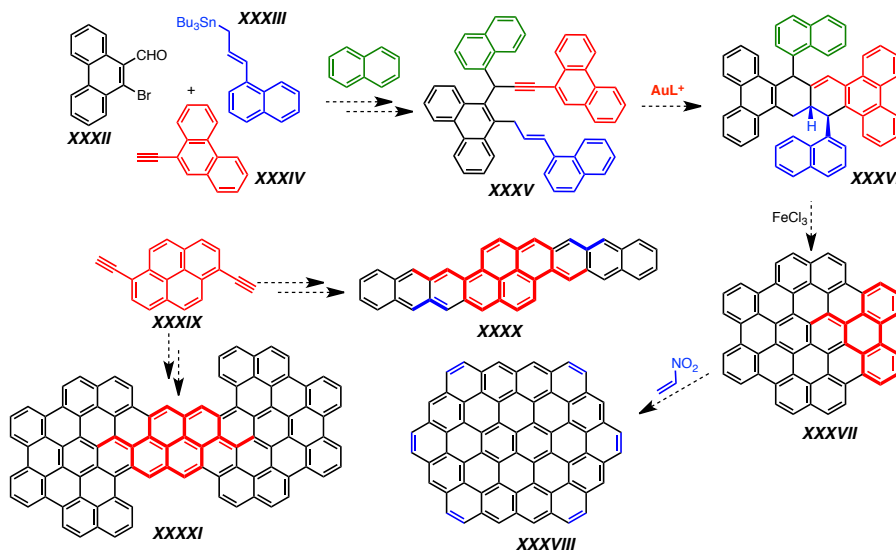
60. Yang, X.; Dou, X.; Rouhanipour, A.; Zhi, L.; Räder, H. J.; Müllen, K. *J. Am. Chem. Soc.* **2008**, *130*, 4216.

61. An isomer (tribenzo[*jk,mn,pq*]dibenzo[5,6:7,8]pentapheno[2,1,14,13,12-*stuvabcd*]ovalene) has been synthesized: Iyer, V. S.; Yoshimura, K.; Enkelmann, V.; Epsch, R.; Rabe, J. P.; Mullen, K. *Angew. Chem. Int. Ed.* **1998**, *37*, 57.

62. (a) Fort, E. H.; Donovan, P. M.; Scott, L. T. *J. Am. Chem. Soc.* **2009**, *131*, 16006. (b) Fort, E. H.; Scott, L. T. *Angew. Chem. Int. Ed.* **2010**, *49*, 6626.

63. A low HOMO-LUMO gap has been calculated for nanographene **81**: Feng, C.; Lin, C. S.; Fan, W.; Zhang, R. Q.; Van Hove, M. A. *J. Chem. Phys.* **2009**, *131*, 194702.

diethynylpyrene **XXXIX**,⁶⁴ other acenes like **XXXX** and nanographenes such as **XXXXI** could be obtained.



Scheme 8: Proposed synthesis for different PAHs.

Many other variations could be conceived for the synthesis of a wide variety of derivatives ranging from simple linear acenes to large nanographenes with a variety of shapes and functionalities.

64. Sarobe, M.; Flink, S.; Jennekens, L. W.; van Poecke, B. L. A.; Zwikker, J. W. *Chem. Commun.* **1995**, 2415.

UNIVERSITAT ROVIRA I VIRGILI

GOLD-CATALYZED CYCLIZATIONS FOR THE SYNTHESIS OF SMALL AND MEDIUM-SIZED ARENES

Claudia Alejandra de León Solís

Dipòsit Legal: T. 196-2013

2. Objectives

We plan to develop new strategies for the rational synthesis of well-defined molecular-sized sections of graphite single layers (nanographenes) and other acenes based on Au(I)-catalyzed reactions.

We propose a new synthesis of semibuckminsterfullerenes from tribromotruene by a Au(I)-catalyzed reaction via C-H activation. In a parallel approach, we will use trialkynes available from truxenetriones for the synthesis of using a gold-catalyzed annulation or other methods. This approach could be applied for the synthesis of fully conjugated C₅₄ derivative by a triple Pd-catalyzed arylation. Other bowl-shaped polyarenes could be obtained from semibuckminsterfullerenes using similar approaches.

UNIVERSITAT ROVIRA I VIRGILI

GOLD-CATALYZED CYCLIZATIONS FOR THE SYNTHESIS OF SMALL AND MEDIUM-SIZED ARENES

Claudia Alejandra de León Solís

Dipòsit Legal: T. 196-2013

3. Results and Discussion

3.1 Synthesis of linear acenes

Initially, we focused on the synthesis of the linear acenes, trying to optimize the conditions for the synthesis of tetracene and then expand our results to the higher members of the family.⁶⁵

Figure 13 shows compound **5**, the simplest enyne prone to cyclize into the tetracene moiety.

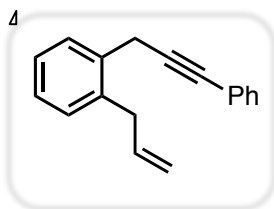
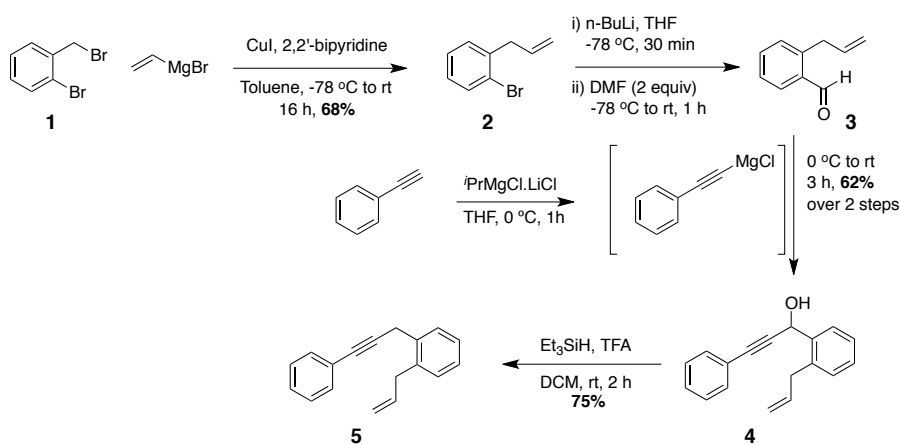


Figure 13: Compound **5**, the key enyne for the synthesis of tetracene

The allyl part of the molecule was introduced by a Kumada coupling of commercially available 1-bromo-2-(bromomethyl)benzene with vinylmagnesium bromide, which provided 1-allyl-2-bromobenzene in 68% yield (Scheme 9).

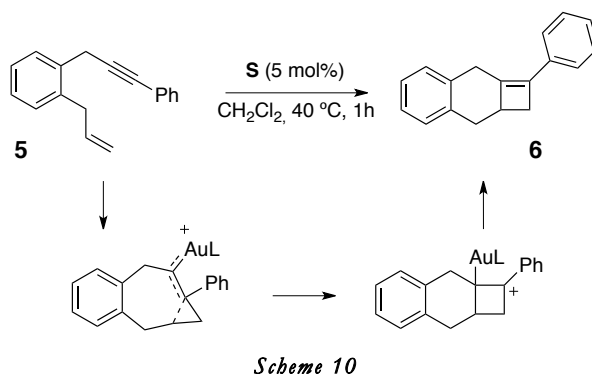


Scheme 9: Synthesis of enyne II-1.

⁶⁵ Work carried out in collaboration of Dr. Paul McGonigal.

The alkyne moiety was then introduced in two steps as described by Curran⁶⁶: first, the lithium-halogen exchange followed by addition of DMF, provided the aromatic aldehyde which was taken without any further purification into the next step. 1-(2-Allylphenyl)-3-phenylprop-2-yn-1-ol (**4**) was formed by addition of freshly prepared (phenylethynyl)magnesium chloride. Compound **5** was finally obtained by reduction with triethylsilane in 75% yield.

With the enyne in hand, we tried the standard conditions that our group had previously developed for the cyclization of 1,6-enynes.⁶⁷ Unfortunately, instead of accessing the desired tetracene, the tricyclic product **6** was obtained through a formal [2+2] cycloaddition reaction mechanism (*Scheme 10*).



It was not possible to isolate the cyclobutene **6** in pure form since it decomposed during the purification by column chromatography but it was possible to identify it by analysis of its ¹H-NMR (*Figure 14*).

⁶⁶ Curran, D. P.; Liu, H.; Josien, H.; Ko, S.-B. *Tetrahedron* **1996**, *52*, 11385.

⁶⁷ Amijs, C. H. M.; López-Carrillo, V.; Raducan, M.; Pérez-Galán, P.; Ferrer, C.; Echavarren, A. M. *J. Org. Chem.* **2008**, *73*, 7721.

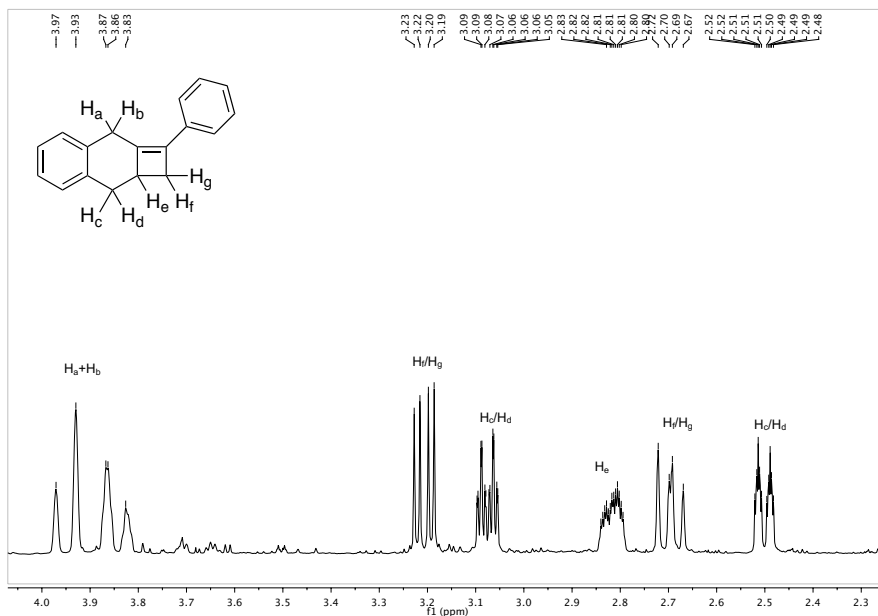
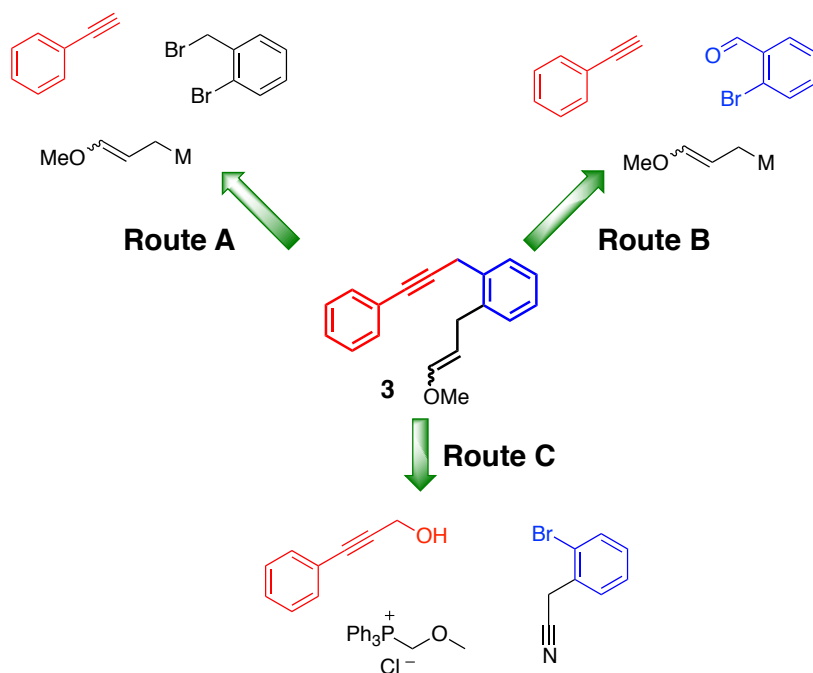


Figure 14: Expansion of the ^1H NMR of the crude cyclobutene 6.

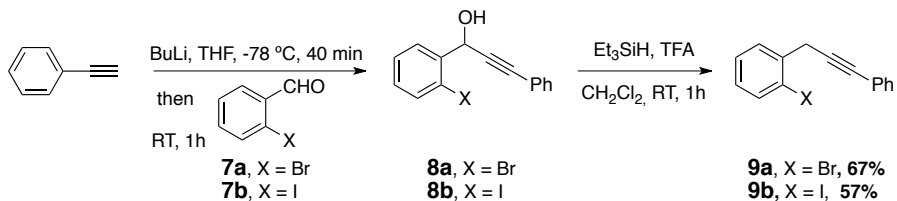
In order to favor the [4+2] cycloaddition reaction, it was determined that having an enoether was essential: the methoxy group would make the alkene more electrophilic and more prone to the attack of the phenyl ring.

Many routes were studied to access the desired enyne tethered with an enoether as shown in the retrosynthetic study in *Scheme 11*.



Scheme 11: Retrosynthetic analysis for the synthesis of enoether 3

The most straightforward seemed to be route B, which was our method of choice. As for compound **5**, the alkyne moiety was introduced by addition of phenylethyne lithium to 2-bromo- or 2-iodobenzaldehyde followed by the reduction of triethylsilane with TFA. The desired compounds were obtained with moderate yields over the two steps: 67 % for the brominated derivative and 57 % for the iodinated one (*Scheme 12*).

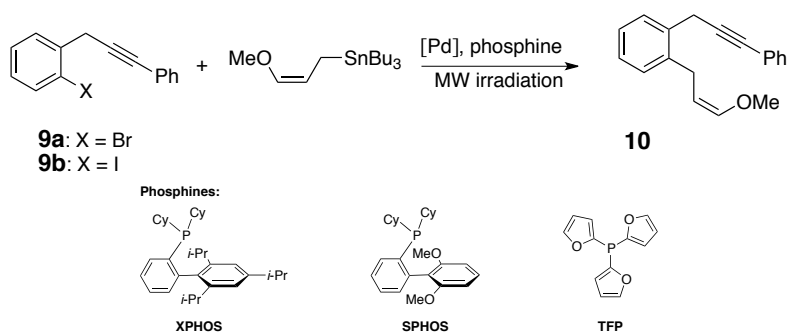


Scheme 12

Then we envisioned a metal-catalyzed allylic coupling to introduce the enolether. We choose to test the Stille coupling, which normally provides good yields for the synthesis of enyne **10**.

Koreeda and Tanaka had already described the synthesis of several alkoxyallyltin compounds, (*Z*)-tributyl(3-methoxyallyl)stannane among them. The *Z*-selectivity is accomplished by complexation of the π -allyl lithium intermediate with TMEDA prior to the addition of tributyltinchloride.⁶⁸ We expected the *Z*-enyne to be more prone to the Au-catalyzed cyclization reaction. The conditions tested for the Stille coupling are shown on *Table 1*. All the reactions were carried out in a microwave reactor.

Table 1



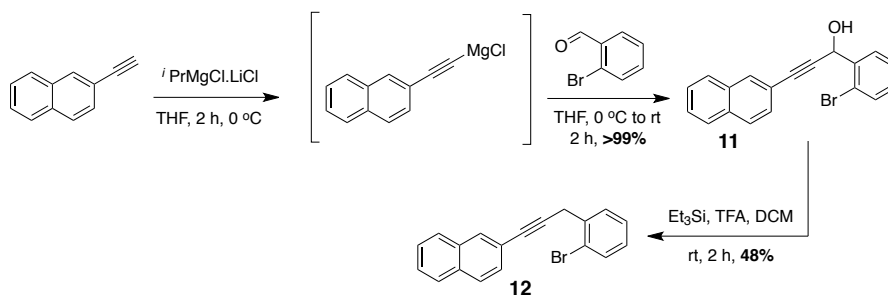
Entry	Substrate	[Pd] (mol%)	Phosphine (mol%)	Solvent	T (°C)	Time (h)	Yield 10 (%)
1	9a	Pd ₂ (dba) ₃ (3.5)	TFP (14)	Toluene	100	1	Traces
2	9a	Pd(PPh ₃) ₄ (7)	none	DMF	110	1	59 ^a
3	9a	PdCl ₂ (CH ₃ CN) ₂ (7)	SPHOS (14)	DMF	120	2	25
4	9a	PdCl ₂ (CH ₃ CN) ₂ (5)	XPHOS (10)	DMF	120	2	35
5	9a	PdCl ₂ (CH ₃ CN) ₂ (7)	XPHOS (14)	DMF	120	2	47
6	9b	PdCl ₂ (CH ₃ CN) ₂ (5)	XPHOS (10)	DMF	120	2	20
9	9b	PdCl ₂ (CH ₃ CN) ₂ (7)	XPHOS (14)	DMF	120	2	25

^a Still contaminated with byproducts after KF treatment.

⁶⁸ Koreeda, M.; Tanaka, Y. *Tetrahedron Lett.* **1987**, *28*, 143.

Even if $\text{Pd}(\text{PPh}_3)_4$ seemed to catalyze the reaction with the best yield, the product was still contaminated with tin residues, which were very difficult to eliminate. Treatment with solid potassium fluoride (KF) and washing of the column with cyclohexane prior to the elution of the compound seemed ineffective. Buchwald's conditions gave the best results for this coupling.⁶⁹ We hypothesized that the resulting enolether was sensitive to the silica in the column chromatography and we tested alumina without improving the yield. We also expected to obtain better yields with iodo compounds but the lower yields indicate that the starting material is more sensitive to the microwave irradiation and might decompose during the reaction.

Even if the yield was moderate, we decided to test the conditions for the synthesis of higher acenes.⁷⁰ Starting from 2-ethynynaphthalene, we prepared the Grignard reagent, which was then added to 2-bromobenzaldehyde followed by reduction. The TFA treatment seemed to be decomposing most of the product since the addition gave almost quantitative yields but we only recovered 48 % yield after the reduction (*Scheme 13*).



Scheme 13

Unfortunately, the conditions that were satisfactory for alkynes **9a** and **9b**, failed for alkyne **12** and the starting material was recovered.

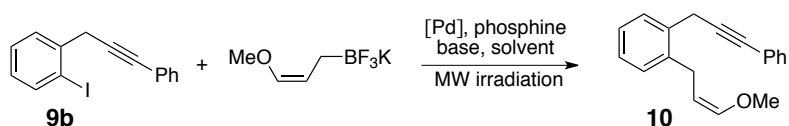
Since the yields for the Stille coupling were not encouraging and the conditions tested were not useful for the synthesis of higher acenes, we decided to test conditions for the Suzuki coupling of potassium (*Z*)-(3-methoxyallyl)trifluoroborate with compound **9b** (scheme in *Table 2*).

⁶⁹ Billingsley, K. L.; Anderson, K. W.; Buchwald, S. L. *Angew. Chem. Int. Ed.* **2006**, *45*, 3484.

⁷⁰ Work carried out in collaboration of Dr. Paul McGonigal.

The trifluoroborate salt was prepared similarly to the alkoxytin analogue but the π -allyl intermediate was trapped with trimethyl borate followed by treatment with KHF_2 as described by Batey.⁷¹ The optimization of the reaction conditions is shown in *Table 2*. Trying to avoid using the microwave reactors, we tested conditions described by Molander.⁷² The yields were low and in the worst cases, we only obtained the decomposition of the starting material. We then tested conditions described by Alam⁷³ which did not provide better yields.

Table 2



Entry	[Pd] (mol%)	Base (equiv)	Phosphine (mol%)	Solvent	T (°C)	Time (h)	Yield 10 (%)
1	$\text{PdCl}_2(\text{CH}_3\text{CN})_2$ (5)	None	XPHOS (10)	DMF	120	2	decomposition
2	$\text{PdCl}_2(\text{CH}_3\text{CN})_2$ (5)	Cs_2CO_3 (3)	XPHOS (10)	THF/ H_2O	85	22	decomposition
3	PdCl_2 (5)	Cs_2CO_3 (3)	XPHOS (10)	THF/ H_2O	85	22	16
4	PdCl_2 (5)	Cs_2CO_3 (3)	PPh_3 (10)	THF/ H_2O	85	22	21
5	$\text{PdCl}_2(\text{PPh}_3)_2$ (6)	DIPA (3)	---	n-PrOH	120	0.5 ^a	12
6	$\text{PdCl}_2(\text{dppf})$ (6)	DIPA (3)	---	n-PrOH	120	0.5 ^a	17
7	$\text{PdCl}_2(\text{dppf})$ (5)	K_2CO_3 (2)	---	IPA/ H_2O	120	0.5 ^a	29
8	$\text{PdCl}_2(\text{dppf})$ (5)	K_2CO_3 (2)	---	IPA/ H_2O	80	24	24
9	$\text{PdCl}_2(\text{dppf})^{\text{b}}$ (5)	K_2CO_3 (2)	---	IPA/ H_2O	120	0.5 ^a	26

^a Reactions performed in a microwave reactor. ^b Reaction done at 0.1M instead of 0.2 M.

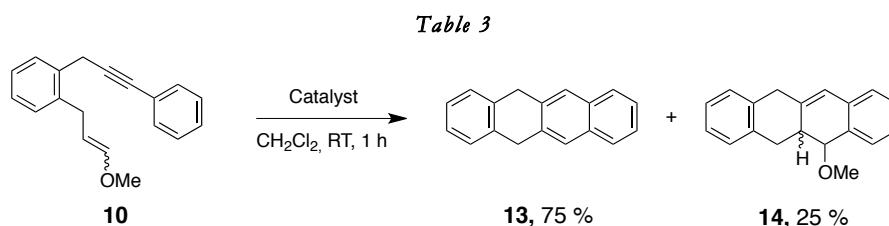
⁷¹ Batey, R. A.; Thadani, A. N.; Smil, D. V. *Tetrahedron Lett.* **1999**, *40*, 4289.

⁷² Molander, G. A.; Brown, A. R. *J. Org. Chem.* **2006**, *71*, 9681.

⁷³ Al-Masum, M.; Alam, S. *Tetrahedron Lett.* **2009**, *50*, 5201.

Even with the low yields obtained for the couplings, we were determined to test the Au-catalyzed cyclization reaction.⁷⁴

Our first attempt yielded an unexpected product besides the desired tetrahydrotetracene **13** (see scheme in *Table 3*): introduction of the enol ether proved to be effective since the tetracene core was formed but loss of methanol did not ensue and 5-methoxy-5,5a,6,11-tetrahydrotetracene (**14**) was obtained in low yields which was corroborated by GC-MS and analysis of the ¹H-NMR. Stirring the reaction longer did not substantially affect the ratio between the two products but increasing the catalyst loading from 5 to 10 mol% did. We also expected that higher temperatures would favor the methanol loss and stirring the reaction under reflux proved to be effective. The optimization of the reaction conditions is summarized in *Table 3*.



Entry	Catalyst (mol%)	T (°C)	Time (h)	Conversion ^a (%)	Yield 13 (%) ^{a,b}	Yield 14 (%) ^a
1	E (10)	23	1	≥ 99	95	5
2	S (10)	23	1	≥ 99	95	5
3	K (10)	23	1	≥ 99	85 ^c	0
4	E (5)	23	1	≥ 99	75	25
5	E (5)	23	2	≥ 99	77	23
6	E (5)	40	1	≥ 99	≥ 99 (96)	0
7	E (2.5)	40	1	≥ 99	≥ 99 (95)	0
8	E (1)	40	1	≥ 99	90 (84)	10

^a Conversion and yields estimated from crude ¹H NMR spectra. ^b Isolated yields given in parentheses. ^c Unknown cycloisomerization product observed in 15%.

⁷⁴ Work carried out in collaboration of Dr. Paul McGonigal and César Rogelio Solorio-Alvarado.

Entries 6 and 7 show the best conditions for the Au(I)-catalyzed cycloisomerization of enyne **10**. Reduction of the catalyst loading from 5 to 2.5 mol% does not affect the conversion nor the isolated yield.

Figure 15 shows the X-Ray crystal structure of 5,12-dihydrotetracene (**10**), which is stable under atmospheric conditions.

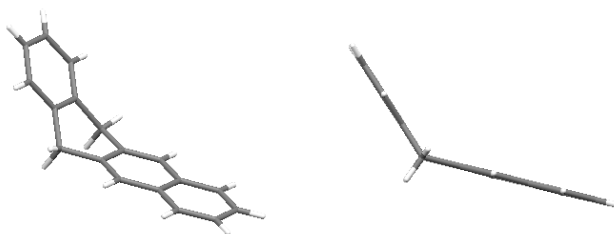


Figure 15: X-Ray crystal structure of 5,12-dihydrotetracene (10)

The Au(I)-catalyzed cycloisomerization reaction is reliable for the late stage cyclization of this kind of enoether tethered enynes into tetrahydroacenes. These reduced molecules could be stored since they are air and light stable and could be aromatized just previously to being deposited on top of the surfaces for the electronic devices.

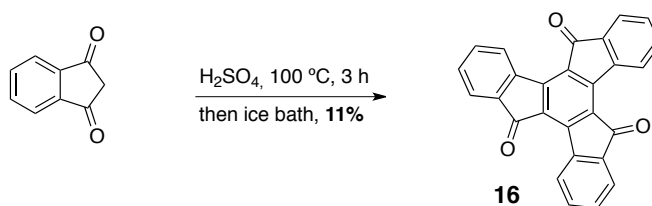
3.2 Synthesis of precursors of semi-buckminsterfullerenes (buckybowls)

For the synthesis of semi-buckminsterfullerenes, we proposed that appropriately tethered truxene derivatives could be cyclized by a Au(I)-catalyzed cyclization reaction via a C-H activation.

The first issue that we had to address was the purification of truxentrione: it has been reported that simple trimerization of 1,3-indendione affords truxentrione in yields over 90 %.⁷⁵ However, every time we tried this approach we obtained a green solid and not the desired bright yellow that has been

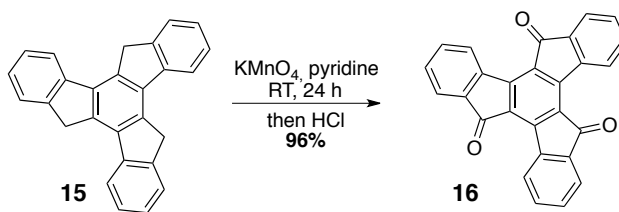
⁷⁵ Dehmlow, E.V.; Kelle, T. *Synth. Commun.* **1997**, *27*, 2021-2031.

reported. Further purification of the green solid by Soxhlet extraction only provided low yields of truxentrione **16** (11 %) (*Scheme 14*).



Scheme 14

We proposed that oxidation of truxene **15** with KMnO_4 followed by HCl treatment to reduce the MnO_2 byproduct to a water-soluble Mn species, would give us better results. Truxene **15** was prepared by the reported acid-catalyzed trimerization of 1-indenone^{75,76} with high yields. Then we submitted this compound to the oxidation conditions⁷⁷ and we obtained compound **16** in 96% yield with high purity (*Scheme 15*).



Scheme 15

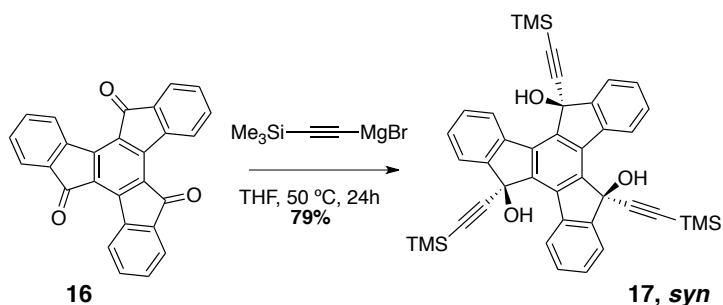
The addition of alkynyl lithium compounds to truxentrione has already been reported by our group.⁷⁸ In this case, a 1:1.5 mixture of *syn/anti* product was obtained, which could be separated by flash chromatography. Following these results, the same addition was attempted using Grignard reagents. Addition of

⁷⁶ Elmorsy, S. S.; Pelter, A.; Hursthouse, M. B.; Ando, D. *Tetrahedron Lett.* **1992**, *33*, 821-824.

⁷⁷ Bagala-Rampazzo, L.; Matiello, L. **2010**, WO/2010/038252

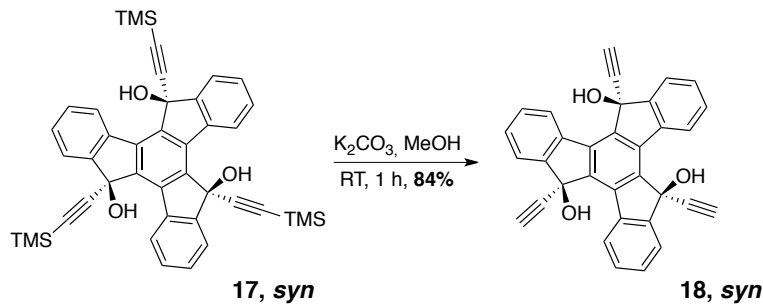
⁷⁸ Gómez-Lor, B.; Frutos, Óscar d.; Ceballos, Plácido A.; Granier, T.; Echavarren, Antonio M. *Eur. J. Org. Chem.* **2001**, *2001*, 2107.

trimethylsilylethynylmagnesium bromide to truxentrione afforded only the *syn* product with high yields.⁷⁹



Scheme 16

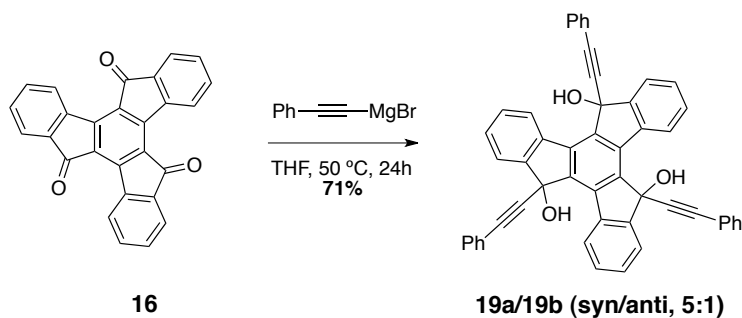
Then simple deprotection of the silyl group with K_2CO_3 in methanol afforded the free trialkyne **18**.



Scheme 17

Complexation of magnesium seemed to favor the formation of the *syn* product, which was the desired one for the Au(I)-catalyzed cyclization reaction to form the buckybowls. These results encouraged us to test other Gignard reagents such as phenylethynylmagnesium bromide. The addition proceeded well but a 5:1 mixture of *syn/anti* product was obtained in 71% yield (Scheme 18).

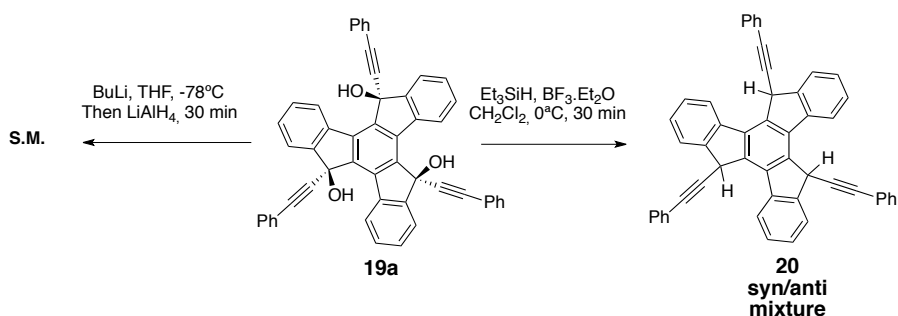
⁷⁹ García-Cuadrado, D. 2006, Unpublished results.



Scheme 18

We hypothesized that the *syn* product could be the kinetic product while the *anti* would be the more thermodynamically stable. Running the reaction for 16 h instead of 24 h, improved the selectivity of the **19a**, which was obtained in 72 % yield. Consequently, running the reaction for 40 hours provided only **19b**, which was confirmed by $^1\text{H-NMR}$.

Then we tried the reduction of **19a** to form **20**. Two methods were tested: reduction with BuLi/LiAlH_4 and reduction with $\text{Et}_3\text{SiH/BF}_3\cdot\text{OEt}_2$. The former did not work and the starting material was recovered, and the latter afforded a mixture of the *syn* and *anti* products.



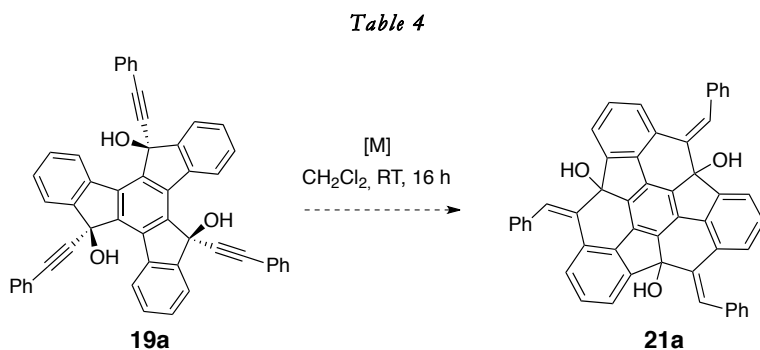
Scheme 19

No stereoselective reduction conditions were found and the attempted isomerization of the mixture with KO^tBu in $^t\text{BuOH}$ led only to decomposition. It is believed that a trisallenic product is formed, which is unstable under the reaction conditions.⁷⁸

We decided to attempt the cyclization with the free alcohol to obtain the desired buckybowl **21a** (see scheme in

Table 4). The reaction provided a black shiny solid using different metals as depicted in

Table 4. The product was not soluble in any solvent, which made difficult its characterization, and mass spectrometry only confirmed that the product had the same mass of the starting material.



Entry	[M] (mol%)	Time (h)	Product
1	GaCl ₃ (15)	24	S. M.
2	FeCl ₃ (15)	24	Black solid
3	E (15)	24	Black solid
4	E (15)	12	Black solid
5	E (5)	72	S. M. + Black solid
6	K (15)	16	S. M. + Black solid

Reducing the catalyst loading as in entry 5 just slowed the reaction and by ¹H NMR we could determine there was still some starting material left. Since the product was not soluble, we could not determine the % conversion. Attempts to obtain a crystal structure were unsuccessful: the solid did not scatter the light. Possible structures of the product are drawn in *Figure 16* but none of them could be unequivocally related to the solid we obtained since we have little information to draw some conclusions.

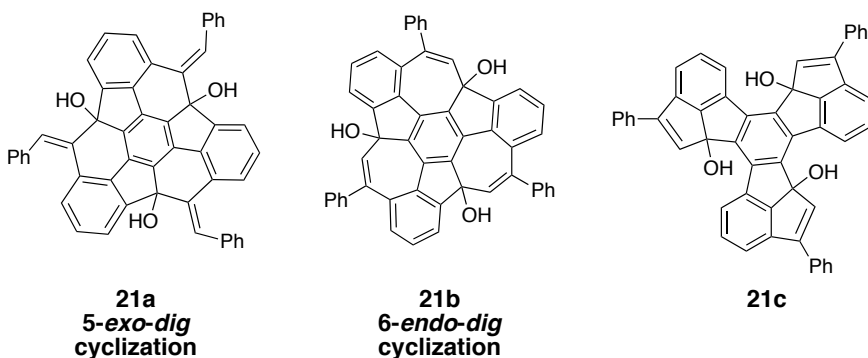


Figure 16

We also analyzed the sample by TEM techniques, which did not shed any light on the kind of compound we were obtaining (clusters, symmetric aggregates, etc.).

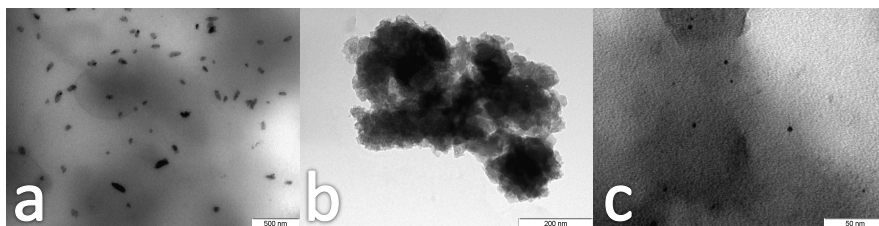
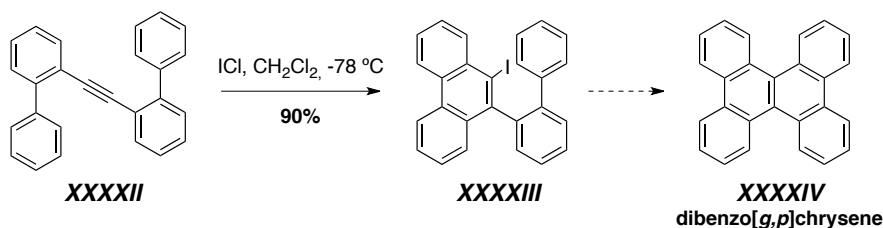


Figure 17: TEM images of 21 taken at a) 40 000 \times (200 nm) b) 150 000 \times (200 nm) and c) 500 000 \times (50 nm) magnification

We also attempted the synthesis of the desired buckybowl with iodine monochloride (ICl).⁸⁰ Li and co-workers had reported the use of this reagent for the synthesis of dibenzo[*g,b*]chrysenes from bis(biaryl)acetylenes by formation of a iodophenanthrene (*Scheme 20*).⁸¹

⁸⁰ Work carried out in collaboration with Dr. Paul McGonigal.

⁸¹ Li, C.-W.; Wang, C.-I.; Liao, H.-Y.; Chaudhuri, R.; Liu, R.-S. *J. Org. Chem.* **2007**, *72*, 9203.



Scheme 20

We hypothesized that either isomer of byckybowl **22a** illustrated in *Figure 18* could be accessed using the same conditions.

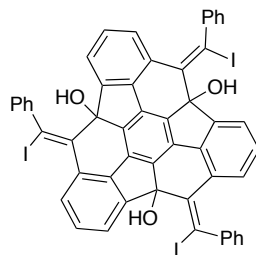


Figure 18: Possible outcome of the ICl-promoted cyclization

Indeed, treatment of compound **19a** with three equiv of ICl in CH_2Cl_2 at $-78\text{ }^\circ\text{C}$ afforded a mixture of products. One of them could be isolated but its analysis by NMR did not shed any light on the structure of the product. However, an X-ray crystal structure was obtained and the product was unequivocally identified as Propeller **23** (*Figure 19*), a mixture of two enantiomers, which was obtained in 37 % yield. The *syn* product as well but it was not detected.

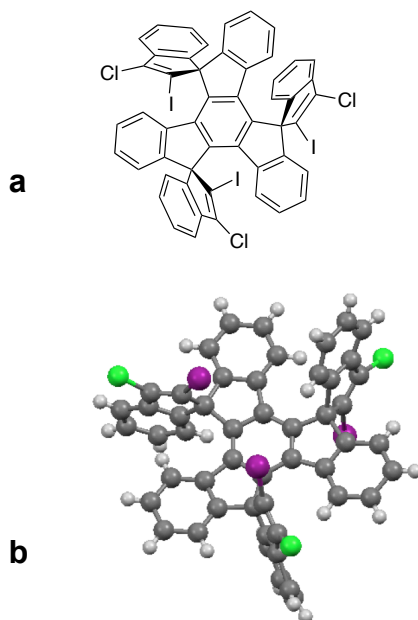
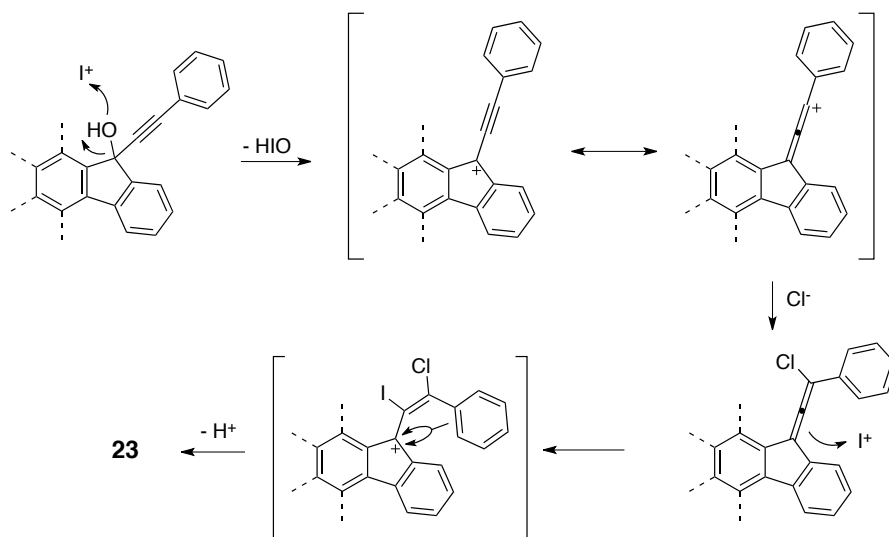


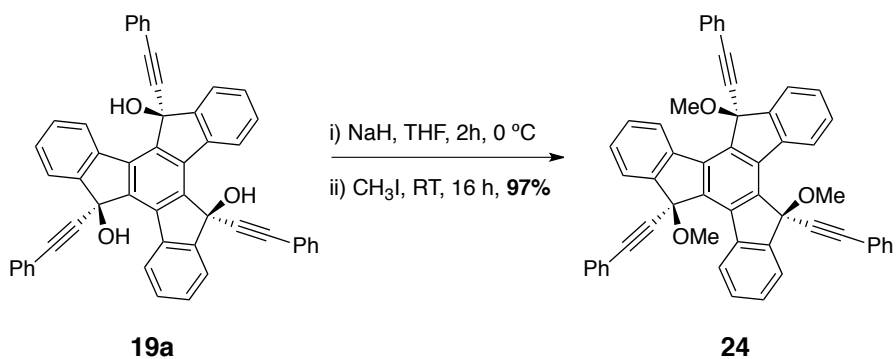
Figure 19: a) Structure of propeller 23 b) X-Ray crystal structure of the mixture of enantiomers.

The mechanism for the formation of this propeller is depicted in *Scheme 21*. We would expect the highly activated alcohol (propargylic and benzylic) to attack the iodonium and form the tertiary carbocation by loss of hypoiodous acid. The cation is stabilized by the adjacent triple bond, which is subsequently trapped by chloride. A second molecule of iodine monochloride activates the allene, iodine is added and a Friedel-Crafts cyclization ensues. Steric effects might be accounted for the selective formation of the *anti* propeller.



Scheme 21

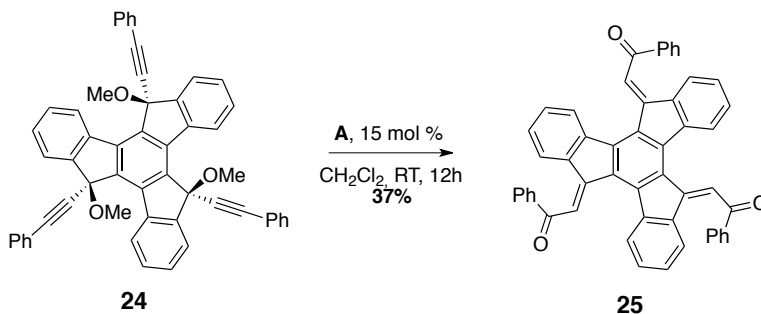
We decided to protect the free alcohol before proceeding with the cyclization reaction. Many protecting groups were tested (MOM, TES, TBDMS) but the hindrance of the tertiary alcohol only allowed the protection with a methyl group. The reaction proceeded smoothly with iodomethane and compound **24** was obtained in excellent yields (97%).



Scheme 22

Gold-catalyzed cyclization afforded an orange solid, which was subsequently identified as compound **25**, the product of a Meyer-Schuster type

rearrangement. The low yield (37%) suggested that decomposition of the product might be taking place.



Scheme 23

Another interesting feature of fullerene derivatives is their ability to encapsule metals and other small molecules. We envisioned that truxenes tethered with alkyl groups bearing a pyridone moiety at the end would self-assemble through hydrogen bonds in a capsule-type mode (*Figure 20*). We attempted the synthesis of **26** from truxene **15**.

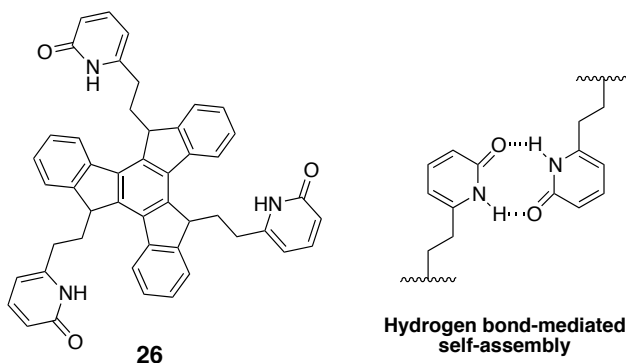
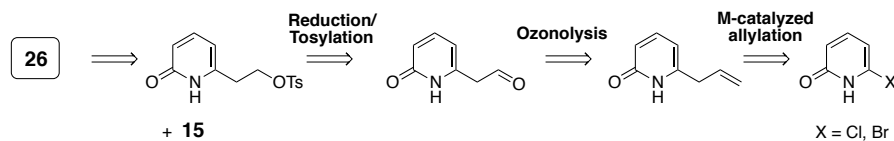
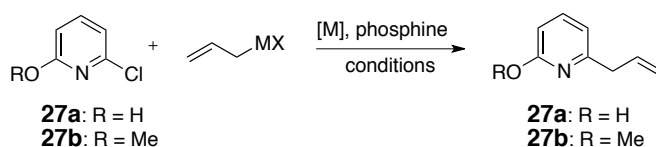


Figure 20

First, we had to address the synthesis of the ethylpyridone moiety that could be introduced to the benzyl position by a nucleophilic substitution reaction. The retrosynthetic approach is illustrated in *Scheme 24*.

*Scheme 24*

We first attempted the direct coupling of commercially available 6-chloropyridin-2(1H)-one with different allyl compounds to no avail. The ring seemed to be too deactivated to engage in the coupling reaction. We decided to protect the oxygen with a methyl group. A Stille coupling using Buchwald's conditions gave the desired product in good yields (*Table 5*, entry 9).

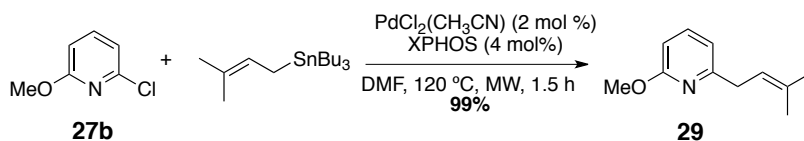
Table 5

Entry	Substrate	MX	[M] (mol%)	Phosphine (mol %)	Conditions	Product (%)
1	27a	SnBu ₃	PdCl ₂ (PPh ₃) (3.5)	---	DMF 120 °C 30 min ^a	No reaction
2	27a	MgBr	Co(acac) ₂ (10)	---	Dioxane 25 °C 30 min	No reaction
3	27a	SnBu ₃	Pd ₂ (dba) ₃ (3.5)	---	DMF 120 °C 1.5 h ^a	No reaction
4	27a	SnBu ₃	Pd(OAc) ₂ (3.5)	---	DMF 120 °C 1 h ^a	No reaction
5	27a		Pd ₂ (dba) ₃ (1)	P(Cy) ₃ (2.4)	Dioxane H ₂ O 100 °C 24 h ^b	No reaction
6	27a	SnBu ₃	PdCl ₂ (CH ₃ CN) ₂ (2)	SPHOS (4)	DMF 120 °C 1 h	No reaction

7	27b	SnBu ₃	Pd ₂ (dba) ₃ (3.5)	---	DMF 120 °C 30 min ^a	No reaction
8	27b	SnBu ₃	PdCl ₂ (PPh ₃) (3.5)		DMF 120 °C 30 min ^a	Homocoupling
9	27b	SnBu ₃	PdCl ₂ (CH ₃ C N) ₂ (2)	SPHOS (4)	DMF 120 °C 1 h	28b (86%)

^a Reaction was carried out in a microwave reactor. ^b K₃PO₄ (1.7 equiv) was added.

Unexpectedly, the coupling of the protected pyridone with tributyl(3-methylbut-2-en-1-yl)stannane was unsuccessful using the optimized conditions. Changing the phosphine for a bulkier one like XPHOS, proved to be effective for the coupling of these substituted allyl stannanes (*Scheme 25*).



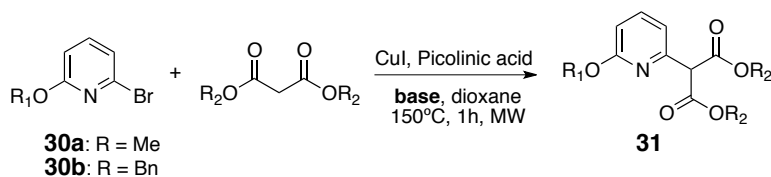
Scheme 25

Two different conditions were tested for the oxidative cleavage of the double bond: ozonolysis and the reaction with the RuCl₃-NaIO₄-phase transfer catalyst. Both of them delivered complex mixtures. We decided to avoid oxidative conditions since it was possible to oxidize the nitrogen atom in the pyridone ring.

Kwong and co-workers had reported the copper-catalyzed α -arylation of malonates at room temperature.⁸² We decided to test their conditions with 6-bromopyridones, which had a protecting group on the oxygen atom. To compensate for the lower reactivity of our substrates, we increased the temperature of the reaction. We were disappointed to notice that the reaction did not work with dimethyl nor with diethyl malonate. Using other bases only

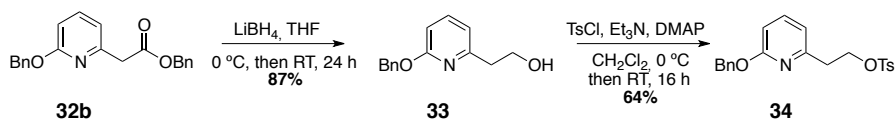
⁸² Yip, S. F.; Cheung, H. Y.; Zhou, Z.; Kwong, F. Y. *Org. Lett.* **2007**, *9*, 3469.

generated the decomposition of the starting materials. Fortunately, dibenzyl malonate afforded products **32a** and **32b** with moderate yields (*Table 6*). The excess of base and the increased temperatures promoted the decarboxylation of the expected pyridonyl-malonate.

Table 6

Entry	R1	R2	Base	Product (%)
1	Bn	Me	Cs ₂ CO ₃	No reaction
2	Bn	Et	Cs ₂ CO ₃	No reaction
3	Bn	Me	CsOH	No reaction
4	Bn	Me	Phosphazene P ₁	Decomposition
5	Bn	Me	NaH	Decomposition
6	Bn	Et	NaH	Decomposition
7	Me	Bn	Cs ₂ CO ₃	 32a (64)
8	Bn	Bn	Cs ₂ CO ₃	 32b (55)

Compound **32b** was selected for the synthesis due to the milder conditions required for the deprotection of the benzyl group in the pyridone ring. Reduction of **32b** to **33** was achieved with LiBH₄ in good yields. Tosylation to yield **34** gave moderate yields, which we attributed to decomposition of the product in the purification process (*Scheme 26*).

*Scheme 26*

With compound **34** in hand, we tested the reaction with truxene. The trianion was prepared with *n*-BuLi at -78 °C for 2 h, and then the tosyl compound was added. After 48 h of stirring, a complex mixture was obtained, which not only derived from the formation of the *anti* and *syn* products. Further tests, such as letting the trianion warm to 0°C before addition of the electrophile, only gave the same results. Using bromohexane as electrophile also gave complex mixtures, which made us believe that β -elimination might be responsible for the results.

4. Conclusions

We have demonstrated that gold-catalyzed cyclization of enynes is a useful tool to prepare linear acenes. Preparation of the key enynes still needs to be optimized and other routes like those shown in *Scheme 11* are currently underway.

Alkynyl truxentriols could be selectively prepared in their *syn* configuration from truxentriene and the Grignard reagents of the corresponding alkyne. The methyl-protected product undergoes a Meyer-Schuster rearrangement with loss of the methyl group.

A method for effective allylation of O-protected chloropyridones was established which had a potential for the preparation of 6-alkylpyridones.

5. Experimental section

5.1 General Methods

Unless otherwise stated, reactions were carried out under argon atmosphere in solvents dried by passing through an activated alumina column on a PureSolv™ solvent purification system (Innovative Technologies, Inc., MA). Analytical TLC was performed on precoated silica gel plates (0.2 mm thick, Gf234, Merck, Germany) and observed under UV light. Flash column chromatography purifications were carried out using flash grade silica gel (SDS Chromatogel 60 ACC, 40-60 μm) as the stationary phase. Preparative TLC was performed on 20 cm × 20 cm silica gel plates (2.0 mm thick, catalogue number 02015, Analtech). NMR spectra were recorded at 298 K on a Bruker Avance 400 Ultrashield and Bruker Avance 500 Ultrashield apparatus. Chemical shifts are reported in parts per million and referenced to residual solvent. Coupling constants (*J*) are reported in hertz (Hz). Mass spectra were recorded on a Waters LCT Premier Spectrometer (ESI and APCI) or on an Autoflex Bruker Daltonics (MALDI and LDI) or on an AgilentMSD-5975B (GC-MS). Melting points (M.p.) were determined using a Büchi melting point apparatus. TEM images were recorded using a transmission electron microscope JEOL 1011.

Unless otherwise stated, all reagents were purchased from commercial sources and used without further purification. Gold complexes were synthesized according to literature procedures (C. H. M. Amijs, V. López-Carrillo, M. Raducan, P. Pérez-Galán, C. Ferrer, A. M. Echavarren, *J. Org. Chem.* **2008**, *73*, 7721–7730) except (acetonitrile)[(2-biphenyl)di-*tert*-butylphosphine]gold(I) hexafluoroantimonate **E** which was purchased from Aldrich.

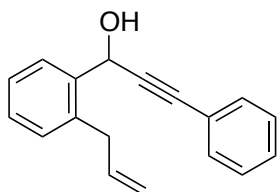
Products 1-allyl-2-bromobenzene¹ (**2**), 2-allylbenzaldehyde² (**3**), 1-bromo-2-(3-phenylprop-2-yn-1-yl)benzene³ (**9a**), 1-iodo-2-(3-phenylprop-2-yn-1-yl)benzene³ (**9b**) and truxene⁴ (**15**) were synthesized as previously reported.

¹ Königs, C. D. F.; Oestreich, M. *Synthesis* **2011**, 2062.

² Watson, I. D. G.; Ritter, S.; Toste, F. D. *J. Am. Chem. Soc.* **2009**, *131*, 2056.

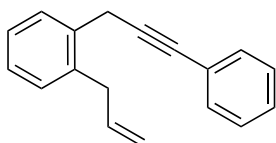
³ Oku, M.; Arai, S.; Katayama, K.; Shioiri, T. *Synlett* **2000**, 493.

1-(2-Allylphenyl)-3-phenylprop-2-yn-1-ol (4)

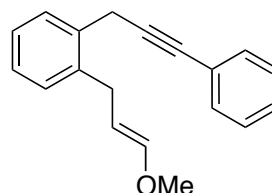
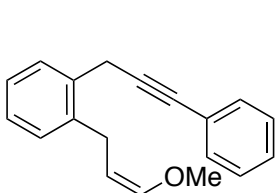


Isopropylmagnesium chloride lithium chloride complex solution (1.3 M in THF, 2.2 mL, 2.9 mmol, 1.1 equiv) was added to a solution of phenylacetylene (0.32 mL, 2.9 mmol, 1.1 equiv) in THF (5 mL) at 0 °C and it was stirred for 1 h. A solution of 2-allylbenzaldehyde (387 mg, 2.6 mmol) in THF (5 mL) was added and the resulting mixture was allowed to warm to room temperature over 3 h. Diethyl ether (50 mL) was added and the organic phase was washed with water (2x50 mL) and brine (1x50 mL). The organic phase was separated, dried over MgSO₄ and the solvents were evaporated under reduced pressure. The crude was purified by column chromatography (cyclohexane/CH₂Cl₂, 1:1, 1:4 and finally with pure CH₂Cl₂) to afford **4** as a yellow oil (424 mg, 1.7 mmol, 66%). ¹H NMR (500 MHz, CDCl₃) δ 7.80 – 7.76 (m, 1H), 7.48 – 7.44 (m, 2H), 7.34 – 7.29 (m, 5H), 7.25 – 7.21 (m, 1H), 6.06 (ddt, *J* = 16.4, 10.1, 6.3, 1H), 5.90 (d, *J* = 5.3, 1H), 5.11 (dq, *J* = 10.1, 1.6, 1H), 5.06 (dq, *J* = 17.1, 1.7, 1H), 3.64 (qdt, *J* = 16.0, 6.2, 1.5, 2H), 2.23 (d, *J* = 5.6, 1H). ¹³C NMR (126 MHz, CDCl₃) δ 138.66, 137.79, 137.52, 131.94, 130.55, 128.96, 128.77, 128.51, 127.44, 127.10, 122.72, 116.40, 100.20, 88.90, 86.85, 62.84, 36.94. HRMS-APCI *m/z* = 271.1107 [M+Na]⁺, calc. for C₁₈H₁₆NaO: 271.1093.

⁴ Dehmlow, E. V.; Kelle, T. *Synthetic Commun.* **1997**, *27*, 2021.

1-Silyl-2-(3-phenylprop-2-yn-1-yl)benzene (5)

To a solution of 1-(2-allylphenyl)-3-phenylprop-2-yn-1-ol (420 mg, 1.7 mmol) and triethylsilane (0.54 mL, 3.4 mmol, 2 equiv) in CH_2Cl_2 (17 mL) was added trifluoroacetic acid (1.3 mL, 17 mmol, 10 equiv) over 5 minutes. The mixture was stirred for 2 h at room temperature. Then aqueous HCl (10%, 50 mL) was added and the aqueous phase was extracted with diethyl ether (3x50 mL). The organic phase was separated, dried over MgSO_4 and the solvents were evaporated under reduced pressure. The crude was purified by column chromatography (cyclohexane, then cyclohexane/ CH_2Cl_2 , 95:5) to afford **5** as a yellow oil (293 mg, 1.3 mmol, 74%). ^1H NMR (500 MHz, CDCl_3) δ 7.56 – 7.52 (m, 1H), 7.45 – 7.41 (m, 2H), 7.28 – 7.25 (m, 3H), 7.24 – 7.20 (m, 2H), 7.18 (dt, $J = 7.2, 3.2, 1\text{H}$), 5.98 (ddt, $J = 16.4, 10.1, 6.3, 1\text{H}$), 5.11 – 5.07 (m, 1H), 5.05 – 5.00 (m, 1H), 3.78 (s, 2H), 3.47 (dt, $J = 6.2, 1.3, 2\text{H}$). ^{13}C NMR (126 MHz, CDCl_3) δ 137.70, 136.55, 135.13, 131.79, 129.84, 128.99, 128.40, 127.95, 127.28, 126.92, 123.94, 116.23, 87.62, 83.15, 37.39, 23.58. HRMS-APCI $m/z = 231.1181$ $[\text{M}-\text{H}]^+$, calc. for $\text{C}_{18}\text{H}_{15}$: 231.1168.

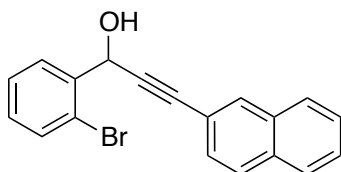
(Z)-1-(3-methoxyallyl)-2-(3-phenylprop-2-yn-1-yl)benzene (10a) and (E)-1-(3-methoxyallyl)-2-(3-phenylprop-2-yn-1-yl)benzene (10b)

An oven-dried microwave vial was charged with 1-bromo-2-(3-phenylprop-2-yn-1-yl)benzene (554 mg, 2.04 mmol), (*Z*)-tributyl(3-methoxyallyl)stannane (959 mg, 2.66 mmol, 1.3 equiv), PdCl₂(CH₃CN)₂ (37 mg, 0.14 mmol, 7 mol%), and XPHOS (136.4 mg, 0.28 mmol, 14 mol%). The vial was evacuated and back-filled with argon three times. Finally, DMF (12 mL) were added and the vial was sealed and heated at 120 °C for 2 h in a microwave reactor. The vial was allowed to cool to room temperature and KF (404 mg, 6.95 mmol, 3.4 equiv) was added to the reaction mixture and it was stirred at room temperature for 3 h. Ice-cold EtOAc was added (100 mL) and the solids were filtrated through a pad of celite. The solvents were removed under reduced pressure and the crude material was purified by column chromatography (hexane, then hexane/EtOAc, 95:5) to afford a yellow oil, **10a** and **10b** as a 4.5:1 mixture of isomers (254 mg, 0.97 mmol, 47%). ¹H NMR (400 MHz, CDCl₃) δ 7.56 – 7.53 (m, 1H), 7.49 – 7.44 (m, 2H), 7.33 – 7.31 (m, 3H), 7.28 – 7.22 (m, 3H), 6.40 (d, *J* = 12.7 Hz, 0.81H, **10a**), 6.03 (dt, *J* = 6.3, 1.3 Hz, 0.17H, **10b**), 4.92 (dt, *J* = 12.9, 7.0 Hz, 0.84H, **10a**), 4.53 (q, *J* = 7.3 Hz, 0.19H, **10b**), 3.85 (d, *J* = 4.3 Hz, 2H), 3.68 (s, 0.52H, **10b**), 3.54 (s, 2.52H, **10a**), 3.53 – 3.49 (m, 0.42H, **10b**), 3.39 (d, *J* = 6.9 Hz, 1.69H, **10a**).

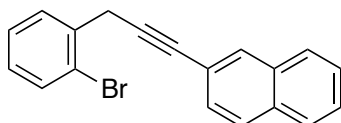
10a: ¹³C NMR (126 MHz, CDCl₃) δ 148.40, 139.17, 134.80, 131.72, 129.29, 128.94, 128.34, 127.90, 127.21, 126.68, 123.85, 100.99, 87.57, 83.04, 56.07, 31.21, 23.55.

10b: ¹³C NMR (126 MHz, CDCl₃) δ 146.83, 138.28, 137.75, 131.74, 129.15, 128.68, 128.32, 127.82, 127.09, 126.47, 123.78, 116.79, 104.58, 81.50, 56.64, 27.75, 23.26.

HRMS-ESI *m/z* = 285.1248 [M+H]⁺, calc. for C₁₉H₁₈NaO = 285.1250

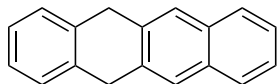
1-(2-Bromophenyl)-3-(naphthalen-2-yl)prop-2-yn-1-ol (11)

Isopropylmagnesium chloride lithium chloride complex solution (1.3 M in THF, 0.51 mL, 0.66 mmol, 1.0 equiv) was added to a solution of 2-ethynynaphthalene (100 mg, 0.66 mmol) in THF (5 mL) at 0 °C and the resulting mixture was stirred for 2 h at this temperature. 2-bromobenzaldehyde (0.12 mL, 0.99 mmol, 1.5 equiv) was added and it was stirred for further 2 h at room temperature. CH₂Cl₂ (20 mL) was added and the organic phase was washed with water (1x20 mL) and brine (1x50 mL). The organic phase was separated, dried over MgSO₄ and the solvents were evaporated under reduced pressure. The crude was purified by column chromatography (cyclohexane/EtOAc, 9:1 then 4:1) to afford **11** as an orange oil (188 mg, 0.56 mmol, 85%). ¹H NMR (500 MHz, CDCl₃) δ 7.99 (s, 1H), 7.88 (dd, *J* = 7.7, 1.7, 1H), 7.81 – 7.74 (m, 3H), 7.59 (dd, *J* = 8.0, 1.2, 1H), 7.51 – 7.45 (m, 3H), 7.39 (td, *J* = 7.6, 1.2, 1H), 7.23 – 7.18 (m, 1H), 6.06 (d, *J* = 5.0, 1H), 2.67 (d, *J* = 5.3, 1H). ¹³C NMR (126 MHz, CDCl₃) δ 139.73, 133.30, 133.16, 133.04, 132.05, 130.20, 128.91, 128.51, 128.19, 128.16, 127.98, 127.96, 127.05, 126.79, 123.02, 119.75, 88.13, 87.34, 64.99.

2-(3-(2-Bromophenyl)prop-1-yn-1-yl)naphthalene (12)

To a solution of 1-(2-bromophenyl)-3-(naphthalen-2-yl)prop-2-yn-1-ol (400 mg, 1.19 mmol) and triethylsilane (0.38 mL, 2.38 mmol, 2 equiv) in CH₂Cl₂ (15 mL) was added trifluoroacetic acid (0.92 mL, 12.0 mmol, 10 equiv) over 30 minutes. The mixture was stirred for 2 h at room temperature. Then aqueous HCl (10%, 20 mL) was added and the aqueous phase was extracted with diethyl ether (3x20 mL). The organic phase was separated, dried over MgSO₄ and the solvents were evaporated under reduced pressure. The crude was purified by column chromatography (cyclohexane, then cyclohexane/ CH₂Cl₂, 95:5) to afford **12** as a brown waxy solid (162 mg, 0.50 mmol, 42%). ¹H NMR (500 MHz, CDCl₃) δ 7.98 (s, 1H), 7.83 – 7.76 (m, 3H), 7.74 (d, *J* = 7.7 Hz, 1H), 7.58 (d, *J* = 8.0 Hz, 1H), 7.52 (dt, *J* = 8.4, 1.7 Hz, 1H), 7.50 – 7.45 (m, 2H), 7.34 (d, *J* = 7.5 Hz, 1H), 7.15 (t, *J* = 7.6 Hz, 1H), 3.96 (s, 2H). ¹³C NMR (126 MHz, CDCl₃) δ 136.28, 133.15, 132.82, 132.71, 131.49, 129.92, 128.75, 128.54, 128.05, 127.87, 127.79, 126.62, 126.61, 124.06, 120.92, 27.04. HRMS-MALDI *m/z* = 320.0214 [M]⁺, calc. for C₁₉H₁₃Br: 320.0195

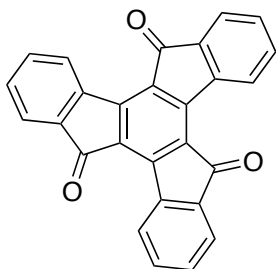
5,12-Dihydrotetracene (13)



A microwave vial was charged with 1-(3-methoxyallyl)-2-(3-phenylprop-2-yn-1-yl)benzene (14.3 mg, 0.055 mmol) and gold catalyst A (1.1 mg, 2.5 mol%). CH₂Cl₂ (HPLC grade, 0.45 mL) was added, the vial was sealed and the reaction was heated at 40 °C for 1 h. Then, it was allowed to cool to room temperature and the reaction was quenched with few drops of Et₃N. The solvents were evaporated under reduced pressure and the product was recrystallized from refluxing cyclohexane to afford **11** as white needles (11.9 mg, 0.052, 95%). ¹H NMR (400 MHz, CDCl₃) δ 7.78 (dd, *J* = 6.3Hz, *J* = 3.3Hz, 2H), 7.75 (s, 2H), 7.41 (dd, *J* = 6.2Hz, *J* = 3.2Hz, 2H), 7.34 (dd, *J* =

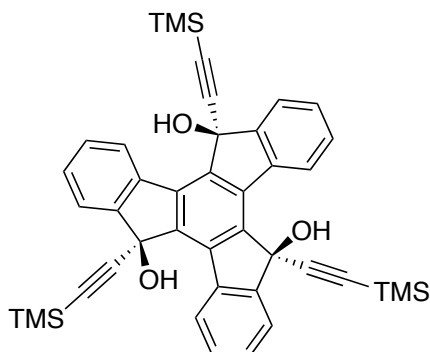
5.4Hz, $J = 3.4\text{Hz}$, 2H), 7.21 (dd, $J = 5.5\text{Hz}$, $J = 3.3\text{Hz}$, 2H), 4.09 (s, 4H); ^{13}C NMR (101 MHz, CDCl_3) δ 137.1, 135.7, 132.3, 127.21, 127.19, 126.2, 125.2, 125.1, 36.8. The spectroscopic data were consistent with those previously reported: Luo, J.; Hart, H. *J. Org. Chem.* **1987**, *52*, 4833.

5H-diindeno[1,2-a:1',2'-c]fluorene-5,10,15-trione (16)



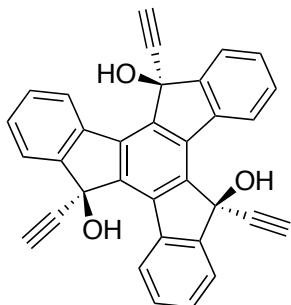
Solid KMnO_4 (5.54 mg, 35.0 mmol, 12 equiv) was added to an ice bath cooled suspension of truxene (1.0 g, 2.9 mmol) in pyridine (55 mL). The resulting mixture was stirred for 24 h leaving the ice bath to melt overnight. Water was added (10 mL) and the flask was cooled in an ice bath. Reduction of MnO_2 with concentrated HCl was ensued adding few drops at a time until no brown precipitate was visible. Then the resulting yellow solid was washed with water, acetone and hexane to afford **16** (1.075 g, 2.80, 96%). The spectroscopic data were consistent with those previously reported: Jacob, K.; Sigalov, M.; Becker, James Y.; Ellern, A.; Khodorkovsky, V. *Eur. J. Org. Chem.* **2000**, 2047.

(5S,10S,15S)-5,10,15-tris(trimethylsilyl)ethynyl-10,15-dihydro-5H-diindeno[1,2-a:1',2'-c]fluorene-5,10,15-triol (17)



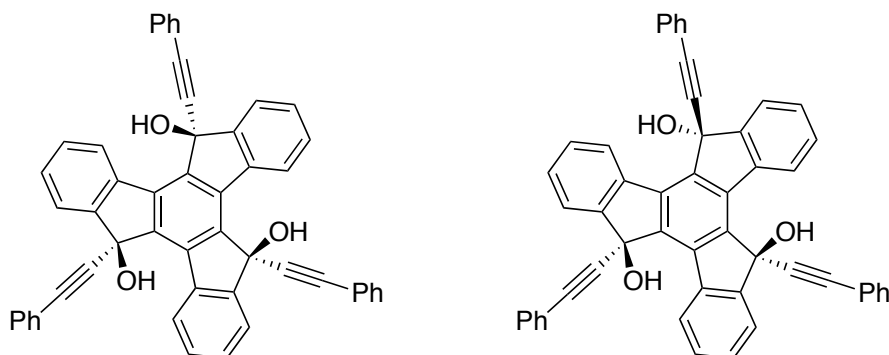
Ethyl magnesium bromide (1.0 M in THF, 2.4 mL, 2.34 mmol, 9 equiv) was added over a solution of trimethylsilylacetylene (370 μ L, 2.60 mmol, 10 equiv) in THF (2 mL) at 0 $^{\circ}$ C. The resulting mixture was warmed to room temperature and stirred for 2 h. This solution was then cannulated into a suspension of 5H-diindeno[1,2-a:1',2'-c]fluorene-5,10,15-trione (100 mg, 0.26 mmol) in THF (3 mL) at 0 $^{\circ}$ C and then it was stirred at 50 $^{\circ}$ C for 16 h. The reaction mixture was concentrated and partitioned between EtOAc (5 mL) and brine (5 mL). The organic phase was separated, dried over MgSO₄ and the solvents evaporated under reduced pressure. The crude was purified by column chromatography (cyclohexane/ EtOAc, 85:15) to afford the desired product **17** as a light yellow solid (117 mg, 0.17 mmol, 66 %). M.p.: decomposes over 225 $^{\circ}$ C. ¹H NMR (500 MHz, CDCl₃) δ 8.81 – 8.71 (m, 3H), 7.84 (dd, J = 7.4, 1.3 Hz, 3H), 7.48 (pd, J = 7.4, 1.5 Hz, 6H), 2.57 (s, 3H, OH), 0.20 (s, 27H). ¹³C NMR (101 MHz, CDCl₃) δ 148.15, 139.80, 138.54, 136.10, 129.21, 129.17, 127.11, 123.64, 103.38, 89.94, 74.70, -0.32. HRMS-MALDI m/z = 678.2318 [M]⁺, calc. for. C₄₂H₄₂O₃Si₃: 678.2436.

(5S,10S,15S)-5,10,15-triethynyl-10,15-dihydro-5H-diindeno[1,2-*a*:1',2'-*c*]fluorene-5,10,15-triol (**18**)



To a solution of (*5S,10S,15S*)-5,10,15-tris((trimethylsilyl)ethynyl)-10,15-dihydro-5H-diindeno[1,2-*a*:1',2'-*c*]fluorene-5,10,15-triol (92 mg, 0.13 mmol) in methanol (HPLC grade, 5.6 mL) was added solid K_2CO_3 (122 mg, 0.88 mmol, 6.5 equiv) and the resulting green solution was stirred at room temperature for 2 h. The reaction was quenched with water (20 mL) and a solid precipitated. The solid was separated by filtration and purified by column chromatography (Cyclohexane/EtOAc, 8:2 then 1:1) to afford the desired product **18** as a light yellow solid (52 mg, 0.11 mmol, 84 %). 1H NMR (500 MHz, $CDCl_3$) δ 8.72 (d, $J = 7.7$ Hz, 3H), 7.85 (d, $J = 7.4$ Hz, 3H), 7.61 – 7.49 (m, 6H), 2.53 (s, 3H, OH), 2.52 (s, 3H). ^{13}C NMR (126 MHz, $CDCl_3$) δ 148.21, 139.80, 138.81, 136.20, 130.00, 129.67, 127.20, 123.85, 82.40, 74.56, 72.74. The spectroscopic data were consistent with those previously reported: Dehmlow, E. V.; Kelle, T. *Synthetic Commun.* **1997**, 27, 2021.

(5S,10S,15S)-5,10,15-tris(phenylethynyl)-10,15-dihydro-5H-diindeno[1,2-a:1',2'-c]fluorene-5,10,15-triol (19a) and (5R,10S,15S)-5,10,15-tris(phenylethynyl)-10,15-dihydro-5H-diindeno[1,2-a:1',2'-c]fluorene-5,10,15-triol (19b)

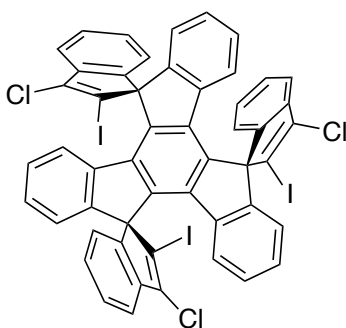


Ethyl magnesium bromide (1.0 M in THF, 11.7 mL, 11.7 mmol, 9 equiv) was added over a solution of phenylacetylene (1.43 mL, 13.0 mmol, 10 equiv) in THF (10 mL) at 0 °C. The resulting mixture was warmed to room temperature and stirred for 2 h. This solution was then cannulated into a suspension of 5H-diindeno[1,2-a:1',2'-c]fluorene-5,10,15-trione (500 mg, 1.30 mmol) in THF (15 mL) at 0 °C and then it was stirred at 50 °C for 16 h. The reaction mixture was concentrated and partitioned between EtOAc (25 mL) and brine (25 mL). The organic phase was separated, dried over MgSO₄ and the solvents evaporated under reduced pressure. The crude was purified by column chromatography (cyclohexane/ EtOAc, 85:15) to afford **19a** as a light yellow solid (529 mg, 0.77 mmol, 59 %) and **19b** as an ocre solid (104 mg, 0.15 mmol, 12%).

19a: ¹H NMR (500 MHz, CDCl₃) δ 8.83 (dd, *J* = 7.7, 0.9 Hz, 1H), 7.89 (dt, *J* = 7.2, 0.9 Hz, 3H), 7.57 (td, *J* = 7.6, 1.3 Hz, 3H), 7.51 (td, *J* = 7.4, 1.2 Hz, 3H), 7.39 – 7.35 (m, 6H), 7.27 – 7.20 (m, 9H). ¹³C NMR (126 MHz, CDCl₃) δ 148.44, 140.13, 138.36, 136.14, 132.00, 129.64, 129.36, 128.56, 128.11, 126.86, 123.83, 122.23, 87.43, 84.12, 74.95.

19b: ^1H NMR (500 MHz, CDCl_3) δ 8.82 – 8.91 (m, 3 H), 7.85 – 7.92 (m, 3H), 7.41 – 7.59 (m, 6 H), 7.29 – 7.35 (m, 6 H), 7.14 – 7.24 (m, 9 H), 2.74 (s, 1H, OH), 2.70 (s, 1H, OH), 2.66 (s, 1H, OH). The spectroscopic data were consistent with those previously reported: Dehmlow, E. V.; Kelle, T. *Synthetic Commun.* **1997**, 27, 2021.

Propeller 23



In an oven-dried microwave vial was placed (5S,10S,15S)-5,10,15-trimethoxy-5,10,15-tris(phenylethynyl)-10,15-dihydro-5H-diindeno[1,2-a:1',2'-c]fluorene (200 mg, 0.29 mmol) in CH_2Cl_2 (19 mL) under an argon atmosphere. Then the mixture was cooled to $-78\text{ }^\circ\text{C}$ and iodine monochloride (1.0 M in CH_2Cl_2 , 1.45 mL, 1.45 mmol, 5.0 equiv) was added dropwise over 10 min. The reaction was allowed to warm to room temperature in the acetone bath over 4 h, then the reaction was stirred at this temperature for 3 h. The reaction was quenched with aqueous NaS (sat, 3 mL) and the aqueous phase was extracted with CH_2Cl_2 (3x1 mL). The solvents were evaporated and the crude residue was purified by flash chromatography (cyclohexane/EtOAc, 2:1) to afford the title compounds **23a** and **23b** as a mixture of enantiomers (219 mg, 0.20 mmol, 67%). ^1H NMR (500 MHz, CDCl_3) δ 7.74 – 7.66 (m, 3H), 7.44 – 7.34 (m, 3H), 7.15 – 6.68 (m, 14H), 6.64 – 6.57 (m, 4H). ^{13}C NMR (126 MHz, CDCl_3) δ 146.59, 146.57, 146.46, 145.14, 145.03, 144.99, 144.93, 143.05, 142.98, 142.97,

141.68, 141.61, 141.48, 141.38, 140.83, 140.68, 140.61, 140.53, 139.48, 139.42, 139.33, 137.12, 137.05, 137.03, 137.00, 128.31, 128.27, 128.18, 128.13, 128.11, 128.09, 128.01, 127.99, 127.97, 127.91, 127.84, 127.81, 127.66, 124.29, 124.27, 123.21, 123.11, 122.83, 121.95, 121.79, 121.76, 119.83, 119.81, 119.7, 106.43, 106.31, 106.09, 105.94, 72.53, 72.48, 72.44, 72.42. LRMS-MALDI m/z = 1121.0 [M]⁻, calc. for. C₅₁H₂₄Cl₃I₃: 1121.81.

X-Ray Crystal Structure.

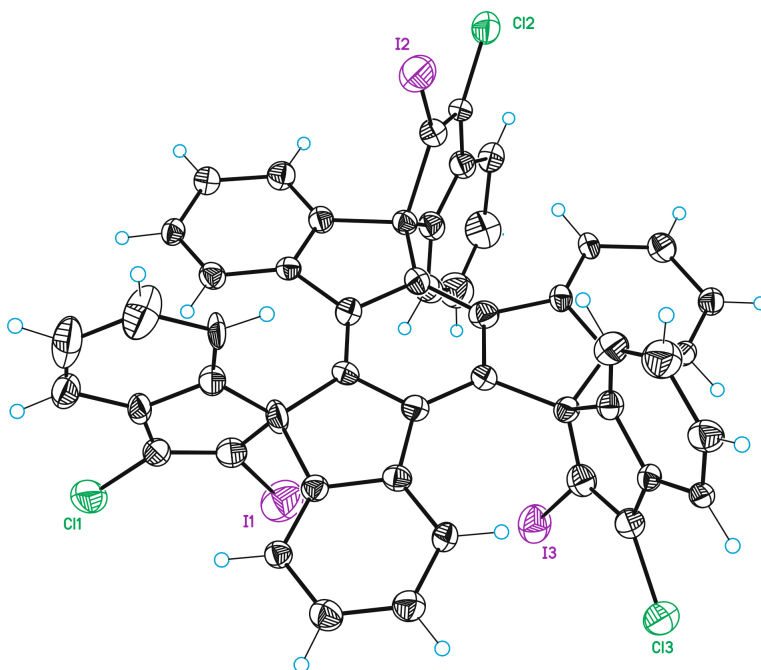


Table 1. Crystal data and structure refinement for PM2_040_C2c.

Identification code	PM2_040_C2c
Empirical formula	C52 H26 Cl5 I3
Formula weight	1208.68
Temperature	100(2) K
Wavelength	0.71073 Å
Crystal system	Monoclinic
Space group	C2/c

Unit cell dimensions	a = 13.4446(4) Å	a = 90.00 °.
	b = 22.7868(6) Å	b = 98.8400(10)
	c = 30.4262(10) Å	g = 90.00 °.
Volume	9210.6(5) Å ³	
Z	8	
Density (calculated)	1.743 Mg/m ³	
Absorption coefficient	2.362 mm ⁻¹	
F(000)	4656	
Crystal size	0.10 x 0.10 x 0.05 mm ³	
Theta range for data collection	1.81 to 30.66 °.	
Index ranges	-15 ≤ h ≤ 19, -32 ≤ k ≤ 32, -	
	43 ≤ l ≤ 40	
Reflections collected	78977	
Independent reflections	14163 [R(int) = 0.0475]	
Completeness to theta = 30.66 °	99.4%	
Absorption correction	Empirical	
Max. and min. transmission	0.7981 and 0.7183	
Refinement method	Full-matrix least-squares on	
F ²		
Data / restraints / parameters	14163 / 726 / 1004	
Goodness-of-fit on F ²	1.159	
Final R indices [I > 2σ(I)]	R1 = 0.1339, wR2 = 0.3081	
R indices (all data)	R1 = 0.1402, wR2 = 0.3111	
Largest diff. peak and hole	1.928 and -1.649 e.Å ⁻³	

Table 2. Bond lengths [Å] and angles [°] for PM2_040_C2c.

Bond lengths----

C1-C6	1.391(12)
C1-C2	1.420(12)
C1-C7	1.475(12)
C2-C3	1.379(12)

C2-C13	1.523(12)
C3-C4	1.415(12)
C3-C22	1.489(12)
C4-C5	1.390(12)
C4-C28	1.499(19)
C5-C6	1.414(12)
C5-C37	1.476(12)
C6-C43	1.55(2)
C7-C8	1.394(13)
C7-C12	1.407(12)
C8-C9	1.402(13)
C9-C10	1.368(14)
C10-C11	1.386(14)
C11-C12	1.386(12)
C12-C13	1.514(14)
C22-C23	1.384(13)
C22-C27	1.404(12)
C23-C24	1.382(13)
C24-C25	1.397(13)
C25-C26	1.393(14)
C26-C27	1.377(13)
C27-C28	1.55(2)
C37-C42	1.381(13)
C37-C38	1.386(13)
C38-C39	1.385(14)
C39-C40	1.426(14)
C40-C41	1.402(13)
C41-C42	1.381(13)
C42-C43	1.55(2)
C1'-C6'	1.391(12)
C1'-C2'	1.420(12)
C1'-C7'	1.475(12)

C2'-C3'	1.379(12)
C2'-C13	1.557(13)
C3'-C4'	1.415(12)
C3'-C22'	1.489(13)
C4'-C5'	1.391(12)
C4'-C28'	1.54(2)
C5'-C6'	1.414(12)
C5'-C37'	1.476(12)
C6'-C43'	1.49(2)
C7'-C8'	1.394(13)
C7'-C12'	1.407(13)
C8'-C9'	1.402(13)
C9'-C10'	1.368(14)
C10'-C11'	1.386(14)
C11'-C12'	1.386(12)
C12'-C13	1.549(14)
C22'-C23'	1.384(13)
C22'-C27'	1.404(12)
C23'-C24'	1.382(13)
C24'-C25'	1.397(13)
C25'-C26'	1.393(14)
C26'-C27'	1.378(13)
C27'-C28'	1.51(3)
C37'-C42'	1.380(13)
C37'-C38'	1.385(13)
C38'-C39'	1.385(14)
C39'-C40'	1.426(14)
C40'-C41'	1.402(14)
C41'-C42'	1.382(13)
C42'-C43'	1.56(3)
C13-C14	1.523(13)
C13-C21	1.524(12)

C14-C15	1.336(12)
C14-I1	2.050(10)
C15-C16	1.453(14)
C15-C11	1.708(9)
C16-C17	1.403(12)
C16-C21	1.413(11)
C17-C18	1.347(17)
C18-C19	1.411(18)
C19-C20	1.317(15)
C20-C21	1.515(19)
C12-C30	1.661(15)
I2-C29	1.927(17)
C28-C36	1.30(2)
C28-C29	1.78(2)
C29-C30	1.37(2)
C30-C31	1.41(2)
C31-C36	1.41(2)
C31-C32	1.58(3)
C32-C33	1.58(3)
C33-C34	1.45(3)
C34-C35	1.39(2)
C35-C36	1.43(2)
C12'-C30'	1.662(16)
I2'-C29'	1.926(17)
C28'-C36'	1.30(2)
C28'-C29'	1.78(2)
C29'-C30'	1.37(2)
C30'-C31'	1.41(2)
C31'-C36'	1.41(2)
C31'-C32'	1.58(3)
C32'-C33'	1.58(3)
C33'-C34'	1.45(3)

C34'-C35'	1.39(2)
C35'-C36'	1.43(2)
C13-C45	1.751(17)
I3-C44	2.156(17)
C43-C44	1.30(2)
C43-C51	1.76(2)
C44-C45	1.39(2)
C45-C46	1.43(2)
C46-C51	1.38(2)
C46-C47	1.41(2)
C47-C48	1.30(2)
C48-C49	1.41(2)
C49-C50	1.45(2)
C50-C51	1.20(2)
C13'-C45'	1.750(17)
I3'-C44'	2.158(17)
C43'-C44'	1.30(2)
C43'-C51'	1.76(2)
C44'-C45'	1.39(2)
C45'-C46'	1.43(2)
C46'-C51'	1.38(2)
C46'-C47'	1.42(2)
C47'-C48'	1.30(2)
C48'-C49'	1.41(2)
C49'-C50'	1.45(2)
C50'-C51'	1.20(2)
C11S-C1S#1	1.66(5)
C11S-C1S	1.79(2)
C11S-C12S	2.688(16)
C12S-C12S#1	1.32(3)
C12S-C1S	1.56(5)
C12S-C1S#1	1.81(4)

C1S-C1S#1	0.79(8)
C1S-C11S#1	1.66(5)
C1S-C12S#1	1.81(4)
C1T-C12T	1.7790
C1T-C11T	1.7943
C1T*-C11*	1.7566
C1T*-C12*	2.1752
Angles-----	
C6-C1-C2	119.6(8)
C6-C1-C7	131.7(9)
C2-C1-C7	108.7(8)
C3-C2-C1	119.4(8)
C3-C2-C13	131.4(9)
C1-C2-C13	109.2(8)
C2-C3-C4	121.3(8)
C2-C3-C22	130.8(8)
C4-C3-C22	107.9(8)
C5-C4-C3	119.2(8)
C5-C4-C28	128.9(11)
C3-C4-C28	111.4(10)
C4-C5-C6	119.8(8)
C4-C5-C37	131.5(8)
C6-C5-C37	108.7(8)
C1-C6-C5	120.5(9)
C1-C6-C43	128.6(11)
C5-C6-C43	110.6(10)
C8-C7-C12	118.8(8)
C8-C7-C1	132.6(9)
C12-C7-C1	108.3(8)
C7-C8-C9	119.3(9)
C10-C9-C8	120.9(10)
C9-C10-C11	120.7(10)

C10-C11-C12	119.0(9)
C11-C12-C7	121.2(9)
C11-C12-C13	128.5(9)
C7-C12-C13	109.9(8)
C23-C22-C27	118.6(9)
C23-C22-C3	132.4(9)
C27-C22-C3	108.5(8)
C24-C23-C22	119.3(9)
C23-C24-C25	121.9(9)
C26-C25-C24	118.9(10)
C27-C26-C25	118.9(10)
C26-C27-C22	122.1(9)
C26-C27-C28	128.0(10)
C22-C27-C28	109.8(9)
C42-C37-C38	119.2(9)
C42-C37-C5	108.6(8)
C38-C37-C5	132.1(9)
C39-C38-C37	119.6(9)
C38-C39-C40	121.2(10)
C41-C40-C39	118.2(9)
C42-C41-C40	118.8(9)
C41-C42-C37	122.8(9)
C41-C42-C43	124.9(10)
C37-C42-C43	112.2(9)
C6'-C1'-C2'	119.5(8)
C6'-C1'-C7'	131.7(9)
C2'-C1'-C7'	108.5(8)
C3'-C2'-C1'	119.6(8)
C3'-C2'-C13	128.1(10)
C1'-C2'-C13	110.5(8)
C2'-C3'-C4'	121.2(9)
C2'-C3'-C22'	130.8(8)

C4'-C3'-C22'	108.0(8)
C5'-C4'-C3'	119.1(8)
C5'-C4'-C28'	130.2(11)
C3'-C4'-C28'	110.1(11)
C4'-C5'-C6'	120.0(8)
C4'-C5'-C37'	131.2(9)
C6'-C5'-C37'	108.8(8)
C1'-C6'-C5'	120.5(9)
C1'-C6'-C43'	129.0(12)
C5'-C6'-C43'	110.4(11)
C8'-C7'-C12'	118.8(8)
C8'-C7'-C1'	132.8(9)
C12'-C7'-C1'	108.4(8)
C7'-C8'-C9'	119.2(9)
C10'-C9'-C8'	121.0(10)
C9'-C10'-C11'	120.8(10)
C10'-C11'-C12'	118.9(10)
C11'-C12'-C7'	121.3(9)
C11'-C12'-C13	126.8(9)
C7'-C12'-C13	111.5(8)
C23'-C22'-C27'	118.7(9)
C23'-C22'-C3'	132.7(9)
C27'-C22'-C3'	108.6(8)
C24'-C23'-C22'	119.3(10)
C23'-C24'-C25'	121.9(10)
C26'-C25'-C24'	119.0(10)
C27'-C26'-C25'	118.9(10)
C26'-C27'-C22'	122.1(9)
C26'-C27'-C28'	126.8(10)
C22'-C27'-C28'	111.0(9)
C42'-C37'-C38'	119.3(9)
C42'-C37'-C5'	108.7(8)

C38'-C37'-C5'	132.1(9)
C39'-C38'-C37'	119.6(10)
C38'-C39'-C40'	121.0(10)
C41'-C40'-C39'	118.2(10)
C42'-C41'-C40'	118.7(10)
C37'-C42'-C41'	122.6(9)
C37'-C42'-C43'	109.9(10)
C41'-C42'-C43'	127.2(11)
C12-C13-C2	102.8(7)
C12-C13-C14	101.6(10)
C2-C13-C14	110.8(10)
C12-C13-C21	112.8(9)
C2-C13-C21	124.7(9)
C14-C13-C21	102.0(7)
C12-C13-C12'	12.8(10)
C2-C13-C12'	102.6(7)
C14-C13-C12'	113.1(10)
C21-C13-C12'	103.7(9)
C12-C13-C2'	102.5(7)
C2-C13-C2'	12.6(10)
C14-C13-C2'	122.7(10)
C21-C13-C2'	114.7(10)
C12'-C13-C2'	99.5(8)
C15-C14-C13	109.9(9)
C15-C14-I1	127.6(8)
C13-C14-I1	122.1(6)
C14-C15-C16	110.7(8)
C14-C15-C11	126.2(8)
C16-C15-C11	123.0(7)
C17-C16-C21	121.0(9)
C17-C16-C15	130.8(8)
C21-C16-C15	108.2(7)

C18-C17-C16	116.6(9)
C17-C18-C19	122.6(11)
C20-C19-C18	126.7(14)
C19-C20-C21	111.5(11)
C16-C21-C20	121.3(8)
C16-C21-C13	108.0(8)
C20-C21-C13	130.0(8)
C36-C28-C4	122.8(18)
C36-C28-C27	110.0(18)
C4-C28-C27	102.1(9)
C36-C28-C29	100.0(10)
C4-C28-C29	115.1(15)
C27-C28-C29	106.0(14)
C30-C29-C28	101.7(12)
C30-C29-I2	127.7(13)
C28-C29-I2	130.1(11)
C29-C30-C31	112.1(16)
C29-C30-C12	126.9(12)
C31-C30-C12	121.0(15)
C30-C31-C36	108.7(17)
C30-C31-C32	125.7(17)
C36-C31-C32	125.6(15)
C31-C32-C33	104.5(16)
C34-C33-C32	127.8(18)
C35-C34-C33	118.9(17)
C34-C35-C36	120.8(15)
C28-C36-C31	116.8(15)
C28-C36-C35	121.1(16)
C31-C36-C35	122.1(16)
C36'-C28'-C27'	111.0(19)
C36'-C28'-C4'	126(2)
C27'-C28'-C4'	102.2(9)

C36'-C28'-C29'	99.8(10)
C27'-C28'-C29'	105.9(16)
C4'-C28'-C29'	110.6(15)
C30'-C29'-C28'	101.8(12)
C30'-C29'-I2'	128.5(13)
C28'-C29'-I2'	129.7(11)
C29'-C30'-C31'	112.2(17)
C29'-C30'-CI2'	126.5(13)
C31'-C30'-CI2'	121.3(15)
C30'-C31'-C36'	108.5(17)
C30'-C31'-C32'	126.2(17)
C36'-C31'-C32'	125.2(15)
C31'-C32'-C33'	104.4(17)
C34'-C33'-C32'	127.7(18)
C35'-C34'-C33'	118.8(17)
C34'-C35'-C36'	120.7(16)
C28'-C36'-C31'	116.7(15)
C28'-C36'-C35'	121.1(17)
C31'-C36'-C35'	122.2(16)
C44-C43-C42	113.7(19)
C44-C43-C6	121(2)
C42-C43-C6	99.7(8)
C44-C43-C51	99.2(9)
C42-C43-C51	107.8(16)
C6-C43-C51	115.2(15)
C43-C44-C45	117.8(16)
C43-C44-I3	118.7(13)
C45-C44-I3	123.5(13)
C44-C45-C46	109.3(17)
C44-C45-CI3	124.2(13)
C46-C45-CI3	126.5(15)
C51-C46-C47	119.7(14)

C51-C46-C45	109.2(16)
C47-C46-C45	131.1(18)
C48-C47-C46	114.5(16)
C47-C48-C49	123.7(15)
C48-C49-C50	119.0(14)
C51-C50-C49	114.7(16)
C50-C51-C46	128.4(17)
C50-C51-C43	127.6(15)
C46-C51-C43	103.8(12)
C44'-C43'-C6'	126(2)
C44'-C43'-C42'	109(2)
C6'-C43'-C42'	102.2(9)
C44'-C43'-C51'	99.4(9)
C6'-C43'-C51'	112.9(18)
C42'-C43'-C51'	106.4(17)
C43'-C44'-C45'	117.5(16)
C43'-C44'-I3'	119.1(13)
C45'-C44'-I3'	123.3(13)
C44'-C45'-C46'	109.7(17)
C44'-C45'-Cl3'	124.0(13)
C46'-C45'-Cl3'	126.3(16)
C51'-C46'-C47'	119.7(14)
C51'-C46'-C45'	109.1(16)
C47'-C46'-C45'	131.2(18)
C48'-C47'-C46'	114.2(16)
C47'-C48'-C49'	123.3(16)
C48'-C49'-C50'	119.0(15)
C51'-C50'-C49'	114.6(17)
C50'-C51'-C46'	128.3(17)
C50'-C51'-C43'	127.8(16)
C46'-C51'-C43'	103.9(12)
C1S-C1IIS-C1S#1	26(3)

C1S-C11S-C12S#1	41.3(13)
C1S-C11S-C12S	33.8(17)
C12S-C12S-C1S#1	77.5(17)
C12S#1-C12S-C1S#1	57.1(18)
C1S-C12S-C1S#1	26(2)
C12S-C12S-C11S#1	88.2(7)
C1S-C12S-C11S	39.7(11)
C1S-C12S-C11S#1	37.1(16)
C1S-C1S-C12S#1	95.5(17)
C1S#1-C1S-C11S#1	87(6)
C12S-C1S-C11S#1	133.8(17)
C1S#1-C1S-C12S#1	59(2)
C12S-C1S-C12S#1	45.4(17)
C11S#1-C1S-C12S#1	102(2)
C1S-C1S-C11S#1	67(4)
C12S-C1S-C11S	106(3)
C11S-C1S-C11S#1	117(3)
C12S-C1S-C11S#1	110.3(19)
C12T-C1T-C11T	102.0
C11*-C1T*-C12*	89.5

Symmetry transformations used to generate equivalent atoms:

#1 -x+1, y, -z+1/2

Table 3. Torsion angles [°] for PM2_040_C2c.

C6-C1-C2-C3	1(3)
C7-C1-C2-C3	-177.8(19)
C6-C1-C2-C13	-179.1(18)
C7-C1-C2-C13	2(2)
C1-C2-C3-C4	-2(3)
C13-C2-C3-C4	177.6(18)

C1-C2-C3-C22	178(2)
C13-C2-C3-C22	-3(4)
C2-C3-C4-C5	4(3)
C22-C3-C4-C5	-176(2)
C2-C3-C4-C28	176.0(18)
C22-C3-C4-C28	-4(2)
C3-C4-C5-C6	-4(3)
C28-C4-C5-C6	-175(2)
C3-C4-C5-C37	176(2)
C28-C4-C5-C37	6(4)
C2-C1-C6-C5	-1(3)
C7-C1-C6-C5	177(2)
C2-C1-C6-C43	-174(2)
C7-C1-C6-C43	4(4)
C4-C5-C6-C1	3(3)
C37-C5-C6-C1	-178(2)
C4-C5-C6-C43	176.9(19)
C37-C5-C6-C43	-3(2)
C6-C1-C7-C8	0(4)
C2-C1-C7-C8	178(2)
C6-C1-C7-C12	-174(2)
C2-C1-C7-C12	5(2)
C12-C7-C8-C9	-1(3)
C1-C7-C8-C9	-174(2)
C7-C8-C9-C10	1(3)
C8-C9-C10-C11	-2(3)
C9-C10-C11-C12	3(3)
C10-C11-C12-C7	-3(3)
C10-C11-C12-C13	-175.1(18)
C8-C7-C12-C11	2(3)
C1-C7-C12-C11	176.5(19)
C8-C7-C12-C13	175.5(17)

C1-C7-C12-C13	-10(2)
C2-C3-C22-C23	-3(4)
C4-C3-C22-C23	177(2)
C2-C3-C22-C27	-174(2)
C4-C3-C22-C27	6(2)
C27-C22-C23-C24	-3(3)
C3-C22-C23-C24	-174(2)
C22-C23-C24-C25	-2(3)
C23-C24-C25-C26	4(3)
C24-C25-C26-C27	-2(3)
C25-C26-C27-C22	-3(3)
C25-C26-C27-C28	-178.7(18)
C23-C22-C27-C26	6(3)
C3-C22-C27-C26	179.0(19)
C23-C22-C27-C28	-177.9(17)
C3-C22-C27-C28	-5(2)
C4-C5-C37-C42	-175(2)
C6-C5-C37-C42	5(3)
C4-C5-C37-C38	0(4)
C6-C5-C37-C38	-179(2)
C42-C37-C38-C39	0(3)
C5-C37-C38-C39	-175(2)
C37-C38-C39-C40	-1(3)
C38-C39-C40-C41	-2(3)
C39-C40-C41-C42	5(3)
C40-C41-C42-C37	-6(3)
C40-C41-C42-C43	178.9(18)
C38-C37-C42-C41	3(3)
C5-C37-C42-C41	179(2)
C38-C37-C42-C43	178.8(18)
C5-C37-C42-C43	-5(3)
C6'-C1'-C2'-C3'	0(3)

C7'-C1'-C2'-C3'	-175(2)
C6'-C1'-C2'-C13	165.9(19)
C7'-C1'-C2'-C13	-9(2)
C1'-C2'-C3'-C4'	-3(3)
C13-C2'-C3'-C4'	-166.4(19)
C1'-C2'-C3'-C22'	178(2)
C13-C2'-C3'-C22'	15(4)
C2'-C3'-C4'-C5'	5(3)
C22'-C3'-C4'-C5'	-176(2)
C2'-C3'-C4'-C28'	177.3(19)
C22'-C3'-C4'-C28'	-4(3)
C3'-C4'-C5'-C6'	-4(4)
C28'-C4'-C5'-C6'	-174(2)
C3'-C4'-C5'-C37'	176(2)
C28'-C4'-C5'-C37'	5(4)
C2'-C1'-C6'-C5'	1(4)
C7'-C1'-C6'-C5'	175(2)
C2'-C1'-C6'-C43'	-174(2)
C7'-C1'-C6'-C43'	0(4)
C4'-C5'-C6'-C1'	1(4)
C37'-C5'-C6'-C1'	-179(2)
C4'-C5'-C6'-C43'	177(2)
C37'-C5'-C6'-C43'	-3(3)
C6'-C1'-C7'-C8'	9(5)
C2'-C1'-C7'-C8'	-177(3)
C6'-C1'-C7'-C12'	-173(3)
C2'-C1'-C7'-C12'	1(3)
C12'-C7'-C8'-C9'	2(4)
C1'-C7'-C8'-C9'	-180(2)
C7'-C8'-C9'-C10'	-1(3)
C8'-C9'-C10'-C11'	-1(4)
C9'-C10'-C11'-C12'	2(4)

C10'-C11'-C12'-C7'	-1(4)
C10'-C11'-C12'-C13	171.3(19)
C8'-C7'-C12'-C11'	-1(4)
C1'-C7'-C12'-C11'	-179(2)
C8'-C7'-C12'-C13	-175(2)
C1'-C7'-C12'-C13	7(3)
C2'-C3'-C22'-C23'	0(5)
C4'-C3'-C22'-C23'	-179(3)
C2'-C3'-C22'-C27'	-178(2)
C4'-C3'-C22'-C27'	3(3)
C27'-C22'-C23'-C24'	-2(4)
C3'-C22'-C23'-C24'	-179(2)
C22'-C23'-C24'-C25'	-1(3)
C23'-C24'-C25'-C26'	2(3)
C24'-C25'-C26'-C27'	0(3)
C25'-C26'-C27'-C22'	-3(3)
C25'-C26'-C27'-C28'	-179.2(18)
C23'-C22'-C27'-C26'	3(4)
C3'-C22'-C27'-C26'	-179(2)
C23'-C22'-C27'-C28'	-180(2)
C3'-C22'-C27'-C28'	-2(3)
C4'-C5'-C37'-C42'	-176(3)
C6'-C5'-C37'-C42'	4(3)
C4'-C5'-C37'-C38'	5(5)
C6'-C5'-C37'-C38'	-176(3)
C42'-C37'-C38'-C39'	3(4)
C5'-C37'-C38'-C39'	-178(3)
C37'-C38'-C39'-C40'	-4(4)
C38'-C39'-C40'-C41'	-2(4)
C39'-C40'-C41'-C42'	7(4)
C38'-C37'-C42'-C41'	3(4)
C5'-C37'-C42'-C41'	-176(2)

C38'-C37'-C42'-C43'	176(2)
C5'-C37'-C42'-C43'	-3(3)
C40'-C41'-C42'-C37'	-8(4)
C40'-C41'-C42'-C43'	179(2)
C11-C12-C13-C2	-176(2)
C7-C12-C13-C2	11.0(19)
C11-C12-C13-C14	-61(2)
C7-C12-C13-C14	125.7(15)
C11-C12-C13-C21	47(2)
C7-C12-C13-C21	-125.8(15)
C11-C12-C13-C12'	93(3)
C7-C12-C13-C12'	-80(2)
C11-C12-C13-C2'	171(2)
C7-C12-C13-C2'	-1.9(19)
C3-C2-C13-C12	172(2)
C1-C2-C13-C12	-8.0(19)
C3-C2-C13-C14	65(2)
C1-C2-C13-C14	-115.8(15)
C3-C2-C13-C21	-58(3)
C1-C2-C13-C21	121.8(14)
C3-C2-C13-C12'	-174(2)
C1-C2-C13-C12'	5.2(19)
C3-C2-C13-C2'	-97(3)
C1-C2-C13-C2'	82(2)
C11'-C12'-C13-C12	-80(3)
C7'-C12'-C13-C12	93(3)
C11'-C12'-C13-C2	-172(2)
C7'-C12'-C13-C2	1(2)
C11'-C12'-C13-C14	-53(2)
C7'-C12'-C13-C14	120.4(17)
C11'-C12'-C13-C21	57(2)
C7'-C12'-C13-C21	-129.9(17)

C11'-C12'-C13-C2'	175(2)
C7'-C12'-C13-C2'	-11(2)
C3'-C2'-C13-C12	164(2)
C1'-C2'-C13-C12	-1(2)
C3'-C2'-C13-C2	71(3)
C1'-C2'-C13-C2	-93(3)
C3'-C2'-C13-C14	51(2)
C1'-C2'-C13-C14	-113.3(16)
C3'-C2'-C13-C21	-73(2)
C1'-C2'-C13-C21	122.1(15)
C3'-C2'-C13-C12'	177(2)
C1'-C2'-C13-C12'	12.2(19)
C12-C13-C14-C15	106.1(9)
C2-C13-C14-C15	-145.2(8)
C21-C13-C14-C15	-10.5(9)
C12'-C13-C14-C15	100.2(10)
C2'-C13-C14-C15	-140.6(9)
C12-C13-C14-II	-67.3(9)
C2-C13-C14-II	41.3(10)
C21-C13-C14-II	176.1(6)
C12'-C13-C14-II	-73.2(10)
C2'-C13-C14-II	45.9(12)
C13-C14-C15-C16	7.2(10)
II-C14-C15-C16	-179.9(6)
C13-C14-C15-C11	-170.5(6)
II-C14-C15-C11	2.4(12)
C14-C15-C16-C17	179.3(9)
C11-C15-C16-C17	-2.9(13)
C14-C15-C16-C21	-0.4(10)
C11-C15-C16-C21	177.4(6)
C21-C16-C17-C18	2.2(14)
C15-C16-C17-C18	-177.5(10)

C16-C17-C18-C19	-2.7(18)
C17-C18-C19-C20	-2(2)
C18-C19-C20-C21	6(2)
C17-C16-C21-C20	2.6(13)
C15-C16-C21-C20	-177.7(8)
C17-C16-C21-C13	173.9(7)
C15-C16-C21-C13	-6.4(9)
C19-C20-C21-C16	-6.6(15)
C19-C20-C21-C13	-175.7(11)
C12-C13-C21-C16	-98.2(10)
C2-C13-C21-C16	136.1(10)
C14-C13-C21-C16	10.0(9)
C12'-C13-C21-C16	-107.7(9)
C2'-C13-C21-C16	144.9(9)
C12-C13-C21-C20	72.0(13)
C2-C13-C21-C20	-53.6(15)
C14-C13-C21-C20	-179.8(9)
C12'-C13-C21-C20	62.5(13)
C2'-C13-C21-C20	-44.8(14)
C5-C4-C28-C36	49(3)
C3-C4-C28-C36	-123(2)
C5-C4-C28-C27	172(2)
C3-C4-C28-C27	1(2)
C5-C4-C28-C29	-73(3)
C3-C4-C28-C29	115.3(18)
C26-C27-C28-C36	-50(3)
C22-C27-C28-C36	134.5(17)
C26-C27-C28-C4	178(2)
C22-C27-C28-C4	3(2)
C26-C27-C28-C29	57(2)
C22-C27-C28-C29	-118.3(16)
C36-C28-C29-C30	8(2)

C4-C28-C29-C30	141.6(16)
C27-C28-C29-C30	-106.3(16)
C36-C28-C29-I2	-180(2)
C4-C28-C29-I2	-46(2)
C27-C28-C29-I2	66(2)
C28-C29-C30-C31	-7(2)
I2-C29-C30-C31	-179.7(17)
C28-C29-C30-CI2	171.1(15)
I2-C29-C30-CI2	-1(3)
C29-C30-C31-C36	4(3)
CI2-C30-C31-C36	-174.0(16)
C29-C30-C31-C32	-177(2)
CI2-C30-C31-C32	4(3)
C30-C31-C32-C33	178(2)
C36-C31-C32-C33	-4(3)
C31-C32-C33-C34	0(3)
C32-C33-C34-C35	4(4)
C33-C34-C35-C36	-6(3)
C4-C28-C36-C31	-135(2)
C27-C28-C36-C31	105(2)
C29-C28-C36-C31	-6(3)
C4-C28-C36-C35	46(3)
C27-C28-C36-C35	-74(3)
C29-C28-C36-C35	175(2)
C30-C31-C36-C28	2(3)
C32-C31-C36-C28	-176(2)
C30-C31-C36-C35	-179(2)
C32-C31-C36-C35	3(4)
C34-C35-C36-C28	-179(2)
C34-C35-C36-C31	3(3)
C26'-C27'-C28'-C36'	40(3)
C22'-C27'-C28'-C36'	-137.3(19)

C26'-C27'-C28'-C4'	176(2)
C22'-C27'-C28'-C4'	-1(2)
C26'-C27'-C28'-C29'	-68(2)
C22'-C27'-C28'-C29'	115.2(18)
C5'-C4'-C28'-C36'	-59(3)
C3'-C4'-C28'-C36'	130(2)
C5'-C4'-C28'-C27'	174(2)
C3'-C4'-C28'-C27'	3(2)
C5'-C4'-C28'-C29'	61(3)
C3'-C4'-C28'-C29'	-110(2)
C36'-C28'-C29'-C30'	-7(3)
C27'-C28'-C29'-C30'	108.7(18)
C4'-C28'-C29'-C30'	-141.3(19)
C36'-C28'-C29'-I2'	175(2)
C27'-C28'-C29'-I2'	-69(2)
C4'-C28'-C29'-I2'	40(3)
C28'-C29'-C30'-C31'	1(3)
I2'-C29'-C30'-C31'	180(2)
C28'-C29'-C30'-C12'	179.8(18)
I2'-C29'-C30'-C12'	-2(4)
C29'-C30'-C31'-C36'	4(3)
C12'-C30'-C31'-C36'	-174.4(18)
C29'-C30'-C31'-C32'	-178(3)
C12'-C30'-C31'-C32'	3(4)
C30'-C31'-C32'-C33'	-168(3)
C36'-C31'-C32'-C33'	10(4)
C31'-C32'-C33'-C34'	-10(4)
C32'-C33'-C34'-C35'	9(5)
C33'-C34'-C35'-C36'	-5(4)
C27'-C28'-C36'-C31'	-102(2)
C4'-C28'-C36'-C31'	134(2)
C29'-C28'-C36'-C31'	10(3)

C27'-C28'-C36'-C35'	79(3)
C4'-C28'-C36'-C35'	-45(3)
C29'-C28'-C36'-C35'	-170(2)
C30'-C31'-C36'-C28'	-10(3)
C32'-C31'-C36'-C28'	172(3)
C30'-C31'-C36'-C35'	169(2)
C32'-C31'-C36'-C35'	-8(4)
C34'-C35'-C36'-C28'	-175(3)
C34'-C35'-C36'-C31'	5(4)
C41-C42-C43-C44	-51(3)
C37-C42-C43-C44	133.4(19)
C41-C42-C43-C6	179(2)
C37-C42-C43-C6	3(2)
C41-C42-C43-C51	58(2)
C37-C42-C43-C51	-117.6(18)
C1-C6-C43-C44	49(3)
C5-C6-C43-C44	-125(2)
C1-C6-C43-C42	174(2)
C5-C6-C43-C42	0(2)
C1-C6-C43-C51	-71(3)
C5-C6-C43-C51	115.4(19)
C42-C43-C44-C45	107(2)
C6-C43-C44-C45	-135(2)
C51-C43-C44-C45	-7(3)
C42-C43-C44-I3	-73(2)
C6-C43-C44-I3	46(3)
C51-C43-C44-I3	172.7(16)
C43-C44-C45-C46	5(3)
I3-C44-C45-C46	-175.2(16)
C43-C44-C45-CI3	-176(2)
I3-C44-C45-CI3	4(3)
C44-C45-C46-C51	1(3)

C13-C45-C46-C51	-177.6(18)
C44-C45-C46-C47	-179(2)
C13-C45-C46-C47	2(4)
C51-C46-C47-C48	2(3)
C45-C46-C47-C48	-178(2)
C46-C47-C48-C49	-2(3)
C47-C48-C49-C50	0(3)
C48-C49-C50-C51	2(3)
C49-C50-C51-C46	-2(4)
C49-C50-C51-C43	-175.0(19)
C47-C46-C51-C50	0(4)
C45-C46-C51-C50	-180(3)
C47-C46-C51-C43	174.7(19)
C45-C46-C51-C43	-5(2)
C44-C43-C51-C50	-178(3)
C42-C43-C51-C50	64(3)
C6-C43-C51-C50	-47(3)
C44-C43-C51-C46	8(2)
C42-C43-C51-C46	-111.0(17)
C6-C43-C51-C46	138.7(17)
C1'-C6'-C43'-C44'	-59(4)
C5'-C6'-C43'-C44'	125(3)
C1'-C6'-C43'-C42'	177(3)
C5'-C6'-C43'-C42'	1(2)
C1'-C6'-C43'-C51'	63(3)
C5'-C6'-C43'-C51'	-113(2)
C37'-C42'-C43'-C44'	-134(2)
C41'-C42'-C43'-C44'	39(3)
C37'-C42'-C43'-C6'	1(3)
C41'-C42'-C43'-C6'	174(3)
C37'-C42'-C43'-C51'	120(2)
C41'-C42'-C43'-C51'	-67(3)

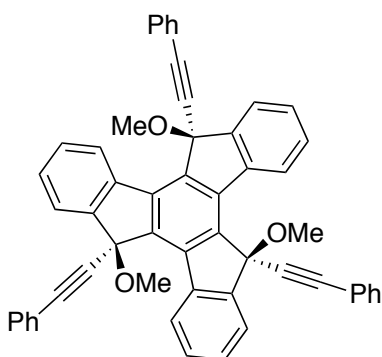
C6'-C43'-C44'-C45'	134(2)
C42'-C43'-C44'-C45'	-105(2)
C51'-C43'-C44'-C45'	6(3)
C6'-C43'-C44'-I3'	-50(3)
C42'-C43'-C44'-I3'	72(2)
C51'-C43'-C44'-I3'	-177.2(15)
C43'-C44'-C45'-C46'	-6(3)
I3'-C44'-C45'-C46'	178.3(16)
C43'-C44'-C45'-C13'	177(2)
I3'-C44'-C45'-C13'	1(3)
C44'-C45'-C46'-C51'	1(3)
C13'-C45'-C46'-C51'	178.1(19)
C44'-C45'-C46'-C47'	-180(3)
C13'-C45'-C46'-C47'	-3(4)
C51'-C46'-C47'-C48'	-9(4)
C45'-C46'-C47'-C48'	172(3)
C46'-C47'-C48'-C49'	11(4)
C47'-C48'-C49'-C50'	-7(4)
C48'-C49'-C50'-C51'	-1(4)
C49'-C50'-C51'-C46'	3(5)
C49'-C50'-C51'-C43'	-178(2)
C47'-C46'-C51'-C50'	2(5)
C45'-C46'-C51'-C50'	-179(3)
C47'-C46'-C51'-C43'	-177(2)
C45'-C46'-C51'-C43'	3(3)
C44'-C43'-C51'-C50'	176(3)
C6'-C43'-C51'-C50'	40(4)
C42'-C43'-C51'-C50'	-71(3)
C44'-C43'-C51'-C46'	-5(3)
C6'-C43'-C51'-C46'	-141.3(18)
C42'-C43'-C51'-C46'	107.4(18)
C1S#1-C11S-C12S-C12S#1	30.9(19)

C1S-C11S-C12S-C12S#1	73(3)
C1S#1-C11S-C12S-C1S	-42(4)
C1S-C11S-C12S-C1S#1	42(4)
C12S#1-C12S-C1S-C1S#1	-35(6)
C11S-C12S-C1S-C1S#1	68(5)
C12S#1-C12S-C1S-C11S#1	56(3)
C1S#1-C12S-C1S-C11S#1	91(7)
C11S-C12S-C1S-C11S#1	159(5)
C1S#1-C12S-C1S-C12S#1	35(6)
C11S-C12S-C1S-C12S#1	102(2)
C12S#1-C12S-C1S-C11S	-102(2)
C1S#1-C12S-C1S-C11S	-68(5)
C12S-C11S-C1S-C1S#1	-89(2)
C1S#1-C11S-C1S-C12S	89(2)
C1S#1-C11S-C1S-C11S#1	-74(4)
C12S-C11S-C1S-C11S#1	-163(4)
C1S#1-C11S-C1S-C12S#1	41.3(15)
C12S-C11S-C1S-C12S#1	-48(2)

Symmetry transformations used to generate equivalent atoms:

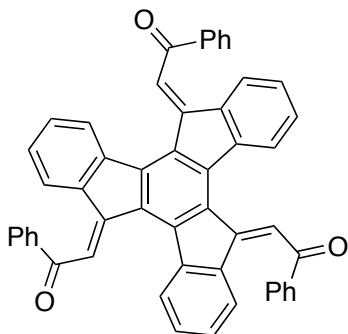
#1 -x+1, y, -z+1/2

(5S,10S,15S)-5,10,15-trimethoxy-5,10,15-tris(phenylethynyl)-10,15-dihydro-5H-diindeno[1,2-a:1',2'-c]fluorene (24)



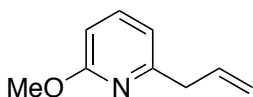
An oven-dried flask was charged with NaH (114 mg, 0.28 mmol, 4 equiv) and THF (0.5 mL). A solution of (5R,10S,15S)-5,10,15-tris(phenylethynyl)-10,15-dihydro-5H-diindeno[1,2-a:1',2'-c]fluorene-5,10,15-triol (50 mg, 0.072 mmol) in THF (0.5 mL) was added to the suspension at 0 °C and the mixture was stirred at this temperature for 3 h. Then it was allowed to warm to room temperature and the mixture was stirred for 16 h. The reaction was quenched with aqueous NH₄Cl (saturated, 10 mL) and the organic phase was separated, dried over MgSO₄ and the solvents evaporated under reduced pressure. The crude product was pure enough and the title compound **24** was obtained as an orange solid (51 mg, 0.07 mmol, 97 %). M.p.: decomposes over 245 °C. ¹H NMR (400 MHz, CDCl₃) δ 8.90 (dt, *J* = 7.9, 0.8 Hz, 1H), 7.89 (dt, *J* = 7.2, 0.9 Hz, 1H), 7.62 (td, *J* = 7.5, 1.3 Hz, 1H), 7.55 (td, *J* = 7.4, 1.2 Hz, 1H), 7.42 – 7.35 (m, 2H), 7.30 – 7.18 (m, 3H), 3.04 (s, 3H). ¹³C NMR (126 MHz, CDCl₃) δ 144.87, 140.26, 137.91, 136.74, 132.07, 129.70, 129.08, 128.48, 128.07, 126.72, 124.41, 122.35, 87.08, 84.20, 80.23, 50.79. HRMS-MALDI *m/z* = 732.2495 [M]⁺, calc. for. C₅₄H₃₆O₃: 732.2659.

(2*E*,2'*E*,2''*E*)-2,2',2''-(5*H*-diindeno[1,2-*a*:1',2'-*c*]fluorene-5,10,15-triylidene)tris(1-phenylethanone) (25)



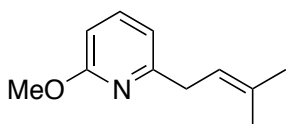
Catalyst **E** (7.2 mg, 0.009 mmol, 15 mol%) was added to a solution of (5*S*,10*S*,15*S*)-5,10,15-trimethoxy-5,10,15-tris(phenylethynyl)-10,15-dihydro-5*H*-diindeno[1,2-*a*:1',2'-*c*]fluorene (45 mg, 0.06 mmol) in CH₂Cl₂ (HPLC grade, 0.6 mL). The reaction was stirred at room temperature for 16 h. The resulting orange solid was filtrated and washed with hexane to afford **25** (16 mg, 0.02 mmol, 37%). M.p.: decomposes over 270 °C. ¹H NMR (400 MHz, CDCl₃) δ 8.56 – 8.52 (m, 1H), 8.45 (s, 1H), 8.44 – 8.40 (m, 1H), 8.08 (dd, *J* = 8.4, 1.4 Hz, 2H), 7.63 – 7.58 (m, 1H), 7.53 – 7.46 (m, 2H), 7.39 (td, *J* = 7.5, 1.5 Hz, 1H), 7.34 (td, *J* = 7.5, 1.4 Hz, 1H). ¹³C NMR (101 MHz, CDCl₃) δ 192.41, 147.13, 138.02, 133.64, 130.23, 129.22, 129.06, 128.97, 128.88, 128.59, 127.65, 127.16, 123.72, 121.33, 111.56. HRMS-MALDI *m/z* = 690.2248 [M]⁺, calc. for. C₅₁H₃₀O₃ = 690.2189.

2-Allyl-6-methoxypyridine (27b)



In a microwave vial were placed 2-chloro-6-methoxypyridine (479 mg, 3.4 mmol) and allyl tributyltin (1.03 mL, 3.4 mmol, 1 equiv) in degassed DMF (18 mL). Then $\text{PdCl}_2(\text{CH}_3\text{CN})_2$ (17 mg, 0.07 mmol, 2 mol%) was added followed by SPHOS (55 mg, 0.13 mmol, 4 mol%). The vial was sealed and heat at 120 °C for 1.5 h in a microwave reactor. The mixture was allowed to cool to room temperature and potassium fluoride (585 mg, 10.1 mmol, 3.4 equiv) was added. The reaction was stirred for three hours then cool ethyl acetate (100 mL) was added and all was filtered through a pad of celite. The solvents were removed under reduced pressure and the residue was purified by column chromatography to afford the desired product **27b** as an oil (429 mg, 2.87 mmol, 86 %). ^1H NMR (400 MHz, CDCl_3) δ 7.27 – 7.22 (m, 1H), 6.49 (d, J = 9.1 Hz, 1H), 6.04 (d, J = 6.7 Hz, 1H), 5.90 (ddt, J = 16.5, 10.2, 6.0 Hz, 1H), 5.25 (dd, J = 10.2, 1.5 Hz, 1H), 5.11 (dd, J = 17.2, 1.6 Hz, 1H), 3.53 (s, 3H), 3.38 (d, J = 5.9 Hz, 2H). ^{13}C NMR (101 MHz, CDCl_3) δ 164.18, 147.76, 138.66, 132.70, 118.77, 118.08, 106.61, 37.91, 31.09. The spectroscopic data were consistent with those previously reported: Struk, Ł.; Sośnicki, J. G. *Synthesis* **2012**, 735.

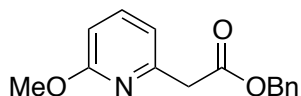
2-Methoxy-6-(3-methylbut-2-en-1-yl)pyridine (29)



In a microwave vial were placed 2-chloro-6-methoxypyridine (71.3 mg, 0.5 mmol) and tributyl(3-methylbut-2-en-1-yl)stannane (168 μL , 0.5 mmol, 1 equiv) in degassed DMF (2 mL). Then $\text{PdCl}_2(\text{CH}_3\text{CN})_2$ (2.6 mg, 0.01 mmol, 2 mol%) was added followed by XPHOS (9.5 mg, 0.02 mmol, 4 mol%). The vial was sealed and heat at 120 °C for 1.5 h in a microwave reactor. The mixture was allowed to cool to room temperature and potassium fluoride (99 mg, 1.7 mmol, 3.4 equiv) was added. The reaction was stirred for three hours then

cool ethyl acetate (100 mL) was added and all was filtered through a pad of celite. The solvents were removed under reduced pressure and the residue was purified by column chromatography to afford the desired product **29** as an oil (88 mg, 4.95 mmol, 99%). ^1H NMR (400 MHz, CDCl_3) δ 7.24 (dd, $J = 9.0, 6.9$ Hz, 1H), 6.48 (d, $J = 9.0$ Hz, 1H), 6.05 (d, $J = 6.8$ Hz, 1H), 5.18 (tt, $J = 6.9, 1.3$ Hz, 1H), 3.54 (s, 3H), 3.31 (d, $J = 6.9$ Hz, 2H), 1.80 (s, 3H), 1.71 (s, 3H). ^{13}C NMR (101 MHz, CDCl_3) δ 164.30, 149.36, 138.79, 136.28, 118.34, 117.54, 105.91, 33.03, 30.93, 25.83, 18.08. HRMS-ESI $m/z = 178.1227$ [$\text{M}+\text{H}$], calc. for $\text{C}_{11}\text{H}_{16}\text{NO}$: 178.1226.

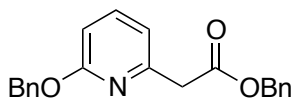
Benzyl 2-(6-methoxypyridin-2-yl)acetate (32a)



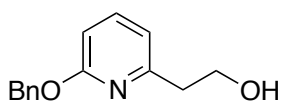
An oven-dried microwave vial equipped with a Teflon coated-sirring bar was charged with CuI (47.6mg, 0.025 mmol, 0.05 equiv), 2-picolinic acid (61.5 mg, 0.5 mmol, 0.1 equiv), cesium carbonate (4.89 g, 15.0 mmol, 3.0 equiv) and 6-(methoxy)-2-bromopyridine (940 mg, 5.0 mmol). The vial was evacuated and backfilled with argon three times. Anhydrous dioxane (5 mL) was added followed by dibenzylmalonate (2.5 mL, 10.0 mmol, 2.0 equiv). The vial was sealed, degassed and heated at 150°C for one hour in a microwave reactor. The mixture was then partitioned between ethyl acetate (3x50 mL) and saturated aqueous NH_4Cl (30 mL). The organic phases were dried over MgSO_4 , filtered and concentrated. The material was purified by flash chromatography (ethyl acetate/hexane 5:95) affording the desired product **32a** as a clear oil (826 mg, 3.21 mmol, 64%). ^1H NMR (400 MHz, CDCl_3) δ 7.51 (dd, $J = 8.3, 7.2$ Hz, 1H), 7.39 – 7.29 (m, 5H), 6.82 (d, $J = 7.2$ Hz, 1H), 6.62 (d, $J = 8.3$ Hz, 1H), 5.18 (s, 2H), 3.86 (d, $J = 0.7$ Hz, 3H), 3.79 (s, 2H). ^{13}C NMR (101 MHz, CDCl_3) δ 170.72, 163.85, 151.97, 139.09, 136.02, 128.63, 128.31, 128.26,

116.37, 109.14, 66.70, 53.42, 43.75. HRMS-ESI $m/z = 280.0956$ $[M+Na]^+$, calc. for. $C_{15}H_{15}NNaO_3 = 280.0944$.

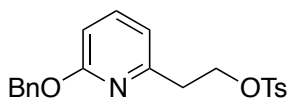
Benzyl 2-(6-(benzyloxy)pyridin-2-yl)acetate (32b)



An oven-dried microwave vial equipped with a Teflon coated-sirring bar was charged with CuI (9.5mg, 0.05 equiv), 2-picolinic acid (12.3 mg, 0.1 equiv), cesium carbonate (0.98 g, 3.0 equiv) and 2-(benzyloxy)-6-bromopyridine (264.1 mg, 1.0 mmol). The vial was evacuated and backfilled with argon three times. Anhydrous dioxane (1 mL) was added followed by dibenzylmalonate (568.6mg, 2.0 equiv). The vial was sealed, degassed and heated at 150°C for one hour in a microwave reactor. The mixture was then partitioned between ethyl acetate (3x20mL) and saturated aqueous NH_4Cl (10mL). The organic phases were dried over $MgSO_4$, filtered and concentrated. The material was purified by flash chromatography (ethyl acetate/hexane 5:95) affording the desired product **32b** as a clear oil (0.256 g, 0.55 mmol, 55%). 1H NMR (400 MHz, $CDCl_3$) δ 7.52 (dd, $J = 8.3, 7.2$ Hz, 1H), 7.45 – 7.41 (m, 2H), 7.38 – 7.27 (m, 8H), 6.84 (dd, $J = 7.3, 0.7$ Hz, 1H), 6.68 (dd, $J = 8.3, 0.7$ Hz, 1H), 5.30 (s, 2H), 5.17 (s, 2H), 3.79 (s, 2H). ^{13}C NMR (101 MHz, $CDCl_3$) δ 170.70, 163.31, 151.88, 137.57, 136.00, 128.65, 128.52, 128.35, 128.28, 127.90, 116.64, 109.62, 67.65, 66.74, 43.77. HRMS-ESI $m/z = 356.1275$ $[M+Na]^+$, calc. for. $C_{21}H_{19}NNaO_3 = 356.1257$.

2-(6-(Benzyloxy)pyridin-2-yl)ethanol (33)

LiBH₄ (487 mg, 22.3 mmol, 5.1 equiv) in THF (7.5 mL) was added to a solution of benzyl 2-(6-(benzyloxy)pyridin-2-yl)acetate (1.46g, 4.4 mmol) in dry THF (15 mL) at 0°C (following the procedure of Furuta, T.; Yamamoto, J.; Kitamura, Y.; Hashimoto, A.; Masu, H.; Azumaya, I.; Kan, T.; Kawabata, T. *J. Org. Chem.* **2010**, *75*, 7010). The resulting mixture was allowed to warm to room temperature and was stirred for 24 h. The reaction was quenched with water and extracted with EtOAc. The organic layer was washed with brine, dried over MgSO₄ and the solvent evaporated under reduced pressure. The residue was purified by column chromatography to afford the desired product **33** as a yellow oil (871 mg, 3.8 mmol, 87%). ¹H NMR (400 MHz, CDCl₃) δ 7.55 (dd, J = 8.3, 7.3 Hz, 1H), 7.47 (dd, J = 7.9, 1.0 Hz, 2H), 7.43 – 7.37 (m, 2H), 7.37 – 7.31 (m, 1H), 6.77 (dd, J = 7.2, 0.5 Hz, 1H), 6.72 (d, J = 8.3 Hz, 1H), 4.07 – 3.93 (m, 2H), 3.84 (s, 1H), 3.00 – 2.90 (m, 2H). ¹³C NMR (101 MHz, CDCl₃) δ 163.11, 158.16, 139.50, 137.19, 128.65, 128.01, 127.86, 116.21, 109.09, 67.78, 62.05, 38.67. HRMS-ESI *m/z* = 252.0986 [M+Na]⁺, calc. for C₁₄H₁₅NNaO₂ = 252.0995.

2-(6-(Benzyloxy)pyridin-2-yl)ethyl 4-methylbenzenesulfonate (34)

To a solution of 2-(6-(benzyloxy)pyridin-2-yl)ethanol (674 mg, 2.9 mmol), Et₃N (492 μL, 3.5 mmol, 1.2 equiv) and DMAP (4 mg, 0.04 mmol, 1.2 mol%)

in CH₂Cl₂ (2.3 mL) was added dropwise a solution of tosyl chloride (561 mg, 2.94 mmol, 1 equiv) in CH₂Cl₂ (3.7 mL) at 0 °C. The resulting mixture was allowed to warm to room temperature and was stirred for 48 h. The mixture was diluted with EtOAc (5 mL), transferred into a separatory funnel and washed with aqueous NaOH (10%, 10 mL) and brine (10 mL). The organic phase was dried over MgSO₄ and the solvents were vaported under reduced pressure. The residue was purified by column chromatography to afford the desired product **34** as an off-white solid (722 mg, 1.88 mmol, 64%). M.p.: 51.5 – 53.0 °C. ¹H NMR (400 MHz, CDCl₃) δ 7.66 (d, *J* = 8.3 Hz, 2H), 7.45 (dd, *J* = 8.3, 7.2 Hz, 1H), 7.42 – 7.28 (m, 5H), 7.24 (d, *J* = 8.0 Hz, 2H), 6.69 (dd, *J* = 7.2, 0.8 Hz, 1H), 6.61 (dd, *J* = 8.3, 0.8 Hz, 1H), 5.16 (s, 2H), 4.45 (t, *J* = 6.5 Hz, 2H), 3.00 (t, *J* = 6.5 Hz, 2H). ¹³C NMR (126 MHz, CDCl₃) δ 163.27, 154.01, 144.70, 139.11, 137.58, 133.13, 129.82, 128.57, 128.08, 127.96, 127.90, 116.62, 109.31, 69.42, 67.44, 37.04, 21.72. HRMS-ESI *m/z* = 384.1282 [M+H]⁺, calc. for. C₂₁H₂₂NO₄S = 384.1264.